A N N U A L R E P O R T

1965

U. S. WATER CONSERVATION LABORATORY
Southwest Branch
Soil and Water Conservation Research Division
Agricultural Research Service
United States Department of Agriculture
Phoenix, Arizona

ADMINISTRATIVELY CONFIDENTIAL

This report contains unpublished and confidential information concerning work in progress. The contents of this report may not be published or reproduced in any form without the prior consent of the research workers involved.

LABORATORY STAFF

Professional

Dr. H. Bouwer, Research Hydraulic Engineer
Mr. K. J. Brust, Agricultural Engineer
Dr. W. L. Ehrler, Research Plant Physiologist
Mr. L. J. Erie, Research Agricultural Engineer
Mr. G. W. Frasier, Agricultural Engineer
Dr. L. J. Fritschen, Research Meteorologist
Dr. R. D. Jackson, Research Physicist
Mr. L. E. Myers, Research Hydraulic Engineer and Director
Dr. F. S. Nakayama, Research Chemist
Mr. R. J. Reginato, Research Soil Scientist
Dr. J. A. Replogle, Research Agricultural Engineer
Mr. R. C. Rice, Agricultural Engineer
Dr. C. H. M. van Bavel, Research Physicist

Technicians:

F. L. Combs, Physical Science Aid
R. G. Flores, Engineering Draftsman
O. F. French, Hydraulic Engineering Technician
J. L. Gale, Physical Science Aid
L. P. Girdley, Engineering Draftsman
J. R. Griggs, Physical Science Technician
A. N. Lehman, Physical Science Aid
R. B. MacIntyre, Physical Science Aid
J. B. Miller, Physical Science Technician
S. T. Mitchell, Physical Science Technician
K. G. Mullins, Physical Science Technician
J. M. Pritchard, Physical Science Technician
B. A. Rasnick, Physical Science Technician
C. M. Wakefield, Physical Science Aid

Administrative, Clerical and Maintenance:

O. J. Abeyta, Laborer
E. D. Bell, General Machinist
E. E. De La Rosa, Janitor
A. V. Figueroa, Laborer
B. E. Fisher, Library Assistant
D. S. Fry, Clerk-Stenographer
C. E. Hansen, Secretary
C. G. Hiesel, General Machinist
R. C. Klapper, Refrigeration and Air Conditioning Mechanic

Administrative, Clerical and Maintenance (Continued)

J. M. R. Martinez, Laborer
R. S. Miller, Administrative Assistant
A. H. Morse, Clerk-Dictating Machine Transcriber
M. E. Olson, Clerk-Stenographer
M. A. Seiler, Clerk-Stenographer
M. F. Witcher, Clerk-Stenographer
M. M. Zamora, Laborer

CHANGES IN PERSONNEL

The Laboratory staff has been strengthened during 1965 by the addition of four new members. They are as follows:

F. L. Combs, Physical Science Aid
L. P. Girdley, Engineering Draftsman
J. M. Pritchard, Physical Science Technician
C. M. Wakefield, Physical Science Aid

During 1965 there were four resignations. They are as follows:

R. G. Flores, Engineering Draftsman
A. N. Lehman, Physical Science Aid
R. B. MacIntyre, Physical Science Aid
A. V. Figueroa, Laborer

The Laboratory staff is now essentially at full strength with one or two exceptions.

TABLE OF CONTENTS 1/

TITLE	SECTION
Dynamic Similarity in Elbow Flow Meters. J. A. Replogle, L. E. Myers, K. J. Brust	2
Calibration and Evaluation of Net Radiometers. L. J. Fritschen	6
Soil Treatment to Reduce Infiltration and Increase Precipitation Runoff. L. E. Myers, G. W. Frasier	7
Application of Hexadecanol-Octadecanol Monofilms to Small Ponds. L. E. Myers, G. W. Frasier	9
Measurement and Calculation of Unsaturated Conductivity and Soil-Water Diffusivity. R. D. Jackson	13
Field Application of Falling-Head Technique for Seepage Meters and of Double-Tube Method for Hydraulic Conductivity Measurement. H. Bouwer, R. C. Rice	14
Components of the Radiation Balance of Field Crops Under Irrigated Conditions. L. J. Fritschen	18
Evaporation From the Soil Surface and Soil Moisture Movement. J. Conaway, C. H. M. van Bavel	19
Measuring Horizontal and Vertical Hydraulic Conductivity of Soil with the Double-Tube Method. H. Bouwer, R. C. Rice	25
Water Absorption, Transpiration, and Internal Water Balance of Cotton Plants as Affected by Changes in Evaporative Demands. W. L. Ehrler, C. H. M. van Bavel	29
Quantitative Measurement of Water Flow with Chemical Tracers. J. A. Replogle, L. E. Myers, K. J. Brust	30
Water Vapor Diffusion in Soils. R. D. Jackson, C. H. M. van Bavel	31
Micrometeorological Determinations of Water Loss From Various Surfaces. L. J. Fritschen	32

1/ Research outlines that have been terminated or that are inactive are not listed.

TITLE	SECTION
Direct Measurement of Evapotranspiration and the Energy Balance of Irrigated Crops. C. H. M. van Bavel, K. J. Brust, W. L. Ehrler, J. Conaway	33
Water Management for the Efficient Irrigation of Sugar Beets. L. J. Erie, O. F. French	36
Clay Dispersants for the Reduction of Seepage Losses from Reservoirs. R. J. Reginato, L. E. Myers	37
Waterborne Sealants to Reduce Seepage Losses from Unlined Channels and Reservoirs. R. J. Reginato, L. E. Myers	38
Crack Sealants for Concrete Lined Canals. R. J. Reginato, L. E. Myers	39
Dispersion and Flocculation of Soil and Clay Materials as Related to the Na and Ca Status of the Ambient Solution. F. S. Nakayama	40
Field Measurement of Critical Pressure Head of Soils. H. Bouwer and R. C. Rice	41
Materials and Methods for Water Harvesting and Water Storage in the State of Hawaii. L. E. Myers, G. W. Frasier	42
Integrating Velocity Profile Meters. J. A. Replogle	43
Manuscripts Approved and/or Published in 1965	AI

WORK AND LINE PROJECTS AND RESEARCH OUTLINES 1/

Work Project	Line Project	Research Outline Code No. 2/	Title
SWC-4		Ariz.-WCL	Conservation of Water Supplies for Agricultural Use.
	gG1		Measurement, Evaluation and Control of Seepage Losses.
		14	Field Application of Falling-Head Technique for Seepage Meters and of Double-Tube Method for Hydraulic Conductivity Measurement. H. Bouwer, R. C. Rice.
		25	Measuring Horizontal and Vertical Hydraulic Conductivity of Soil with the Double-Tube Method. H. Bouwer, R. C. Rice.
		37	Clay Dispersants for the Reduction of Seepage Losses from Reservoirs. R. J. Reginato, L. E. Myers.
		38	Waterborne Sealants to Reduce Seepage Losses from Unlined Channels and Reservoirs. R. J. Reginato, L. E. Myers.
		39	Crack Sealants for Concrete Lined Canals. R. J. Reginato, L. E. Myers.
		41	Field Measurement of Critical Pressure Head of Soils. H. Bouwer, R. C. Rice.
	gG2		Atmospheric and Related Boundary Mechanisms in Water Vapor Losses from Plant, Soil and Water Surfaces.
		6	Calibration and Evaluation of Net Radiometers. L. J. Fritschen.

1/ Research outlines that have been terminated or are inactive are not listed.

2/ Research outline code number also indicates section number.

Work Project	Line Project	Research Outline Code No.	Title
SWC-4	gG2	9	Application of Hexadecanol-Octadecanol Monofilms to Small Ponds. L. E. Myers, G. W. Frasier.
		18	Components of the Radiation Balance of Field Crops Under Irrigated Conditions. L. J. Fritschen.
		32	Micrometeorological Determinations of Water Loss from Various Surfaces. L. J. Fritschen.
		33	Direct Measurement of Evapotranspiration and the Energy Balance of Irrigated Crops. C. H. M. van Bavel.
	gG3		Measurement, Evaluation and Control of Infiltration to Conserve Water.
		7	Soil Treatment to Reduce Infiltration and Increase Precipitation Runoff. L. E. Myers, G. W. Frasier.
		40	Dispersion and Flocculation of Soil and Clay Materials as Related to the Na and Ca Status of the Ambient Solution. F. S. Nakayama.
		42	Materials and Methods for Water Harvesting and Water Storage in the State of Hawaii. L. E. Myers, G. W. Frasier.
	gG4		Physical Processes in the Soil Affecting Preventable Losses of Water by Surface Evaporation.
		13	Measurement and Calculation of Unsaturated Conductivity and Soil-Water Diffusivity. R. D. Jackson.
		19	Evaporation from the Soil Surface and Soil Moisture Movement. C. H. M. van Bavel, R. D. Jackson, R. J. Reginato.
		31	Water Vapor Diffusion in Soils. R. D. Jackson.

Work Project	Line Project	Research Outline Code No.	Title
SWC-4	gG5		Water Measurement and Control for Water Conservation.
		2	Dynamic Similarity in Elbow Flow Meters. J. A. Replogle, K. J. Brust, L. E. Myers.
		30	Quantitative Measurement of Water Flow with Chemical Tracers. J. A. Replogle, K. J. Brust, L. E. Myers.
		43	Integrating Velocity Profile Meters. J. A. Replogle.
SWC-5			Irrigation Principles, Requirements, Practices and Facilities for Efficient Use of Water on Farms.
	g2		Irrigation Requirements of Forage and Cultivated Crops in the Southwest.
		36	Water Management for Efficient Irrigation of Sugar Beets. L. J. Erie, O. F. French.
SWC-11			Soil, Water, and Plant Relations as They Affect Use of Land and Water Resources.
	gG1		Uptake and Disposal of Water by Plants in an Arid Climate.
		29	Water Absorption, Transpiration, and Internal Water Balance of Cotton Plants as Affected by Changes in Evaporative Demands. W. L. Ehrler, C. H. M. van Bavel, F. S. Nakayama.

TITLE: DYNAMIC SIMILARITY IN ELBOW FLOW METERS

LINE PROJECT: SWC 4-gG5 CODE NO.: Ariz.-WCL-2

INTRODUCTION:

See Annual Report for 1964.

PROCEDURE:

Experimental procedures described in 1964 were extended to include the remaining 10"-diameter elbow flow meters. All elbow radii of bend were measured by a casting plaster technique. Plaster castings of a strip of each elbow interior along the inside and outside of the bend were made. This provided an accurate representation of the flow path along the elbow wall and over the manometer taps.

The plaster castings of the elbow interior were easily obtained by oiling the surface to be cast and troweling a ribbon of casting plaster along the bend an inch or so wide and about an inch thick, depending on the elbow size. Before the plaster set, wire mesh was pressed into it for reinforcement. The bend profile was transferred to drawing paper by using a slide projector as a light source and tracing the shadow profile of the casting. From this tracing, the radius of curvature was constructed graphically, based on the center 2/3 of the bend.

RESULTS AND DISCUSSION:

Due to inconsistencies in some preliminary data collected from the 3-inch elbows, it was erroneously concluded that detrimental effects on the calibration were caused by misalignment and by abrupt changes in effective diameter caused by flanges that were not completely threaded onto the pipe. To assure alignment and provide smooth passage into the 3-inch elbows, a thin sleeve insert was constructed to fit tightly in both the elbow and the pipe. See Annual Report for 1960. The sleeve, 2.5 inches long, was gently tapered to a knife edge on both the upstream and downstream ends. The maximum thickness of the insert wall was approximately 0.08 inch. The entire lot of 3-inch elbows was calibrated under this arrangement. This problem of misalignment of joints was reinvestigated. Deliberate misalignment was introduced in the standard 3-inch piping arrangement by moving the flange of the upstream pipe section approximately 1/4 inch toward the inside of the

elbow bend before bolting and calibrating. This produced an indicated flow rate that was about 0.7 percent too low. A similar position was likewise tested with the pipe shifted to the opposite direction, but no significant change could be detected in the indicated discharge rate. Downstream offsets likewise caused no significant changes in discharge rate.

Further checks for effects due to misalignment were conducted with a 12-inch and a 6-inch elbow. On these elbows, a flow was established through the elbow. The elbow flanges were clamped and the bolts removed. This permitted an offset in alignment of either face of the elbow by slight loosening of the clamps and offsetting the pipe while still maintaining the same discharge. On the 12-inch elbow, severe offsets on the order of 1/4 to 1/2 the bolt-hole diameter were necessary to produce approximately one-half percent difference in indicated discharge rate. An upstream offset, as with the 3-inch elbows, produced more severe effects than a similar downstream offset. Similar results were obtained with the 6-inch elbow.

The influence of the space which is formed when the pipe is not completely threaded through the flange was checked. A space at the upstream elbow connection, approximately 3/8-inch wide and 1/4-inch deep, caused less than 0.2 percent decrease in indicated discharge for both the long and short radius 3-inch elbows.

Representative 3-inch elbows were rechecked with and without the sleeve insert. The influence of the insert was so insignificant that it was not detectable. The original calibrations were concluded valid and retained for analysis.

It is concluded that sources of error caused by misalignment are small and can be prevented by aligning the flange-bolt holes with tight-fitting bolts or pins. Also, the influence of minor upstream disturbances such as flange joints are insignificant if they affect the velocity profile symmetrically with respect to the centerline of the approaching pipe flow.

The construction of the manometer taps perpendicular to the interior elbow surface is important. Manometer taps inclined into the

flow will read pressures that are too high, and those inclined in the opposite direction will read too low. This causes differences in the pressure differential discharge relation when the flow direction is reversed. All cases of poor reversibility were associated with improper manometer tap alignment that was observable by sighting through the two manometer taps. Normal machine shop procedures should prevent this by drilling undersized pilot holes and manually correcting observed misalignment when reaming to the desired full size.

Manometer tap misalignment is not the only factor that can affect reversibility of an elbow meter. This is partly illustrated by a 12-inch elbow (No. 42, Table 1), which displayed nearly 11 percent difference in the pressure-differential discharge relation between alternate flow directions, but had only minor manometer tap misalignment. The inside bend radius was found to vary considerably from flange to flange. Also, the elbow was not round at the section containing the manometer taps and, even though they appeared to be only slightly misaligned when observed from outside the elbow, they were considerably nonperpendicular to the flow boundary. The combination of variable radius of curvature and nonperpendicular manometer taps are believed to have produced the large bias with regard to direction of elbow installation.

When the inside radius of the above mentioned 12-inch elbow was changed with a power grinder to improve the symmetry and roundness of the elbow interior, radical changes in calibration of over 10 percent occurred. Similar grinding along the outside bend caused no detectable change in calibration. The regularity of the radius of curvature of the inside bend was concluded to be critical for accurately characterizing elbows. Because of the relative insensitivity of the elbow meter to the outside bend radius, it was subsequently not used to determine $\bar{r}$. The simpler procedure of simply adding D/2 to the inside radius determined with plaster castings was found to be adequate. If examination of this inside-bend profile shows it to be symmetrical, it is likely that the sand mold casting is within the tolerances necessary to meet the qualifications of the calibrations reported herein. Elbow No. 42 was the only elbow with significant asymmetry. If asymmetry is noted

such that corresponding points of symmetry differ by 1/16 inch or more, the elbow should be discarded for use as a meter unless calibrated in place.

Calibration Results. An empirical equation of the form

$$Q = MH^E \qquad [1]$$

was chosen for each elbow calibration. In equation [1], M and E are the intercept and slope, respectively, of a log-log plot of discharge, Q, versus pressure differential, H. The values of M and E were determined for each calibration by the least squares method. These values are listed in columns 4 and 5 of Table 1 for both directions of flow through each elbow.

An equation (see Annual Report 1964) including a discharge coefficient, k, may be written for flow in an elbow meter of diameter, D, and centerline bend radius, $\bar{r}$, as

$$Q = k \sqrt{2g} \frac{\pi D^2}{4} \sqrt{\frac{\bar{r}}{2D}} H^E \qquad [2]$$

or

$$Q = kM' H^E \qquad [3]$$

and M of equation [1] becomes

$$M = kM' = k \sqrt{2g} \frac{\pi D^2}{4} \sqrt{\frac{\bar{r}}{2D}} \qquad [4]$$

The value of k was calculated for each elbow type and size group and is simply

$$k = \frac{M}{M'} \qquad [5]$$

Here, M is the average calibration value in equation [1] for the elbow size group and M' is calculated with equation [4]. The average group dimensions, the average calibration values for M and E, and the calculated values of k and kM' are tabulated in Table 1.

Both E and k were generally found to increase linearly with elbow diameter. This increase is believed to be associated with the strength of secondary currents in the bend. The values for E increase according to the equation

$$E = 0.0377\ D + 0.489 \qquad [6]$$

The values for k show approximate linearity for the 6-, 10-, and 12-inch elbows, Figure 1, but do not follow through for the 3-inch elbow sizes.

The error in Q resulting from errors in the various factors of equation [2] can be expressed by

$$\frac{\Delta Q}{Q} = \frac{\Delta k}{k} + \frac{\Delta \bar{r}}{2\bar{r}} + \frac{3\Delta D}{2D} + E\,\frac{\Delta H}{H} + \Delta E \log H. \qquad [7]$$

The major error in Q, excluding manometer errors in determining H, is made up of those factors incorporated into M, equation [4]. The error caused by deviations in E are small by comparison. Thus, an estimate of how well the calculated equation compares with the laboratory calibrated equation for each elbow can be obtained by comparing the respective values for kM' with M. This comparison is expressed in Table 1 as a percent deviation, ΔQ. For this comparison, M is averaged for the alternate flow directions. These alternate direction values for M are also given in Table 1. The first value listed corresponds to the initial direction of installation and the second value to the reverse direction.

In all cases, the average calibration result for flow in both directions through an elbow was described within $\pm$ 3 percent by equation [2], using the measured elbow dimensions and the corresponding values of k and E. (Note the values of ΔQ, Table 1.)

Several elbows, namely Nos. 21, 30, 32, 33, and 42, had calibration equations for individual flow directions which exceeded the $\pm$ 3 percent value. In all cases the manometer taps were not correctly aligned and, as explained earlier, No. 42 was also asymmetric. However, the average of the value of M for the two flow directions in these cases produced calibration results within $\pm$ 2 percent of equation [2]. The fact that

the average of the alternate direction values for M agrees so well with the computed values for kM' suggests a field calibration procedure for elbows as poor as those cited above. This calibration procedure requires a steady discharge source that can be shut down and reestablished to the same discharge rate. A monometer reading is obtained and the elbow reversed for a second manometer reading. The two apparent discharges are calculated using equation [2]. The correct discharge is the average of these two. Therefore, kM' can then be adjusted by one-half the percentage difference in the apparent discharge rates determined for the two flow directions. This equation then should predict discharge through the elbow accurate to $\pm$ 3 percent.

In all but four cases which involve elbows Nos. 7, 8, 33, and 42, the average equation for a particular size grouping of elbows is sufficiently accurate to predict the flow rate through a member of the same group to within $\pm$ 5 percent. This reflects variations in the dimensional uniformity of the sand cast elbows and indicates the degree of accuracy that may be expected even if no measurements are made on an uncalibrated elbow.

Six die-molded plastic elbows, 3 inches in diameter, were among those calibrated. The pertinent data concerning them are presented in Table 1. Significant here is the excellent reproducibility from elbow to elbow. The die-molded elbows, as expected, are more uniformly manufactured than is possible with the sand casting techniques used on cast iron elbows. These elbows can be expected to agree well within 2 percent of the calibration equation of an elbow of the same type. These elbows are also somewhat directional with a definite calibration bias associated with the direction of flow. This produced no special problem since the molded plastic elbows had sufficient manufacturing markings to permit selection of a standard orientation.

SUMMARY AND CONCLUSIONS:

Flow meters, constructed from pipe elbows, have the unique advantages of replacing an existing elbow, ability to measure flow rate in either direction, and contributing no additional head loss to the piping system. The utility of the elbow flow meter would be increased many times if

calibration in place were not necessary. Uncalibrated elbow flow meters have been previously regarded as only $\pm$ 10 percent devices.

In a laboratory study, a number of flanged, 90-degree commercial pipe elbows of several sizes, ranging from 3 inches to 12 inches in diameter, were calibrated as flow meters. The accuracy to which a calibration equation can be predicted for an elbow flow meter, without calibration in place and using only the nominal elbow size, is $\pm$ 5 percent. This accuracy can be obtained using the equation

$$Q = MH^E$$

where Q is the discharge, H is the differential pressure produced by the flow around the elbow flow meter and M and E are constants previously derived by calibrating several elbows of the type and size under consideration.

Accurate dimensional data, obtained with plaster castings of the elbow interior, permit the measurement of the elbow radius of curvature and the subsequent calculation of a pressure differential discharge equation for the elbow flow meter which is accurate to $\pm$ 3 percent. Without calibrating the elbow in place, this accuracy can be obtained with the equation

$$Q = k \frac{\pi D^2}{4} \sqrt{\frac{g\bar{r}}{D}} \; H^E$$

where k is a constant derived from previous calibrations on several elbows of the nominal size and type under consideration, D is the elbow diameter, g is the gravitational constant, $\bar{r}$ is the centerline radius of bend for the elbow flow meter, and E is obtained from the empirical equation

$$E = 0.0377\ D + 0.489$$

Elbow meters should have at least 25 to 30 diameters of upstream straight piping. This distance was sufficient to reduce the effects of all disturbance elements to less than 1 percent.

The shape of the inside bend of the elbow interior is critical to the calibration of the elbow; the outside bend is much less so.

Molded plastic elbows are uniform enough that a single calibration of one in a group manufactured from the same die can characterize the group to within 2 percent.

Pressure taps should be radially opposed, perpendicular to the elbow interior surface, free from burrs, and located approximately at the midpoint of the bend, in the plane of the bend. Small deviation in construction of the pressure taps and in elbow asymmetry can be detected and compensated for by a simple field calibration technique that involves reversing the elbow installation and noting the change in pressure differential at the same flow rate.

PERSONNEL: J. A. Replogle, L. E. Myers, K. J. Brust

TABLE 1: Comparison of Calculated and Calibrated Elbow Meter

Equation of the Form $Q = MH^E$

Short Radius — Cast Iron, 3-inch,

Elbow No.	D a/ ft	$\bar{r}$ b/ ft	Calibrated c/ M	Calibrated c/ E	k d/	Calculated e/ kM'	Calculated e/ E	ΔQ f/ %
1	0.242	0.382	0.325 g/	0.508	0.994	0.324	0.498	-0.3
			0.325 g/	0.503				
2	0.242	0.391	0.329	0.504	"	0.330	0.498	+0.6
			0.327	0.504				
3	0.250	0.339	0.321	0.500	"	0.332	0.498	+0.6
			0.320	0.497				
4	0.251	0.333	0.325	0.501	"	0.322	0.498	0.0
			0.319	0.499				
7	0.249	0.378	0.347	0.499	"	0.333	0.498	-2.9
			0.347	0.494				
8	0.248	0.379	0.339	0.497	"	0.337	0.498	-0.3
			0.338	0.503				
11	0.250	0.366	0.331	0.490	"	0.334	0.498	+0.6
			0.332	0.495				
12	0.250	0.363	0.329	0.493	"	0.333	0.498	+1.5
			0.328	0.490	"			
17	0.248	0.356	0.323	0.499	"	0.326	0.498	0.0
			0.328	0.501				
18	0.249	0.349	0.330	0.497	"	0.326	0.498	-0.6
			0.326	0.496				
Ave.	0.248	0.364	0.329	0.498	0.994	--	--	--

TABLE 1: (Continued)

3 inch, Cast Iron, Long Radius

Elbow No.	D a/ ft	$\bar{r}$ b/ ft	Calibrated c/ M	Calibrated c/ E	k d/	Calculated e/ kM'	Calculated e/ E	ΔQ f/ %
5	0.248	0.557	0.411	0.497	1.014	0.411	0.498	+0.2
			0.409	0.494				
6	0.247	0.575	0.408	0.498	"	0.415	0.498	+2.5
			0.403	0.496				
9	0.250	0.569	0.421	0.490	"	0.420	0.498	-0.5
			0.422	0.498				
10	0.251	0.555	0.412	0.502	"	0.418	0.498	-1.7
			0.410	0.500				
13	0.248	0.528	0.403	0.502	"	0.401	0.498	-0.2
			0.400	0.502				
14	0.247	0.520	0.401	0.495	"	0.395	0.498	-1.5
			0.401	0.495				
15	0.249	0.539	0.406	0.498	"	0.407	0.498	-0.2
			0.410	0.500				
16	0.249	0.536	0.405	0.494	"	0.406	0.498	-1.2
			0.417	0.502				
Ave.	0.249	0.547	0.409	0.498	1.014	--	--	--

TABLE 1: (Continued)

	Elbow No.	D a/ ft	$\bar{r}$ b/ ft	Calibrated c/ M	Calibrated c/ E	k d/	Calculated e/ kM'	Calculated e/ E	ΔQ f/ %
6-inch, Cast Iron	20	0.496	0.570	1.129	0.509	0.983	1.152	0.508	+1.8
				1.133	0.511				
	21	0.496	0.558	1.158	0.514	"	1.140	0.508	+0.7
				1.105	0.519				
	22	0.491	0.588	1.198	0.504	"	1.153	0.508	-2.8
				1.174	0.506				
	23	0.491	0.597	1.173	0.514	"	1.161	0.508	-0.3
				1.158	0.513				
	Ave.	0.494	0.578	1.15	0.508	0.983	--	--	--
10-inch, Cast Iron	30	0.829	0.785	3.17	0.515	1.021	3.02	0.520	-2.0
				2.99	0.516				
	31	0.826	0.804	3.15	0.521	"	3.06	0.520	-2.5
				3.13	0.523				
	32	0.833	0.788	3.13	0.516	"	3.06	0.520	+1.7
				2.89	0.514				
	33	0.828	0.777	2.90	0.523	"	3.01	0.520	+0.7
				3.08	0.520				
	34	0.833	0.776	3.00	0.529	"	3.04	0.520	+2.0
				2.95	0.529				
	Ave.	0.830	0.787	3.04	0.520	1.021	--	--	--

TABLE 1: (Continued)

Elbow No.	D a/ ft	$\bar{r}$ b/ ft	Calibrated c/ M	Calibrated c/ E	k d/	Calculated e/ kM'	Calculated e/ E	ΔQ f/ %
12-inch, Cast Iron								
40	1.000	0.845	4.23	0.533	1.048	4.28	0.527	+0.7
			4.26	0.534				
41	0.996	0.885	4.38	0.513	"	4.36	0.527	+0.5
			4.30	0.519				
42	1.000	0.857	4.05	0.542	"	4.32	0.527	+0.9
			4.51	0.551				
43	0.997	0.893	4.51	0.502	"	4.38	0.527	-2.5
			4.47	0.510				
Ave.	0.998	0.870	4.33	0.525	1.048	--	--	--
ABS Plastic. Long Turn.								
P_1	0.256	0.378	0.348	0.498	0.965	0.340	0.498	-0.3
			0.334	0.502				
P_2	0.256	0.378	0.338	0.504	"	0.340	0.498	+1.8
			0.330	0.500				
P_3	0.256	0.378	0.346	0.502	"	0.340	0.498	0.0
			0.335	0.496				
Ave.	0.256	0.378	0.340	0.500	0.965	--	--	--
ABS-Plastic. Short turn.								
P_4	0.256	0.323	0.298	0.502	0.920	0.300	0.498	0.0
			0.303	0.504				
P_5	0.256	0.323	0.297	0.500	"	0.300	0.498	+0.7
			0.299	0.492				
P_6	0.256	0.323	0.300	0.504	"	0.300	0.498	-0.3
			0.302	0.496				
Ave.	0.256	0.323	0.300	0.500	0.920	--	--	--

a/ Elbow diameter; average diameter of both faces.
b/ Average bend radius; inside bend radius plus D/2.
c/ M and E are the intercept and slope, respectively, of a log-log plot of discharge, Q, versus pressure differential, H.
d/ Calibration coefficient adjusting the average calculated to the average calibrated values of M.
e/ Values of kM' and E obtained with equations 4 and 6.
f/ 100 (M - kM')/M.
g/ Two values are for alternate flow directions.

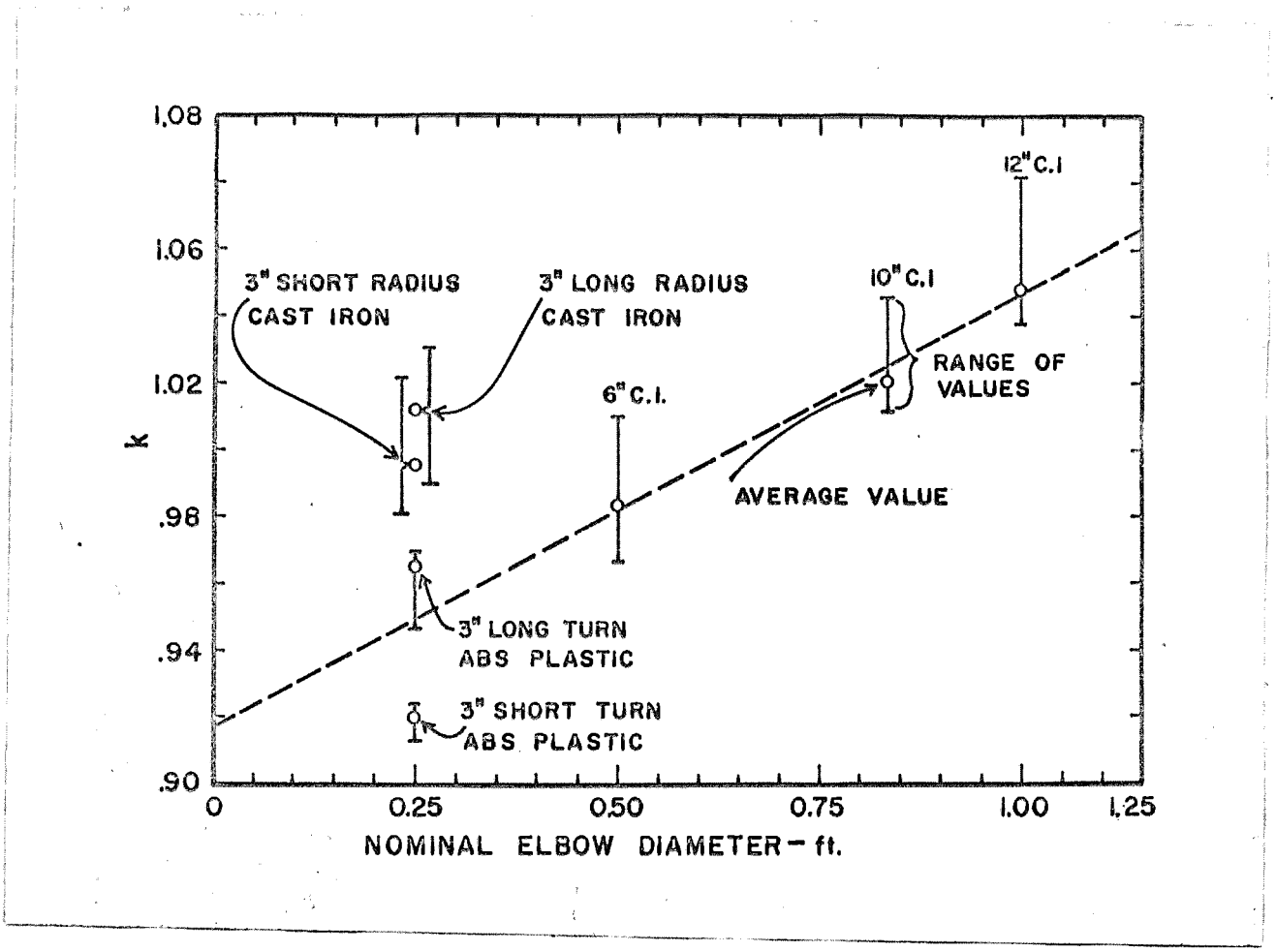

Figure 1. Experimentally determined values of k for 3-, 6-, 10-, and 12-inch elbow flow meters.

TITLE: CALIBRATION AND EVALUATION OF NET RADIOMETERS

LINE PROJECT: SWC 4-gG2 CODE NO.: Ariz.-WCL-6

The miniature net radiometer design, described in (1), has been changed to facilitate replacement of the hemispherically shaped polyethylene wind shields in the field. The changes include omitting the stem from the top brass clamping ring, casting the thermal transducer into an aluminized epoxy-resin frame to protect the circuitry, and including a small bull's eye level in the frame. Details of the changes are described in WCL Report 5.

In order to supply the Division with net radiometers, molds, jigs, and components have been acquired to construct 300 net radiometers.

Individual calibration of large numbers of net radiometers has proven to be too time consuming. A facility has been constructed which will permit simultaneous calibration of 6 miniature net radiometers. With this facility periodic recalibration of net radiometers may be accomplished rapidly.

REFERENCES:

(1) Fritschen, Leo J.
1965. Miniature net radiometer improvements.
Jour. Appl. Meteorology 4: 528–532.

PERSONNEL: Leo J. Fritschen

TITLE: SOIL TREATMENT TO REDUCE INFILTRATION AND INCREASE PRECIPITATION RUNOFF

LINE PROJECT: SWC 4-gG3 CODE NO.: Ariz.-WCL-7

INTRODUCTION:

Recent laboratory studies have been concerned with the analysis of discolored runoff water collected from asphalt-treated plots. Standards were developed for qualitative comparison of water samples and for preliminary evaluation of materials applied to asphalt surfaces to reduce water discoloration.

At the Granite Reef testing site 8 new plots were constructed. Also, underground electrical power was installed at 15 plots to expedite the measurement of the collected runoff water. A series of 23 newly installed raingages within the test area and an automatic recording system of wind speed and direction at two locations are helping to characterize the rainfall patterns within the test area.

In a continuation of our field evaluation of different surface treatments, two new experimental operational water harvesting structures were installed in cooperation with the Bureau of Indian Affairs, along with a re-treatment of the Metate catchment. Also, a small unitized catchment and storage to provide water for bees and firefighting was developed and is undergoing evaluation.

PART I. ANALYSIS OF RUNOFF WATER:

The runoff water from exposed asphalt-treated surfaces is often discolored by the byproducts of asphalt deterioration. The degree of discoloration is also an indication of the rate of asphalt deterioration. The discolored water is not believed harmful to livestock and the discoloration can be removed from the water by standard water-treatment procedures. For agricultural uses treatment of the water is not economically feasible; therefore, it is desirable to reduce or prevent the water discoloration. This can be done by spraying materials on the catchment surface which reduce the rate of asphalt deterioration. To qualitatively evaluate the effectiveness of the surface treatments, it is necessary to analyze the discolored water.

Using a Beckman DU spectrophotometer, an absorption spectrum of a sample of discolored runoff water was constructed. The measurements showed no absorption maximum, and it was concluded the amount of discoloration from a sample is a factor of dilution only. This allows a qualitative analysis of the water to be made by color comparison with standards of known concentrations. The preparation of color standards and the preliminary results were as follows.

Procedure. With a sample of runoff water collected 23 June 1965 from plot L-5 at Granite Reef as a base, a set of 13 standards with known concentrations of discolored water was prepared. The base water sample was filtered through a sheet of No. 2 Whatman filter paper to remove suspended impurities; then, diluted with distilled water to the required concentration and sealed in a 15 × 125 mm test tube. Following is a list of the standards prepared:

Water color index	0	0.1	0.5	1	2	3	4	5	6	7	8	9	10
Percent distilled water	100	99.0	95.0	90	80	70	60	50	40	30	20	10	0
Percent base water	0	1.0	5.0	10	20	30	40	50	60	70	80	90	100

Runoff water samples were collected from the asphalt plots at Granite Reef after each rain. After filtering each sample through a sheet of No. 2 Whatman filter paper, the electrical conductivity and pH were measured, using standard laboratory procedures. The samples were then placed in 15 × 125 mm test tubes, and the water discoloration was determined by color comparison with the standards, using a Wallace & Tiernan color comparator.

Primary interest was given to the water samples from plots L-5 and L-6 at Granite Reef. Plot L-5 is a two-phase asphalt treatment with a sealcoat of roofing asphalt-clay emulsion at 0.5 kg asphalt m^{-2}

applied 25 January 1965. Plot L-6, also a two-phase asphalt treatment, had a top spray of flaked aluminum dispersed in asphalt and solvent, applied at 0.08 kg solution m^{-2} in January 1965.

Results. The pH of the water samples varied from 5.1 to 7.2, with no apparent correlation to the degree of discoloration. The conductivity varied from 0.01 to 0.97 millimhos (less than 50 to 600 ppm) — within wide limits the higher the conductivity, the more discolored the water. It was anticipated that the degree of discoloration would generally be inversely proportional to the quantity of runoff water and directly proportional to the days between rains. This correlation is shown in Figure 1, where the days between rains divided by the runoff in millimeters are plotted against the water color index. The correlation appeared linear, corresponding to the general equation

$$y = ax + b \quad .$$

A best-fit line of the equation was computed by the least-squares method for the data from plots L-5 and L-6 for the period 3 March 1965 to 16 October 1965. For plot 5 the best-fit line was

$$y = 0.46x + 1.51 \quad ,$$

and for plot 6 the best-fit line was

$$y = 0.29x + 0.66 \quad .$$

This shows the top spray of flaked aluminum on plot 6 reduced the discoloration of runoff water by approximately 40 percent.

PART II. OPERATIONAL FIELD CATCHMENTS:

Nelson Road catchment. The treatment installed on the Nelson Road catchment of MC-250 basecoat and clay emulsion sealcoat during the summer of 1964 was in excellent condition when inspected on 7 December 1965. There was some very minor damage to the plot surface from deer, which was easily repaired with asphalt emulsion poured from a can on the hoof marks. The asphalt-fiberglas pit appeared to be in good shape, with approximately 40,000 liters of stored water. Rainfall had been low in the area during the summer. It is thought the pit may be slowly leaking. The lining will be carefully inspected and possibly resprayed with asphalt in the spring of 1966.

Blue Mountain catchment. The Blue Mountain catchment treatment of MC-250 basecoat and SS-2 emulsion sealcoat, installed during the summer of 1964, was in good condition when inspected in December 1965. The upper half, which has a top spray of flaked aluminum, was in excellent condition. On the lower half, with no aluminum top spray, a few yucca plants were growing, and there were several small places where the asphalt pavement was soft. The yucca plants were treated with concentrated soil sterilant and the soft pavement locations sealed with asphalt emulsion poured out of a can. Preliminary indications are that the aluminum spray is protecting the asphalt. The catchment has been in operational use and is considered to be performing with a high degree of success.

Metate catchment. The Metate catchment had been treated in June 1964 with an MC-250 basecoat and 1.5-mil black polyethylene bonded to the soil with SS-2 emulsion. Upon inspection in March 1965 the catchment was considered to be in fair shape. A few holes had been torn in the sheeting and several yucca plants were growing. Another inspection of the catchment on 13 July 1965 revealed an increased number of holes in the sheeting, even though the sheeting was bonded to the soil over most of the area. The plastic had been laid over scattered gravel on the catchment surface, and at each rock there was a small area of film not bonded. At these spots the sheeting was partially free to move, and abrasion on the rock underneath eventually wore holes in the film.

On 20 July 1965 the entire catchment was re-treated. All loose pieces of the old polyethylene were removed and the entire area was rolled with a self-propelled vibrating roller to push all gravel into the soil surface. The catchment was then sprayed with RSK asphalt emulsion and new 2-mil low-density black polyethylene installed. The new polyethylene is believed to have better tear and weathering resistance than the material previously used. The storage pit asphalt-fiberglas lining was still in good condition but did not appear completely watertight. To seal the lining a spray application of 80 parts MC-250 and 30 parts RSK emulsion was applied at a rate of 0.62 kg asphalt m^{-2}. The mixture was heated to 180F and applied in two applications one day apart.

Inspection on 2 November 1965 revealed the catchment to be in excellent condition. The pit lining appeared in good condition, but there were indications the pit was still leaking. Seepage cylinders were placed on the lining to determine if the lining was leaking through the seal or only at lap joints of the fiberglas, which were not completely sealed. These cylinder studies indicated the pit was probably leaking at lap joints which were not completely sealed. The lap joints will be sprayed with an asphaltic crack sealer in the spring of 1966.

Hopi No. 1. The treatment on this catchment of RC-Special basecoat and clay emulsion sealcoat, applied in September 1964, was considered in good condition when inspected in December 1965, even though the asphalt application rate for the basecoat had been too low. This catchment has survived only because a good sealcoat has protected the poor basecoat against water penetration and subsequent frost damage. To preserve the catchment, approximately one-third of the area will have to be re-treated in the spring. The rainfall in the area was low for the year, and the water in the storage tank was discolored from asphalt deterioration.

Flagstaff cinders catchment. The Flagstaff cinders catchment, stabilized with RSK emulsion and sealed with clay emulsion during the summer of 1964, was in excellent condition when inspected in December 1965. It now appears that the catchment should perform satisfactorily for several years with only minor maintenance.

Mescal catchment. This new catchment was installed on the Fort Apache Indian Reservation in eastern Arizona. The catchment is 30 × 30 m on a 10 percent slope diagonal to one corner. The water is taken from the plot by an 8-inch diameter corrugated steel pipe to a 40,000-gallon steel tank with a 22-mil vinyl plastic bottom liner. The catchment soil was sterilized after smoothing and allowed to weather for two months to obtain compaction by alternate wetting by rain and drying between rains. On 26 September 1965 the catchment was covered with an experimental 20-mil thick sheeting of modified polyethylene. This sheeting is easily field seamed with solvent and has high puncture and tear resistance when new. The catchment was inspected in December 1965 and was in good condition. There were a few small holes where yucca was growing through, but these were easily repaired. Rain had fallen on the catchment and the collected water was being used.

San Vicente catchment. The San Vicente catchment was installed on the Papago Indian Reservation in southern Arizona in June 1965. The catchment is 30 × 30 m on a 5 percent slope and was covered with 20-mil modified polyethylene. The storage for the catchment consisted of a pit excavated at the lower end of the catchment, which was lined and covered by seaming two 15 × 15 m sheets of the film at the edges to form a 50,000-gallon bag. Water flows from the catchment to the bag through a 12-inch rigid-plastic pipe. On 12 July 1965 the catchment was inspected and was in fair condition. There were two small holes in the catchment surface where ants had eaten through the sheeting. The ants were killed with chlordane applied under the sheeting and the holes repaired. Inspection of the bag revealed that it had been punctured by a small stick on the lower side.

In November 1965 a report was received that rodents had torn some holes in the sheeting which allowed wind to get under the sheeting and cause severe damage. At the same time, coyotes had ripped the bag in an attempt to get to the stored water. The bag was considered completely destroyed. The catchment and storage will be redesigned and rebuilt in early 1966.

A major part of the trouble with this structure was caused by a change in the plastic sheeting formulation which the manufacturer had made without our knowledge. The original material we tested had very high resistance to tearing and puncturing. The material furnished for the San Vicente catchment had subsequently been modified to reduce flammability. This modification drastically reduced puncture and tear resistance. New material for the catchment will eliminate the modification and the tearing problem. Nevertheless, the catchment and storage structures will be redesigned to reduce the possibility of animal and wind damage.

Bee catchment. Preliminary work was started on the development of small unitized catchments and storage to provide water for bees and firefighting. These catchments are designed to collect and store up to 1,500 gallons of water. They consist of a collection apron, approximately 6 × 6 m, with a storage bag or lined pit with evaporation-retardent cover. The design criterion is for low-cost and easy installation with a minimum of labor and equipment.

In November 1965 a small unit was installed south of Florence, Arizona, to provide water for a bee apiary. The rancher has been hauling water at the rate of 250 to 500 gallons per month a distance of 20 miles to provide adequate water for the bees during peak honey production. Primary interest is in the possibility of damage to the installation by rodents and small animals, which are abundant in the area. Also, the relative sizes of catchment and storage for most efficient and economical performance must be determined. Similar units will be installed in 1966 to provide water for fighting forest fires.

PART III. GRANITE REEF TESTING SITE

During the summer of 1965 electrical power was brought into the Granite Reef testing site. Within the plot area the wiring was run underground to 15 of the large test plots. Pumping sumps and submersible pumps were connected to the storage tanks at each of the plots. The water is pumped from the tanks through a precalibrated water meter at each plot. The sump pumps are set to start automatically when the water in the tanks reaches a depth of 60 cm. This permits the collection of data from storms when the runoff is in excess of the capacity of the storage tanks. Also, for storms where the runoff does not fill the tanks to the pump automatic-start level, a calibration check of the point gage volumetric reading versus water meter reading is obtained as the tanks are emptied.

The instrumentation of Granite Reef was enlarged with the installation of a second set of directional wind vane and anemometer connected to a high-speed multipoint recorder. Also, water-stage recorders were installed in the storage tanks on three large plots to measure the rate of precipitation runoff. The wind system, water-stage recorders, and a fast time-scale weighing raingage are automatically started at the start of a rain. The system normally operates from line electrical power, but automatically switches to a power supply derived from a 12-VDC battery and a power inverter in case of electrical outage.

The rainfall patterns within the test area are being studied through the use of a series of twenty-three 7.62-cm diameter raingages, two 8-inch diameter weighing gages, one 8-inch storage gage, and a vecto-pluviometer. The data from the raingages, coupled with observations during storms, indicate the rainfall is quite variable. Rainfall variation must be considered in evaluating differences in runoff measured from separated plots. Until additional data are obtained, all runoff values are being compared to a single standard raingage.

The total rainfall at Granite Reef for the year 1965 was almost double the average annual precipitation, with December 1965 being one of the wettest in the past 34 years. For the year a total of 47 separate storms was measured, with 17 storms occurring in December. A total of

166.4 mm was measured in December, compared to an average of 27.9 mm. Rainfall for the year was 395.5 mm, compared to an average of 221 mm. Following are the results of the runoff measured from the different plot.

Small 9.3-m^2 plots. For the fourth consecutive year the total runoff from the 30-mil butyl sheeting on plot 2 averaged over 100 percent of the raingage catch, while the untreated soil (plot 4) averaged 28 percent for the year. Plot 8 was treated 14 April 1965 with a 12-mil modified butyl sheeting bonded to the soil with SS-2 Special asphalt emulsion applied at a rate of 0.7 kg asphalt m^{-2}. This plot is primarily a weathering test, but it has averaged 97 percent runoff since installation. Plot 16, a weathering test also, treated in July 1964 with a basecoat of MC-250 at 2.5 kg asphalt m^{-2} and a sealcoat of clay emulsion at 1.0 kg asphalt m^{-2}, averaged 92 percent runoff. Both plot 8 and plot 16 are weathering satisfactorily to date. A water repellant designated R-9, applied to plot 18 in May 1963 at a rate of 0.113 kg m^{-2} on the upper half and 0.057 kg m^{-2} on the lower half, yielded 47 percent runoff.

Esso plots. The four-plot test unit constructed in cooperation with Esso Research Corporation of Linden, New Jersey, is performing satisfactorily. The plots, installed in December 1964 with a one-phase treatment of Eastern asphalt, are in good condition one year later. Plot E-1, treated with 1.95 kg asphalt m^{-2}, averaged 89 percent runoff; plot E-2, treated with 1.85 kg asphalt m^{-2}, averaged 89 percent runoff; plot E-3, which is smoothed—untreated soil, averaged 42 percent runoff; and plot E-4, treated with 2.2 kg asphalt m^{-2}, averaged 92 percent runoff.

Watersheds. The runoff from the three 450-m^2 watersheds is presented in Table 1. Watersheds 1 and 2 are completely untreated with respect to smoothing or brush removal. Watershed 3 has had the brush hand-removed with a minimum of soil disturbance. Runoff occurs from these areas only from storms of high total rainfall or high intensity, or if the soil is completely saturated from previous storms. A saturated soil condition existed for many of the storms when runoff occurred in

December. For the year, watersheds 1 and 2 yielded 23 and 22 percent runoff, respectively. Runoff from cleared watershed 3 was 28 percent.

Large 230-m^2 plots. Treatments applied to the 230-m^2 plots are listed in Table 2, and the runoff results are presented in Table 3. The bonded 1.5-mil black polyethylene, plot L-1, averaged 96 percent runoff for the year. The sheeting has wrinkled considerably, which has increased the retention and reduced the runoff. The wrinkling has been found to be caused by absorption of the asphalt adhesive and a swelling of the film.

Runoff from the smoothed—untreated plot L-2 averaged 33 percent, while plot L-3, treated with a low-cost water repellant designated R-9, has averaged 94 percent since installation on 4 August 1965. Although the water repellant does not stabilize the soil, the erosion on plot L-3 is only slightly higher than on plot L-2. For storms on 17 August, 2 September, 19 September, 16 October, and all the December storms, the quantity of soil eroded from the plots and deposited in the tanks was dried and weighed. For these storms the smoothed—untreated plot eroded 2.2 g soil per liter of runoff, compared to 3.0 g per liter for the water-repellent plot. Particle size analysis of the sediment is being conducted to evaluate possible differences in the size of soil particles being eroded.

Plot L-4, the butyl sheeting standard, has no observed deterioration and runoff averaged 100 percent. To determine if the asphalt bonding the butyl to the soil was damaging the butyl, strips of the sheeting were taken from both bonded and unbonded areas of the plot. The pieces, trimmed to 10.2-cm width, were placed in the testing machine, and the strength of the material was measured at a cross-head traverse speed of 5 cm min^{-2}. The gripping clamps of the testing machine were initially set 6 cm apart. Both samples were stretched 50 cm, from an initial length of 6 cm to a final length of 56 cm. The final loading was 14 kg for the unbonded butyl and 11 kg for the asphalt-bonded butyl. Both samples were extremely ductile. Although the asphalt may have slightly reduced the tensile strength of the butyl, the

ductility was certainly not adversely affected. The asphalt has not damaged the butyl sheeting after 4 years of exposure.

Plots L-5 and L-6 are treated with a two-phase asphalt treatment. The runoff from both plots averaged 98 percent for 1964, although for individual storms there was as much as 30 percent difference. The differences measured were attributed to the fact that the plots slope in different directions and therefore had different wind exposures during the storms. To determine the possibility of increasing runoff by slowing wind movement over the plot surface, a 1.2-m high snow fence was placed around the outside of the two plots. On plot L-5, which slopes north, the fence was placed on the north and west sides. On plot L-6, which slopes east, the fence was placed on the south and east sides. Vectopluviometer data, presented in Table 4, show that 48 percent of the rain fell while the wind was blowing from the north and west and 52 percent came from the south and east. Runoff from plot 5, with fence on the north and west, was 96 percent. Runoff from plot 6, with fence on the south and east, was 101 percent. Definite conclusions cannot be reached until an analysis of individual storm data is completed. It appears that during some storms the fence intercepted rainfall and reduced runoff. On a preliminary basis, however, the annual averages indicate that snow fence on the upwind side of the plots did increase total rainfall collection.

Plot L-7a, which was covered with 1-mil Tedlar, bonded to the soil with asphalt, failed in the spring of 1965. Shrinking of the material occurred which tore the sheeting. Wind then severely damaged a 2×15 m area and the remaining film was removed in March. Runoff from the plot before damage occurred averaged 104 percent.

A new cover of a modified 10-mil black polyethylene film was installed on plot L-7 in June 1965. This sheeting was bonded to the old basecoat with RSK emulsion, applied at a rate of 0.7 kg asphalt m^{-2}. Inspection on 28 July 1965 found that asphalt was migrating up through the sheeting, and the water collected from a rain on 28 July was discolored by asphalt deterioration byproducts. Another inspection in August found a number of small holes in the sheeting. The holes result

from deterioration of the film, which has been accelerated because the sheeting was installed under considerable tension. Runoff has averaged 96 percent since installation.

Ridge and furrow plots. Three years of records from the smoothed–untreated plot L-2 at GraniteReef show that over 30 percent of the rainfall has been collected. The plot is on a 5 percent slope, with no provisions for channeling the water into collection ditches. Runoff should be increased by increasing the slope, but the length of the sloped surface should be decreased to reduce erosion hazard. The best way to obtain large areas of short but steep slopes is through the construction of large ridges draining into furrows which convey the water to the storage reservoir. Accordingly, eight 6.1 × 30.4 m ridge and furrow plots were constructed at Granite Reef in March 1965 with a road grader. Longitudinal slope on all plots is 3 percent. Four plots run east and west, and four run north and south. Four plots have 10 percent side slopes, and four have 20 percent side slopes. Orientation and slopes are summarized in Table 5. Each furrow drains into a separate calibrated steel tank, where water volume is measured with a micrometer point gage.

The runoff measured since tank installation in April 1965 is presented in Table 6. For the period 12 May through 19 September the ridge and furrow plots averaged 24 percent runoff and the smoothed–untreated plot L-2 averaged 29 percent of 51.0 mm precipitation. Soil on the ridge and furrow plots was unconsolidated for a period following construction and this reduced runoff. For the entire period since installation the ridge and furrow plots averaged 118.2 mm runoff while plot L-2 yielded 103.8 mm. There were no consistent differences in runoff between the 20-percent slope and the 10-percent slope plots. Measurements of plot erosion were made for the storms of 19 September, 16 October, and for all the December storms combined. The plots with 10 percent slope averaged 7.9 g sediment per liter runoff, while the 20 percent slopes averaged 9.7 g sediment per liter runoff. This is compared to plot L-2 which has 5 percent slope and eroded 1.5 g per liter runoff.

SUMMARY AND CONCLUSIONS:

Water collected from exposed asphalt-treated asurfaces is often discolored by asphalt deterioration byproducts. This is an additional incentive for reducing the rate of asphalt oxidation, which is the primary cause of the discoloration. A spectrophotometric analysis of the discolored water indicated the degree of discoloration was a factor of dilution only, permitting colormetric evaluation of the quantity of coloring material in the water. Runoff water from two asphalt-treated plots at Granite Reef was thus evaluated to determine the relative effectiveness of materials intended to reduce asphalt deterioration. One plot had a sealcoat of standard asphalt-clay roofing emulsion and the other had a top spray of flaked aluminum. The runoff water analyses from both plots showed that the flaked aluminum top spray reduced the water discoloration by approximately 40 percent, compared to the asphalt-clay emulsion.

With one exception the experimental operational catchments have performed satisfactorily. The 1.5-mil black polyethylene treatment on the Metate catchment developed numerous small holes during the winter of 1964-65 because of gravel on the catchment surface and was subsequently re-treated. The plot was rolled to obtain a smooth surface, and stronger 2-mil polyethylene was installed on the catchment during the summer of 1965. Seepage cylinder measurements on the asphalt-fiberglas pit at Metate indicate water is being lost through unsealed lap joints in the lining.

The two-phase asphalt treatments on the Nelson Road, Blue Mountain, and Flagstaff cinders are in excellent condition and are now expected to last many years if a reasonable maintenance program is followed. The Hopi No. 1 asphalt catchment needs re-treatment of one-third of the area, but this was expected, as insufficient asphalt had been applied in the basecoat treatment. The Tedlar covering on the Cedar Mesa catchment suffered severe damage both from cattle walking on the plot and from shrinking of the sheeting. The shrinking damage eventually forced the removal of the entire catchment. The area will be re-treated with another material in the spring of 1966.

Two new catchments of an experimental 20-mil modified polyethylene were installed in cooperation with the Bureau of Indian Affairs. One catchment on the Papago Indian Reservation was severely damaged by ants and rodents, and a 50,000-gallon bag of the sheeting was destroyed by coyotes. The second catchment on the Fort Apache Indian Reservation has suffered only a few small holes from yucca growth, and these were easily repaired.

Small, easily installed unitized catchments and storages were designed to provide water for bees and firefighting. Current work is aimed at the evaluation of potential damage to the installations by small animals and at determining the most efficient relative size of catchment and storage.

Electric pumps and water meters were installed on the collection tanks for 15 plots at Granite Reef. The pumps start automatically when the water reaches a depth of 60 cm. This permits the collection of data from storms when runoff is in excess of the tank capacity. When runoff is insufficient to start the pumps, a check of the point gage volumetric reading versus water meter readings is obtained as the tanks are emptied.

Instrumentation at Granite Reef was expanded with the installation of: (1) two sets of wind-direction vanes and anemometers connected to a high-speed multipoint recorder; (2) twenty-three 7.62-cm diameter raingages; (3) a fast chart-speed weighing raingage; and (4) water-stage recorders on the storage tanks for three catchments. All recording instruments start automatically at the beginning of each rainstorm. Rainfall at Granite Reef was almost double the 34-year average, with 395.5 mm precipitation measured in 47 separate storms.

Runoff from the small 9.3-m^2 plots for 1965 was: butyl sheeting — 100 percent; untreated soil — 28 percent; and water-repellent soil — 47 percent.

Two 450-m^2 uncleared watersheds at Granite Reef averaged 22 percent runoff, and a third one, where the brush was removed, averaged 28 percent. This is compared to a smoothed—untreated plot which averaged 33 percent. A second smoothed plot, treated with a low-cost water

repellant, has averaged 94 percent runoff since installation in August 1965. Erosion from the water-repellent plot has not significantly exceeded that from a similar untreated—smoothed soil plot.

Runoff from three 230-m^2 Granite Reef plots covered with plastic or rubber sheeting has averaged essentially 100 percent of the rainfall. The two 230-m^2 Granite Reef plots treated with a two-phase sprayed asphalt pavement have shown no decrease in runoff effectiveness, averaging over 98 percent.

Preliminary investigation of slope versus runoff and erosion was initiated by constructing eight ridge and furrow plots of 185 m^2. The plots, which are 6.1 m wide and 30.4 m long, consist of ridges with side slopes of 10 and 20 percent draining into furrows with 3 percent longitudinal slope. There were no consistent differences in runoff between 10- and 20-percent side slopes. Runoff averaged from 41 to 48 percent, as compared to 33 percent for the 230-m^2 smoothed soil plot which has 5 percent slope. Average erosion per liter of runoff for 19 comparable storms was: 5 percent — 1.5 g; 10 percent — 7.9 g; and 20 percent — 9.7 g.

Snow fence, 1.2 m in height, was installed adjacent to different sides of two 230-m^2 asphalt-paved plots at Granite Reef to determine the effect on rainfall collection. Runoff data are being compared to wind and rain direction data obtained with the vectopluviometer. Preliminary comparisons show that for some storms the fence intercepted rain and decreased runoff. It appears, however, that average runoff for the year was increased by fence on the upwind side of the plot.

PERSONNEL: L. E. Myers, G W. Frasier

Table 1. Runoff from 450-m^2 watersheds at Granite Reef testing site

Date	Rainfall total	W-1 runoff		W-2 runoff		W-3 runoff	
1965	(mm)	(mm)	(%)	(mm)	(%)	(mm)	(%)
5–6–7 Jan	28.2	1/ 6.1	21.6	1/ 4.2	14.9	1/ 7.0	24.8
20 Jan	2.5	0	0	0	0	0	0
6 Feb	15.7	0	0	0	0	0	0
6 Feb	11.7	0	0	0	0	0	0
7 Feb	3.8	0	0	0	0	0	0
9 Feb	1.1	0	0	0	0	0	0
10–11 Mar	18.0	0	0	0	0	0	0
11 Mar	1.5	0	0	0	0	0	0
12 Mar	0.9	0	0	0	0	0	0
15–16 Mar	3.3	0	0	0	0	0	0
1 Apr	5.0	0	0	0	0	0	0
3–4 Apr	25.6	6.4	25.0	5.4	21.1	7.7	30.0
4 Apr	0.9	0.2	22.2	0.2	22.2	0.3	33.3
9–10 Apr	9.2	1.5	16.3	1.3	14.1	1.7	18.5
10 Apr	1.5	0	0	0	0	0	0
12 Apr	2.2	0	0	0	0	0	0
12 May	5.0	0	0	0	0	0	0
23 Jun	2.3	0	0	0	0	0	0
16 Jul	1.0	0	0	0	0	0	0
18 Jul	4.3	0.5	11.6	0.3	7.0	1.1	25.6
28 Jul	10.2	2.1	20.6	2.0	19.6	3.3	32.4
11 Aug	12.2	5.0	41.0	3.5	28.7	6.1	50.0
17 Aug	6.3	1.1	17.5	0	0	0.3	4.8
30 Aug	1.0	0	0	0	0	0	0
2 Sep	1.5	0	0	0	0	0	0
19 Sep	7.2	0	0	0	0	0	0
16 Oct	6.2	0	0	0	0	0	0
22–23 Nov	25.3	0.7	3.0	0	0	1.3	5.1
25 Nov	15.5	5.5	35.5	3.3	21.3	4.6	29.7

See footnotes at end of table.

Table 1. Runoff from 450-m^2 watersheds at Granite Reef testing site—Continued

Date	Rainfall total	W-1 runoff		W-2 runoff		W-3 runoff	
1965	(mm)	(mm)	(%)	(mm)	(%)	(mm)	(%)
8 Dec	1.3	0	0	0	0	0	0
9 Dec	3.5	0.8	22.9	1.3	37.1	1.9	54.3
9 Dec	7.9	2.9	36.7	1.4	17.7	2.1	26.6
9–10 Dec	19.4	7.1	36.6	5.6	28.9	9.7	50.0
10 Dec	11.1	5.2	46.8	6.0	54.1	3/ 6.7	60.0
10 Dec	23.1	2/ 11.6	50.0	2/ 11.6	50.0	3/ 13.9	60.0
13 Dec	11.7	8.5	72.6	6.1	52.1	8.5	72.6
14 Dec	7.1	1.3	18.3	1.5	21.1	3.0	42.3
14–15 Dec	14.0	5.5	39.3	3.9	27.9	6.3	45.0
15 Dec	1.5	0.3	20.0	0.3	20.0	0.5	33.3
16 Dec	3.5	0.4	11.4	0.3	8.6	0.7	20.0
17 Dec	0.5	0	0	0	0	0	0
22 Dec	25.7	4/ 7.7	30.0	12.3	47.9	5/ 10.3	40.0
22 Dec	22.9	4/ 6.9	30.0	13.2	57.6	5/ 9.2	40.0
22 Dec	6.5	0.6	9.2	0.7	10.8	1.4	21.5
23 Dec	3.2	1.9	59.4	1.5	46.9	2.5	78.1
29 Dec	3.5	0	0	0	0	0	0
Total	395.5	89.8	22.7	85.9	21.7	110.1	27.8

1/ Storage pit leaking – runoff estimated by comparison with untreated 9.3-m^2 plot from storms to 25 November 1965.

2/ Storage overflowed – runoff estimated at 50 percent.

3/ Runoff into storage from outside plot – runoff estimated at 60 percent.

4/ Runoff into storage from outside plot – runoff estimated at 30 percent.

5/ Runoff into storage from outside plot – runoff estimated at 40 percent.

Table 2. Treatments on 230-m^2 plots at Granite Reef testing site

Plot	Treatment date	Treatment
L-1	10 Oct 1963	Basecoat. RC-Special at 2.0 kg asphalt m^{-2}
	1 Feb 1965	Top sheeting. Black polyethylene, 1.5-mil, bonded with mixture of MC-270 and MC-250 at 1.2 kg asphalt m^{-2}
L-2	30 Nov 1961	Smoothed—untreated
L-3	4 Aug 1965	R-9 at 0.057 kg m^{-2}
L-4	30 Nov 1961	Butyl rubber sheeting, 30-mil
L-5	18 Sep 1962	Basecoat. S-1 at 1.04 kg asphalt m^{-2}
	25 Jan 1965	Topcoat. Clay emulsion at 0.5 kg asphalt m^{-2}
L-6	19 Apr 1963	Basecoat. RC-Special at 1.5 kg asphalt m^{-2}
	8 May 1963	Topcoat, south half. SS-2 Special at 0.65 kg asphalt m^{-2}, with 3% butyl latex
	9 Jul 1963	Topcoat, north half. S-1 at 0.5 kg asphalt m^{-2}, with 3% butyl latex
	22 Jan 1965	Top spray. Flaked aluminum at 0.08 kg solution m^{-2}
L-7A	12 Feb 1964	Basecoat. RC-Special at 2.0 kg asphalt m^{-2}
	19 Feb 1964	Top sheeting. Tedlar PVF film, 1-mil, bonded with SS-2B at 0.5 kg asphalt m^{-2}
L-7B	12 Feb 1965	Basecoat. RC-Special at 2.0 kg asphalt m^{-2}
	8 Jun 1965	Top sheeting. Modified polyethylene film, 10-mil, bonded with S-1 at 0.7 kg asphalt m^{-2}

able 3. Runoff results from rainfall on 230-m^2 plots at Granite Reef testing site

ate	Rainfall total	L-1 runoff		L-2 runoff		L-3 runoff		L-4 runoff		L-5 runoff		L-6 runoff		L-7a runoff		L-7b runoff	
965	(mm)	(mm)	(%)	(mm)	(%)	(mm)	(%)	(mm)	(%)	(mm)	(%)	(mm)	(%)	(mm)	(%)	(mm)	(%)
-6 Jan	25.2			6.8	27.0			26.2	104.0	25.3	100.4	25.6	101.6	26.3	104.4		
Jan	3.0			0.7	23.0			3.3	110.0	3.3	110.0	3.0	100.0	3.3	110.0		
) Jan	2.5			0	0			2.9	116.0	3.0	120.0	2.9	116.0	2.7	108.0		
Feb	15.7	13.0	82.8	1.7	10.8			15.7	100.0	15.3	97.5	15.9	101.3	15.5	98.7		
Feb	11.7	11.9	101.7	2.9	24.8			1/ 11.7	100.0	11.4	97.4	1/ 11.7	100.0	1/ 11.7	100.0		
Feb	3.8	5.2	136.8	2.3	60.5			3.9	102.6	5.4	142.1	4.6	121.1	4.8	126.3		
Feb	1.1	1.6	145.5	0	0			1.6	145.5	1.6	145.5	1.1	100.0	1.2	109.1		
)-11 Mar	18.0	18.2	101.1	0.7	3.9			18.3	101.7	17.6	97.8	18.5	102.8	17.8	98.9		
l Mar	1.5	2.3	153.0	0	0			2.5	166.7	2.5	166.7	2.5	166.7	2.9	193.3		
2 Mar	0.9	1.1	122.2	0	0			1.2	109.1	1.1	122.2	1.0	111.1	1.0	111.1		
5-16 Mar	3.3	3.1	93.9	0	0			3.2	97.0	3.3	100.0	3.3	100.0	3.0	90.9		
Apr	5.0	4.4	88.0	0.2	4.0			4.8	96.0	4.8	96.0	5.0	100.0				
-4 Apr	25.6	1/ 25.6	100.0	8.6	33.6			2/ 24.9	97.3	25.6	100.0	1/ 25.6	100.0				
Apr	0.9	0.9	100.0	0	0			1.3	144.4	0.9	100.0	0.8	88.9				
-10 Apr	9.2	9.6	104.3	2.8	30.4			9.9	107.6	9.4	102.2	9.3	101.1				
) Apr	1.5	1.7	113.3	0.4	26.7			1.5	100.0	1.4	93.3	1.0	66.7				
! Apr	2.2	2.0	90.9	0	0			2.3	104.5	2.2	100.0	2.3	104.5				
! May	5.0	5.0	100.0	0	0			5.0	100.0	5.2	104.0	5.2	104.0				
Jun	2.3	1.8	78.3	0	0			2.1	91.3	1.8	78.3	1.8	78.3			1.5	65.2

e footnotes at end of table.

ıble 3. Runoff results from rainfall on 230-m^2 plots at Granite Reef testing site—Continued

ıte	Rainfall total	L-1 runoff		L-2 runoff		L-3 runoff		L-4 runoff		L-5 runoff		L-6 runoff		L-7a runoff		L-7b runoff	
)65	(mm)	(mm)	(%)	(mm)	(%)	(mm)	(%)	(mm)	(%)	(mm)	(%)	(mm)	(%)	(mm)	(%)	(mm)	(%)
5 Jul	1.0	1.9	190.0	0	0			1.4	140.0	0.7	70.0	0.7	70.0			0.7	70.0
3 Jul	4.3	5.0	116.3	2.1	48.8			5.2	121.4	4.7	109.3	5.1	118.6			4.8	111.6
3 Jul	10.2	9.7	95.1	3.5	34.3			9.9	97.1	8.9	87.3	9.0	88.2			9.6	94.1
. Aug	12.2	11.5	94.3	7.4	60.7	11.3	92.6	12.0	98.4	10.8	88.5	10.7	87.7			10.3	84.4
' Aug	6.3	6.0	95.2	0.2	3.2	5.8	92.1	5.9	93.7	5.9	93.7	5.8	92.1			5.8	92.1
) Aug	1.0	1.0	100.0	0	0	0.6	60.0	1.1	110.0	0.8	80.0	0.7	70.0			1.0	100.0
Sep	1.5	1.5	100.0	0	0	1.3	86.7	1.6	106.7	1.5	100.0	1.2	80.0			1.6	106.7
) Sep	7.2	7.9	109.7	1.7	23.6	7.9	109.7	8.3	115.3	7.1	98.6	7.2	100.0			9.1	126.4
Oct	6.2	5.9	95.2	0.6	9.7	5.3	85.5	6.0	96.8	6.1	98.4	5.6	90.3			4.6	74.2
—23 Nov	25.3	21.0	83.0	0	0	3/ 23.9	94.4	23.6	93.3	1/ 25.3	100.0	24.4	98.4			3/ 23.6	93.4
Nov	15.5	14.7	94.8	4.8	31.0	14.9	96.1	15.1	98.7	14.4	92.9	15.0	96.8			14.2	91.6
Dec	1.3	1.2	92.3	0	0	0.6	46.2	1.4	107.7	1.2	92.3	0.9	69.2			0.9	69.2
Dec	3.5	3.7	105.7	2.4	68.6	3.7	105.7	3.4	97.1	3.5	100.0	3.8	108.6			3.5	100.0
Dec	7.9	7.8	98.7	4.8	60.8	7.8	98.7	7.3	92.4	7.6	96.2	7.8	98.7			8.6	108.9
10 Dec	19.4	18.3	94.3	6.0	32.8	4/ 19.0	98.0	20.0	103.1	15.4	79.4	16.7	86.1			19.7	101.5
Dec	11.1	8.1	73.0	4.7	42.3	8.8	79.3	9.6	86.5	9.3	83.8	12.4	111.7			6.9	62.2
Dec	23.1	23.0	99.6	18.0	77.9	20.0	86.6	23.7	102.6	22.9	99.1	26.6	115.2			25.7	111.3
Dec	11.7	10.7	91.5	7.4	63.2	10.2	87.2	11.0	94.0	10.9	93.2	11.4	97.4			11.2	95.7
Dec	7.1	7.1	100.0	1.9	26.8	6.7	94.4	6.8	95.8	7.2	101.4	7.0	98.6			6.8	95.8

e footnotes at end of table.

able 3. Runoff results from rainfall on 230-m^2 plots at Granite Reef testing site—Continued

ate	Rainfall total	L-1 runoff		L-2 runoff		L-3 runoff		L-4 runoff		L-5 runoff		L-6 runoff		L-7a runoff		L-7b runoff	
965	(mm)	(mm)	(%)	(mm)	(%)	(mm)	(%)	(mm)	(%)	(mm)	(%)	(mm)	(%)	(mm)	(%)	(mm)	(%)
4–15 Dec	14.0	13.6	97.1	5.2	37.1	13.4	95.7	13.8	98.6	13.8	98.6	13.7	97.9			13.7	97.9
5 Dec	1.5	1.5	100.0	0	0	1.5	100.0	1.5	100.0	1.4	93.3	1.6	106.7			1.4	93.3
6 Dec	3.5	3.7	105.7	0.3	8.6	3.4	97.1	3.5	100.0	3.8	108.6	3.6	102.9			3.5	100.0
7 Dec	0.5	0.5	100.0	0	0	0.4	80.0	0.6	120.0	0.6	120.0	0.6	120.0			0.7	140.0
2 Dec	25.7	24.0	93.4	15.3	59.5	26.4	102.7	24.8	96.5	20.8	80.9	27.2	105.8			24.9	96.9
2 Dec	22.9	21.0	91.7	15.0	65.5	23.0	100.4	21.8	95.2	21.1	92.1	24.4	106.6			21.9	95.6
2 Dec	6.5	6.2	95.3	1.4	21.6	5.6	86.2	6.0	92.3	5.9	90.8	6.1	93.8			6.2	95.4
3 Dec	3.2	3.1	96.9	1.1	34.4	3.2	100.0	3.2	100.0	3.3	103.1	3.5	109.4			3.3	163.1
9 Dec	3.5	4.1	117.1	0	0	3.1	88.6	4.0	114.3	4.1	117.1	3.9	111.4			3.9	111.4
otal	395.5	351.1	96.2	130.9	33.1	227.8	94.3	394.8	99.8	38.1	96.1	397.7	100.6	90.2	104.0	249.6	96.2

/ Tank overflowed. Runoff estimated at 100 percent.

/ Possible tank overflow.

/ Tank overflowed. Runoff estimated from storms to 25 November 1965.

/ Meter stopped. Runoff estimated at 98 percent from previous storm.

Table 4. Directional rainfall measurements by vector pluviometer at the Granite Reef testing site

Date	Total rainfall collected	Collection by orfice facing direction listed							
		North		East		South		West	
1965	(ml)	(ml)	(%)	(ml)	(%)	(ml)	(%)	(ml)	(%)
5–6 Jan	458	120	26.2	234	51.0	52	11.4	52	11.4
7 Jan	93	9	9.6	21	22.6	10	10.8	53	57.0
20 Jan	34	5	14.7	22	64.7	4	11.8	3	8.8
6 Feb	456	115	25.2	130	28.5	47	10.3	164	36.0
7 Feb	35	12	34.3	7	20.0	3	8.6	13	37.1
9 Feb	14	0	0	0	0	0	0	14	100.0
10–11 Mar	285	54	18.9	160	56.1	50	17.6	21	7.4
11 Mar	11	1	9.1	5	45.4	1	9.1	4	36.4
12 Mar	5	0	0	0	0	2	40.0	3	60.0
15–16 Mar	27	1	3.7	2	7.4	11	40.7	13	48.2
1 Apr	61	4	6.6	3	5.0	17	27.9	37	60.5
3–4 Apr	506	83	16.4	143	28.3	75	14.8	205	40.5
4 Apr	14	2	14.3	5	35.7	6	42.9	1	7.1
9–10 Apr	227	44	19.4	10	4.4	14	6.2	159	70.0
12 Apr	37	2	5.4	0	0	6	16.2	29	78.4
12 May	86	16	18.6	60	69.8	4	4.7	6	6.9
23 Jun	4	2	50.0	0	0	0	0	2	50.0
16 Jul	13	4	30.8	9	69.2	0	0	0	0
18 Jul	23	23	100.0	0	0	0	0	0	0
28 Jul	199	27	13.6	79	39.7	65	32.7	28	14.0
11 Aug	346	57	16.5	18	5.2	192	55.5	79	22.8
17 Aug	131	21	16.0	69	52.7	20	15.3	21	16.0
30 Aug	0	0	0	0	0	0	0	0	0
2 Sep	3	0	0	3	100.0	0	0	0	0
19 Sep	291	159	54.6	86	29.6	0	0	46	15.8

Continued

Table 4 . Directional rainfall measurements by vector pluviometer at the Granite Reef Testing site—Continued

Date	Total rainfall collected	Collection by orfice facing direction listed							
		North		East		South		West	
1965	(ml)	(ml)	(%)	(ml)	(%)	(ml)	(%)	(ml)	(%)
16 Oct	58	9	15.5	35	60.3	0	0	14	24.2
22–23 Nov	529	83	15.7	285	53.8	38	7.3	123	23.2
25 Nov	275	38	13.8	57	20.7	67	24.4	113	41.1
8–9 Dec	47	7	14.9	34	72.3	0	0	6	12.8
9 Dec	80	17	21.3	32	40.0	6	7.5	25	31.2
9–10 Dec	600	78	13.0	163	27.2	170	28.3	189	31.5
10 Dec	131	33	25.2	35	26.7	31	23.7	32	24.4
10 Dec	385	130	33.8	116	30.1	66	17.1	73	19.0
13 Dec	202	65	32.2	39	19.3	17	8.4	81	40.1
14 Dec	88	10	11.4	47	53.4	21	23.8	10	11.4
14–15 Dec	359	54	15.1	161	44.8	89	24.8	55	15.3
15 Dec	41	1	2.4	4	9.8	23	56.1	13	31.7
16 Dec	75	5	6.6	56	74.7	8	10.7	6	8.0
17 Dec	17	0	0	17	100.0	0	0	0	0
22 Dec	510	122	23.9	240	47.1	29	5.7	119	23.3
22 Dec	585	123	21.0	90	15.3	135	23.0	237	40.7
22 Dec	241	26	10.8	101	41.9	70	29.0	44	18.3
23 Dec	17	0	0	0	0	0	0	17	100.0
29 Dec	74	3	4.1	44	59.4	17	23.0	10	13.5
Total	7673	1565	20.4	2622	34.2	1366	17.8	2120	27.6

Table 5. Orientation and slope of ridge and furrow treatments and the Granite Reef testing site, installed March 1965

Plot	Longitudinal direction	Side slope
R-1	North-south	20 percent
R-2	North-south	10 percent
R-3	North-south	20 percent
R-4	North-south	10 percent
R-5	East-west	10 percent
R-6	East-west	20 percent
R-7	East-west	10 percent
R-8	East-west	20 percent

Table 6. Runoff results from rainfall on large ridge and furrow plots at Granite Reef testing site

Date	Rainfall total	R-1 Runoff		R-2 Runoff		R-3 Runoff		R-4 Runoff		R-5 Runoff		R-6 Runoff		R-7 Runoff		R-8 Runoff	
1965	(mm)	(mm)	(%)	(mm)	(%)	(mm)	(%)	(mm)	(%)	(mm)	(%)	(mm)	(%)	(mm)	(%)	(mm)	(%)
12 May	5.0	0	0	0	0	0	0	0	0	0	0	0	0	0	0	0	0
23 Jun	2.3	0	0	0	0	0	0	0	0	0	0	0	0	0	0	0	0
16 Jul	1.0	0	0	0	0	0	0	0	0	0	0	0	0	0	0	0	0
18 Jul	4.3	2.4	55.8	2.3	53.5	2.2	51.2	2.6	60.5	2.5	58.1	2.4	55.8	2.6	60.5	2.3	53.5
28 Jul	10.2	2.9	28.4	3.1	30.4	3.1	30.4	3.1	30.4	3.2	31.4	3.1	30.4	3.6	35.3	3.1	30.4
11 Aug	12.2	5.1 1/	41.8	5.4	44.3	5.1	41.8	5.2	42.6	6.0	49.2	5.6	45.9	6.6	54.1	5.6 3/	45.9
17 Aug	6.3	0.3	4.8	0.1	1.6	0.1	1.6	0	0	0.2	3.2	0.2	3.2	0.1	1.6	0.2 3/	3.2
30 Aug	1.0	0	0	0	0	0	0	0	0	0	0	0	0	0	0	0	0
2 Sep	1.5	0	0	0	0	0	0	0	0	0	0	0	0	0	0	0	0
19 Sep	7.2	1.1	15.3	1.4	19.4	1.1	15.3	1.2	16.7	1.3	18.1	1.3	18.1	1.5	20.8	0.6	8.3
16 Oct	6.2	1.3	21.0	1.6	25.8	1.6	25.8	1.9	30.6	1.6	25.8	1.6	25.8	1.6	25.8	0.7	11.3
22-23 Nov	25.3	1.5 2/	5.9	2.4	9.5	1.5	5.9	2.4	9.5	2.3	9.1	2.2	8.7	2.6	10.1	1.4	5.5
25 Nov	15.5	7.1 2/	48.5	7.6	49.0	7.1	48.5	6.8	43.9	7.8	50.3	7.3	47.1	8.1	52.3	7.6	49.0
8 Dec	1.3	0	0	0	0	0	0	0	0	0	0	0	0	0	0	0	0
9 Dec	3.5	3.1	88.6	2.3	65.7	2.5	71.4	2.8	80.0	2.6	74.3	2.6	74.3	2.9	82.9	2.5	71.4
9 Dec	7.9	5.0	63.3	4.9	62.0	4.6	58.2	4.9	62.0	5.0	63.3	4.6	58.2	4.7	59.5	4.8	60.8
9-10 Dec	30.5	17.9	58.7	11.0	36.1	18.5	60.7	20.8	68.2	14.9	48.9	15.0	49.2	11.2	36.7	21.3	69.8
10 Dec	23.1	14.9	64.5	13.7	59.3	11.9	51.5	20.8	90.0	18.9	81.8	23.1	100.0	18.9	81.8	17.6	76.2
13 Dec	11.7	8.3	70.9	6.7	57.3	7.9	67.5	8.2	70.1	8.0	68.4	7.9	67.5	8.5 4/	72.6	8.7	74.4

1/ Runoff into tank from outside plot, runoff estimated from plot R-3.
2/ Tank leaking, runoff estimated from plot R-3.
3/ Tank leaking, runoff estimated from plot R-6.
4/ Error in reading, runoff estimated from plot R-5.

Table 6. Runoff results from rainfall on large ridge and furrow plots at Granite Reef testing site—Continued

Date	Rainfall total	R-1 Runoff		R-2 Runoff		R-3 Runoff		R-4 Runoff		R-5 Runoff		R-6 Runoff		R-7 Runoff		R-8 Runoff	
1965	(mm)	(mm)	(%)	(mm)	(%)	(mm)	(%)	(mm)	(%)	(mm)	(%)	(mm)	(%)	(mm)	(%)	(mm)	(%)
14 Dec	7.1	2.0	28.2	1.8	25.4	2.0	28.2	1.8	25.4	1.4	19.7	1.6	22.5	2.4	33.8	2.3	32.4
14-15 Dec	14.0	5.6	40.0	5.6	40.0	5.2	37.1	5.1	36.4	4.8	34.3	6.0	42.9	6.6	47.1	5.9	42.1
15 Dec	1.4	0	0	0	0	0	0	0	0	0	0	0	0	0	0	0	0
16 Dec	3.5	0.4	11.4	0.3	8.6	0.2	5.7	0	0	0.2	5.7	0.3	8.6	0.3	8.6	0.3	8.6
17 Dec	0.5	0	0	0	0	0	0	0	0	0	0	0	0	0	0	0	0
22 Dec	25.7	17.9	69.6	16.9	65.8	13.9	54.1	17.4	67.7	17.2	66.9	16.8	65.4	17.9	69.6	18.0	70.0
22 Dec	22.9	15.9	69.4	16.6	72.5	16.0	70.0	11.7	51.1	16.7	72.9	15.4	67.2	17.6	76.9	19.1	83.4
22 Dec	6.5	2.1	32.2	2.1	32.3	1.5	23.1	1.5	23.1	1.5	23.1	1.9	29.2	2.2	33.8	2.0	30.8
23 Dec	3.2	3.3	103.1	1.6	50.0	2.6	81.3	3.2	100.0	2.5	78.1	2.9	90.6	2.9	90.6	2.6	81.3
29 Dec	3.5	0	0	0	0	0	0	0	0	0	0	0	0	0	0	0	0
TOTAL	264.3	118.1	44.7	107.4	40.6	108.6	41.1	121.4	45.9	118.6	44.9	121.8	46.1	122.8	46.5	126.6	47.9

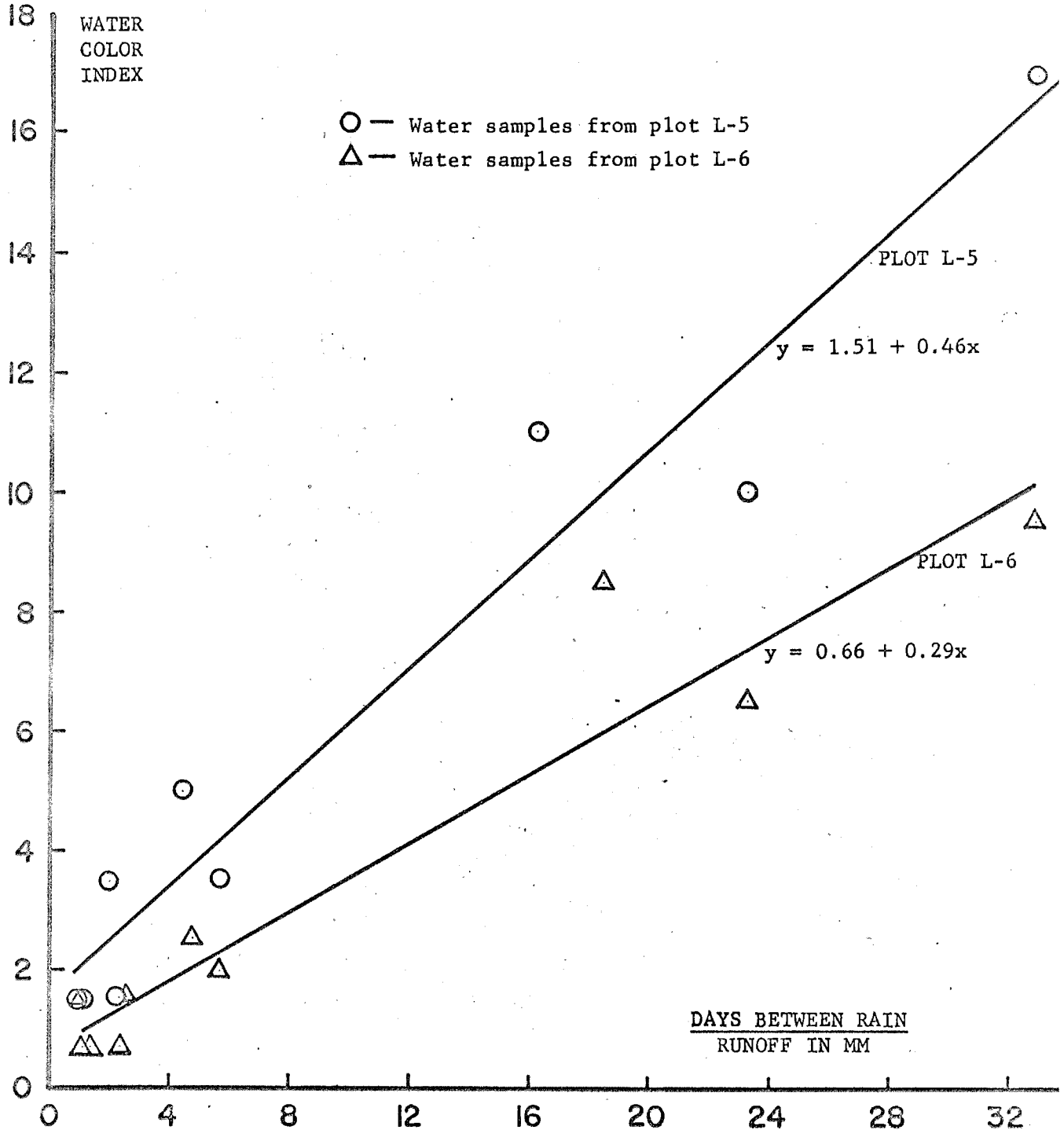

Figure 1. Discoloration of water from asphalt catchments in relation to quantity of runoff and days between rainstorms.

TITLE: APPLICATION OF HEXADECANOL-OCTADECANOL MONOFILMS TO SMALL PONDS

LINE PROJECT: SWC 4-gG2 CODE NO.: Ariz.-WCL-9

INTRODUCTION:

Further studies were conducted to evaluate the long-term effect of floating white granular materials which reduce evaporation by reflecting solar radiation and reducing the water temperature. Also, preliminary studies were conducted to evaluate different designs and sheeting for use as floating covers.

PROCEDURES:

Procedures were the same as outlined in the 1964 Annual Report, with the following additions:

Incoming shortwave radiation incident to and reflected by covered and uncovered water surfaces in 274-cm diameter tanks was measured with Kipp solarimeters. Net radiation measurements were also made with Fritschen miniature net radiometers. The data were recorded at half-hour intervals on a Datex digital recording system. Temperature profiles were measured during the same 24-hour periods with thermocouples at 1, 2, 7, 15, and 80 cm below the water surface, and recorded at 1-hour intervals with a multipoint strip-chart recorder. Radiation and water-temperature measurements were made simultaneously on treated and untreated tanks.

RESULTS AND DISCUSSION:

Floating Granular Materials.

In October 1964 a study was started to determine the effect of weathering of floating granular materials on evaporation reduction. Four kilograms each of 10-mm diameter chopped styrofoam and 1-mm diameter foamed plastic beads were applied to the 274-cm diameter tanks. During the period 30 October through 13 November 1964, when the untreated evaporation was 47 mm, the beads reduced evaporation by 42 percent and the chopped styrofoam reduced evaporation by 60 percent. Evaporation measurements for the next 5 months

showed a gradual reduction in effectiveness by both materials. For the period of 19 April through 23 April when untreated evaporation was 18.8 mm, the beads reduced evaporation by 29 percent and the chopped styrofoam by 12 percent.

On 20 April 1965 the incoming and reflected shortwave radiation was measured over the styrofoam. Incoming radiation was 439 langleys day^{-1} and reflected radiation from this styrofoam was 139 langleys or 31.7 percent, while from the untreated water surface 20 langleys or 4.6 percent was reflected. The following day with an incoming radiation of 506 langleys, the beads reflected 248 langleys or 49.0 percent, and the untreated water reflected 23 langleys or 4.6 percent.

In September 1965 radiation measurements over new covers of styrofoam and beads were made. On 9 September with an incoming radiation of 550 langleys day^{-1}, the beads reflected 235 langleys or 42.7 percent and the untreated water, 28 langleys or 5.1 percent. On 10 September, when the incoming radiation was 510 langleys, the new styrofoam reflected 275 langleys or 53.9 percent and the untreated water reflected 28 langleys or 5.5 percent. For the same periods net radiation was measured over each of the tanks. These measurements, which include longwave radiation in addition to shortwave radiation, are presently being analyzed. Evaporation measurements for the period 10 September through 15 September when the untreated tank lost 23.9 mm showed the styrofoam reduced evaporation 46 percent and the beads, 34 percent.

Further studies of low-cost materials included expanded perlite ore particles, about 0.5 mm average diameter, treated with a silicone water repellent. This material, customarily used as loose-fill insulation, has a very low density and would be less likely to sink when subjected to rain. Two types of perlite were studied. These are designated by S-Perlite which has a single treatment of water repellent and R-Perlite which has a double

water repellent treatment. For the period of 29 September - 14 October, with an untreated evaporation of 63 mm, the R-Perlite reduced evaporation 53 percent and the S-Perlite, 46 percent. For the period 18 October - 5 November, after light rain on 16 October, the untreated evaporation was 60 mm, the R-Perlite reduced evaporation 23 percent, and the S-Perlite, 27 percent.

Further analysis of radiation and water-temperature measurements are being made.

Floating Covers.

Preliminary work was conducted on the evaluation of materials and designs for covers floating on the water surface to reduce evaporation. The first cover was constructed of 30-mil reinforced black butyl sheeting. The edge of the sheeting was cemented to and floated by an air-filled, 3.2-cm diameter, rigid plastic pipe formed into a circle which was slightly smaller than the tank. The tank area is 5.91 m^2 and the covered area was 5.52 m^2, representing a covering of 93.4 percent. The center of the cover was supported by a 30-cm diameter air-filled inner tube. For the period of 3 June - 11 June the uncovered tank evaporated 50.8 mm and the covered tank, 3.6 mm.

For the period of 14 July - 23 July evaporation was measured, along with water temperatures, under the cover and in an uncovered tank. For the interval the uncovered tank evaporated 49 mm of water and the covered tank, 5.1 mm of water for a reduction of 90 percent. Temperature measurements taken during the interval showed a 6 C - 8 C warmer 24-hour mean water temperature at the 1-cm depth in the covered tank than in the uncovered tank. This resulted in a higher rate of evaporation from the open portion of the covered tank, thereby losing more water than is indicated by the percentage of area covered. The cover was then painted with white enamel. For 26 July - 3 August the uncovered tank lost 54.4 mm of water and the white-coated cover lost 2.0 mm for a reduction of 96 percent. Water temperature measurements showed an increase of 2 C mean

temperature at the 1-cm level, compared to the uncovered tank. Rain falling on this cover was trapped on the surface and was subsequently lost by evaporation.

A second cover was constructed of 10-mil modified black polyethylene. An outer rim was formed, using 2.5-cm semirigid nylon tubing which was filled with water and cemented to the sheeting. The center of the sheeting is supported above the water by injecting air under the sheeting forming an air supported dome which shed rain into the tank where it was protected against evaporation by the cover. This cover was 2.6 m in diameter, covering an area of 5.31 m^2 or 89.8 percent of the tank area.

A third cover, 2.6-m diameter, was constructed of 6.4-mm thick white foamed polyethylene. This material has a density less than water and does not need auxiliary support. Evaporation measurements from 29 November - 6 December, when an uncovered tank lost 13.0 mm, showed the domed cover reduced evaporation by 84 percent and the foamed polyethylene, 90 percent. Further studies with the foamed polyethylene will include evaluation of surface treatments to increase life of the sheeting. The unprotected sheeting deteriorates quite rapidly upon exposure to solar radiation.

During the summer of 1965 a field test of the effectiveness of larger floating covers was conducted in cooperation with the Bureau of Indian Affairs on the Hualapai Indian Reservation. A 30-mil butyl cover was constructed for one of the two 6.5-m diameter 40,000-liter steel-rimmed tanks that store water from the Blue Mountain catchment. The other tank, left uncovered, made it possible to measure evaporation from covered and uncovered tanks simultaneously. The butyl sheeting was fastened at the edges to an air-filled 5.1-cm diameter rigid plastic pipe, formed into a 6.4-m diameter circle. The center of the cover was supported by two 1-meter diameter air-filled inner tubes. For the period of 12 June - 18 June the uncovered tank lost 82.6 mm and the covered tank lost 6.4 mm for a

reduction of 92 percent. A second test period 25 June - 3 July, when the uncovered tank evaporated 114.3 mm, the covered tank lost 38.1 mm for a reduction of only 67 percent. This reduced effectiveness was caused by rain that had been collected on top of the cover.

SUMMARY AND CONCLUSIONS:

Studies were continued with floating white granular materials which reduce evaporation by reflecting solar radiation and reducing the water temperature. A 6-month study was conducted on 274-cm diameter tanks to determine the effect of weathering on evaporation reduction by the floating materials. Chopped styrofoam, which initially reduced evaporation 60 percent, gradually decreased in effectiveness to only 12 percent reduction. Foamed plastic beads which initially reduced evaporation 42 percent, decreased in effectiveness to 29 percent reduction.

Preliminary studies were conducted with a low-cost expanded perlite ore, treated with a silicone water repellent. Initially the perlite reduced evaporation approximately 50 percent but decreased to 25 percent after being wetted by rain. Measurements of incoming and reflected solar radiation, net radiation, and water-temperature profiles are currently being evaluated.

Present indications are that evaporation can be reduced 25 to 50 percent for periods of 6 months or more with floating granular materials if wind movement of the materials can be controlled. Further studies on larger areas will be conducted.

Preliminary studies were conducted on the evaluation of materials and designs for floating covers to reduce evaporation. One cover of 30-mil black butyl, covering 93.4 percent of the tank area, reduced evaporation 90 - 93 percent. After painting the same cover white, evaporation was reduced 96 percent.

For sheetings with a density greater than water, an air-supported dome-shaped cover was developed that sheds rain into the tank where it will be protected against evaporation by the cover.

Investigations are being conducted with covers constructed of 6.4-mm thick white foamed polyethylene. This sheeting floats on the water surface without auxiliary support. It reduces water temperatures by reflecting solar radiation by virtue of its white color and insulating properties. Current studies include evaluation of treatments to protect the polyethylene sheeting against deterioration by solar radiation.

A field test of a larger floating cover was conducted in cooperation with the Bureau of Indian Affairs on the Hualapai Indian Reservation. A 6.4-m diameter cover of 30-mil butyl sheeting was constructed and installed on one of two identical tanks on the Blue Mountain catchment. Evaporation measurements for 6 days in June showed the cover reduced evaporation 92 percent. After a rain that ponded water on the cover, evaporation reduction was 67 percent.

PERSONNEL: L. E. Myers, G. W. Frasier.

TITLE: MEASUREMENT AND CALCULATION OF UNSATURATED CONDUCTIVITY AND SOIL-WATER DIFFUSIVITY

LINE PROJECT: SWC 4-gG4 CODE NO.: Ariz.-WCL-13

The objectives and need for study for this project were given in the 1961 Annual Report of the U. S. Water Conservation Laboratory. Further work under this project was reported in 1962 and 1963. This report covers the measurement of the temperature dependence of the hydraulic conductivity of 50-500μ sand. The conductivity measurements were made according to the procedure given in the 1963 Annual Report.

The intrinsic permeability of a porous material is defined as

$$P = \frac{k\eta}{\rho g} \qquad [1]$$

where P is the permeability, k the conductivity, η the viscosity of the fluid, ρ the density, and g the acceleration due to gravity. The units of P are length^2, and in the cgs system it is convenient to use microns^2 (μ^2).

If k is measured at several temperatures and P calculated for each k, then P will be the same for all temperatures of interest if the temperature dependence of k is solely due to the temperature dependence of η/ρ. Experimental verification of equation [1] for unsaturated porous materials has not been published to this writer's knowledge.

Measurements were made of the hydraulic conductivity of 50-500μ sand at four temperatures over a water content range of 0.2 to 0.4. Data presented in Figure 1 show the permeability versus water content for eleven runs at four temperatures. The data fall very nearly on the same line. No significant trends with temperature can be observed. The solid square at $\theta = 0.423$ represents measurement of the saturated hydraulic conductivity at eight temperatures. The latter measurement was made to ascertain whether or not small deviations of conductivity with temperature not accounted for by viscosity occurred but were not measurable with the long column technique. Table 1 shows that for 50-500μ sand, no significant changes of saturated permeability with temperature occurred.

The value of the conductivity at each temperature was obtained by measuring the flux at several different gradients. Usually six to eight gradients with two flux measurements at each gradient were made. Least squares analysis of the data indicated that a zero intercept obtains and no deviations from Darcy's law were evident.

PERSONNEL: R. D. Jackson

Table 1. Conductivity, permeability at several temperatures for 50-500μ sand.

Temperature °C	Conductivity (cm min^{-1})	Permeability $microns^2$
4.0	0.185	4.94
9.7	0.223	5.02
12.2	0.237	4.97
14.1	0.248	4.94
15.5	0.266	5.12
15.5*	0.257	4.94
18.5	0.279	4.98
23.8	0.327	5.13
38.2	0.436	5.06
	Average	5.01

*Two measurements were made at 15.5 C. A 10-day interval and measurements at several other temperatures separated these two measurements.

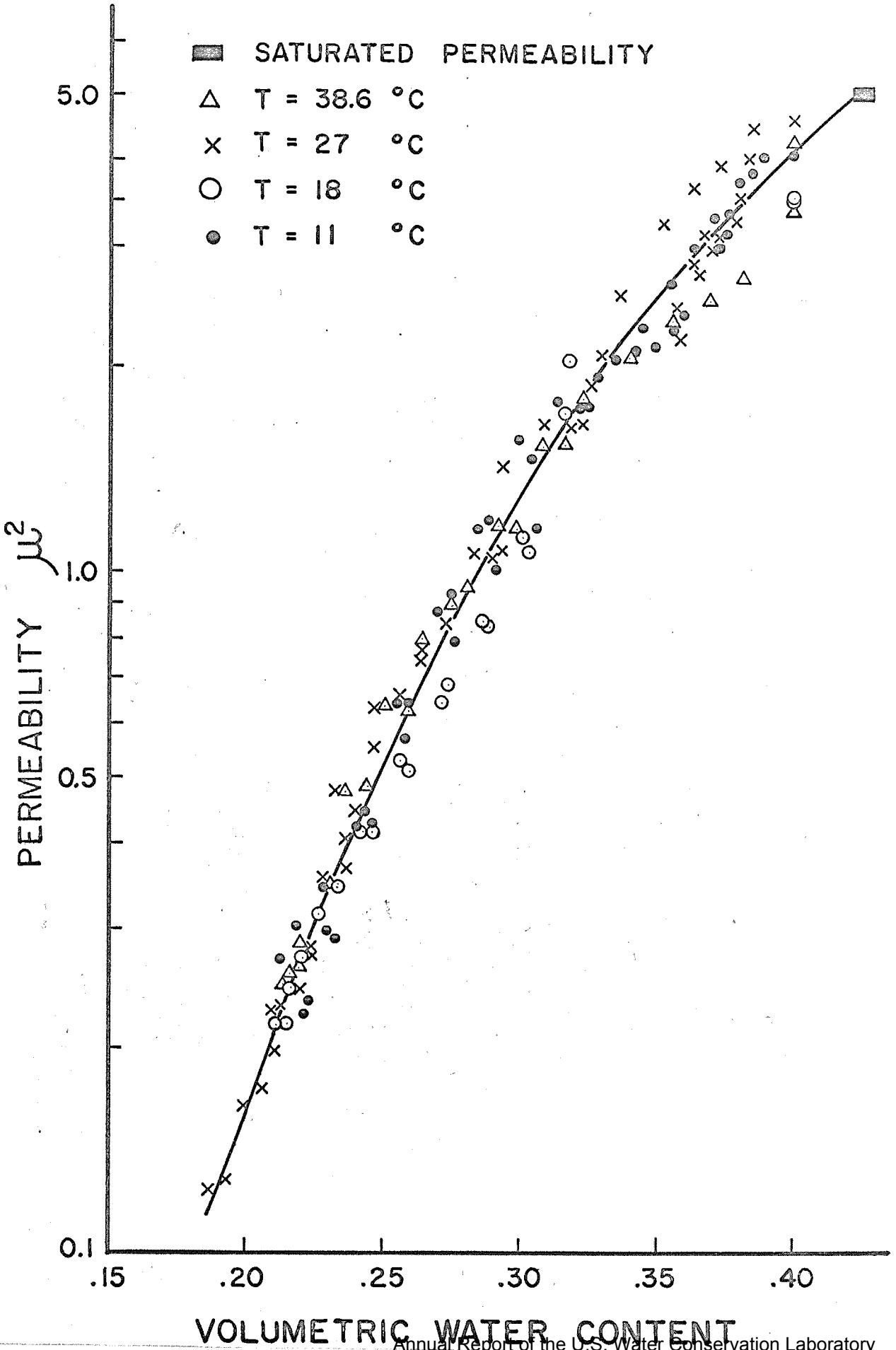
SATURATED PERMEABILITY
T = 38.6 °C
T = 27 °C
T = 18 °C
T = 11 °C
5.0
1.0
0.5
0.1
PERMEABILITY μ²
.15
.20
.25
.30
.35
.40
VOLUMETRIC WATER CONTENT

Figure 1

TITLE: FIELD APPLICATION OF FALLING-HEAD TECHNIQUES FOR SEEPAGE METER AND DOUBLE-TUBE METHOD FOR HYDRAULIC CONDUCTIVITY MEASUREMENTS

LINE PROJECT: SWC 4-gG1 CODE NO.: Ariz.-WCL-14

INTRODUCTION:

The field application of seepage meters was continued in 1965 with studies at Twin Falls, Idaho and at Logan, Utah to compare seepage meter results with those of other techniques for measuring seepage losses from canals.

The top plate of the double-tube apparatus was modified to permit insertion of the inner tube into the soil after the top plate was fastened to the outer tube. The purpose of this modification was to make the device easier to construct and to operate, and to minimize soil disturbance.

PROCEDURE:

Seepage Meter Tests, Twin Falls, Idaho. The seepage meter tests at Twin Falls, Idaho were conducted on a 1/2-mile reach of the north side pumping canal, Minidoka Project, in cooperation with the Snake River Conservation Research Center, the University of Idaho, and the Bureau of Reclamation. The measurements were performed by Robert Worstell and Charles Brockway of Twin Falls. Seepage meter data were collected at 7 stations, 400 ft apart. At each station, seepage was measured in 2 profiles 5 ft apart with 5 tests per profile. The water depth in the canal, normally at 5 to 6 ft, was reduced to 20 to 22 inches for these tests. The cross-section at this shallow depth approached a segment of an 18-ft radius circle. The water velocity was about 0.75 ft/sec. A ponding test was run on the canal section 2 weeks after the seepage meter tests were run.

Logan, Utah, Seepage Meter Tests. Seepage meter tests were conducted on six 8 × 20-ft earth-lined canal sections, which were part of the experimental canal-lining installation at the Logan ARS field station. The results were compared with the seepage for each section calculated from the drainage flow from the concrete bins in which the sections were installed. The type of earth lining is given

in Table 2. The earth blankets were covered by a 4-inch layer of 1-inch diameter gravel to prevent sloughing. This gravel had to be raked away at each seepage meter location before the cylinder could be installed. Twelve to 15 tests were distributed along the center and sides of each section.

Modifications of Double-Tube Equipment. The flexible connecting tubing from the inner tube to the top plate has been replaced by a straight 10 × 1-1/2-inch diameter brass tube (See Figure 1). This tube connects to the inner tube and slides through a slip-joint connection on the top plate. With this arrangement, the inner tube can be inserted into the soil after the top plate is in place. A nut is then tightened against the rubber gasket to obtain a water-tight seal. The method of attaching the standpipes has been changed from O-ring seals to a flange-and-gasket seal. The construction of the outer tube has also been simplified in that a commercially available flange is attached to the outer tube with rivets or machine screws. This eliminates welding of the flange to the outer tube.

RESULTS AND DISCUSSION:

Seepage Meter Tests, Twin Falls, Idaho. Results of the seepage tests are shown in Table 1. The average seepage rates for the different profiles were quite uniform although considerable variation occurred within each profile. This variation appeared to be of a random nature without clear relation to location in the profile or to water depth. The uniform average rates can be explained in part by the uniformity of the soils in the region. The soils are wind-blown loess materials of uniform size mostly in the silt range. No rock or gravel was encountered in the canals. The average seepage meter rate of the entire half-mile section was 0.67 ft/day.

Values of H_b were near or exceeded the water depth in 63 out of the 71 tests. This indicated the presence of a slowly permeable, thin surface layer. The average pressure head below this layer was -5.4 inches water with some values as low as -18 inches. Using an average value for impedance and pressure below the sealing layer, the seepage rate can be projected to the normal operating water

depth of 5 ft (see Annual Report 1963). Considering the canal cross-section as trapezoidal with a bottom width of 7.5 ft and a side slope of 30 degrees, the resulting seepage rate for the 5-ft depth was 1.55 ft/day.

The data from the ponding tests have not been completely processed and are not available at this time. Thus, comparisons between the seepage meter results and the ponding data can not yet be made.

Logan, Utah, Seepage Meter Tests. The results of the seepage meter measurements are summarized in Figures 2, 3, and 4. The average seepage meter rate for each section is presented in Table 2, which shows that the seepage based on drain flow measurement exceeded the average seepage meter rate from 2 to 68 times! Based on the following arguments, the conclusion is made that this large discrepancy is caused by leakage due to thin spots and similar imperfections in the earth lining.

1. The seepage as calculated from the drain outflow has increased several hundreds of times over the period that the linings have been in operation (approximately 10 years).
2. Wave action caused sloughing of the lining material. Annual maintenance consisted of raking the material back on to the canal banks. Later on, the lining was covered with a layer of gravel to keep it in place. This "handling" could have caused a reduction of the effectiveness of the earth linings.
3. The seepage meter results are not erratic but fairly consistent for each section. Occasionally, high rates were observed for the channel banks near the water level. In numerous other studies, seepage meter data have been found to give reliable estimates of local seepage rates. Thus, the seepage meter results are probably valid for the Logan studies.

Modifications of Double-Tube Equipment. The modifications in the double-tube equipment resulted in easier construction and operation of the device. A complete construction drawing of the double-tube equipment was prepared.

SUMMARY AND CONCLUSIONS:

Canal seepage investigations using the falling-head seepage meter technique were conducted in a canal section of 1/2 mile length and approximately 2-ft water depth near Twin Falls, Idaho. Measurements were carried out in 7 duplicate profiles uniformly spaced over the canal section, with 5 seepage meter tests per profile. The average seepage meter rate was rather uniform for each profile. The average of all 71 tests was 0.67 ft/day. A thin, slowly permeable layer with unsaturated conditions beneath it was present throughout most of the canal section. The projected seepage rate for a normal operating depth of 5 ft was calculated as 1.55 ft/day. These data will be compared with results from ponding tests carried out in the same canal.

Seepage meter tests on experimental earth linings at Logan, Utah showed that the seepage rate in the bulk of the lining as indicated by the seepage meter was less than the seepage calculated from the outflow from the drainage system. This difference could be due to weak spots and similar imperfections in the lining, particularly at the upper part of the banks.

Modifications of the double-tube equipment were made to simplify the construction and installation of the equipment. The inner tube can now be inserted into the soil after the top plate is in place, which is more convenient, causes less disturbance of the soil, and permits more accurate evaluation of the depth of penetration.

PERSONNEL: Herman Bouwer and Robert C. Rice.

Table 1. Seepage Data - Twin Falls, Idaho

Station and Water Surface Width	Test	Location[1/]	d in.	I_s ft/day	H_b in.	R_a hr.	h_w in.	P_c in.
51 + 64	1-1	4	1.12	.57			14	
	1-2	1	0.75	.59	15	51	6	-9
15 ft	1-3	7	0.75	.55	27	98	20	-7
	1-4	11	1.25	.44	15.5	70	14	-1.5
	1-5	14	1.62	.85	9.5	22	6	-3.5
	1-6	13	1.75	1.97	3	3	8	
	1-7	8	1.0	.28			20	
	1-8	11	1.25	.39	22.5	115	6	-16.5
	1-9	1	1.0	.94	14.5	31	10	-4.5
	1-10	4	.87	.69	18.2	53	20	
	Average			.73		55		- 5.2
48 + 00	2-1	1.5	1.0	.48	13.5	56	8	-5.5
	2-2	2	1.5	1.66	17.2	52	12	-5.2
16 ft	2-3	4	1.0	.28	26	185	16	-10
	2-4	5	1.5	1.04	26.5	51	21	-5.5
	2-5	10	0.5	.26	17.5	135	18	0
	2-6	1.5	1.0	.23	13.6	118	10	-3.6
	2-7	14.5	1.0	.16	7.0	88	5	-2
	2-8	3.5	1.25	1.20	26.1	43	17	-9.1
	2-9	12	1.5	.56	21	75	12	-9
	2-10	5	1.0	.70	23.5	67	21	-2.5
	Average			.56		70.3		-5.2
44 + 00	3-1	11.5	1.25	.34	13	77	9	-4
	3-2	1.5	1.25	.52	16.6	65	10	-6.6
13 ft	3-3	10	1.5	.90	22	49	18	-4
	3-4	4	2.0	.64	15.5	48	19	
	3-5	6.5	1.25	.33	15.2	92	22	
	3-6	2.5	.87	.25	11.1	89	13	
	3-7	6.5	1.25	.76	15	39	22	
	3-8	5	.75	.60	29	97	21	-7
	3-9	8	1.0	.40	15	74	18	
	3-10	11	1.0	.54	14.6	54	10	-4.6
	Average			.53		68		-2.7

1/ Distance from left water surface edge.

Table 1 (Cont'd). Seepage Data - Twin Falls, Idaho

Station and Water Surface Width	Test	Location[1/]	d in.	I_s ft/day	H_b in.	R_a hr.	h_w in.	P_c in.
40 + 00	4-1	1	.62	1.04	17.2	33	6	-11.2
	4-2	12	1.25	.84	11	26	6	-5
13 ft	4-3	4	1.12	.66	27	82	16	-11
	4-4	9	1.25	.72	24.6	68	16	-8.6
	4-5	6.5	.75	1.60	24	31	18	-6
	4-6	12	1.12	.27	7.2	5.4	5	-2.2
	4-7	1	1.0	.95	14	30	6	-8
	4-8	4	1.0	.72	27.2	76	17	-10.2
	4-9	4	1.25	.60	30.5	52	16	-14.5
	4-10	6.5		.46	20.5	89	19	-1.5
	Average			.79		49.2		-7.8
36 + 00	5-1	11.5	.75	1.82	11	12	5	-6
	5-2	1	1.5	.47	12	51	5	-7
12.5 ft	5-3	4	.5	.70	20.5	59	19	-1.5
	5-4	1	1.5	.86	8.7	20	5	-3.3
	5-5	6	.5	.24	11.3	94	18	
	5-6	6	1	.21	18.5	176	19	0
	5-7	6	.5	.68	19.5	57	17	-2.5
	5-8	1.5	.5	.17	11.2	132	8	-3.2
	5-9	8.5	.5	.58	22.5	78	11	-11.5
	5-10		.5	.20	2.2	22	18	-4
	5-11	11.5	.5	.42	15.5	74	6	-9.5
	Average			.58		70.5		-4.4
32 + 00	6-1	12.5	.5	.38	26.2	137	8	-18.2
	6-2	1.5	1	.37	15.5	84	8	-7.5
14 ft	6-3	10	1.1	.54	23	85	16	-7
	6-4	5	.75	.90	35	78	18	-17
	6-5	7	.5	1.01	9.3	18	22	
	6-6	7	1	2.65	1	0.7	22	
	6-7	9	.75	.96	29	60	18	-11
	6-8	5	.62	.90	34	75	17	-17
	6-9	12.5	.62	.70	1.4	4	9	
	6-10	1	1.25	1.06	16	30	6	-10
	Average			.95		57.2		-8.77

Table 1 (Cont'd). Seepage Data - Twin Falls, Idaho

Station and Water Surface Width	Test	Location 1/	d in.	I_s ft/day	H_b in.	R_a hr.	h_w in.	P_c in.
28 + 00	7-1	12.5	1.25	.26	2.3	18	9	
	7-2	6	1.25	.77	7.2	19	6	-1.2
14 ft	7-3	11	.5	.52	16.7	64	19	
	7-4	10	1.5	.32	18	112	20	
	7-5	1	.75	.48	20.2	84	7	-10.2
	7-6	7	.5	.45	16.7	74	20	
	7-7	13	1	.14	9.5	135	6	-3.5
	7-8	4.5	.75	.94	26.5	58	19	-7.5
	7-9	9	.87	1.12	23	41	18	-5.0
	7-10	7	.25	.52	11.5	44	22	-10.5
	Average			.55		64.9		-3.79

Table 2. Average Seepage Data - Logan, Utah.

Section	Lining Material	No. of Tests	Seepage Rate ft/day	
			Meter	Outflow
1B	Oasis Silt Loam	12	0.03	2.14
2B	Mullville Silt Loam 10 parts bentonite	12	0.13	0.61
4B	Trenton Sandy Loam 20 parts bentonite	13	0.13	1.04
6B	Trenton Sandy Loam 20 parts bentonite	14	0.03	0.25
7B	Trenton Sandy Loam 20 parts bentonite	15	0.07	0.21
8B	Trenton Sandy Loam 10 parts bentonite	14	0.16	0.43

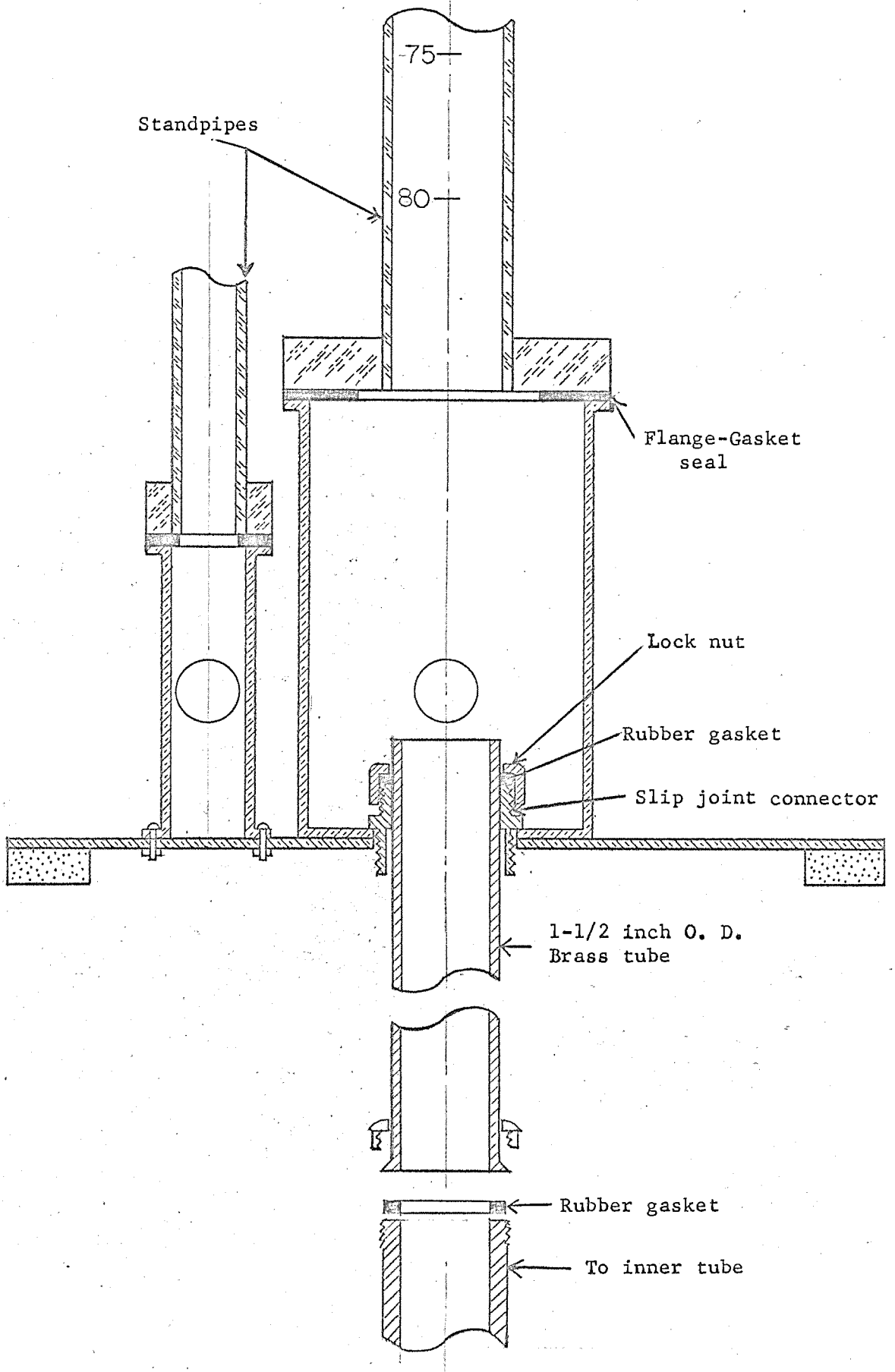

Figure 1. Modified connection of inner tube and standpipes to top plate.

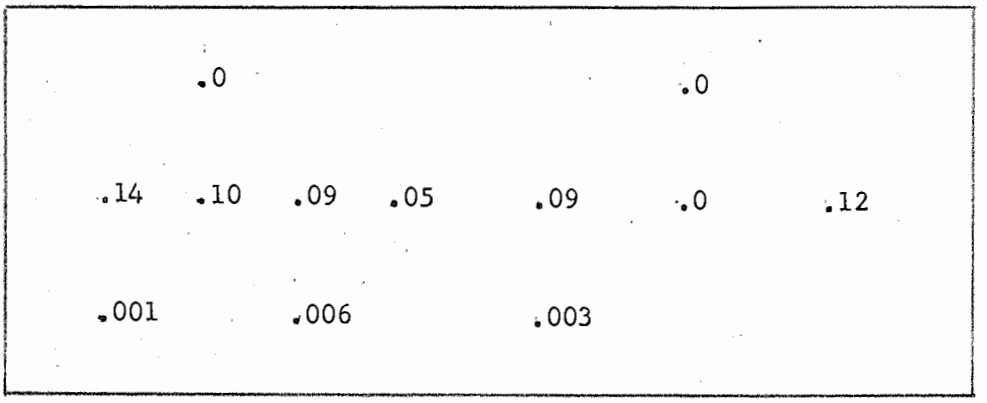

Section 1B

Average Seepage = 0.03 ft/day

N

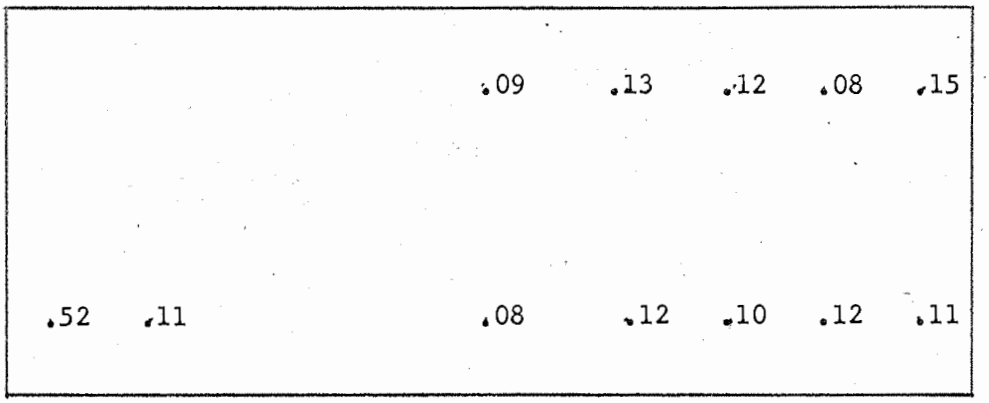

Section 2B

Average Seepage = 0.13 ft/day

Scale 1" = 4'

Figure 2. Location of seepage meter tests, Sections 1B and 2B, Logan, Utah.

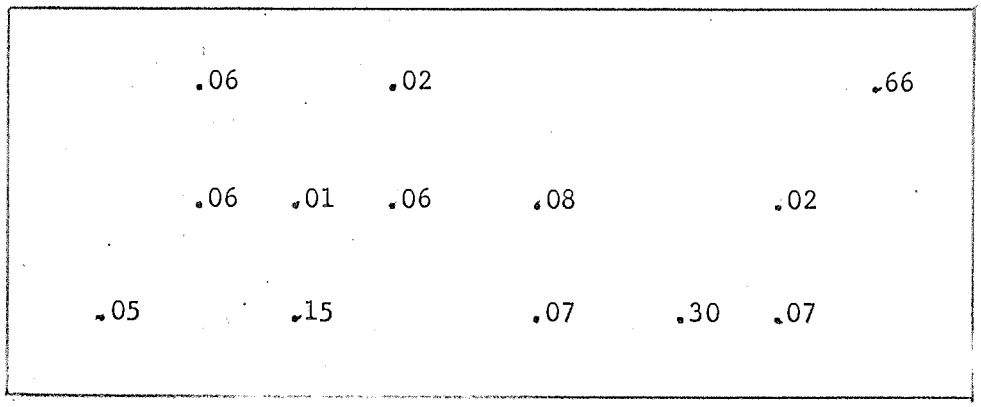

Section 4B

Average Seepage = 0.13 ft/day

N

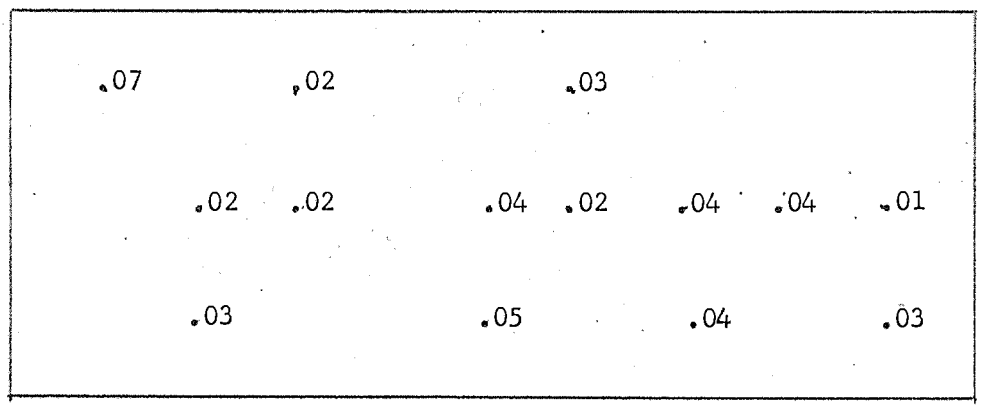

Section 6B

Average Seepage = .034 ft/day

Scale 1" = 4'

Figure 3. Location of seepage meter tests, Sections 4B and 6B, Logan, Utah.

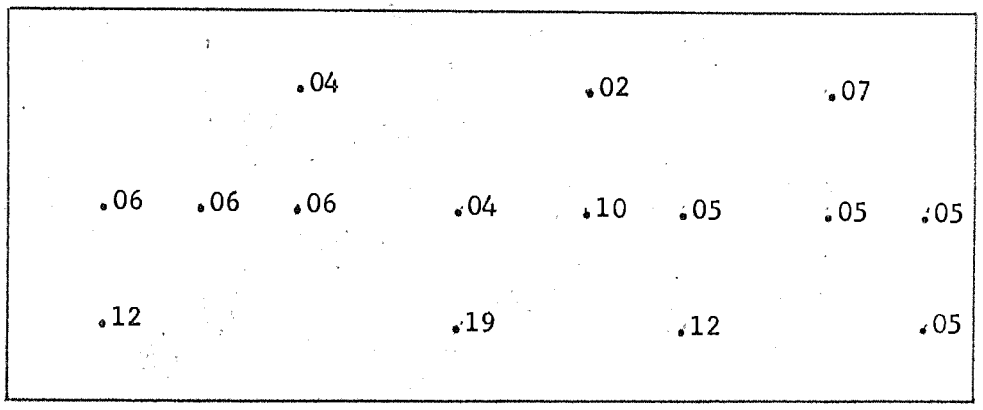

Section 7B

Average Seepage = 0.07 ft/day

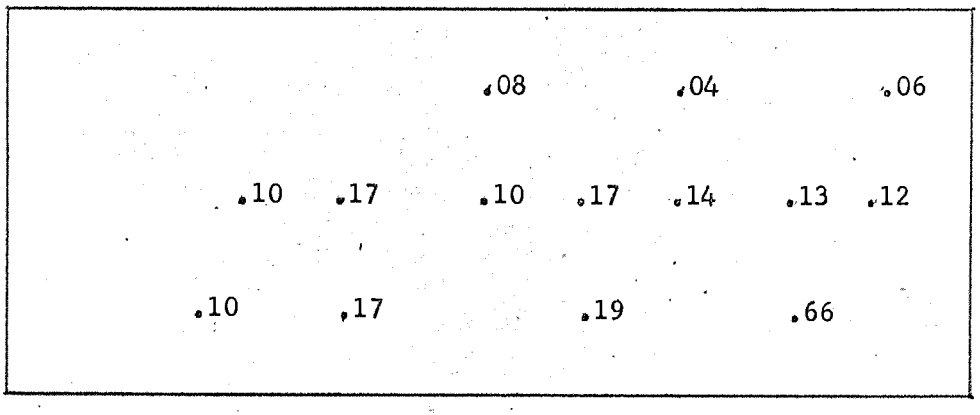

Section 8B

Average Seepage = 0.16 ft/day

Scale 1" = 4'

Figure 4. Location of seepage meter tests, Sections 7B and 8B, Logan, Utah.

TITLE: COMPONENTS OF THE RADIATION BALANCE OF FIELD CROPS UNDER IRRIGATED CONDITIONS

LINE PROJECT: SWC 4-gG2 CODE NO.: Ariz.-WCL-18

A radiometer has been designed to obtain – either by direct measurement or by calculation – the following radiation terms:

Incoming and reflected shortwave radiation,
Incoming and outgoing total hemispherical radiation,
Longwave sky and terrestrial radiation, and
Net and net-solar radiation.

These radiative terms should permit the calculation of the effective sky and terrestrial radiation temperatures.

The instrument, referred to as the 4-component radiometer, consists of four thermal transducers mounted on an aluminum plate. Two of the transducers are on top of the plate and two on the bottom, each pair being located exactly on opposite sides of the plate. The transducers are the same as used in the miniature net radiometer.

Windshielding of the transducers is provided by ground glass and polyethylene hemispheres, one pair being shielded by glass and the other pair by polyethylene. The glass-enclosed transducers are sensitive to shortwave, or solar, radiation. The polyethylene transducers are sensitive to total radiation. If the plate temperature is uniform, then the previously mentioned radiative terms can be obtained.

Evaluation of the 4-component radiometer has not been completed.

PERSONNEL: Leo J. Fritschen

TITLE: EVAPORATION FROM THE SOIL SURFACE AND SOIL MOISTURE MOVEMENT

LINE PROJECT: SWC 4-gG2 CODE NO.: Ariz.-WCL-19

INTRODUCTION:

General methods of estimating energy and mass flux to or from a surface where evaporation is occurring employ temperature gradients above this surface. In the past, most such gradients have been measured using temperature sensors at two or more points above the surface. These have been used with the assumption that the net flux was vertical at the point of measurement. For this assumption to be adequately fulfilled, a certain minimum fetch was required depending on such factors as windspeed, up-wind atmospheric and surface conditions and on the height of the sensors.

Those who have attempted to measure the surface temperature directly in order to find the temperature gradient very near the surface (with the implied reduction in fetch requirement) have had to introduce an instrument that usually affected the temperature they were trying to measure. An instrument which can measure this temperature remotely would not present this difficulty.

PROCEDURE:

We are attempting to measure the temperature of a soil or leaf surface (hopefully at the seat of evaporation) using an Infrared Thermometer (IFT) made by Barnes Engineering Company of Connecticut (Model No. IT-2 Type S). This instrument measures the electromagnetic radiation from a surface in the 8-13μ wave band.

The radiation from such a surface is composed of two parts: (1) that due to the internal energy of the surface molecules, W_e, and (2) that part of the radiation, incident on the surface, which is reflected, W_r.

W_e is a unique function of the temperature of a specific radiating surface as shown in equation [1]

$$W_e = \epsilon \sigma T^4 \int_{\lambda_1}^{\lambda_2} \lambda^{-5} [\exp(c/\lambda T) - 1]^{-1} d\lambda = \epsilon \sigma F(T) T^4 \qquad [1]$$

where

T = temperature

ϵ = emissivity

λ_1 and λ_2 = limits of the wave band viewed (8 and 13μ in our case)

σ = Stephan-Boltzman constant

c = 2nd Planck radiation constant

$$F(T) = \int_{\lambda_1}^{\lambda_2} \lambda^{-5} \left[\exp (c/\lambda T) - 1\right]^{-1} d\lambda$$

Note: The integral is derived from Planck's Radiation Law and was evaluated from Table 2, p. 154 of "Radiation Pyrometry and Its Underlying Principles of Radiation Heat Transfer" by Thomas R. Harrison, Wiley, 1960.

Since, by definition,

$$W_r = r\, W_I = (1 - \epsilon)\, W_I \qquad [2]$$

where

r = reflectivity

W_I = radiation incident on the surface

then

$$f(S_B) = W_T = \epsilon\, \sigma\, F(T)\, T^4 + (1 - \epsilon)\, W_I \qquad [3]$$

where

S_B = millivolt signal from the IFT

W_T = total radiation from the surface

The function f( ) is defined by an empirical calibration technique to be described later.

In order to determine a surface temperature using equation [3], S_B, ϵ, and W_I must be known. S_B, of course, is read from the IFT by means of a millivolt recorder. To get the other variables the following scheme is used:

(1) A stable surface is constructed from an aluminum plate in which thermocouples are embedded just below the surface, and on whose surface a paint is sprayed. This plate is placed in a chamber whose

walls are maintained at a constant temperature, so that W_I is constant. A plot of W_T vs $\sigma F(T_p)T_p^4$ made as T_p is varied will yield a straight line whose slope is the plate emissivity (ϵ_p). When the temperature of the plate is the same as that of the walls of the chamber,

$$\sigma F(T_p)T_p^4 = W_I = W_T$$

Therefore, the intersection of the line of slope ϵ_p and one of slope 1 will give W_I.

(2) With a surface of interest, step one is repeated using, for example, a pan of soil instead of the plate (to yield a soil emissivity, ϵ_s).

(3) Using the plate with its known ϵ_p we can calculate any W_I by measuring S_B and T_p.

Thus, with simultaneous measurement of the plate temperature and radiation from the plate (exposed to the same W_I as the soil) and from the soil surface, and previously determined value of ϵ_s and ϵ_p, one can calculate the surface temperature.

RESULTS AND DISCUSSION:

Calibration. The function $f(S_B) = W_T$ was defined (i.e., the IFT was calibrated) by making use of the concept of a Black Body, a radiator with $\epsilon = 1$. Under these conditions equation [3] reduces to

$$f(S_B) = \sigma\ F(T_{BB})\ T_{BB}^4$$

and simultaneous measurements of S_B and T_{BB} over a range of T's will produce a curve defining f( ).

A cavity with a single small hole in it and with walls at a uniform temperature is a very good approximation to a Black Body when viewed through the hole. Such a cavity was built (Figure 1) and immersed in a controlled temperature bath and used to make the calibration between -15 C and 70 C.

Emissivity. A plate for the measurement of W_I was constructed as follows: three No. 56 holes were drilled in a triangular pattern around the center of a 16.51 cm × 16.51 cm × 0.64 cm aluminum plate within 2 cms

of each other. These holes were drilled from the bottom surface and perpendicular to it, up to very close to the upper surface but never breaking this upper surface. Nylon coated thermocouples were inserted in each hole so that the tip of the junction would make electrical contact with the plate as close to the upper surface as possible. The plate was then nested in a styrofoam box (Figure 2) and its surface sprayed with an appropriate paint.

The question of how well the thermocouples were measuring the conditions at the painted surface was investigated by placing a very fine wire (4 mil) thermocouple across the surface with the junction near the point of contact of the embedded thermocouples. This fine thermocouple was joined to the embedded thermocouples so as to form a thermopile so that the readout signal would indicate temperature difference. This signal was recorded as the plate cooled from 60 C toward ambient (30 C). The signal had considerable variation but its maximum mean (near the start of the cooling test) indicated that the surface thermocouple was about 2.5 C cooler than the plate thermocouple. Since: (1) it was not possible to bring the fine thermocouple into contact with the surface at every point on the wire, (2) the ϵ's of the wires were greater than that of the plate, and (3) the rated accuracy of the Barnes is only within 2 C, this test is considered good evidence that the plate thermocouples are sufficient for our purpose.

It is thought that an $\epsilon_p = 0.5$ would allow us to measure W_I with the least error. Since it was found that aluminum spray paint has an $\epsilon \approx 0.33$, various mixtures of this and a flat black paint were made to get the desired ϵ_p. A mixture of 6 or 7 parts aluminum to 2 parts black gave satisfactory results.

To determine the ϵ of the soil in the lysimeters (Adelanto loam), samples were taken from the surrounding field and were given the usual air drying and dry sieving treatment to get 5 aggregate size fractions (2 - 4.76 mm, 1 - 2 mm, 0.5 - 1 mm, 0.25 - 0.5 mm, and < 0.25 mm). Sheet metal trays were built which fit into styrofoam holders much as the aluminum plates do and will hold a 2.5 cm layer of soil. Thermocouples stick up from the bottom of the tray to just below the surface of the soil.

To make the actual ϵ determination a 56 cm $\times$ 56 cm $\times$ 76 cm plywood box was lined with 5 cm styrofoam and sprayed with a flat black paint. A small viewing hole was cut in the top and concealed vents were cut in the sides to provide for circulation of air at a controlled temperature. By monitoring the wall temperature with thermocouples it was found that the temperature could be controlled within 1/2 C during the course of a measurement. This measurement was made by heating or cooling the object (plate or tray of soil) away from the chamber temperature, placing the object in the view path of the Barnes sensor, and recording S_B and the thermocouple output as the object changed temperature.

This procedure was used to determine the ϵ of an aluminum spray paint ("Aerosol Brand Jet" aluminum 17/78 lacquer type), Parson's optical black paint and an aluminized tape (Permacel aluminized) (see table).

Table 1.

Object	Emissivity
Aluminum Paint	0.33
Black Paint	0.97
Tape	0.75

Plans. The ϵ of the various size fractions of soil in the wet and dry state will be measured. It is supposed that ϵ_s will (1) be independent of aggregate size, (2) be at most a weak function of moisture content, and (3) be quite high. If this proves to be true, then the instruments will be taken outside to make measurements on the lysimeters.

A portable tower and stands are being constructed on which the sensor will be mounted. The tower will be carried between lysimeters to make measurements on bare soil. These measurements will be made in conjunction with measurements of net and solar radiation, air temperature and humidity, windspeed and direction, soil heat flux, evaporation and surface temperature (measured with thermocouples embedded near the surface), which will be used in various transfer equations to judge the effectiveness of surface temperature measurements, made in this manner, in predicting evaporation.

The possibility exists that W_r may be negligible compared to W_e and will not have to be measured. This will be true if ϵ_s is very close to one or if W_I is very small. Such a condition would eliminate two of the three field measurements now necessary to obtain surface temperatures. This aspect will be investigated.

SUMMARY AND CONCLUSIONS:

A method for measuring soil and leaf surface temperature is useful in attempting to evaluate models of heat and moisture flux into the atmosphere. Such a method is being investigated. It is based on measurement of the electromagnetic radiation emitted by these surfaces.

An Infrared Radiation Thermometer (IFT) (Barnes Engineering Co. of Conn.; Model No. IT-2 Type S) is used to measure the total radiant energy flux from a surface in the 8-13μ wave band. This flux (W_T) is composed of two components: that reflected from the surface (W_r) and that emitted by the surface (W_e). W_e can, by knowing the surface emissivity, be related to the surface temperature by the equation, $W_e = \epsilon \sigma F(T) T^4$ from Planck's Radiation Law. W_r can be calculated by measuring W_T from a plate of known temperature and emissivity using the equation

$$W_T = \epsilon \sigma F(T)T^4 + (1 - \epsilon) W_I$$

where W_I = the incident radiation and $W_r = (1 - \epsilon) W_I$.

A controlled temperature Black Body Cavity was built for calibration of the IFT after it was adjusted to have a range from -15 C to 70 C. The millivolt signal was read on a strip chart recorder.

A procedure for measuring surface emissivities was developed and used to obtain the emissivities of a 0.62-cm thick painted aluminum plate. It was decided to have a plate with $\epsilon = 0.5$ for the measurement of W_I. A mixture of 6 or 7 parts of aluminum paint to 2 parts of black paint gave the desired ϵ. This same procedure will be used to measure the ϵ of the soil of the site of outside experiments in preparation for measuring soil surface temperature.

PERSONNEL: J. Conaway, C. H. M. van Bavel

SENSING HEAD
DRY AIR
THERMOCOUPLE
COOLANT
THERMOMETER
HEATER
STIRRER
CAVITY
SIGHT TUBE
BATH
SUPPORT WIRE
BATH
BATH
LEAD WEIGHT
RUBBER TUBE TO CIRCULATE LIQUID

SIMULATED BLACK BODY CAVITY AND BATH, FOR CALIBRATION OF INFRA-RED THERMOMETER

FIG. 1

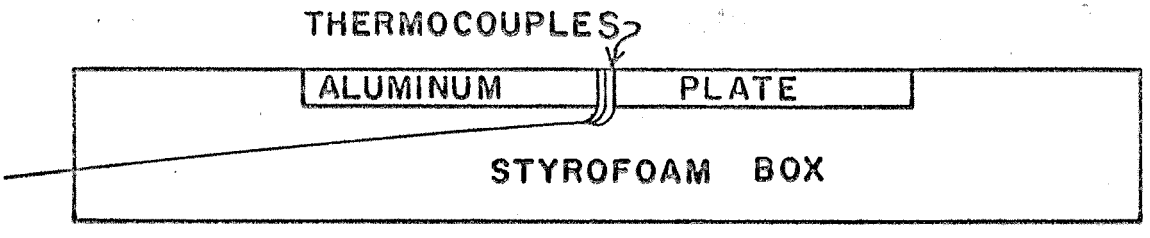

PLATE USED TO MEASURE REFLECTED RADIATION

FIG. 2

TITLE: MEASURING HORIZONTAL AND VERTICAL CONDUCTIVITY OF SOIL WITH THE DOUBLE-TUBE METHOD

LINE PROJECT: SWC 4-gG1 CODE NO.: Ariz.-WCL-25

INTRODUCTION:

The development of fast-response piezometers was continued with a laboratory study of the effect of piezometer design on the type and magnitude of disturbance of the medium and on the response time of the piezometer.

PROCEDURE:

The piezometers were tested by inserting them into 7-cm diameter saturated soil columns in 1-cm increments and measuring the pressure changes (Figure 1). The piezometers were inserted into porous materials by a motorized point gage at speeds of 0.07, 0.28, and 1.33 cm/sec. The motor was turned off by a microswitch arrangement each time after the piezometers had advanced a distance of 1 cm. A certain flow of water was maintained through the columns, using constant head and tail water levels.

Piezometers of different diameters and types of openings were tested. The diameters of the piezometers at the opening were 0.25 inch, 0.15 inch, 0.125 inch, and 0.08 inch. The bodies of the 0.15-inch and 0.08-inch piezometers were tapered while the other two were straight. The openings were an open side hole, a 200-mesh screen opening, a porous glass bead tip, and an open side hole which was shielded (Figure 2). The length of piezometer point beyond the opening on the 0.15-inch screen piezometer was varied from 0.1 inch to 0.8 inch. The different porous materials used were 28-micron glass beads, Laveen loam, Adelanto loam, and Pine silty clay. The pressures were measured with a Sanborn model 267B pressure transducer and a Sanborn model 312 amplifier-indicator. The signal from the amplifier-indicator was recorded on a millivolt recorder.

RESULTS AND DISCUSSION:

Soil Disturbance During Piezometer Insertion. Inserting the piezometers into the soil changes the particle arrangement with attendant change in the void ratio, water content, and pore water

pressure of the soil in the area around the piezometer. Thus, the pressures measured by the piezometer during insertion represent the condition of a local disturbance rather than that of a soil mass as such.

The magnitude of the pressure disturbance depends on the extent of the zone of stress changes, the permeability of the soil, and the consolidation and shearing characteristics of the soil. The change in stress conditions may be from compaction or shear. Compaction will cause a zone of increased pore pressure and may decrease the permeability in the area around the piezometer. If shearing of the soil occurs, the shear strain may either increase or decrease the pore water pressure depending upon the initial density and the stress history of the soil. Soils with a dilatant structure, i.e., soils in which there is a net increase in void ratio as the soil shears, will show a reduction in pore water pressure when shearing. This usually occurs in dense sands and overconsolidated cohesive soils. Soils with a lower density may show increased pore water pressures when shearing.

The type of disturbance was studied by inserting the 0.15-inch diameter piezometer with a screen opening into columns of 28-micron glass beads. The glass beads were used to eliminate effects due to smearing or plugging of the piezometer opening. Tests were run on samples with initial void ratios between 0.5 and 0.6. A typical recorder trace for the different depths of penetration of the piezometer is shown in Figure 3. The arrows indicate the beginning and end of piezometer movement. The solid line is the path of the measured pressure while the dashed line represents piezometric head changes if no disturbance or time lag was occurring in the system. A negative pressure difference is present when the solid line is below the dashed line. A positive pressure difference is present when the solid line is above the dashed line.

The effect of initial void ratio upon the pressure difference is illustrated in Figure 4. The pressure difference when the piezometer movement ceased, Δu_0, is plotted against void ratio

for three different insertion speeds. It appears that Δu_0 was positive for the higher void ratios and negative for the lower void ratios. This shows that the soil disturbance is due to shear rather than compaction.

The pressure difference in a given porous material increases with increasing insertion speed (Figure 4) and increasing diameter of the piezometer. The pressure difference was not affected by the length of piezometer point beyond the opening. The pressure disturbance is also a function of soil permeability. This was indicated by the observation that Δu_0 changed from -22 to -84 cm for a ten-fold decrease in permeability. Thus, the pressure difference is caused by a disturbance that is generated at a faster rate than can be dissipated through the medium.

Effect of Piezometer Opening on Response Time. Response time of a piezometer system is the time required for the pressure in the piezometer to become essentially equal to that of the soil mass at the piezometer opening. This response time is a function of the volume of the fluid that has to flow either in or out of the piezometer, the permeability of the soil, and the size and type of piezometer opening. The response time follows a typical exponential decay curve. The time constant of the piezometer system is expressed by equation

$$T = V F^{-1} k^{-1}$$

where T = the time constant,

k = hydraulic conductivity of the soil,

V = volume of water entering the system per unit head difference,

F = factor that depends on the shape and size of piezometer opening.

The time constant is defined as the time required for a piezometer to register 63 percent of an initial pressure difference. The factors in the right hand part of the equation may change during and after insertion of the piezometer, thus affecting the time constant. Smearing of the soil decreases k in the area adjacent to the piezometer opening. Plugging of the piezometer opening will decrease

the value of F. Gas bubbles in the piezometer system or in the soil will cause some compressibility in the system resulting in larger volume displacement.

The response time of the different piezometer openings was measured in the four different soil materials to determine which design would result in a minimum amount of plugging and smearing of the opening. The response of the piezometers was expressed by the time constant calculated from the pressure vs. time curve resulting from an instantaneously applied pressure difference.

Figure 5 shows the time constant in relation to k of the different soil materials for each piezometer opening tested. The open side hole piezometer did not respond in the Adelanto and Pine soils and is, therefore, not included. The equations on the curves are for the best fitting lines through the points as calculated by the method of least squares. If no smear occurs, the exponent of k should be -1. The exponent of k in the best-fitting equations therefore can be used to express the relative degree of smearing for the different piezometer openings.

The shielded piezometer had a minimum amount of smear with an exponent of -1.58 as compared to -2.09 and -2.18 for the screen opening and porous tip piezometers, respectively. Although the opening on the shielded piezometer has a smaller intake area than either the screen or the porous tip, the shielded opening apparently offered more protection against plugging because the opening is recessed. The screen opening is on the side and is subject to more smear and plugging. Because of its larger opening, however, the response times of the screened opening are comparable to those of the shielded opening. In contrast to the shielded and screen openings, the porous tip is on the end of the piezometer, where it has no protection and, consequently, it is easily plugged. The response of the porous tip was three to four times slower than that of the screen opening. For a soil with a k of 0.001 cm/min, the 95 percent response for both the shielded and the screened piezometer would be between 20 and 25 minutes.

SUMMARY AND CONCLUSIONS:

The dynamic response of different types of piezometers during insertion and the subsequent equilibration were studied on laboratory columns of different soil materials to determine piezometer design features conducive to minimum disturbance and fast response. A pressure transducer of very small volume displacement and a millivolt recorder were used to record the piezometric heads.

Instantaneous pressure distortions during insertion of the piezometer resulted from soil stress changes due to shear. The magnitude of the pressure distortion, which was positive in loose soil and negative in dense soil, increased with increasing diameter of the piezometer, with increasing insertion speed of the piezometer, and with decreasing hydraulic conductivity of the soil.

Measurement of the hydrostatic response time for four different piezometer openings indicated that plugging and smearing were causing an increase in the response time. The effect of plugging and smearing was less in the screen and shielded type piezometer openings. The open side hole piezometer became plugged and did not respond in the heavier soils. Response of the porous bead tip was from 3 to 4 times greater than that for the screen opening.

To obtain fast response and minimum soil and pressure distortion, small-diameter piezometers with shielded (recessed) or screen-covered openings should be used.

PERSONNEL: Herman Bouwer and Robert C. Rice.

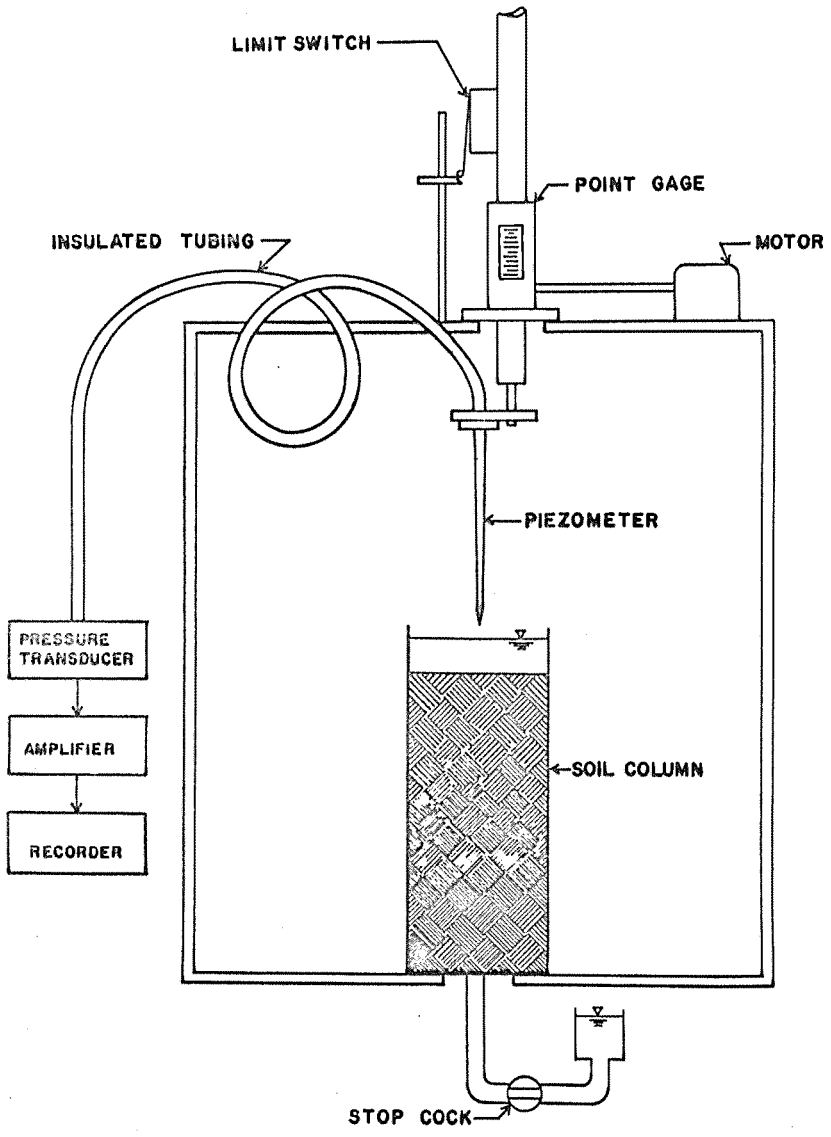

Figure 1. Piezometer testing apparatus.

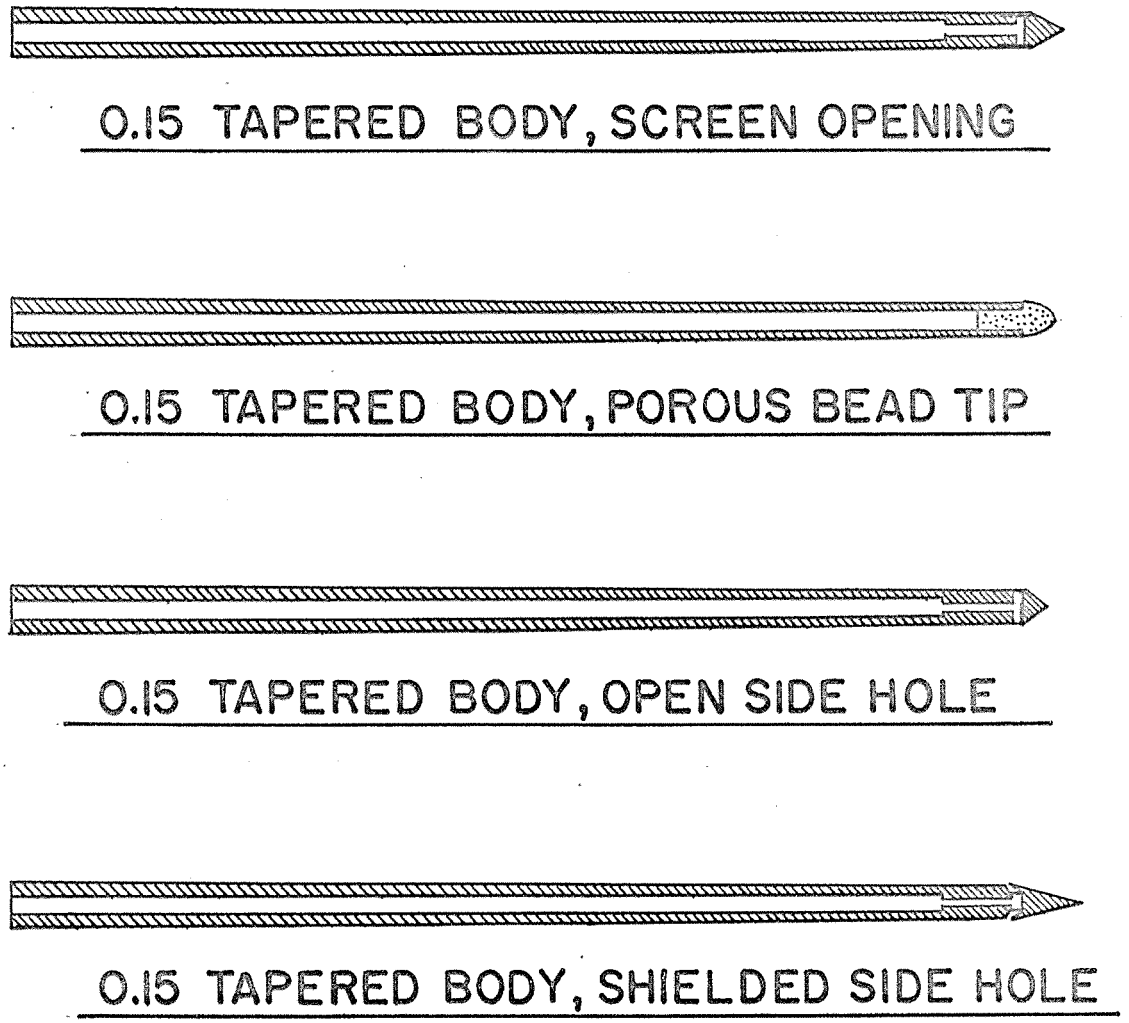

Figure 2. Piezometer openings.

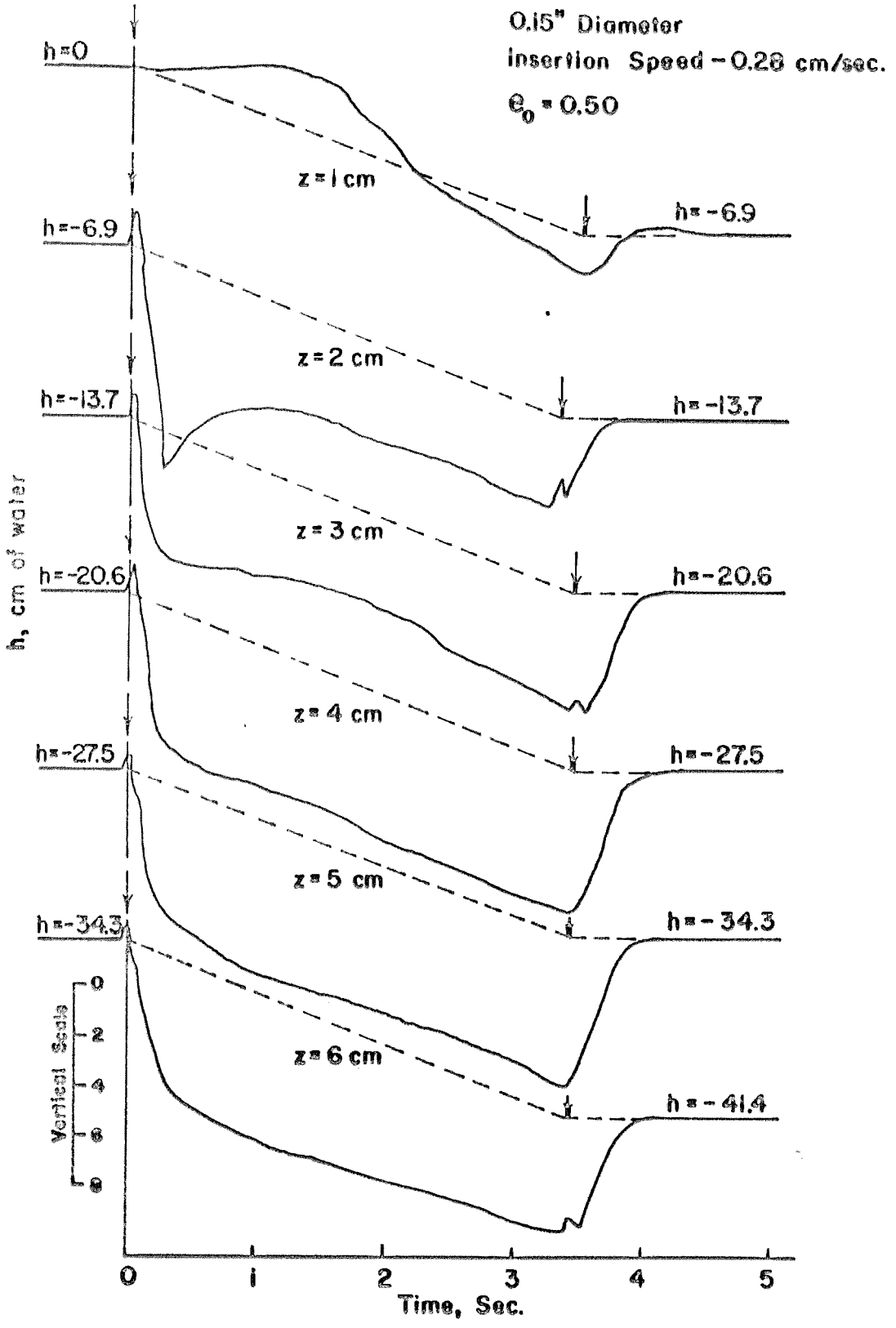

Figure 3. Recorded piezometric head, h, as piezometer is inserted for six successive increments of penetration to a total depth of 6 cm.

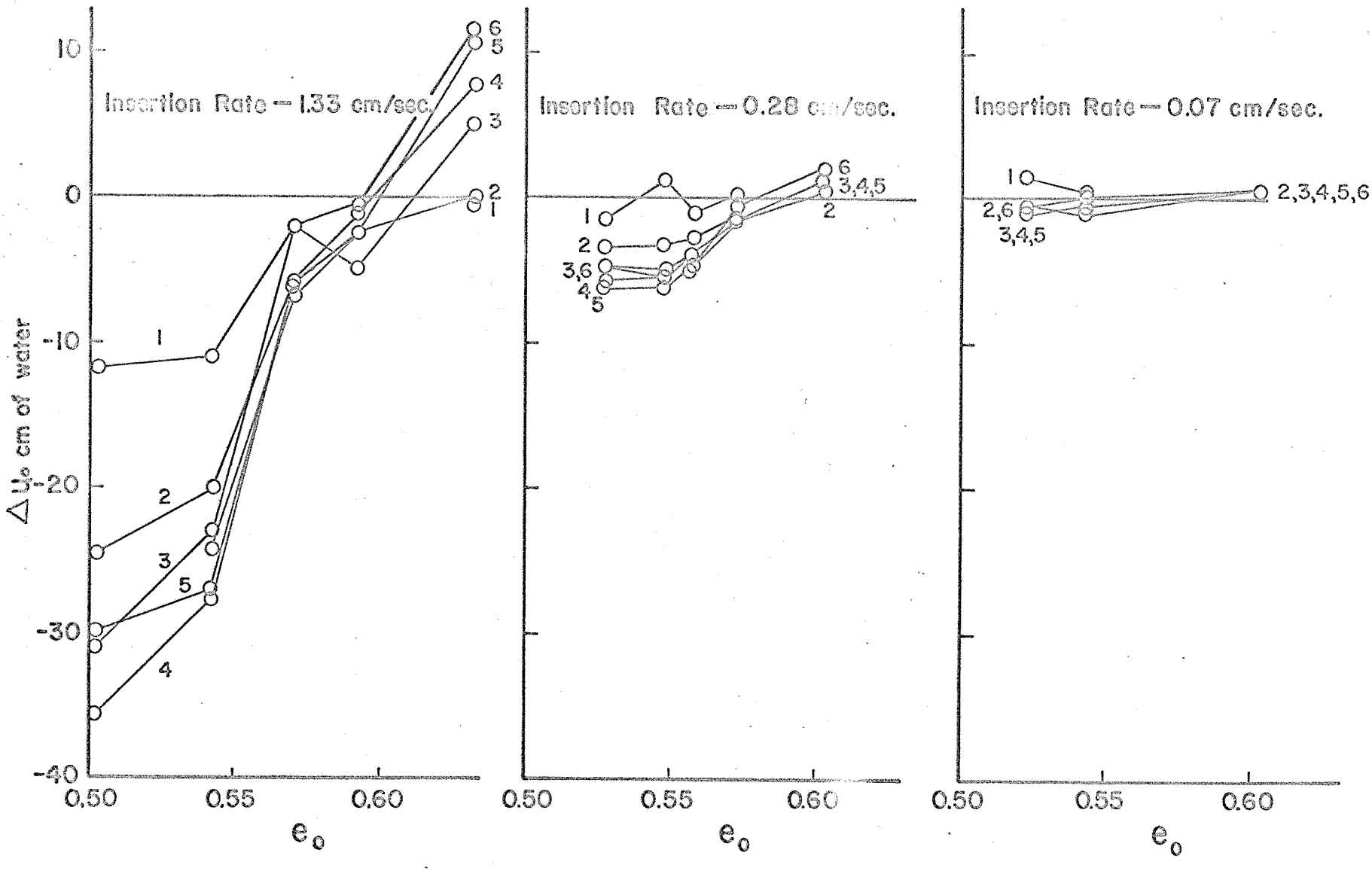

Figure 4. Pressure difference when piezometer movement ceases, Δu_0, in relationship to void ratio, e_o, for different insertion rates and depths of penetration (on the curves).

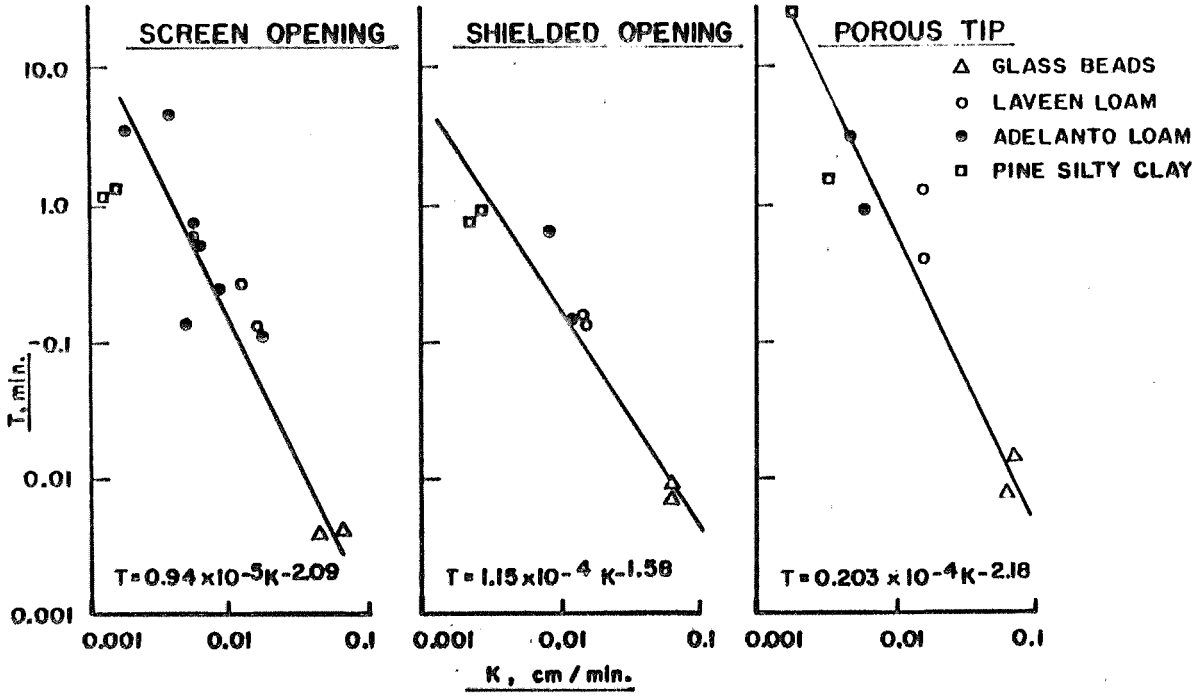

Figure 5. Time constant, T, for different hydraulic conductivity rates, K, and piezometer openings.

TITLE: WATER ABSORPTION, TRANSPIRATION, AND INTERNAL WATER BALANCE OF COTTON PLANTS AS AFFECTED BY CHANGES IN EVAPORATIVE DEMANDS

LINE PROJECT: SWC 11-gG1 CODE NO.: Ariz.-WCL-29

This report is made up of five parts, followed by a General Summary and Conclusions section pertaining to all of the work done.

PART 1. EFFECT OF LIGHT INTENSITY ON LEAF DIFFUSION RESISTANCE OF CROPS

INTRODUCTION:

The information in this section complements similar data presented in the 1964 report. The data as a whole deal with a total of eight species belonging to five plant families, and therefore should lend validity to a generalization about the effect of light intensity on crops. More details can be obtained in the previous report, but a brief restatement of the objective is pertinent here. It was desired to evaluate the effect of the single factor, light intensity, on leaf diffusion resistance without the interaction of leaf water potential or carbon dioxide content of the air. As stomates open, leaf diffusion resistance decreases; another objective was to determine the minimum leaf diffusion resistance obtainable in a controlled environment, as compared to field conditions.

PROCEDURE:

As described more fully in the 1964 report, the plants were grown in nutrient solution in the greenhouse until they reached a vigorous vegetative growth; then they were taken to the controlled environment room. After preconditioning overnight at 30C $\pm$ 0.2 air temperature, 15.0 $\pm$ 0.2 mb vapor pressure, and 375 $\pm$ 10 ppm carbon dioxide content of the air, the plants were exposed to gradual increases of light intensity. Measurements of leaf temperature and leaf diffusion resistance were made periodically, until the maximum fluorescent light intensity obtainable at a given representative leaf was obtained. The two leaves measured on each plant showed essentially parallel results. The data for only the upper leaf are presented graphically in Figures 1, 2, and 3.

RESULTS AND DISCUSSION:

The overall effect of light on alfalfa, lemon, and sorghum is the same as shown previously for five other crops; namely, a decrease in leaf diffusion resistance with increasing illumination, occurring because of stomatal opening. Opening was verified by means of silicone rubber impressions and microscopic measurements.

The apparent difference in response of upper and lower epidermis of alfalfa to a given light intensity was not correlated with stomatal frequency, in contrast to the case for lemon leaves. In lemon only a slight lowering in leaf diffusion resistance occurred in the upper epidermis, even at 3000 ft-c, compared to darkness. The leaf diffusion resistance of the lower epidermis was decreased appreciably by higher light intensity, as in other species. Significantly, the stomatal frequency in the lower epidermis in lemon was 80,000 cm^{-2}, compared to only 4,000 cm^{-2} in the upper epidermis. Lemon was the only species to demonstrate such a clear relationship between the total stomatal aperture and leaf diffusion resistance. Although the stomatal width in the upper epidermis increased greatly as light intensity was raised, an insufficient total area was available for the rapid escape of water vapor.

As in the other species studied, the highest light intensity used (3000 ft-c) was not adequate to induce minimal leaf diffusion resistance, i.e., full stomatal opening, as judged by the nonflattening of the leaf resistance curve with high light intensities. This fact lent considerable support for the decision to convert the light source in the controlled environment room from fluorescent to mercury vapor lamps, which is now in process.

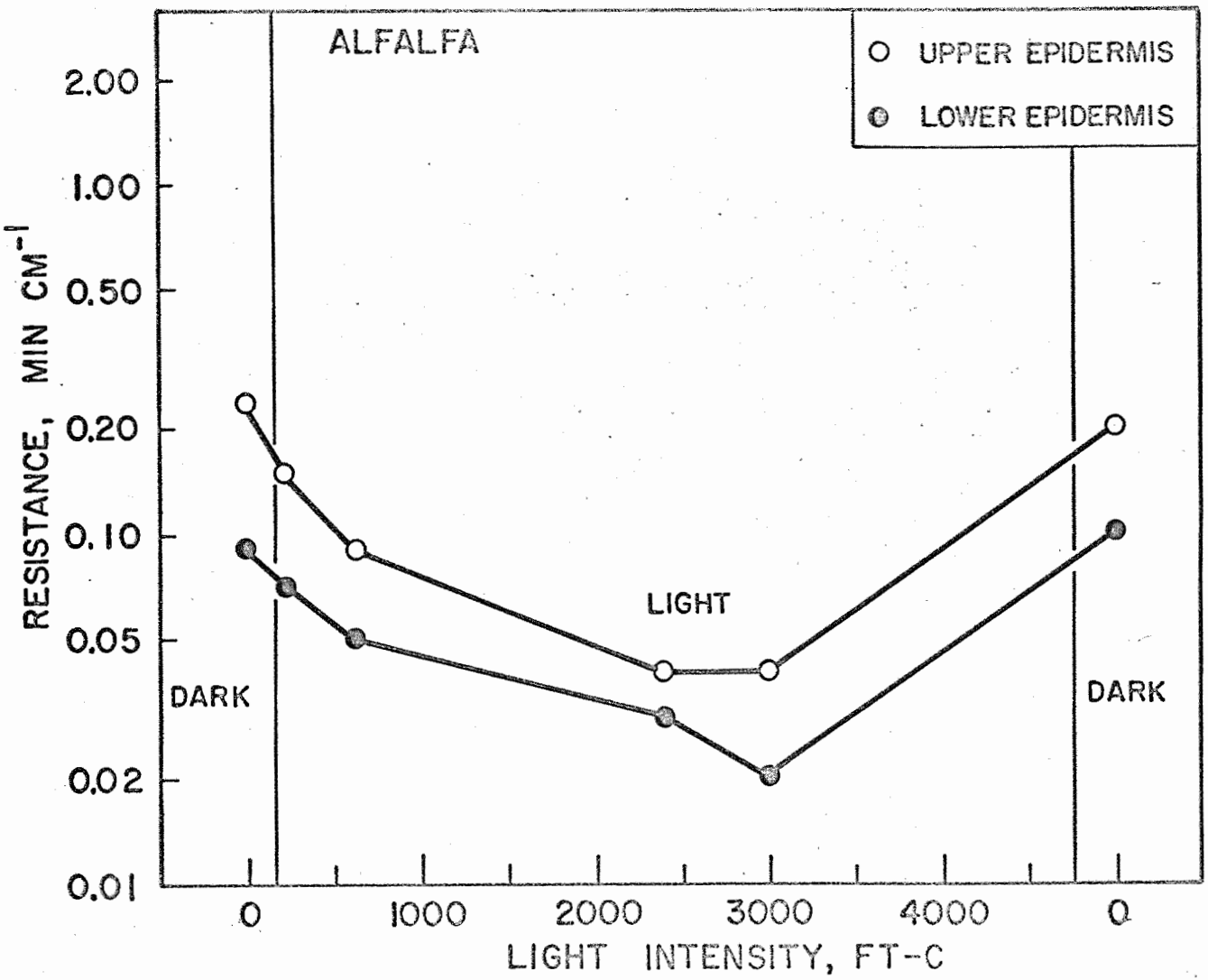

Figure 1. Effect of light intensity on leaf diffusion resistance of alfalfa.

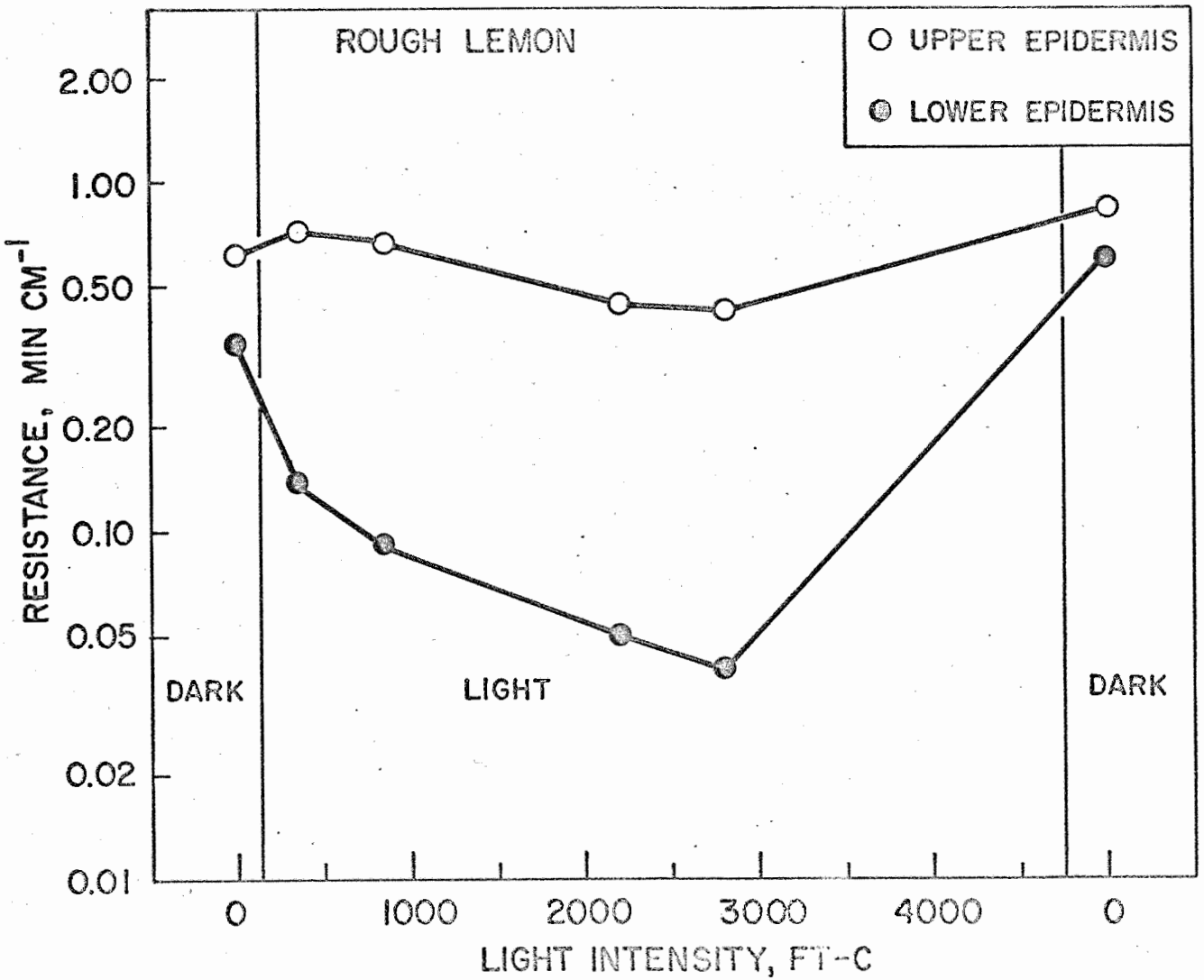

Figure 2. Effect of light intensity on leaf diffusion resistance of Rough Lemon.

Annual Report of the U.S. Water Conservation Laboratory

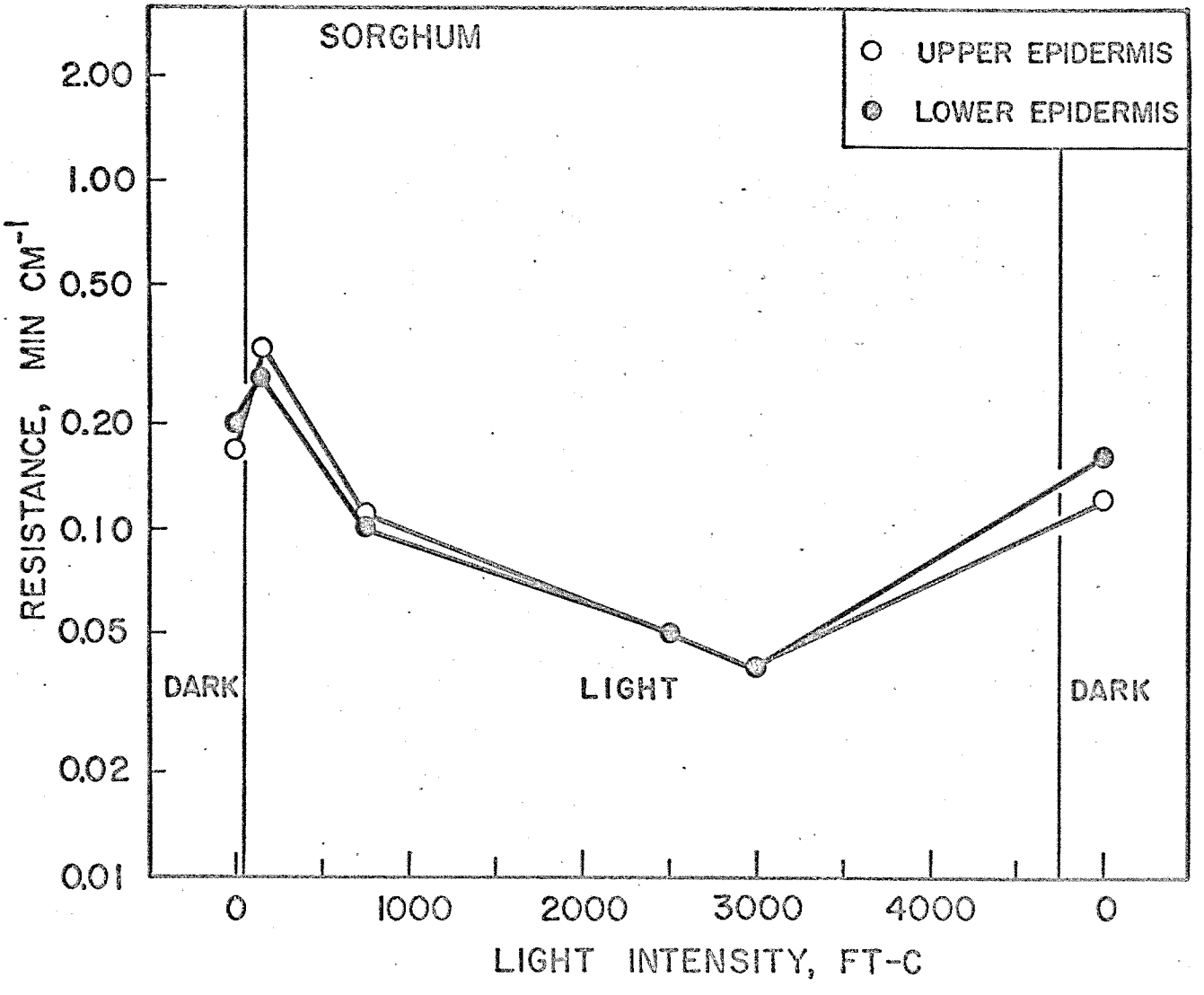

Figure 3. Effect of light intensity on leaf diffusion resistance of sorghum.

PART 2. TRANSPIRATION AND LEAF DIFFUSION RESISTANCE

INTRODUCTION:

Precise measurement of leaf diffusion resistance (R_L), boundary layer resistance (R_A), and the gradient in vapor density from leaf to air (Δd_v) would supply all the information needed to calculate transpiration (E), according to the equation

$$E = \frac{\Delta d_v}{R_A + R_L} \quad .$$

The measured value of transpiration from gravimetric determinations would serve as the reference standard for the calculated values. Good agreement between measured and calculated transpiration rates would enhance our understanding of the whole evapotranspiration process. Experiments were carried out, making use of this model. The data for cotton presented in the 1964 report were extended to sunflower and lemon to make the results more comprehensive.

PROCEDURE:

For greater detail, see the 1964 report. Briefly, the plant in nutrient solution was maintained in a steady aerial environment (30C $\pm$ 0.2 air temperature, 15.0 $\pm$ 0.2 mb vapor pressure, 375 $\pm$ 10 ppm CO_2). Since ambient vapor pressure was held steady, at a known leaf temperature (from thermocouple measurements) Δd_v was known, assuming saturation vapor pressure inside the leaf. Blotter paper measurements from synthetic plants established R_A. Knowledge of R_L from direct measurements on the leaf then permitted calculation of transpiration. This was done in steady conditions of darkness followed by high light intensity for sunflower and Rough Lemon.

RESULTS AND DISCUSSION:

Table 1 shows that calculated values considerably overestimated measured transpiration rates, especially in cotton. The greatest discrepancy was for lemon in the dark. However, this is not believed to be as important as the disagreement in the other comparisons, since with lemon the extremely low transpiration rate in the dark

gave poor accuracy in weight loss measurements. This is in contrast to the data for lemon in the light, as well as to comparisons for the two other species where the measured value (from weight loss measurements) must be considered as accurate. Even when the transpiration rate was high enough to determine weight loss accurately, however, indications are that greater discrepancies occurred at low than at high light intensities.

It should be noted that the best agreement, where calculated was 120 percent of the measured value in both sunflower and lemon, was obtained with two species that differ considerably, both in general morphology and transpiration rate, sunflower's loss being 172 percent that of lemon. Despite differences in leaf shape and size, however, the boundary layer resistance was essentially the same in both species. Therefore, the much greater transpiration rate in sunflower is due primarily to the loss of water vapor from both surfaces of the leaf, in contrast to lemon, in which loss from the upper epidermis is negligible, even in high light intensity.

Although the data demonstrate real progress in measuring all factors pertinent to transpiration, the agreement between calculated and measured values is not acceptable in terms of meeting the objective of a complete characterization of the transpiration process. It is believed that the gradient for water loss and the boundary layer resistance have been measured with satisfactory accuracy, but that leaf diffusion resistance values may be at fault. The value of R_L relative to that of R_A makes R_L a very sensitive determinant of transpiration. For example, for case two, sunflower, an R_L value of 0.060 min cm^{-1}, instead of the listed value of 0.037, would have given equivalent calculated and measured transpiration, assuming other factors the same.

Recalibration of the leaf resistance meter has given the same factor as before (see Part 3) for calculating R_L values. However, this fact merely establishes good precision rather than accuracy. Ultimately a completely different method of calibration may have to be used for confirmation or refutation of R_L values used in the above calculated transpiration.

Table 1. A comparison of measured and calculated evaporation from cotton, sunflower, and Rough Lemon, as affected by both plant and environmental factors*

Species	Light intensity	Leaf temperature	Δd_v	R_A	R_l, mean of all leaves: Lower epidermis	R_l, mean of all leaves: Upper epidermis	Total evaporation: calculated	Total evaporation: measured	Calculated/ Measured
Cotton	87	29.0	18.32	0.029	0.192	0.427	12.30	6.28	1.96
	3800	31.5	22.90	0.029	0.120	0.184	26.20	13.40	1.96
Sunflower	0	28.0	15.89	0.025	0.150	0.319	13.70	8.92	1.53
	3400 (I)	26.9	14.16	0.025	0.023	0.032	54.30	44.60	1.22
	3400 (II)	28.6	16.83	0.025	0.037	0.071	44.60	32.60	1.37
Rough Lemon	0	29.2	16.63	0.024	0.224	0.876	8.55	3.03	2.82
	2800	30.0	18.05	0.024	0.040	0.580	31.20	25.80	1.21

* Light intensity, ft-c; leaf temperature, degree C; Δd_v, $\mu g\ cm^{-3}$; R_A and R_L, $min\ cm^{-1}$; evaporation, $g\ cm^{-2}\ min^{-1} \times 10^{-5}$.

PART 3. RECALIBRATION OF THE LEAF RESISTANCE METER CUPS

INTRODUCTION:

The 1964 report (Part 2, page 29-7) described a direct method to measure transpiration resistance by use of a leaf resistance meter employing a cup attached momentarily to a leaf surface. Since that time, three new cups have been constructed for use with either of the two meters available. Although the cups were replicas of the original, it could not be assumed that they necessarily would have the same calibration factor as the first cup. Therefore, all four cups were calibrated. Calibration permits quantitative expression of leaf diffusion resistance (R_L) in min cm^{-1} or sec cm^{-1}, according to the following:

$$R_L = (S\Delta t - L_o/D)$$

in which S is an instrument constant, or sensitivity in cm min^{-1}, L_o is a characteristic diffusion length for the cup in centimeters, and D is the molecular diffusivity of water vapor in air in cm^2 min^{-1}.

A second objective was to extend the calibration beyond the 40C achieved before to include the range of leaf temperatures encountered in the field.

PROCEDURE:

Calibration consisted of exposing the cup to water-vapor sources of known diffusion resistance by varying the diffusion path length from a free-water source to the cup and recording the transit time. This process was repeated at several temperatures to account for changes in water-vapor diffusivity and response of the humidity sensor in the cup. The temperatures used were 6.0, 16.0, 27.2, 27.5, 41.8, and 47.3C, at path lengths of 0, 1.00, 2.62, and 4.82 cm. Different lengths of lucite cylinders with the same internal diameter as that of the leaf resistance meter cup were inserted instantaneously between a water-saturated porous plate and the cup. Then the time was recorded for water vapor to pass from the free-water surface to the cup, as judged

by a change in electrical resistance on the meter. Separate calibrations were run for half-scale and full-scale readings. A path length of zero — that is, with the cup flush with the wet porous plate — essentially recorded the sensor response time (designated L_o above). The temperature of both the free-water surface and the air surrounding the cup were measured with thermocouples to $\pm$ 0.2C.

Further evaluation followed the procedure outlined in the paper "Measuring transpiration resistance of leaves," C. H. M. van Bavel, F. S. Nakayama, and W. L. Ehrler, Plant Physiology, 40:535–540, 1965. This consisted of plotting diffusion path length against transit time for each temperature. From each of these linear plots the slope of the line was calculated. Also, L_o was obtained by extrapolation to zero path length. The slope at each temperature plotted against temperature gave S, the sensitivity factor mentioned above.

All the data from the four cups at six temperatures were used to obtain S. A computer analysis provided a least-squares best fit, a quadratic equation, and evaluated the constants a, b, and c for this equation. From these data the value of S at each whole degree centigrade from 0C to 50C was tabulated for use in calculating R_L when supplemented with D (water vapor diffusivity), L_o, and Δt (the stop watch transit time).

The S value obtained from the pooled data of four cups was almost identical to that established with the old cup. One change in routine calculations that was inaugurated was expression of R_L in sec cm^{-1} instead of min cm^{-1} to conform with the usage of a majority of present researchers in this field. The tables were calculated so as to include this change without the need of an additional computation.

PART 4. LEAF DIFFUSION RESISTANCE OF SORGHUM IN THE FIELD AS AFFECTED BY SOIL-WATER POTENTIAL

INTRODUCTION:

The increase in leaf diffusion resistance (R_L) during stomatal closure can be measured quantitatively with the leaf resistance meter (Annual Report, 1964). Although stomatal opening or closing is a complex process, under normal conditions it is affected primarily by light intensity (see Part 1 of this section). However, a plant water deficit also can lead to stomatal closure (high value of R_L) even in intense illumination. Change in stomatal aperture can be induced and determined by subjecting a crop to a period of water shortage followed by a heavy irrigation and by making periodic measurements of R_L.

When the boundary layer resistance is suitably low, as it tends to be under moderate wind speeds (greater than 1 m sec^{-1}), high values of R_L bring about lowered transpiration. Therefore, it should be possible to correlate lysimetric weight losses with changes in R_L values as soil-water content decreases with time.

PROCEDURE:

As part of a comprehensive study of the evapotranspiration process with sorghum in the lysimeter field (see WCL-33), R_L was measured both on a routine basis during the growth cycle and intensively at critical stages of soil-water potential. During the intensive periods, lasting 24 hours, R_L was measured about every half-hour, or more frequently when the plants were responding rapidly. Leaf resistance measurements were made on a mature leaf near the tip of the plant on two plants in each of the three lysimeters. Measurement sites were shifted upward as the plants grew, but later in the season remained on the flag leaf, which subtends the inflorescence. At times supplementary R_L measurements were made in two field sites near the lysimeters. On intensive days R_L readings were begun at midnight and continued for 24 hours. They were accompanied by measurements of leaf thickness, leaf temperature, and various soil and meteorological parameters, in addition to precise determinations of evapotranspiration with three lysimeters.

RESULTS AND DISCUSSION:

Soil water was not depleted sufficiently during the June drying cycle to bring about a significant plant response. Therefore, only the data for the July and August series are presented. Figure 4 demonstrates hourly R_L values, each an average of upper and lower epidermes of six leaves, two from each of the three lysimeters. Whether the soil was well irrigated (20 July, soil-water content 0.228 by volume in whole lysimeter profile, 1.6-m depth) or practically devoid of available water (13 July, soil-water 0.163), R_L values were high at night, about 30 sec cm^{-1} or more. The lack of data for the first six periods for 20 July is due to dew formation on the leaves, which precludes meaningful R_L measurements. However, there is no doubt that the stomates were closed during this time (from midnight to 0600), as shown by similar measurements made at night on well-watered plants when dew did not form.

The minimum R_L values during daylight on 20 July, less than 1 sec cm^{-1}, coincided with wide stomatal aperture and high evapotranspiration, and is consistent with the known effects of light on R_L. The significantly higher R_L values on 13 July, around 8 sec cm^{-1}, occurring in strong illumination, demonstrates the effect of low soil-water availability on plant behavior. The lysimeters showed much lower evapotranspiration on 13 July than on 20 July. However, since important meteorological factors are not likely to be identical on two days, a better comparison is the actual evaporation (E) with the potential amount (E_o). On 13 July the increased R_L was associated with a reduction in evapotranspiration to about half the calculated potential rate. The R_L values measured directly on individual leaves are not identical with the canopy or crop surface resistance (R_S), but they are proportional to it.

The August data confirmed the July evidence in that R_L values increased during the greater part of the day whenever soil water was sufficiently depleted for stomates to start closing. That sorghum is resistant to soil-water depletion is shown by a difference in plant response between lysimeters 1 and 2, treated as a unit, compared

to lysimeter 3. Earlier, an accidental overirrigation of lysimeter 3 caused a persistent lag in soil-water depletion, as compared to the two other lysimeters. Later this resulted in a plant response in lysimeters 1 and 2 of sufficient magnitude to necessitate a 24-hour intensive study, although the plants in lysimeter 3 had not reached the stage of significant stomatal closure in daylight.

A comparison of Figures 5 and 6 makes these differences in plant response apparent. In lysimeter 3 the daylight R_L values averaged about 1 sec cm^{-1} for either of two experimental days, 5 and 10 August. In contrast, although the mean R_L values for lysimeters 1 and 2 were low on 10 August, about 1 sec cm^{-1}, they were as high as 18 sec cm^{-1} on 5 August. It is pertinent to point out that the soil-water content values were consistent with the different responses among lysimeters. For example, on 5 August lysimeters 1 and 2 averaged 0.154 volumetric water content in the lysimeter soil profile (1.6-m depth), compared to 0.181 for lysimeter 3. After irrigation the soil-water content in all lysimeters exceeded 0.250, measured 9 August. Apparently sorghum stomates do not close in daylight until the plant is subjected to a severe soil-water deficit. No measurements of plant water potential were available. Instead, leaf water content was measured by means of beta ray gauging (see Part 5, this section).

When loss of plant turgor is sufficient to affect the guard cells, stomates close and thereby build up leaf diffusion resistance enough to diminish evapotranspiration significantly, as demonstrated by the lysimeter records (see WCL-33 of this Annual Report). Thus, the data show the hypotheses stated earlier to be well founded.

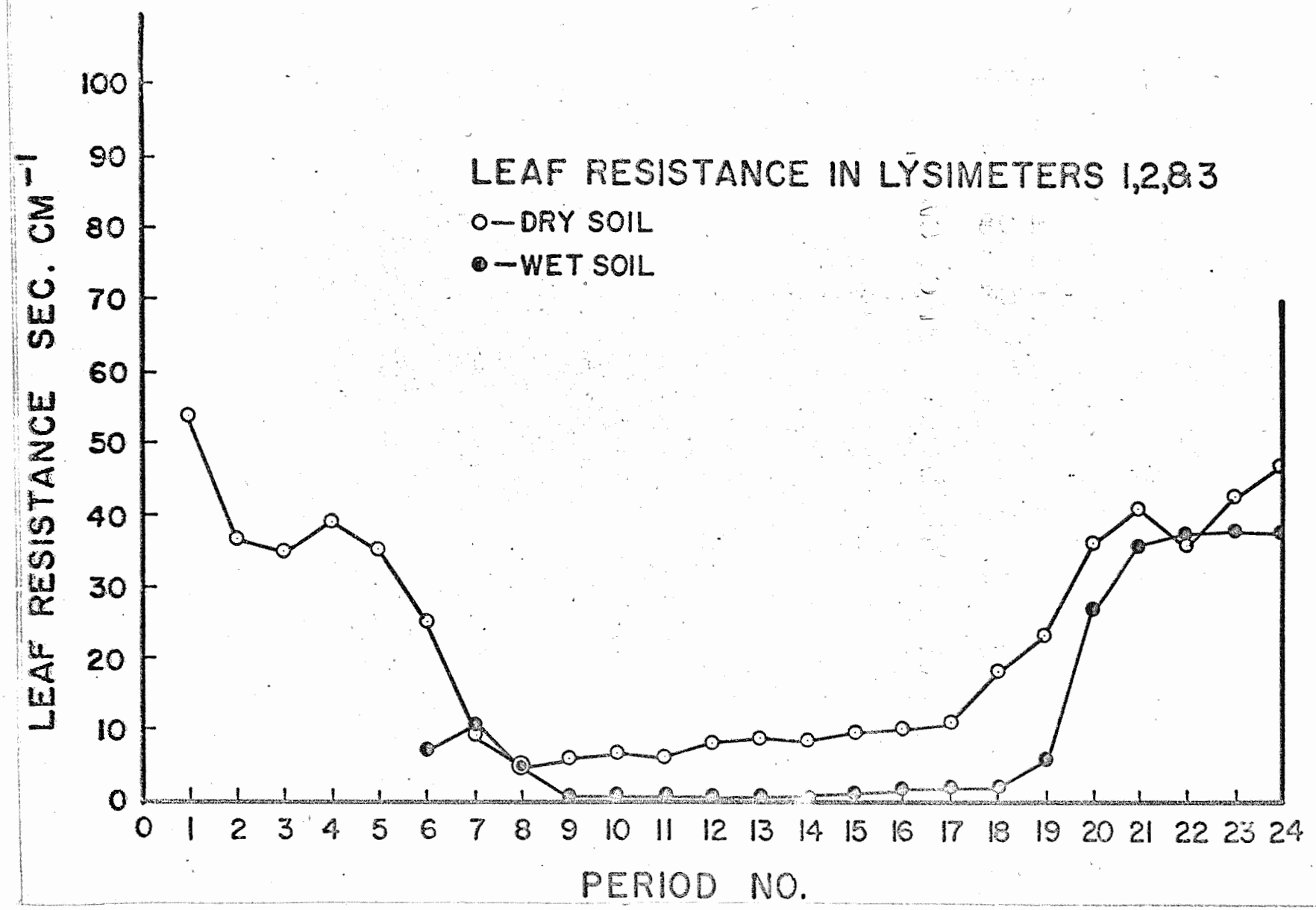

Figure 4. Average leaf diffusion resistance in lysimeters 1, 2, and 3 for a 24-hour period when the soil was dry (13 July 1965) and recently irrigated (20 July).

Annual Report of the U.S. Water Conservation Laboratory

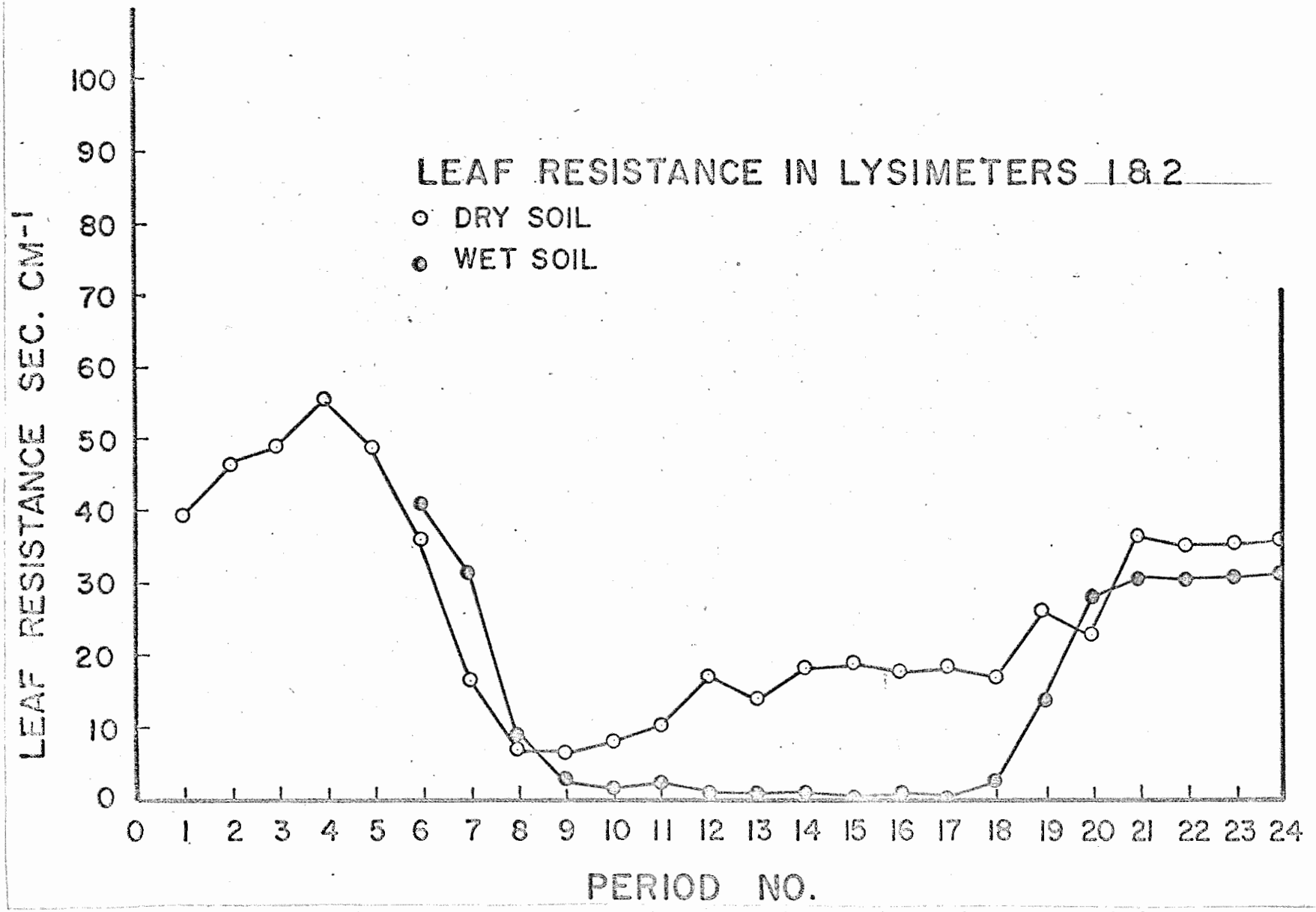

Figure 5. Average leaf diffusion resistance in lysimeters 1 and 2 for a 24-hour period when the soil was dry (5 August 1965) and recently irrigated (10 August).

Annual Report of the U.S. Water Conservation Laboratory

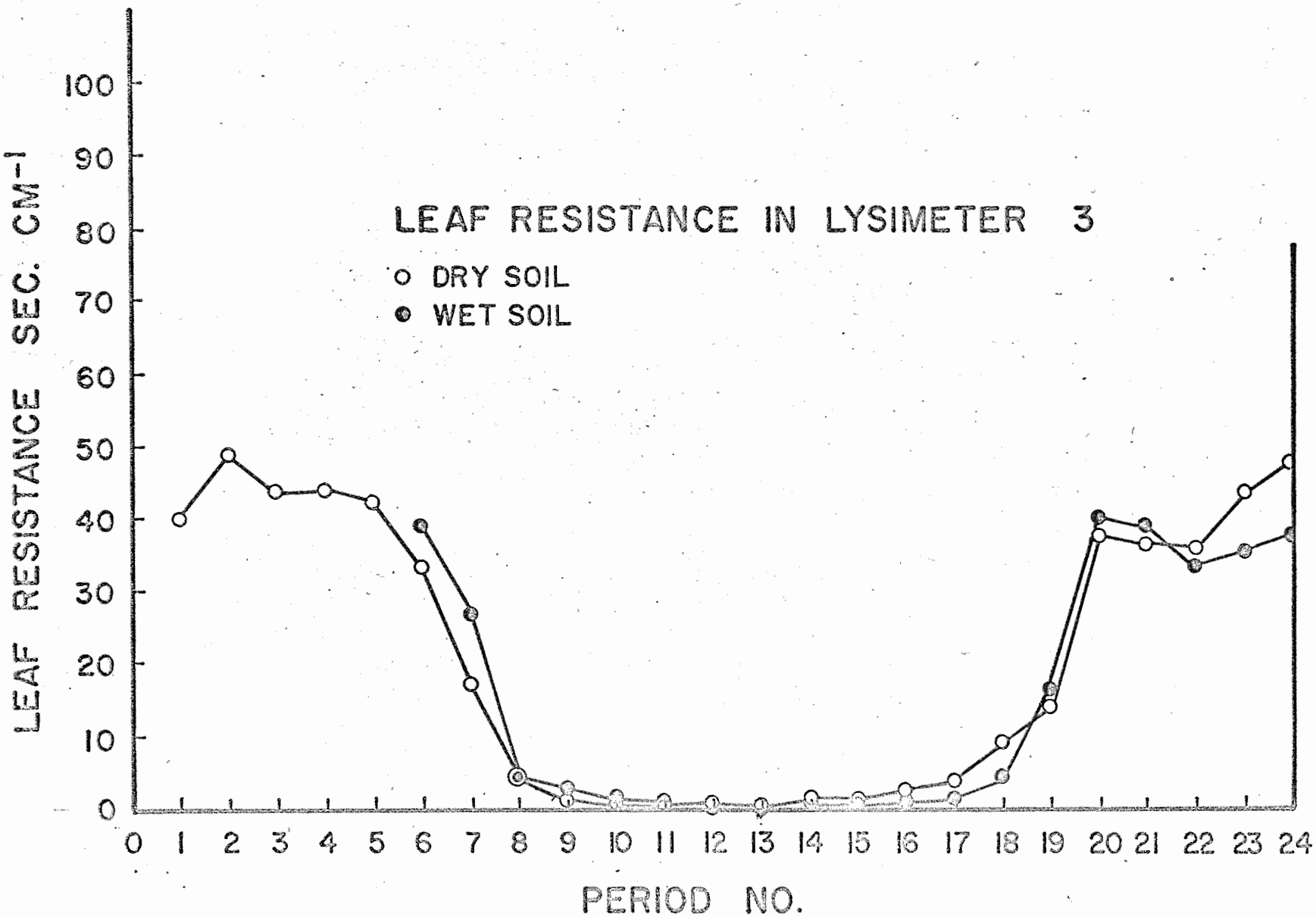

Figure 6. Average leaf diffusion resistance in lysimeter 3 for a 24-hour period when the soil was moderately dry (5 August 1965) and recently irrigated (10 August).

Annual Report of the U.S. Water Conservation Laboratory

PART 5. LEAF WATER CONTENT OF SORGHUM AS AFFECTED BY SOIL-WATER POTENTIAL

INTRODUCTION:

A continuous record of plant water balance can be obtained by measuring changes in the water content of a representative attached leaf by the beta ray gauge technique ("Transpiration, water absorption, and internal water balance of cotton plants as affected by light and changes in saturation deficit," W. L. Ehrler, C. H. M. van Bavel, and F. S. Nakayama, Plant Physiology, January 1966.). In the field leaf water content at dawn is assumed to be maximal, and thus serves as a reference point for the diurnal cycle in plant water balance. The commonly observed decrease in leaf water content during the day follows from relatively fast stomatal opening combined with sluggish transmittal of a water deficit from leaves to roots. Recovery from an internal water deficit is enhanced by stomatal closure and by an increased gradient for water absorption, induced by tissue dehydration.

Diurnal changes in plant water balance were followed in sorghum as a supplement to leaf diffusion resistance (R_L) measurements made in a comprehensive field experiment (see Part 4 of this section). The hypothesis was that the higher values of R_L induced by daytime stomatal closure would be preceded or at least accompanied by a lowered leaf water content. This line of reasoning accepts the commonly held belief that the primary mechanism for stomatal closure is a loss of turgor by guard cells. However, when the turgidity of a whole leaf is used as an indicator of guard cell turgor, this assumes equivalent behavior of guard cells and the other leaf cells. If this assumption is true, one might expect the leaf water content to reach a certain minimal value during daytime stomatal closure. The intensive beta ray gauge measurements were taken to verify this hypothesis.

PROCEDURE:

A beta ray gauge was placed about 20 cm from the apex of a mature leaf on one of the 20 sorghum plants in each of three lysimeters. In some instances the leaf was so narrow that the gauge straddled the midrib. In June the first mature leaf was the third or fourth

back from the tip of the plant (just below the leaf containing a thermocouple). The leaf was carefully selected since its changes in water content had to represent the whole lysimeter. In July and August the beta ray gauge leaf was the next one back from the flag leaf — that is, still being the next one down the stem from where leaf temperatures and R_L measurements were taken.

The gauges were connected by a 100-foot shielded cable to a switch which permitted each gauge to be counted in succession on a Baird-Atomic scaler wired to a rate meter and a Leeds & Northrup strip-chart recorder. The time during which gauge readings were taken on a lysimeter was made to coincide with the readings of leaf resistance during the days of intensive measurement. This gave three intermittent records of leaf water content throughout a 24-hour period beginning at midnight and coinciding with other pertinent measurements. These intensive measurements were made on a total of 6 days (3 pairs of days with contrasting amounts of soil moisture) encompassing irrigation cycles in June, July, and August. Usually it was possible to leave the gauge in place on the leaf at the end of phase I (dry soil), thereby having identical gauge-leaf geometry during phase II, which occurred as soon as feasible after irrigation.

Changes in leaf thickness due to differential gain and loss of water were registered as variations in the count rate of Pm^{147}. By counting different thicknesses of aluminum foil in the gauge, it was possible to express the data from leaves in terms of equivalent aluminum thickness. Calibration was done in the field. The count rate during calibration was read from the rate meter output recorded on a strip chart, rather than directly from the scaler, since the data for changes in leaf thickness during the experiment were obtained in this manner. This procedure was adopted because it permitted overnight records on one gauge during nonintensive periods without an observer.

RESULTS AND DISCUSSION:

All of the six intensive measurement periods showed essentially the same results in regard to change in leaf thickness (leaf water content). Therefore, only one graph is presented to represent the data. Figure 7 shows that leaf water content was greatest at dawn. The leaf underwent a slight dehydration shortly after sunrise and reached its low point of water content in late afternoon. The striking feature is the lack of any appreciable loss in water content. The data are for 13 July, when soil water was severely depleted – enough for leaf diffusion resistance to be high in midday. Despite the lack of easily available soil water, apparently water absorption continued at a rate sufficient to almost balance transpiration. This was reflected in only a slight net loss in leaf water content.

After irrigation, during another 24-hour measurement period, on 20 July, easily available water presumably induced a rate of absorption essentially equal to the rate of transpiration. Therefore, the results were the same as before; namely, essentially no real loss in leaf water content from dawn to midday. This phenomenon undoubtedly is closely related to the abundance of roots that sorghum develops for a given leaf area and is consistent with literature references citing its good drought tolerance.

Since the leaf diffusion resistance measurements on 13 July demonstrated a significant degree of stomatal closure in full daylight, presumably the guard cells underwent a loss of turgidity. Nevertheless, this was associated with no appreciable decrease in overall leaf water content. In reference to the hypothesis set forth in the introduction, it must be concluded that in sorghum, overall leaf turgidity is not closely correlated with that of guard cells. This result from the field is not in accord with the behavior of cotton in the controlled environment room (laboratory), where loss of leaf turgidity, as indicated both by the beta ray gauge and visible wilting symptoms, was closely correlated with stomatal closure; i.e., increased leaf resistance. No research with the beta ray gauge has been done with sorghum in the laboratory, however. Therefore, it must be assumed

that cotton and sorghum react similarly to an internal water deficit.

The lack of correlation between daylight stomatal closure and a decrease in leaf water content in the field, as contrasted with a high degree of correlation between these two parameters in the laboratory, may be due to the difference in the rate of plant dehydration. In the laboratory leaf dehydration was due to a very rapid acceleration in transpiration, occurring in a half-hour or less. In the sorghum field, however, plant dehydration proceeded very slowly and was brought about by a combination of rapid transpiration during midday and a gradually diminishing soil-water availability.

If it is assumed that guard cells have a lower dehydration threshold than other leaf cells, the divergent plant behavior in field and laboratory can be rationalized. When tissue dehydration occurred gradually, as in sorghum, the guard cells were affected before the leaf as a whole, due to their lower threshold of sensitivity. On the other hand, when tissue dehydration was induced rapidly, as in the laboratory, the loss of turgor became quite general throughout the leaf, and thus became grossly detectable by the beta ray gauge, which necessarily is a multicell integrating type of instrument. Further work would be required to test the validity of this hypothesis. This line of reasoning suggests that a rapid plant dehydration of sorghum would be detectable by the beta ray gauge, just as in cotton. It seems desirable to carry out controlled experiments on beta ray gauging of sorghum before additional field experimentation is undertaken. A simple, alternative explanation is that the beta ray gauge just is not so sensitive as the leaf resistance meter, perhaps because the meter is responding primarily to a difference in turgidity of guard cells and other cells, whereas the gauge is responding to an absolute decrease in overall cell turgidity. Therefore, a certain minimum rate of cell dehydration must occur before an appreciable decrease in leaf thickness is detected by the gauge.

One bit of documentation for the hypothesis that the beta ray gauge is sensitive to rapid changes in overall leaf water content was obtained in a side test carried out in the sorghum field between intensive measurement periods. Rapid plant dehydration, admittedly of an extreme nature, was induced by excising a leaf, the cut being made near the sheath, and in air (no water supplied to the detached leaf), when leaf water content was at a steady value. This was done at 0745 on 3 August, and again at 1420 on 4 August (on a similar leaf) with the same results. Leaf water content diminished rapidly immediately after leaf excision, at a faster rate in the afternoon than in the early morning, due undoubtedly to the greater transpiration rate later in the day. On 4 August the counting rate rose from a steady 26,000 cpm to 39,700 cpm in only one-half hour, which represents a decrease in leaf thickness of 4.7 mg cm^{-2}. This decrease is much greater than that shown in Figure 7 for a period of several hours. Even in the early morning (3 August) of the leaf excision test, leaf water content decreased 3.5 mg cm^{-2} in an hour's time following excision (leaf cut in air). These two leaf excision tests seem to demonstrate the validity of the previous hypothesis; that is, when the rate of change in leaf water content is high, the beta ray gauge can detect these losses in overall leaf water content.

The conclusion as to the results of the intensive measurements is still the same: Sorghum in the field undergoes only a slight leaf dehydration, even under an extremely high evaporative demand and practically no available soil water in the whole profile. One approach that might be undertaken in the future is to increase the sensitivity of the beta ray gauge in order to have it more compatible in sensitivity with the leaf resistance meter.

GENERAL SUMMARY AND CONCLUSIONS:

A controlled environment permitted light intensity to be the single variable regulating stomatal aperture; that is without the interaction of internal water balance of the plant or of ambient carbon dioxide level. The general response of 8 plant species was similar, about a 50-fold lowering of the leaf diffusion resistance (R_L) over the range investigated, from darkness to 4000 ft-c. Since the lowest R_L attained still was not as low as field measurements, greater illumination is needed in the laboratory to achieve a realistic radiation environment.

In a controlled environment, transpiration has been calculated from measurements of leaf temperature, ambient vapor pressure, leaf diffusion resistance (R_L), and boundary layer resistance. For cotton, sunflower, and lemon, the calculated values were consistently higher than those of the standard obtained by weighing. However, progress in evaluating all parameters relevant to the transpiration process is demonstrated by achievement of only a 20 percent disparity between calculated and measured values in the two best instances (sunflower and lemon in high light intensity). It is believed that R_L values are responsible for lack of better agreement rather than the other parameters. Since recalibration of the leaf resistance meter gave the same results as before, an entirely different calibration technique may be the only hope of improving the calculated transpiration.

Calibration of four leaf resistance meter cups confirmed the values previously found for the old cup and extended the data to three new ones, over a range from 6C to 50C. The method consisted of simulating stomatal resistances by interposing known diffusion path lengths between cup sensor and a free-water source, and recording the transit time and water vapor diffusivity as affected by temperature and an instrument constant.

Half-hourly measurements of leaf diffusion resistance were carried out on sorghum in three lysimeters. These data were in conjunction with other intensively measured plant and meteorological

parameters and were obtained during two contrasting periods, one wherein soil water content was depleted, followed in a few days by one with freely available soil water. Measurements were made during drying cycles in June, July, and August. In recently irrigated soils, R_L values showed the typical diurnal cycle – high values in the dark, followed by a gradual decrease after sunrise to a minimum of about 1 sec cm^{-1} or less throughout the bulk of the day, and then an increase to the original dark value after sunset. In contrast, when available soil water had been almost completely depleted, which was about one month after irrigation, midday R_L values averaged 10 to 15 sec cm^{-1}, an appreciable resistance due to partial stomatal closure, and were correlated with lysimetric evapotranspiration losses less than half of the potential rate. This increase in R_L demonstrates the effect of plant water deficit on the stomatal mechanism.

A beta ray gauge was installed in each of three lysimeters to detect changes in leaf water content during six 24-hour periods of intensive measurements on sorghum. During the same three drying cycles mentioned above, the results were essentially the same regardless of soil-water content: the leaf lost only a small amount of water content from dawn to midday. This lack of an appreciable loss in turgor by the whole leaf, occurring when stomates were partially closed over the greater part of a clear day, presumably due to turgor loss, may indicate that guard cells are more sensitive to lowered turgidity than other leaf cells. On the other hand, it may be only a reflection of differences in instrument sensitivity (leaf resistance meter versus beta ray gauge). Under conditions that induced a greater rate of change in leaf water content than occurred during normal field measurements, the beta ray gauge reflected plant response as quickly and completely as the leaf resistance meter.

These results still lead to the conclusion that during the intensive experiments sorghum apparently absorbed water at a fast enough rate to resist leaf dehydration, despite low availability of soil water, a capability that may be related to its favorable root-shoot

ratio. Attempts to increase gauge sensitivity might be advisable for future studies of sorghum, by substitution of technetium-99 for promethium-147 as a beta ray emitter.

PERSONNEL: W. Ehrler and C. H. M. van Bavel

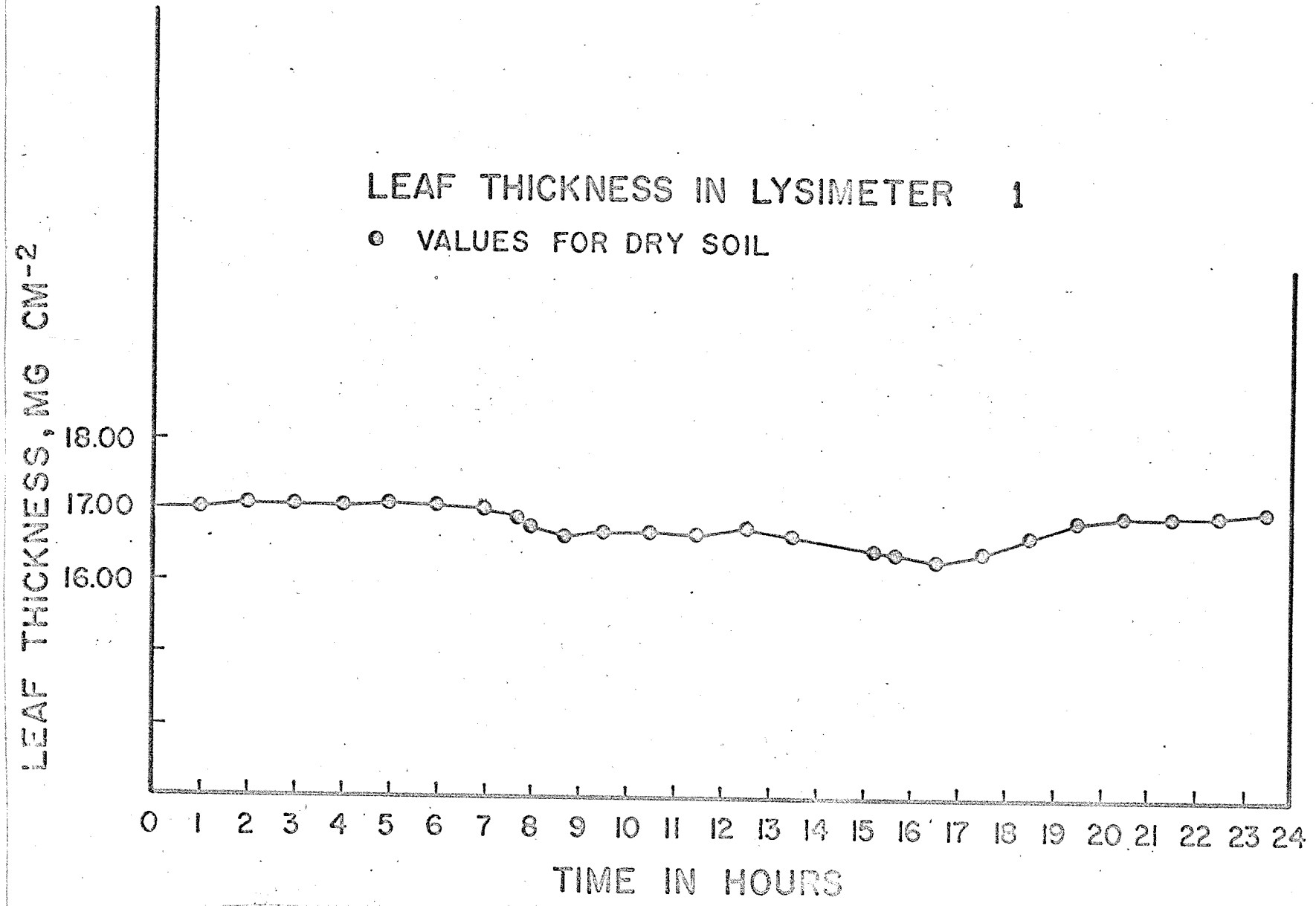

Figure 7. Leaf thickness in lysimeter 1 during a 24-hour period when the soil was dry (13 July 1965). Changes in leaf thickness are assumed to be due to changes in leaf water content.

Annual Report of the U.S. Water Conservation Laboratory

TITLE: QUANTITATIVE MEASUREMENT OF WATER FLOW WITH CHEMICAL TRACERS

LINE PROJECT: SWC 4-gG5 CODE NO.: Ariz.-WCL-30

INTRODUCTION:

See Annual Report for 1964.

PROCEDURE:

Same as for 1964 except as noted.

The procedures for constructing the comparison standards were changed slightly to assure more accurate and reproducible results. One-part-per-billion standards were consistantly and accurately constructed in the following manner:

A laboratory analytical balance was used to weigh 0.2500 ± 0.0002 grams of 20 percent Rhodamine WT solution from the same lot used in the stream flow measurement. This was then washed into 10,000 ± 1 grams of stream water to produce a 5-parts-per-million dilution (± 0.1 percent error). A calibrated 10-ml pipet, found to be repeatable to ± 0.03 percent, was used to transfer 10 ml of the 5-ppm dilution into 50,000 grams of the stream water (approximately 110.23 pounds weighed on a 200-pound capacity platform scales) to obtain a 1-ppb solution. To determine the fluorescence, the solution was recirculated through the fluorometer and back into the 50,000-gram container (20-gallon plastic garbage can) and a second 10 ml of 5-ppm solution added to obtain the 2-ppb fluorescence reading, etc.

Standards were constructed for a range of fluorescence readings covering those of the samples. Since the fluorometer responds linearly for dye concentrations below 100 ppb, only 3 points were needed to establish and check the fluorescence response curve. In these studies, the usual practice was to develop the least-squares linear-regression line using 5 or more points.

The accumulative addition of as many as 10 of the pipet volumes to the 50,000-gram container caused a systematic error of only 0.2 percent in the standards. Thus, errors associated with the dye dilution method of stream flow measurement are essentially those imposed by insufficient mixing, nonuniform sampling rates, and limitations in the accuracy of the fluorometer. The effects of fluctuations of the

fluorometer dial, approximately 1/2 division or less, can be minimized by choosing an instrument sensitivity setting that causes the fluorescence readings of the samples to be near full scale on the dial.

RESULTS AND DISCUSSION:

The fluorescence-temperature response curve of the Rhodamine WT was obtained by a slightly different method than had been used in similar determinations by Pontacyl Pink and Rhodamine B. The previous method produced results slightly lower than that reported in the literature (see Annual Report, 1964).

The temperature recorded on the sample in practice is that obtained in the sample container before the sample has advanced through the connecting hoses and into the fluorometer. The temperature actually occurring while reading is not necessarily the temperature recorded, but since the measuring techniques require a comparison standard to be read with the same hose and pump system, this temperature shift, if any, would effect the comparison standard similarly. Therefore, a test series was arranged to evaluate the temperature coefficient, n, suitable for application to this method of reading samples. The sample was cooled in a water bath to the lower limit of the temperature range of interest, then warmed slowly to the upper limit of interest (10 C to 35 C). By knowing the travel time through the hose to the instrument and continuously monitoring both the temperature rise of the sample and the instrument response, it was possible to plot a semi-logarithmic curve of fluorescence versus temperature, the slope of which corresponded to n. For the Rhodamine B, $n = -0.0269\ C^{-1}$, which agrees with $n = -0.027\ C^{-1}$, reported in the literature. Rhodamine WT had a value for n of $-0.0261\ C^{-1}$. Based on the close agreement for Rhodamine B, the value for Pontacyl Pink B, also reported in the literature, $n = -0.029\ C^{-1}$, was accepted as adequate and not rechecked.

For purposes of further checking the relative adsorption on suspended materials in stream waters, a comparison test was conducted for the three dyes. Two highly turbid solutions were prepared for each dye, one with 1 gram per liter of high-sodium bentonite clay and the other with 1 gram per liter of local canal sediments, both in tap

water with 10-ppb dye concentrations. The sediment concentrations were high compared to those naturally occurring in streams, except perhaps in the bed load of a flash flood. This was intended to exaggerate the effects of adsorption.

Relative fluorescence indications were obtained immediately after the dry sediments were stirred into the solutions and were checked again after about 16 hours without further agitation. After 16 hours, in the canal sediment materials 41 percent of the Rhodamine B dye was no longer detectable while only 6 percent of the Rhodamine WT had been adsorbed. Pontacyl Pink B was not significantly different from Rhodamine WT, indicating a 5 percent loss. In a similar time, bentonite clay adsorbed 96 percent of the Rhodamine B, 65 percent of the Pontacyl Pink B, and 28 percent of the Rhodamine WT. The Rhodamine WT thus appears to be the most suitable of the fluorescent dyes.

The laboratory study, on tracer flow techniques, was extended to include measurements with Rhodamine WT. The laboratory procedures were similar to those used for previous measurements made with Pontacyl Brilliant Pink B (see Annual Report, 1964).

Four sampling pumps were installed in the laboratory channel but could not be placed in the same stream cross section because of their size. Instead, they were randomly scattered in the last 6 to 8 feet of the channel. Table 1 lists the pertinent data for the tests conducted with the Rhodamine WT. The standard deviation was a maximum of 1.9 percent averaging approximately $\pm$ 0.9 percent for all runs. The discharge computed from the four samples in each series varied a maximum of 1.3 percent, averaging only 0.6 percent, from the actual discharge which was determined gravimetrically to $\pm$ 0.5 percent. These differences can be attributed to mixing inadequacies, slight changes in channel flow (noted to be on the order of 0.5 percent due to power fluctuations to the recirculating pump) and limitations in the fluorometer readout. From the laboratory measurements it was concluded that accurate stream flow measurements could be obtained if the effects of tracer losses through adsorption on banks, etc., and inadequate lateral mixing were reduced to negligible amounts.

Field Studies. Field measurements of discharge using Rhodamine B were reported in the Annual Report of 1964. These were conducted in the Arizona Canal about 1 mile east of Scottsdale, Arizona. At that time there was indication that there might be some significant loss of the Rhodamine B to the canal bank. Consequently, a study was set up attempting to evaluate the tracer losses in the canal. This conceivably could be done in the following manner: (a) Inject the tracer at station 1, (b) Sample at downstream station 2 as the tracer wave passes, and (c) Sample either the same wave or a companion wave as it passes station 3 which will be located even further from the injection station. Since the effects of seepage in the canal will not be detected once adequate mixing is achieved, the above procedure would indicate tracer losses as an apparent increase in discharge. The comparison study, as planned, consisted of 2 injections each of the Rhodamine B, the Rhodamine WT, and the Pontacyl Brilliant Pink B, and sampling each dye wave as it passed the 1.2-mile station and the 3-mile station. Due to the physical difficulty of sampling the wave and then moving quickly enough to sample the same wave downstream, the system was designed to use duplicate drops and to calculate the dye lost from the subsequent discharge measurements. However, the study was not completed. Two attempts were aborted, one due to electrical failure in the equipment, and one due to unanticipated rain. This portion of the project will be continued in the forthcoming irrigation season.

Other measurements, designed to check the field comparison with another reliable field method were set up in a 5259-ft long, nominal 4-ft diameter concrete pipe. Rhodamine WT was used. The discharges were compared with those determined with a Cole pitometer supplied and operated by Salt River Project personnel. The pitometer was calibrated in our laboratory by traversing the flow in a 12-inch pipe. The flow rate determined with the pitometer was compared with the weighed discharge. The pitometer curves delivered with the instrument were found to need correction by -5.4 percent. This calibration was then used in the field studies.

Measurements were made on the same pipe on two days, 12 July and 14 July. In addition to the pitometer data obtained by the Salt River Project personnel and the dilution measurements, time of travel measurements from the time of injection until the arrival of the peak were also obtained. The pertinent data are summarized in Table 2. On the first day, the time of travel comparison with the dye dilution method indicated that there might be approximately 4.75 inches of silt in the bottom of the pipe. On the second day 5.5 inches of silt were indicated. These depths represent the reduction in flow area necessary to rectify the time of travel measurements to the dye dilution measurements. Subsequent examination of the pipe after the flow stopped indicated that there was a uniform 5-inch depth of silt in the pipe. When the pitometer values were corrected for this change in flow area, the discharge measurements by the chemical tracer and by the pitometer method agreed for the 12 July measurement and differed by only 0.4 percent for the 14 July measurement. These tests indicate no tracer loss of the Rhodamine WT dye to the walls of the pipe and demonstrates the high accuracy that can be obtained in field applications.

SUMMARY AND CONCLUSIONS:

Laboratory studies, conducted to obtain information relative to the accuracy and precision with which fluorescent dyes can be used to determine stream discharge, were extended to include a new dye, Rhodamine WT. The results, as with previous measurements with Rhodamine B and Pontacyl Brilliant Pink B, indicated that dye concentrations of less than 10 parts per billion can be quantitatively detected in most natural stream waters with errors of less than $\pm$ 1 percent. This accuracy is possible with commercially available equipment which compares fluorescence of samples with accurately prepared standards that are readily constructed for each stream flow measurement. Stream gauging by dye dilution techniques to this same order of accuracy is thus possible if sufficient mixing of tracer with the stream flow can be obtained and adsorption of the dye on stream boundaries is negligible.

Reliable criteria for guaranteeing sufficient lateral mixing require further study. Sampling at several points in the stream cross

section indicates whether mixing was achieved, but this deserves improvement.

Data indicate that Rhodamine WT is not significantly adsorbed on channel boundaries. Comparisons of discharges by the dye dilution method using Rhodamine WT with discharges determined with a Cole Pitometer, both in a 48-inch diameter pipe, gave identical values for 1 day's runs and only 0.4 percent difference for a second day's results. Thus, no loss of Rhodamine WT was indicated. Laboratory studies also show a relatively low adsorption rate on suspended materials as compared to Rhodamine B and Pontacyl Pink B. This adsorption on suspended materials appears to be undetectable in ordinary applications.

PERSONNEL: J. A. Replogle, L. E. Myers, and K. J. Brust

Table 1. Laboratory discharge measurements using Rhodamine WT as the tracer with weighed discharge comparisons.

Series	y 1/	$\bar{V}$ 2/	R_R 3/	S 4/	Δt 5/	$\bar{c}$ 6/	σ_c 7/	Q_s 8/	Q_W 9/	ΔQ 10/
	ft	ft/sec		gm	min	μg/L	%	cfs	cfs	%
1	.60	0.62	370,000	0.100	6.00	26.27	± 1.2	0.375	0.373	+ 0.5
2	.60	0.62	370,000	0.100	6.00	26.28	± 0.4	0.374	0.369	+ 1.3
3	.68	0.90	640,000	0.100	6.00	15.97	± 0.3	0.616	0.614	+ 0.3
4	.68	0.90	640,000	0.100	6.00	15.97	± 1.9	0.616	0.613	+ 0.5
5	.75	1.08	890,000	0.100	5.00	14.65	± 1.8	0.806	0.818	- 0.5
6	.75	1.08	890,000	0.100	5.00	14.41	± 0.2	0.820	0.809	+ 1.3

1/ Flow depth in laboratory channel near sampling stations.
2/ Average velocity in flume near sampling stations.
3/ Reynolds number based on hydraulic radius = $\frac{VR}{\nu}$.
4/ Amount of dry weight tracer used.
5/ Sampling time length.
6/ Average concentration derived from four collected samples; μg/L ≈ ppb.
7/ Standard deviation computed for four samples from each series.
8/ Discharge determined by tracer dilution technique.
9/ Discharge determined gravimetrically by weight-time relation.
10/ $100(Q_s - Q_W)/Q_W$.

Table 2. Discharge comparison in cast-in-place concrete pipe using pitometer and dye-dilution methods.

Date	Pipe diameter	Pipe length	Dye time of travel	$\bar{v}_t$ time of travel method	$\bar{v}_p$ pitometer	Depth of silt in pipe	Net pipe area	Q_p pitometer method	Q_d dye dilution method
1965	ft	ft	sec	ft/sec	ft/sec	in	ft^2	ft^3/sec	ft^3/sec
12 July	3.943	5259	4490	1.172	1.167	5.0	1.152	13.44	13.44
14 July	3.943	5259	3890	1.353	1.368	5.0	1.152	15.75	15.68

TITLE: WATER VAPOR DIFFUSION IN SOILS

LINE PROJECT: SWC 4-gG4 CODE NO.: Ariz.-WCL-31

The objectives and need for study for this project were reported in the 1963 Annual Report of the U. S. Water Conservation Laboratory. The results reported in the 1964 Annual Report have been published. The majority of the work done under this project during 1965 concerned the development of a "survival still" for obtaining emergency drinking water from soil and plant materials. This development has been published in Science (Vol. 149, pp. 1377-1379) and over 1300 copies of a mimeographed report (WCL-4) have been distributed upon request. Numerous newspaper and magazine articles describing the survival still have appeared. Since the still is amply described elsewhere, this report will only cover aspects not previously published.

The "survival still" in essentially its present form was conceived on the afternoon of 3 February 1965. The previous evening calculations were made using diffusion theory for water flow through soil to determine possible water yields from soils using solar distillation. Assuming that the soil is uniformly wet to great depth at a water content θ_i and at time t = 0 the water content at the surface is reduced and maintained at $\theta = \theta_o$, then in the first approximation the amount of water evaporating is given by

$$q = 2\ (\theta_i - \theta_o)\ \sqrt{\frac{Dt}{\pi}}\ . \qquad [1]$$

To obtain an order of magnitude for q let $\theta_i - \theta_o = 0.1$ and choose $D = 3.6 \times 10^{-5}\ cm^2\ sec^{-1}$. This value of D is a measured value for the desorption of water from relatively dry Adelanto loam ($\approx$ 3% water by volume). Putting the area as 1 m^2 and q in liters and time in days and differentiating to get the yield per day we have

$$q = \frac{1}{\sqrt{t}}\ . \qquad [2]$$

We can now calculate a theoretical yield for 1 m^2.

Table 1. Theoretical yield in liters from 1 m^2.

Day	Yield
1	1
4	0.5
49	0.143
100	0.100

After 3 1/3 months, 100 ml per day is theoretically possible. These calculations, made before the first still was constructed, showed the theoretical feasibility of mining water from soil by solar distillation.

After data had been collected for a period of time, more refined calculations were made.

Data from the 1961 Annual Report (page 165) showing evaporative water losses from the lysimeters plotted versus the square root of time is reproduced in Figure 1. The relationship is nearly linear. With the slope yielding $D = 19.6\ cm^2\ day^{-1}$ (2.26×10^{-4} cm sec^{-1}), the measured water content difference ($\theta_i - \theta_o$) was about 0.2.

Figure 2 shows the accumulative yield from a survival still constructed in Adelanto loam, the same soil type in which the lysimeters are located. Neglecting the non-zero intercept, a D of 20.7 $cm^2\ day^{-1}$ was calculated from the line in Figure 2. This is very near the 19.6 $cm^2\ day^{-1}$ obtained from lysimeter data. This value of D was used to calculate the daily yield from the still. Figure 3 shows daily yield versus time, the circles are experimental and the line is theoretical.

These data indicate that yields from survival stills, at least in the first approximation, can be predicted from soil-water diffusion theory.

PERSONNEL: R. D. Jackson and C. H. M. van Bavel

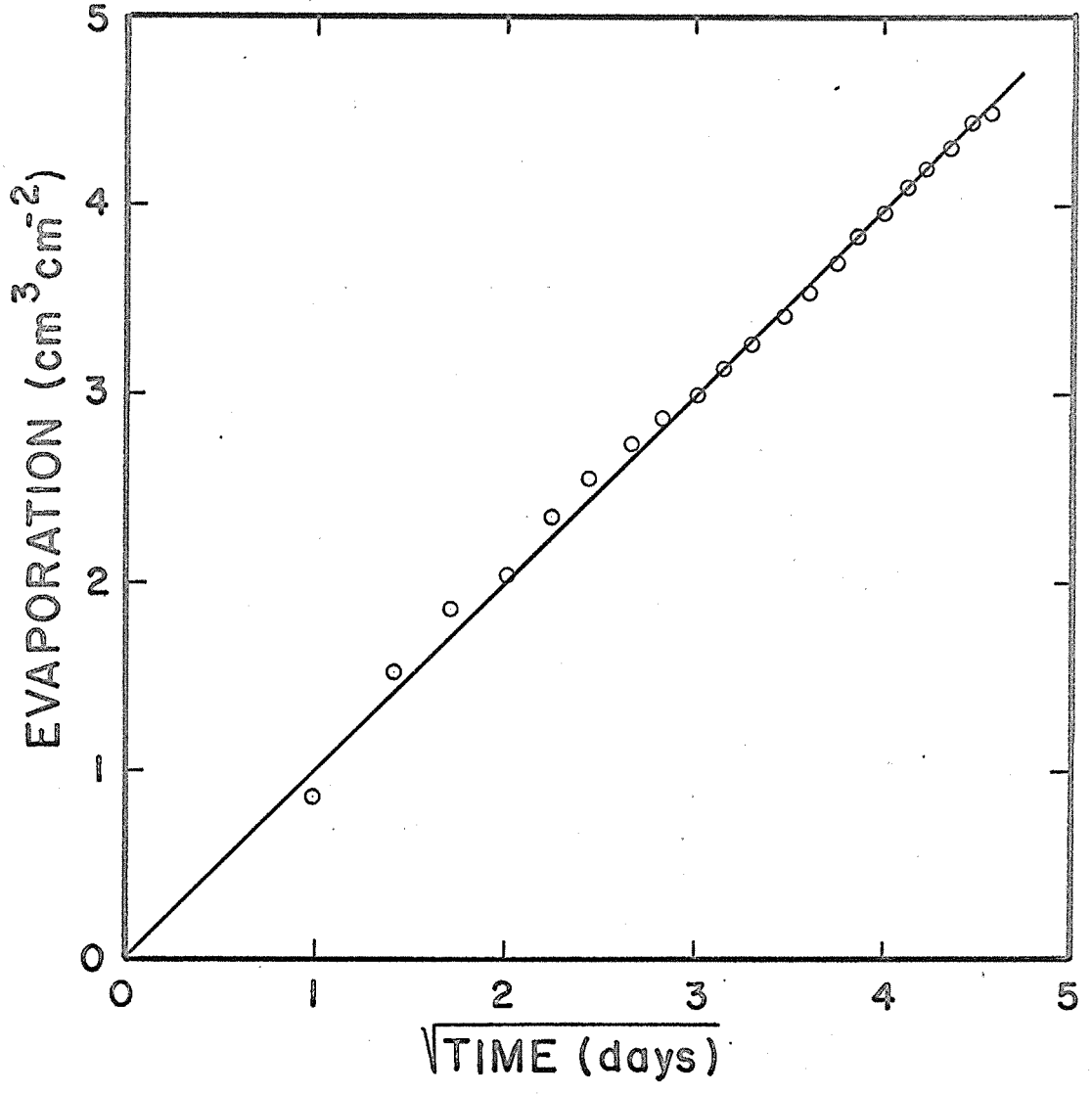

Figure 1. Evaporation from lysimeters versus the square root of time.

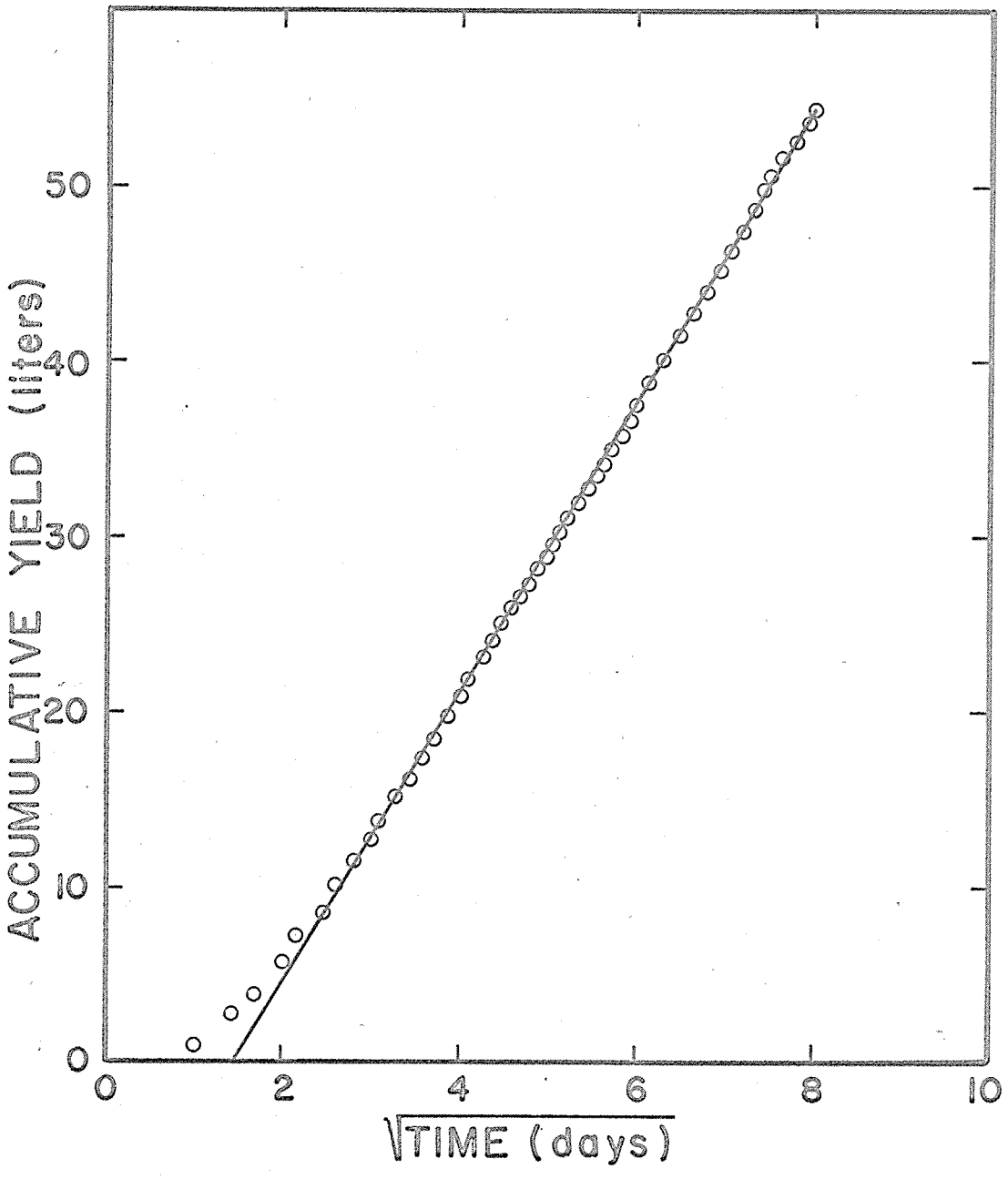

Figure 2. Accumulative yield from a survival still versus the square root of time.

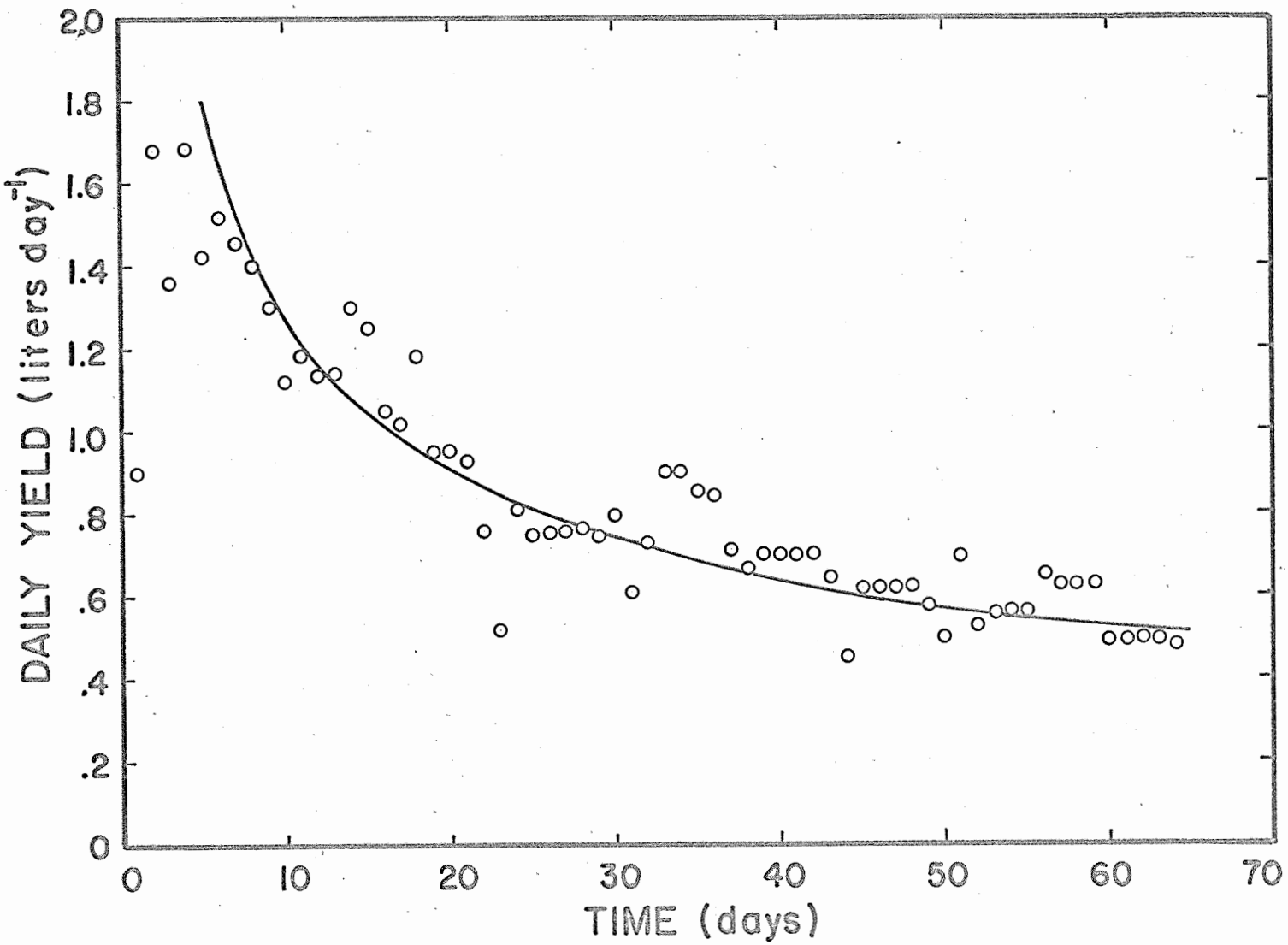

Figure 3. Daily yield from a survival still.

TITLE: MICROMETEOROLOGICAL DETERMINATIONS OF WATER LOSS FROM VARIOUS SURFACES

LINE PROJECT: SWC 4-gG2 CODE NO:: Ariz.-WCL-32

INTRODUCTION:

Micrometeorological research was concentrated on two types of problems. The first was to determine the relative magnitude of local advection versus air-mass advection. A total of four runs (A5-1, A5-2, C5-4, and C5-5) and three transects (SJ5-1, SJ5-2, and SJ5-3) were made for this purpose. Secondly, a profile study (C5-3) was conducted to determine the relative contribution of various portions of a cotton plant canopy to evapotranspiration and to measure profiles of air temperature, vapor pressure, and wind speed.

Evapotranspiration of cotton was determined for 2 by 2 skip-row and solid-planted cotton near Bakersfield, California, at the request of the California Department of Water Resources (C5-1, C5-2).

A total of 31 days' data was collected. Not all of the data have been analyzed; consequently, will not be reported at this time.

EXPERIMENTAL PROCEDURES:

A5-1. Similar instruments were located at 13, 27, 34.5, and 109.5 m from the middle of the south edge of a 50-acre field of alfalfa on the Arizona State University farm. Immediately south of the alfalfa was a 50-acre field of barley stubble, which was to be the local source of advected energy. The alfalfa was 65 cm in height.

At each of the locations the following measurements were made: air temperature and vapor pressure at 5 and 40 cm above the plant canopy, net radiation at two sites, soil heat flow at 5 cm, and average soil temperature from 2 mm to 5 cm. See Fritschen (2) for instrument details. Wind-speed profiles (4 levels) at the 13- and 109.5-m locations and incoming and reflected solar radiation were also measured. Data were recorded at 10-minute intervals.

A5-2. In this experiment three sets of instruments were located at the southwest corner of the alfalfa field at 4, 33, and 53 m from the south edge. The fourth set of instruments was located to the west

of the 53-m site in another alfalfa field for normalizing purposes. The 50-acre field south of the 3-location field was barley stubble.

Instruments, heights, and recording frequency were the same as for A5-1, with the exception that the wind profiles were at the 53-m and westerly locations.

The alfalfa was 25 and 50 cm in height on the east and west fields, respectively. The east field was irrigated at 1530 on 6 July.

C5-1. The experiment was conducted to determine the instrumentation required for evapotranspiration determination from 2 by 2 skip-row cotton on 38-inch centers. Three sets of instruments, necessary to determine evapotranspiration by the Bowen ratio method, were set up in a field of north-and-south planted cotton near Buttonwillow, California. One set was located over the blank rows, the second set was located over the rows, and the third set was located over both cotton and blank rows. Air temperatures and vapor pressure were sampled spatially at location 3, but not at locations 1 and 2.

A fourth set of instruments, similar to that of location 3, was located in a field of 2 by 2 skip-row cotton planted in an east—west direction.

Instruments, heights, and recording frequencies were the same as A5-1. Wind-speed profiles were measured in both the east—west and north—south planted fields.

C5-2. Evapotranspiration of solid-planted cotton was determined by the Bowen ratio method, with duplicate sets of instruments, near Arvin, California. At this location the soil was quite sandy. Instruments, heights, and recording frequencies were the same as for A5-1, except spatial sampling of air temperature and vapor pressure was provided. A single wind profile was used in this study.

C5-3. In this study the instruments were located 300 feet from the east edge and 114 feet from the north edge of a 600-foot-square field of cotton. The experimental field is in the middle of the Cotton Research Experimental Farm at Phoenix, Arizona. The cotton ranged from 100 to 150 cm in height, averaging 120 cm.

Measurements consisted of net radiation within the canopy at 5, 40, 75, and 110 cm, and 1 m above the canopy; plant temperatures at 5, 40, 75 cm, and at the top of the canopy; air temperature and vapor pressure at 5, 40, 75, 110, 145, 180, 215, and 250 cm; wind speeds at 5, 40, 75, 110, and 145 cm, using heated thermocouple anemometers; wind speeds at 145, 167.5, 185, 202.5, 220, 235.5, 255, and 272.5 cm, using sensitive cup-type anemometers; soil heat flow at 5 cm; average soil temperature, 2 mm to 5 cm; incoming and reflected solar radiation; and wind direction.

Data were recorded at 10-minute frequency. The run was timed to collect data before and after irrigation. During the run thunderstorm activity wetted the entire area, thus reducing advected energy.

C5-4. The cotton field selected for this study was the same as in C5-3. It was 600 feet square and bordered on the east, southeast, southwest, and northwest by at least 1,200 feet of irrigated cotton, and on the south and west by 1,200 feet of disked fallow ground.

Four sets of instruments were set up on a north–south line, 29 m from the east edge of the field, the locations being 5.7, 25.7, 45.7, and 65.7 m from the south edge. Instruments used in this study were the same as A5-1. Wind profile measurements were made at the 5.7- and 65.7-m location. The cotton in this portion of the field averaged 80 cm at the 5.7-m location and increased to 90 cm at the 65.7-m location.

C5-5. The field and instruments were the same as in C5-4, with exception of location. This time the instruments were set up on an east–west line, 21 m from the south edge and at 0, 27, 53, and 80 m from the west edge. Wind profiles were recorded at the 0- and 80-m locations.

SJ5-1, 2, and 3. These runs were transects of the lower San Joaquin Valley. In SJ5-1, the route started 24 miles west of Bakersfield, proceeded east 10 miles, and then back to the starting point. The route for SJ5-2 and 3 started 24 miles west of Bakersfield, proceeded east 10 miles, south 10 miles, and then east 15 miles. SJ5-2 was terminated after the first 10 miles because of cloudy weather. The routes traversed large irrigated and desert areas, and mixed irrigated and desert areas.

Measurements consisted of air temperature and vapor pressure at 65, 100, 365, and 400 cm above the surface, net and solar radiation for normalizing purposes, wind speed at 365 cm and direction. The data were recorded at 5-minute intervals in SJ5-1 and at 1-minute intervals in SJ5-2 and 3. The traverse speed was 4.6 m sec^{-1}; thus the time constant of the temperature and vapor-pressure sensors (4 to 5 minutes) amounted to a distance constant of 1.2 km, or 0.7 mile.

Instrumental Changes

Air-temperature and vapor-pressure sensor. The sensing portion of the air-sampling tower described in "Accuracy of Evapotranspiration Determinations by the Bowen Ratio Method" (2) has been redesigned. The new design, Appendix I, facilitates more accurate and reliable measurement of temperature and vapor-pressure differences.

Anemometers. Measurement of wind profiles over a surface of limited fetch requires a sensitive anemometer that is physically small. Similarly, measurement of wind profiles within a canopy requires a small, sensitive anemometer without moving parts. To meet these needs a cup-type and a heated-thermocouple anemometer were designed and tested. Details of design and calibration are given in Appendix II.

RESULTS AND DISCUSSION:

A5-1. The purpose of this run was to determine the relative magnitude of local versus air-mass advection. The site and local advection source were ideal. Unfortunately, the wind did not blow from the prevailing direction, and scattered thunderstorms modified the air mass. Consequently, the objective could not be realized.

Totals of the energy balance components for periods of positive net radiation are shown in Table 1. Since the winds were from the north to northeast on both days, the results obtained from the four locations should not reflect edge effects. Variation between locations may be due to differences in the alfalfa stand or instrumental error. The increase in net radiation from the edge of the field inward suggests that the surface as viewed from the radiometer was cooler toward the center of the field. This would imply a more complete and rapidly transpiring surface near the center of the field. Calculation of

evapotranspiration by the Bowen ratio method confirms greater evapotranspiration near the center of the field. However, the calculated evapotranspiration at the 27- and 34.5-m locations was lower than at the other locations. This could be due to the method of sampling air-temperature and vapor-pressure differences. These differences were not sampled spatially at the 27- and 34.5-m locations. Furthermore, the sensor intakes were orientated to the south. Thus the sensor housing could have affected the difference.

A5-2. The purpose of this run was to determine the relative magnitude of local versus air-mass advection as affected by irrigation. Three stations were set up to determine horizontal temperature and vapor-pressure gradients; a fourth station was established in an adjacent field for normalizing to establish the effect of irrigation.

These results were not achieved because the wind — except for a few hours — did not blow from the prevailing direction, and a burnt valve in the generator engine caused the run to be terminated the day after irrigation.

Totals of the energy balance components for periods of positive net radiation are shown in Table 2. The results from the 4-, 33-, and 53-m locations reveal a decrease in net radiation and calculated evapotranspiration from the edge of the field inward, the decrease being related to the number of hours of southerly winds and the wind speed. The greatest difference occurred on 7 July when the wind was southwesterly in the morning and variable in the afternoon.

The calculations of evapotranspiration at the 4 m and sometimes at the 33 m location are not valid because the basic assumption of the method — that is, vertical fluxes — was not met. These calculations were made to obtain an estimate of the error from improper use of the method. Part of the difference in calculated evapotranspiration between the 4- and 53-m location is due to net radiation and may be due to variation in the surface, but the bulk of the difference is attributed to improper use of the method.

The proper fetch-to-height ratio for valid results has not been established. Previous investigations (Fritschen, 2) indicated a ratio of 68 was adequate under light wind conditions. Dyer (1), using simple diffusion theory, calculated the time and fetch required for profile adjustment. His results, extended to a 40-cm height, are summarized in Table 3. They indicate a fetch of 60 m or 20 sec is necessary for 90 percent adjustment at the 40-cm height. This means that the wind speed would have to be less than 60 m/20 sec, or 3 m sec^{-1}, for 90 percent adjustment. Another way of interpreting these results is that for 90 percent adjustment at the 40-cm height the fetch in meters should be 20 times the wind speed in m sec^{-1}. Thus with a wind speed of 5 m sec^{-1} a 100-m fetch is required. Larger fetches are required for greater heights.

Air-temperature differences at 40 cm between the 4-, 33-, and 53-m locations were computed for periods of southerly winds on 6 and 7 July. The wind speed was less than 2 m sec^{-1} during these periods. The results revealed a small or negative temperature difference between the 33- and 53-m location and a large positive difference between the 4- and 53-m location, indicating that adjustment in air temperature was completed in 33 m at the 40-cm height.

The temperature difference (4- to 53-m location) appeared to be a function of the wind speed. The plot of temperature difference versus wind speed was nearly linear (Figure 1). The 90 percent adjustment value would suggest an intercept at 0.2 m sec^{-1}, which would agree with the experimental data.

Calculation of horizontal advection was not attempted because of the brief period of southerly winds.

C5-1. Data from C5-1 are summarized in Table 4. Location 1 represents the blank rows, location 2 the crop rows, and location 3 both blank and crop rows on the north—south planted cotton. Location 4 is the same as 3 but on the east—west planted cotton. The data from 14 and 16 July represent partial days. Soil heat flow averaged for locations 1, 2, and 3 were used in the analysis.

The average on 15 July represents the combination of all data; that is, the air-temperature differences for locations 1, 2, and 3 were averaged for each hour. Vapor-pressure differences and net radiation were treated similarly. The Bowen ratio equation was then solved, using the averaged data.

If the averaged computation were assumed to represent the true value, then the stationary sampling stations were less than 4 percent low, while the spatial sampling station was 15 percent high. The small difference in evapotranspiration between locations of extreme conditions suggests that spatial sampling may not be too critical, although the location differences may be somewhat masked by the use of average soil heat-flow data.

C5-2. The two locations were set up about 25 meters apart to obtain replication. The results, given in Table 5, reveal substantial differences between the locations in net radiation, heat flow, and calculated evapotranspiration. Duplicate net radiometers at each location agreed. The location differences must be real, since net radiation is one of the most conservative measurements made. The question that needs to be answered is: What caused the differences?

The field was sprinkler irrigated at night with five laterals. Each day the laterals were moved east by one-fifth of the distance between laterals. The last irrigation was made the night of the eighteenth. By the nineteenth the east location had been irrigated 2 days previous, while the west plot had been irrigated 4 days previous. Evapotranspiration was divided by solar radiation and plotted versus days after irrigation. The results, Figure 2, suggest a linear relation between water use and days after irrigation or soil moisture content. Thornthwaite and Mather (4) proposed a linear relation based on observations made at O'Neill, Nebraska. These results should be investigated at a future date in more detail.

C5-3, 4, and 5. Data from runs C5-3, C5-4, and C5-5 have not been analyzed completely and will be reported later.

SJ5-1, 2, and 3. The San Joaquin transects will be reported in detail elsewhere (Fritschen and Nixon, 3). Briefly, the results indicate that the microclimate is modified by irrigation. The air is cooler and more humid over the irrigated areas, the degree of modification depending upon the height of measurement above the surface in relation to the upwind fetch. At 1 m above the surface the modification is less than 5C or 10 mb.

Strong surface heating and light winds, usually found in arid regions, favor convection over advection, thus limiting the aerial extent of microclimatic modification. Cooler and more humid air has been detected downwind from an irrigated area. The detectable distance ranged from a few meters to 500 meters, and appears to be a function of the wind speed and the size of the wetted area. Certainly, the bulk of the modification was noted within 30 m downwind from the field. In general, the effects of irrigation are of limited aerial extent and duration and, in the main, do little to the microclimate.

The transect revealed a temperature maximum between 1 and 2 m above the surface. This maximum existed in the desert, as well as in the irrigated areas, and must be considered in determining evapotranspiration by meteorological means, because this shallow layer of warm air is the source of advected energy. Measurements should be made below the temperature maximum for valid results.

Potential irrigation requirements of an anticipated project can be calculated with existing temperature, humidity, and wind-speed data, and an estimation of net radiation based on solar radiation. The potential thus calculated would be from 5 to 15 percent high, depending upon the average wind speed, but certainly good enough for broad planning purposes.

REFERENCES:

(1) Dyer, A. J.
1963. The adjustment of profiles and eddy fluxes.
Quart. Jour. Roy. Met. Soc. 89:276–280.

(2) Fritschen, Leo J.
1965. Accuracy of evapotranspiration determinations
by the Bowen ratio method.
Bul. Internatl. Assoc. Sci. Hydrol. 10(2):38–48.

(3) Fritschen, Leo J., and Nixon, Paul R.
[196] The microclimate, before and after irrigation.
[manuscript form.]

(4) Thornthwaite, C. W., and Mather, J. R.
1955. The water budget and its use in irrigation.
U.S. Dept. Agr. Yearbook 1955:346–358.

Table 1. Solar radiation R_{sd}, and net radiation R_n, soil heat flow S + S', evapotranspiration LE, and sensible heat A for periods of positive net radiation from 65-cm alfalfa on the Arizona State University Farm, 1965

Date	Location	R_{sd}	R_n	S+S'	LE	A
June	meters	<		langleys		>
23	13	360	214	–17	–291	94
	27		221	–21	–231	–11
	34.5		234	–21	–231	–18
	109.5		253	–13	–319	82
24	13	734	442	–35	–525	118
	27		458	–32	–466	40
	34.5		475	–33	–467	25
	109.5		501	–35	–570	104

Table 2. Solar radiation R_{sd}, and net radiation R_n, soil heat flow S + S', evapotranspiration LE, and sensible heat A for periods of positive net radiation from 25- and 50-cm alfalfa on the Arizona State University Farm, 1965

Date	Location	R_{sd}	R_n	S+S'	LE	A
July	meters	<		langleys		>
4	4	679	434	–57	–432	55
	33		440	–71	–393	24
	53		399	–68	–345	14
	west		531	–46	–610	125
5	4	656	449	–46	–617	214
	33		433	–49	–481	97
	53		396	–52	–475	131
	west		511	–39	–736	264
6	4	561	390	–55	–483	148
	33		378	–64	–380	66
	53		349	–45	–372	68
	west		433	–34	–555	156
7	4	542	390	–48	–531	189
	33		385	–56	–451	122
	53		353	–23	–362	32
	west		429	–41	–521	133

Table 3. Fetch, fetch-to-height ratio, and time required for percent of profile adjustment

% Adjustment	Fetch	$\frac{\text{Fetch}}{40\text{ cm}}$	Time
	m		sec
0.9	60.0	150	20.0
.8	24.0	60	9.0
.7	15.0	38	5.5
.6	9.5	24	3.5
.5	6.5	16	2.5
.4	5.0	12	1.8
.3	3.8	10	1.5
.2	2.8	7	1.0
.1	1.0	2	0.7

Table 4. Solar radiation R_{sd}, and net radiation R_n, soil heat flow $S + S'$, latent heat LE, and sensible heat A for periods of positive net radiation from 2 × 2 skip-row cotton near Buttonwillow, California, 1965

Date	Location	R_{sd}	R_n	S+S'	LE	A
July		<		langleys		>
14	1	194	67	33	–119	19
	2		83	33	–123	7
	3		68	33	–126	25
	4		97	33	–178	46
15	1	669	371	–60	–356	44
	2		413	11	–364	11
	3		429	11	–425	56
	Average		405	11	–369	25
	4		500	–52	–558	109
16	1	172	70	5	–77	2
	2		79	11	–85	1
	3		88	11	–110	17
	4		102	7	–202	93

Table 5. Solar radiation R_{sd}, and net radiation R_n, soil heat flow $S + S'$, latent heat LE, and sensible heat A for periods of positive net radiation from solid-plant cotton near Arvin, California, 1965

Date	Location	R_{sd}	R_n	S+S'	LE	A
July		<		langleys		>
19	West	618	389	–53	–397	60
	East		433	–40	–464	71
20	West	684	421	–64	–401	43
	East		465	–44	–470	49
21	West	690	431	–63	–421	53
	East		459	–50	–439	31

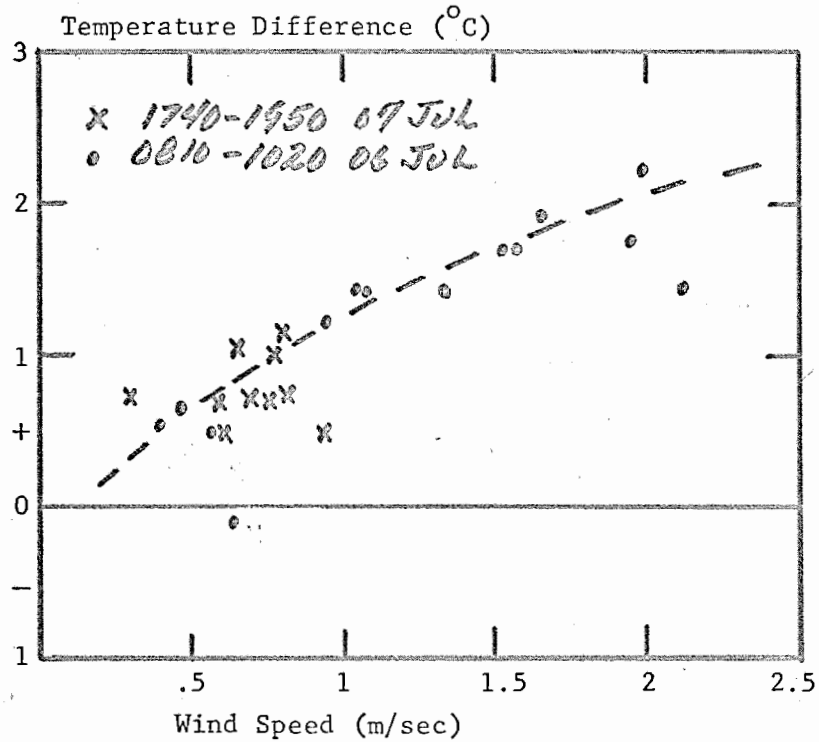

Figure 1. Temperature difference at 40 cm between the 4-m and 53-m location versus wind speed.

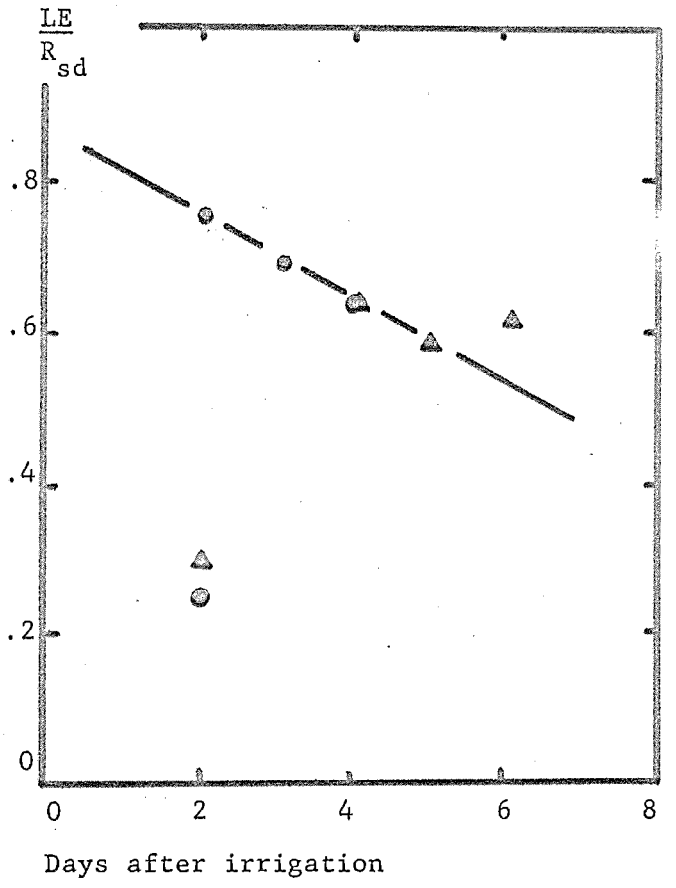

Figure 2. The relation between the ratio of evapotranspiration of cotton to solar radiation and days after irrigation, Arvin, California.

APPENDIX I. CONSTRUCTION DETAILS OF THE SPATIAL AIR-SAMPLING TOWER

Table of Contents

	Page
Drawing of the air-sampling tower.	32-18
Part list for the air-sampling tower	32-19
Drawing of the air-sampling head	32-20
Part list for the air-sampling head.	32-21
Photograph of the air-sampling head mechanism.	32-22
Part list for the air-sampling head mechanism.	32-23
Layout for the air-sampling head mechanism box	32-24
Wiring diagram for the air-sampling head mechanism	32-25

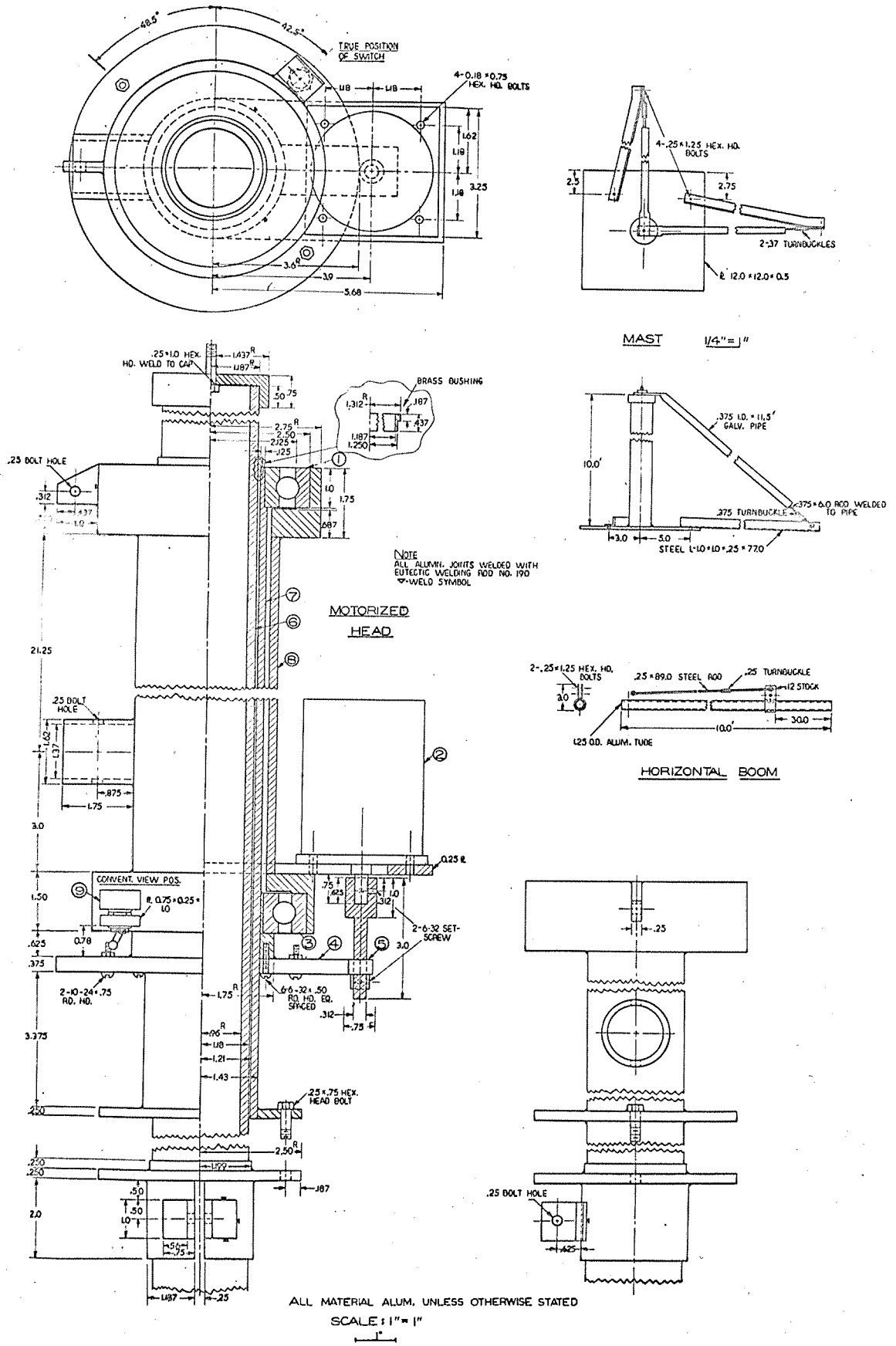

Air Sampling Tower

Air-sampling Tower Parts

1. Fahnir grease-shield ball bearing
   125-mm O.D.; 70-mm I.D ; 24-mm wall

2. R.M.S. Motor Corporation BG5PIK

3. Fahnir grease-shield ball bearing
   130-mm O.D.; 75-mm I.D.; 25-mm wall

4. Boston spur gear (6-spoke – cast-iron), NA 144

5. Boston spur gear (6-spoke – cast-iron), NA 12B

6. Extra-heavy aluminum pipe
   2.375-in. O.D.; 1.939-in. I.D.; 0.218-in. wall; 10 feet long

7. Standard aluminum pipe
   2.875-in. O.D.; 2.469-in. I.D.; 0.203-in. wall; 32-1/8 inches long

8. Standard aluminum pipe
   3.500-in. O.D.; 3.068-in. I.D.; 0.216-in. wall; 24-1/4 inches long

9. Toggle switch, Arrow H & H 34-062

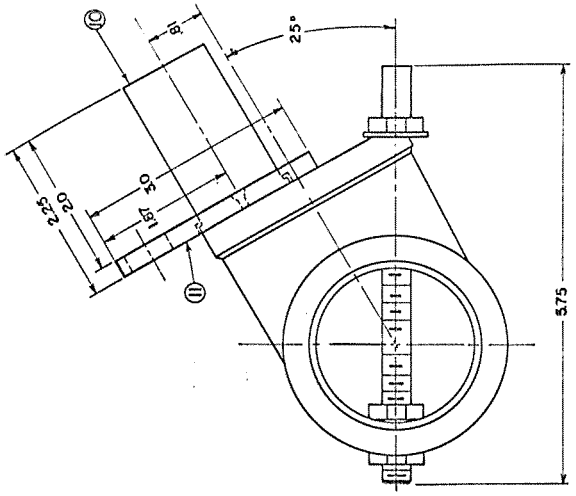

AIR SAMPLING HEAD

SCALE: 1" = 1"

/////LUCITE

PVC

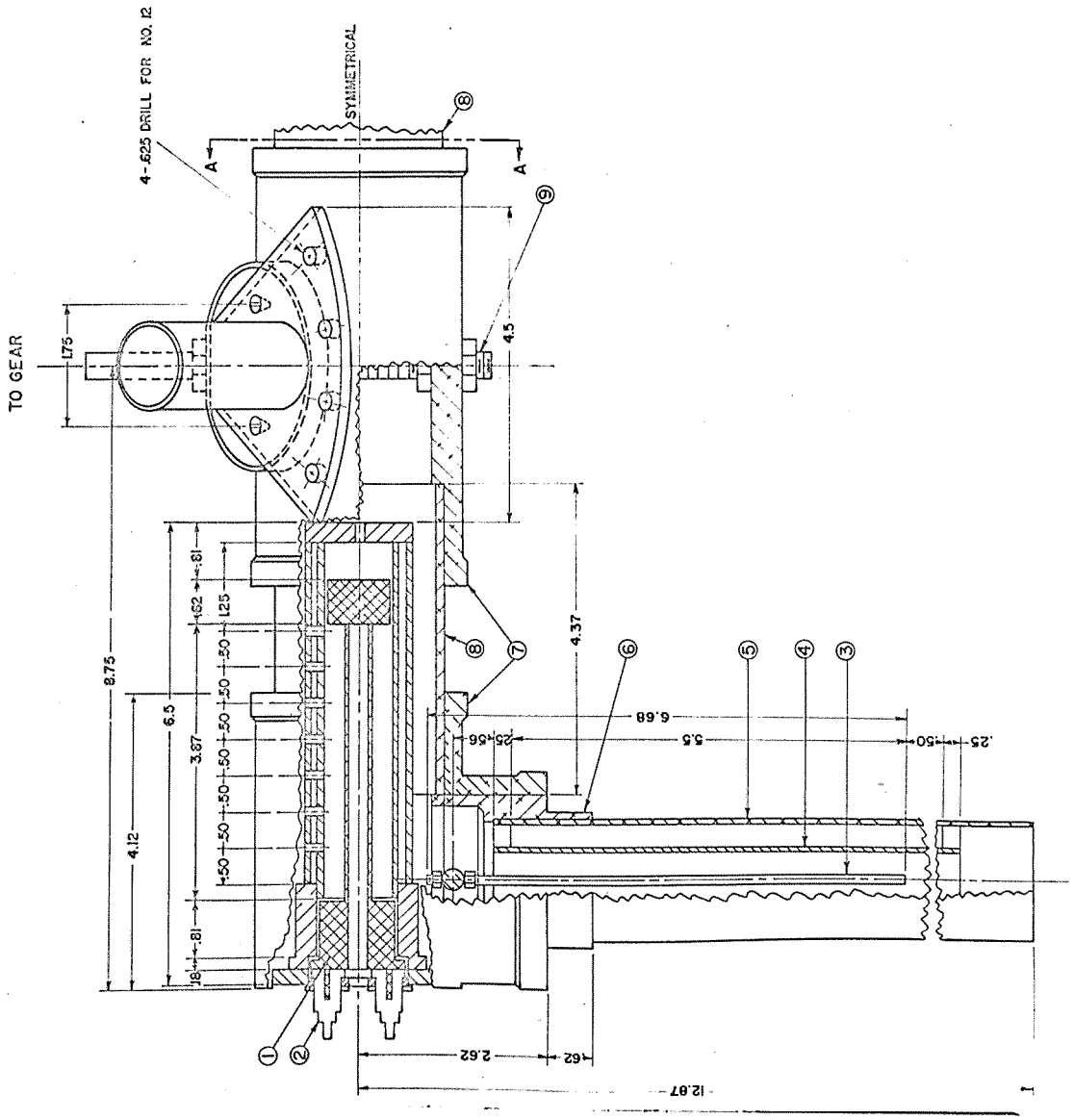

Air-sampling Head

1. Minneapolis-Honeywell Dewprobe bobbin, SSP129Z005
2. H. H. Smith tip jack, #240
3. Brazing rod, 1/8-inch O.D.
4. Lucite cylinder, 3.4-inch I.P., 1/16-inch wall
5. PVC pipe, 1-1/4 inch
6. PVC reducer, 2 inch to 1-1/4 inch
7. PVC tee, 2 inch
8. PVC pipe, 2 inch
9. Cold-rolled shafting, 3/8-inch O.D.
10. Hose swivel
11. Lucite connector and swivel holder

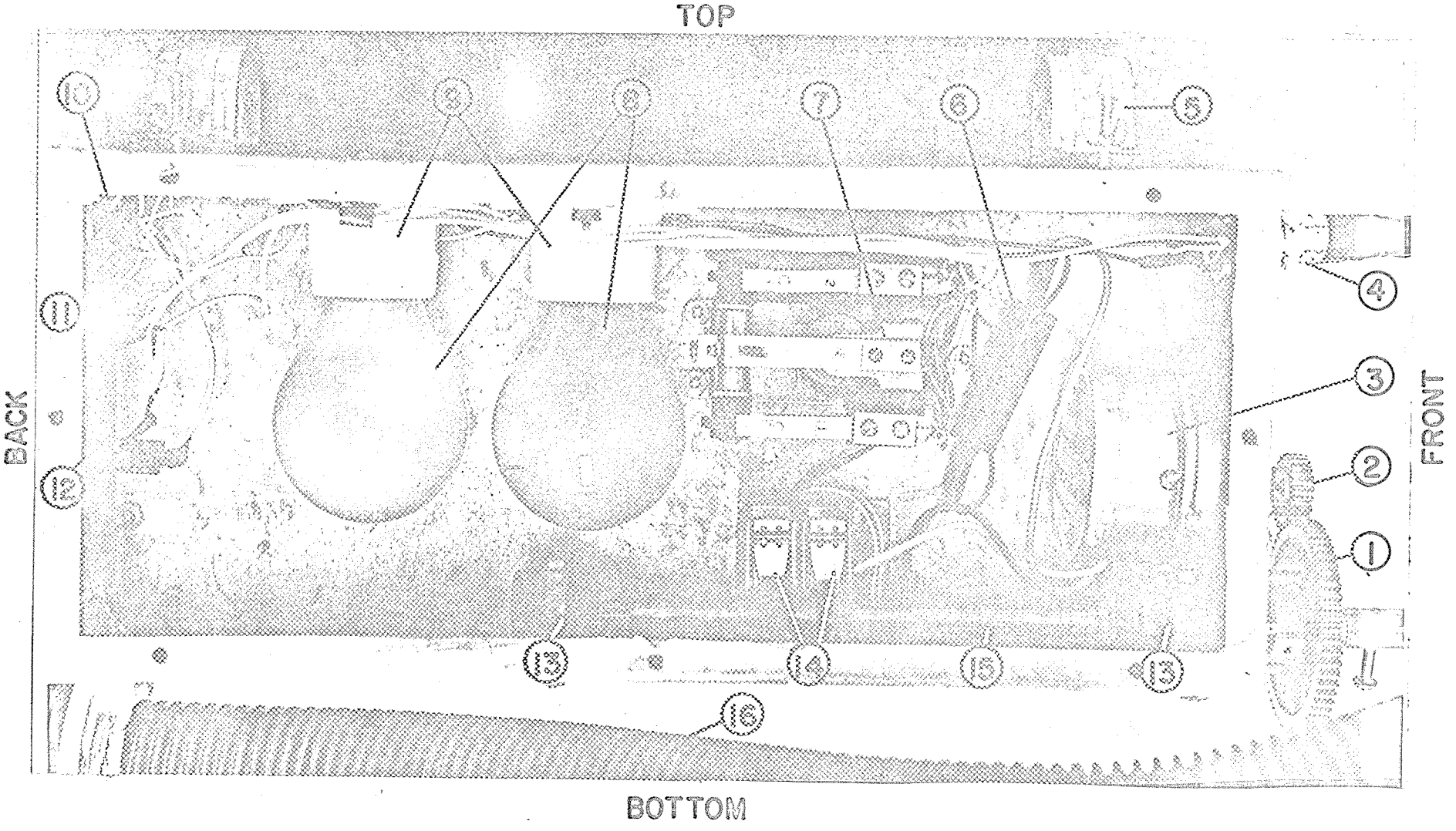

Air-sampling head mechanism

Air-sampling Head Mechanism

1. Boston brass spur gear, Y2460, 60 teeth
2. Boston brass spur gear, Y2421, 12 teeth
3. Hurst synchronous motor, DA series, 4 rpm
4. Amphenol connector, 80MC2M
5. Pipe strap, 1.25 inch
6. Capacitor supplied with Hurst motor
7. Potter & Brumfield impulse relay, AP17A
8. Light bulb, 25-watt, 30-volt
9. Lamp holder, GE 5655-7
10. Amphenol connector, 80-PC2F
11. Military-type connector, MS 3102A 14S-6P
12. Fuse holder, 3AG
13. Boston cast-iron pillow block, SRP6, 3/8-inch shaft
14. Acro snap-action switch, BRD2-LW8
15. Cold-rolled shaft, 3/8-inch O.P.
16. Kirby vacuum cleaner hose

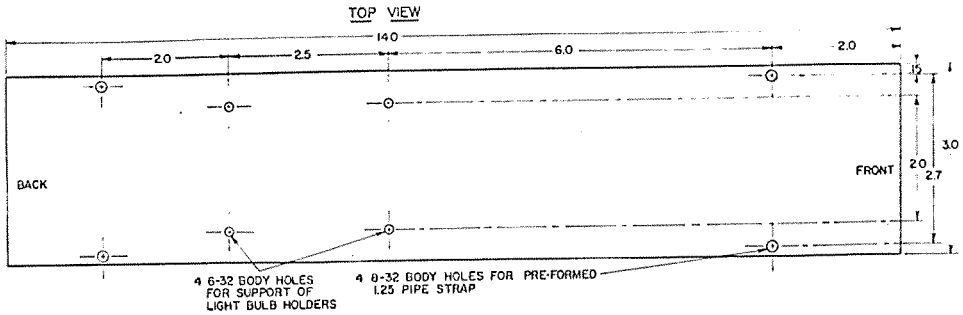

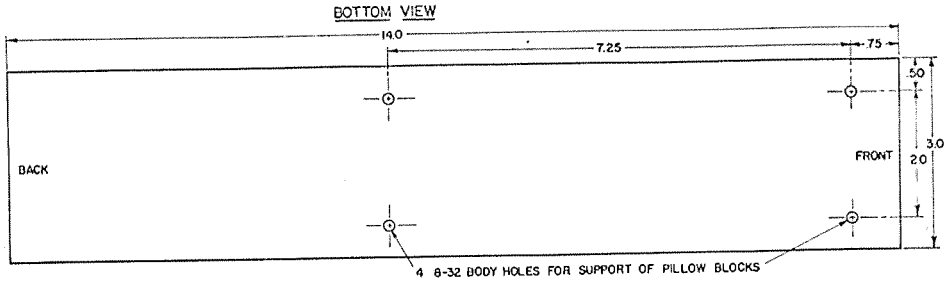

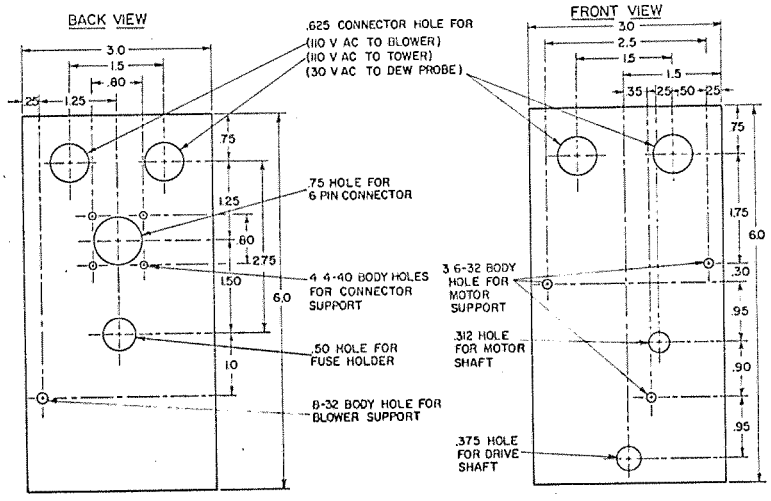

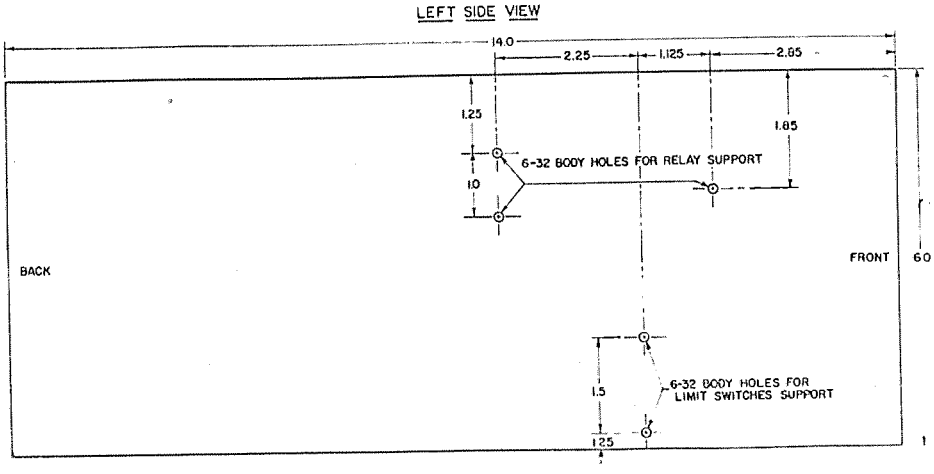

Air-sampling head box

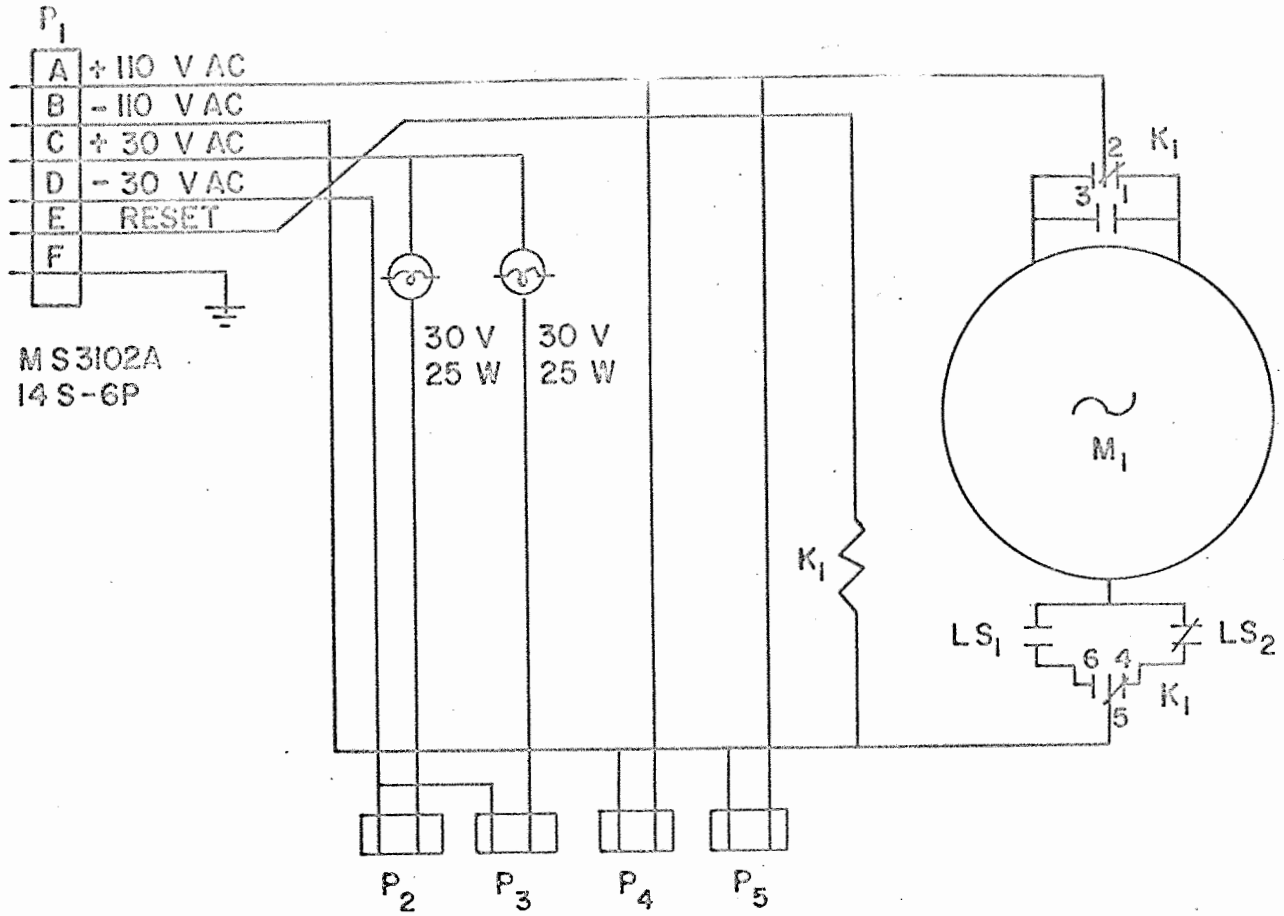

P_2 TO DEW PROBE 1

P_3 TO DEW PROBE 2

P_4 TO BLOWER

P_5 TO TOWER

P_1 - MS 3102A 14S-6P

P_2, P_3, P_4, P_5 - AMPHENOL 80-PC2F

K_1 - POTTER & BRUMFIELD-AP17A

LS_1, LS_2, - MICROSWITCH 287 5023 00

M_1 - HURTS DA 4 RPM

CABLE BELDEN 8446

Air-sampling head mechanism wiring

APPENDIX II. CONSTRUCTION AND EVALUATION OF ANEMOMETERS

Table of Contents

Page

PART I. A SENSITIVE CUP-TYPE ANEMOMETER

Introduction 32-27

Design 32-28

Calibration. 32-29

Summary. 32-31

References 32-32

Table
1. Characteristics of anemometer cup assemblies 32-33

Figure
1. Construction details for a sensitive cup-type anemometer
   Part A 32-34
   Part B 32-35
   Part C 32-36
2. Circuit for the sensitive cup-type anemometer. 32-37
3. Calibration results of the sensitive cup-type anemometer with USWCL cup assemblies, with and without edges, and the Beckman and Whitley cup assembly 32-38

PART II. A HEATED THERMOCOUPLE ANEMOMETER

Introduction 32-39

Construction details 32-40

Calibration results. 32-40

Summary. 32-41

References 32-41

Figure
1. Construction details for the heated thermocouple anemometer 32-42
2. Calibration curves for two heated thermocouple anemometers 32-43

PART I. A SENSITIVE CUP-TYPE ANEMOMETER

1. Introduction

Measurement of wind profiles over areas of limited horizontal extent for the purpose of determining surface characteristics or transport coefficients demands the following requirements for cup-type anemometers:

1) The anemometer, including cup assembly and transmitter, should be physically small, so that several anemometers can be stacked vertically and still be within the boundary layer of the field.
2) With limited horizontal extent wind measurements must be obtained close to the surface, where wind speeds are lowest; therefore, a very sensitive anemometer is required — that is, one with a low starting speed and small response length.
3) For ease of operation the assembly should be simple and contain a minimum of electronics.
4) A linear response is necessary where wind speeds are integrated over a period of time.

The literature contains descriptions of many types of cup assemblies. Patterson (6) found that the 3-cup anemometer system yields a more uniform torque than 2- or 4-cup systems. The 3-cup anemometer is preferred because of more uniform torque and a greater torque per unit weight (5). Conical-shaped cups seem to be preferred over hemispherical-type cups because they run slower (4), and the relation between cup speed and wind speed is more linear (7). Beaded cups are more sensitive to variations in wind-stream turbulence than plain cups (7). The overrun caused by increased turbulence is much less with beaded cups than with smooth cups. The variation in size of the bead seems to be of secondary importance in cup performance (4).

The relation between arm length and cup size has been investigated by several workers. Brazier (1) in Middleton and Spilhaus (5) concluded that the relations between cup speed and wind speed will be linear when the cup arm is equal to the cup radius. This arm length is short compared with those of most anemometers. Patterson (6) concluded that the relation will be linear with very short arms; however, the torque will be smaller. Sheppard (7) found a linear relation between the rate of rotation and wind speed when the arm length is approximately 1.5 times the cup diameter. After careful consideration Patterson (6) and Fergusson (2) decided the best design includes an arm length 1.5 times the cup radius. This criterion prevails in commercially available anemometers.

Of the commercially available anemometers, the design produced by Thornthwaite Associates, Centerton, New Jersey, appears to meet most of the above requirements. However, better response and simpler electrical system prompted the design and construction of a similar type anemometer. This report contains the design and response characteristics of a sensitive cup anemometer.

2. Design

The sensitive cup anemometer was designed to utilize as many commercially available components as possible. Details of construction and assembly are shown in Figure 1, Parts A, B, and C.

The cups are made by vacuumforming 15-mil cellulose acetate in a 7.6 cm right-angle cone mold. Heat for the molding process is supplied by a single tungsten-filament photoflood bulb mounted approximately 5 cm above the cellulose acetate.

Wind speed is recorded by an electromechanical counter actuated by a photoelectric chopper through an intermediate relay. The circuit of the sensitive cup anemometer is shown in Figure 2. Components R, L, and P are located in the transmitter assembly, and component K is located near a counter unit. Although the relay K is rated at 6 VDC (pulling power, 20 milliwatts), the series arrangement of the photocell in the light and the relay allows enough current to pass to energize the relay, but not enough to cause overheating under

continuous duty. The relay contacts are used to actuate an electromechanical counter.

In practice the anemometer bearings are operated without oil. A strobe disk with nine patterns, weighing 10.3 gm, is used to test the bearing friction. To be satisfactory the shaft must turn at least 600 revolutions, or 128 seconds, from the major strobe pattern to stop.

3. Calibration

The linearity and response length of the sensitive cup anemometer were investigated in the wind tunnel at White Sands Missile Range, New Mexico. The response of three types of cups was investigated because of the uncertainty in the literature about the arm length – cup size relation and the presence of beads on the cups. The characteristics of the cup assemblies – USWCL cups, with and without edges, and the Beckman and Whitley cup assembly – are listed in Table 1, along with those of two other types of cups.

The results of the wind tunnel tests are shown in Figure 3. The points plotted are an average of two 1-minute counting periods, generally agreeing within 1 rpm. Linear regression was used to compute the relation between cup revolutions and wind speed. Only the two extreme relations are shown. All three relations are highly significant, having correlation coefficients of 0.9999. The standard deviation from regression is less than 13 cm sec^{-1}. Over the range investigated, it appears all cups had linear responses. Contrary to the literature, the Beckman and Whitley cups appeared to rotate faster than the cups with the shorter cup arm. The cups with the beaded edge appeared to rotate slightly faster than the cups without the edge.

Extrapolating the regression lines to zero leads one to conclude that the starting speeds of the USWCL cups, with and without edges, and the Beckman and Whitley cups would be 6, 9, and 7 cm sec^{-1}, respectively. However, when the transmitter with cup assemblies was mounted on a trolley and towed at constant speed over a 3-m course in still air (timed over the center 2 meters), a speed of 6, 9, and

9 cm sec^{-1} was required for continuous rotation of the USWCL cups, with and without edges, and the Beckman and Whitley cups, respectively. It was surprising to see that the cups with edges, having a larger surface area, had a larger starting speed than the cups without edges. The edges tended to cause the cups to rotate backward. Thus, it appears that specific weight (Table 1) may be a good criterion for starting speed.

The response length was investigated in the wind tunnel by releasing the cup assembly in a 4 m sec^{-1} wind. The revolutions of the cup assembly displayed on an XY-plotter indicate that the cup assembly reached full speed in less than one-half revolution. Therefore, it was not possible to determine the response length. This point should be investigated with at least a 4-hole chopper at lower wind speeds. The anemometers sold by C. W. Thornthwaite Associates are said to have a distance constant of 83 cm and a starting speed of 9 cm sec^{-1}, although no indication is given as to how the starting speed was obtained. Frenzen (3) indicated that a low-inertia, high-torque anemometer had been developed at Argonne National Laboratory, with a response length of 70 cm.

The overshoot was investigated by counting revolutions to stop after the anemometer mounted on a trolley traveling at 2.5 m sec^{-1} was suddenly stopped. Expressed in centimeters of air, the USWCL cups with edges stopped in 134 cm, the cups without edges required 167 cm, and the Beckman and Whitley cups required 198 cm. This may not be a valid test for the overshoot, because the air adjacent to the cups must have been in motion and required time to settle down. Apparently, cups with beads or flanged edges would be more sensitive to turbulent fluctuations.

As stated previously, measurement of wind-speed profiles over areas of limited fetch requires that several anemometers be stacked close together. In the wind tunnel, a second anemometer was mounted with its cups 17.5 cm above or below the cups of the first transmitter. The cup revolutions were increased by 1.9 percent at 2 m sec^{-1} and 1.3 percent at 15.5 m sec^{-1}. Other locations were not investigated.

4. Summary

A sensitive cup-type anemometer was designed to facilitate wind-profile analyses over crops of limited horizontal extent. This required a sensitive and physically small anemometer with a linear response. The anemometer was designed, using commercially available parts and a minimum of electronic components. It may be quickly dismantled for cleaning. The cup assembly contains three 7.6 cm right-angle cone cups, molded from 15-mil cellulose acetate mounted on 3.2-mm-diameter arms. The arm length is equal to the radius of the cup. The revolutions of the cup assembly are determined by a photoelectric chopper arrangement using a photoresistive-type cell in series with a sensitive relay. This arrangement eliminates the necessity of amplifying the photoelectric output.

The response of three types of cup assemblies, USWCL cups with and without edges and Beckman and Whitley cups, was investigated. A linear response was obtained for all assemblies from 0.2 to 18 m sec^{-1}. The USWCL cups without edges had the lowest starting speed, 6 cm sec^{-1}, and the USWCL cups with edges had the least overshoot. Assuming that the low starting is more important, the USWCL cup assembly without edges was selected for field use.

REFERENCES:

(1) Brazier, C. E.
1920. Mémoires. Annales du Bureau Central Mét. de France, 1914, Paris, Gautier-Villars, 157–300.

(2) Fergusson, S. P.
1934. The sensitiveness of anemometers. Bul. Amer. Met. Soc. 15:95–99.

(3) Frenzen, P.
1965. Determination of turbulence dissipation by Eulerian variance analysis. Quart. Jour. Roy. Met. Soc. 91:28–34.

(4) Marvin, C. F.
1934. Recent advances in anemometry. Monthly Weather Review 62:115–120.

(5) Middleton, W. E. K., and Spilhaus, A. F.
1953. Meteorological Instruments, University of Toronto Press.

(6) Patterson, J.
1926. The cup anemometer. Trans. Roy. Soc. Canada, Section III, 20:1–54.

(7) Sheppard, P. A.
1940. An improved design of cup anemometer. Jour. Sci. Instruments 17:218–221.

Table 1. Characteristics of anemometer cup assemblies

Characteristic	USWCL[1/] With edge	USWCL[1/] Without edge	B & W[2/]	T[3/]	C[4/]
Diameter (cm)	7.6	7.4	5.1	5.1	5.6
Arm length (cm)	4.1	4.1	4.3	[5/]4.3	4.6
Assembly weight (grams)	11.1	10.3	11.4	7.0	37.5
Beaded edge	0.13-cm flange	no	no	no	yes
Distance between lower cup edge and horizontal support (cm)	3.8	3.8	...	[5/]7.6	...
Cup material	molded plastic	molded plastic	molded plastic	molded plastic	aluminum
Specific weight[6/]	32	33	12	20	5

1/ USWCL — U.S. Water Conservation Laboratory, Phoenix, Arizona.

2/ B & W — Beckman & Whitley, San Carlos, California, Model 170-40.

3/ T — C. W. Thornthwaite Associates, Centerton, New Jersey.

4/ C — C. F. Casella & Co. Ltd., London, England.

5/ Measured on a photograph.

6/ Surface area of 1 cup × wheel radius ÷ cup assembly weight.

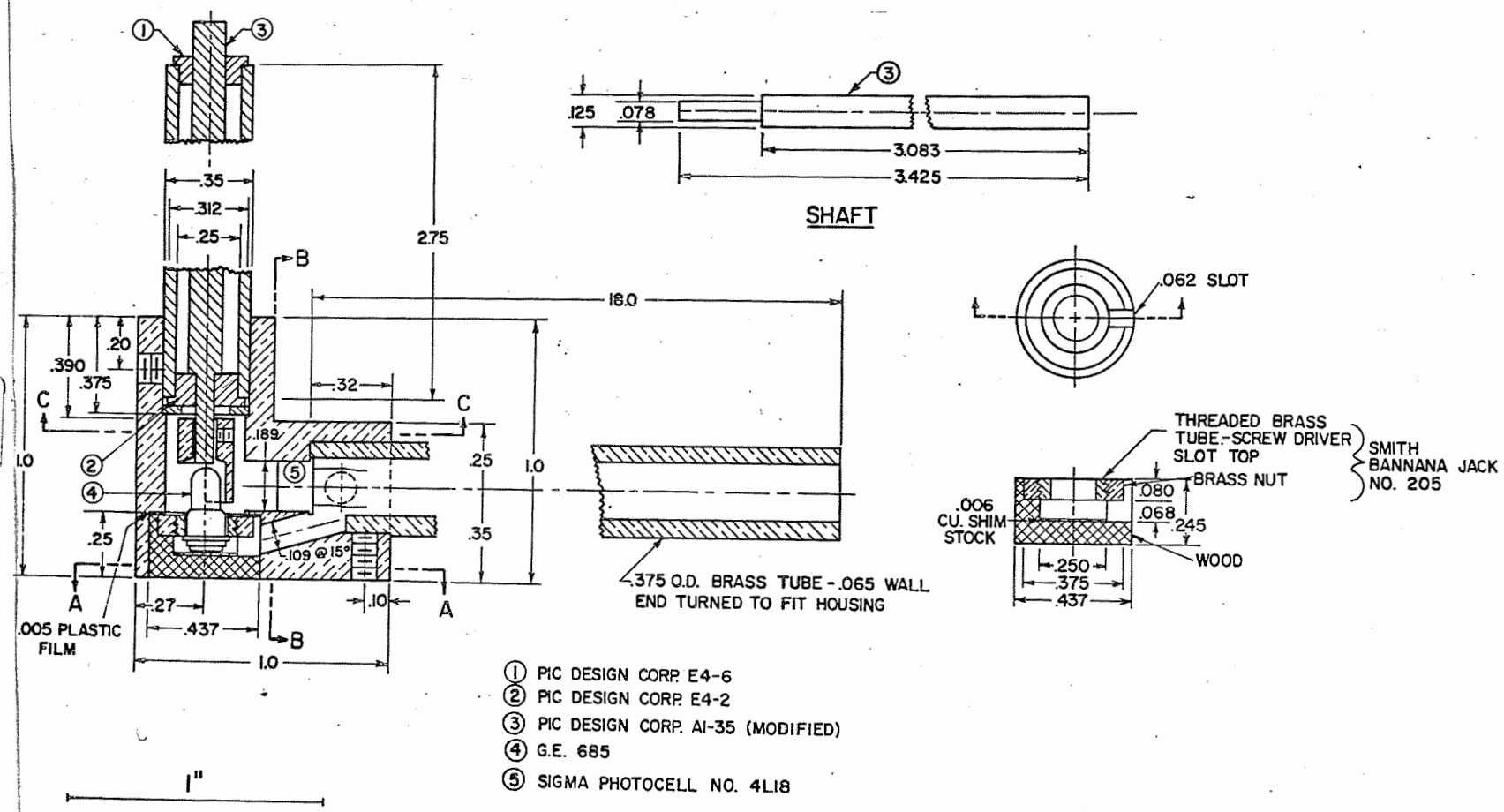

Fig. 1. Construction details for a sensitive cup-type anemometer, Part 1.

Annual Report of the U.S. Water Conservation Laboratory

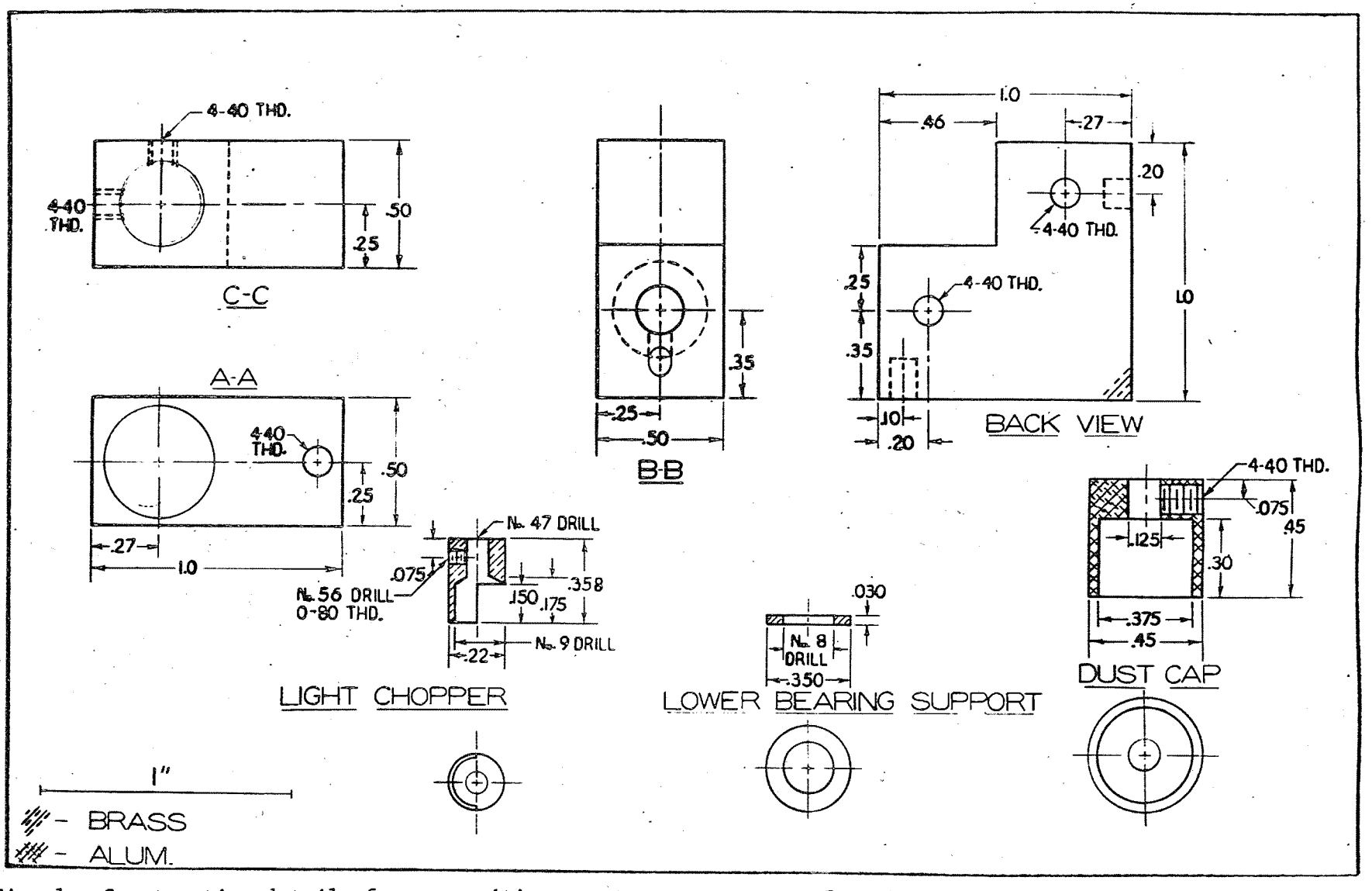

Fig. 1. Construction details for a sensitive cup-type anemometer, Part B.

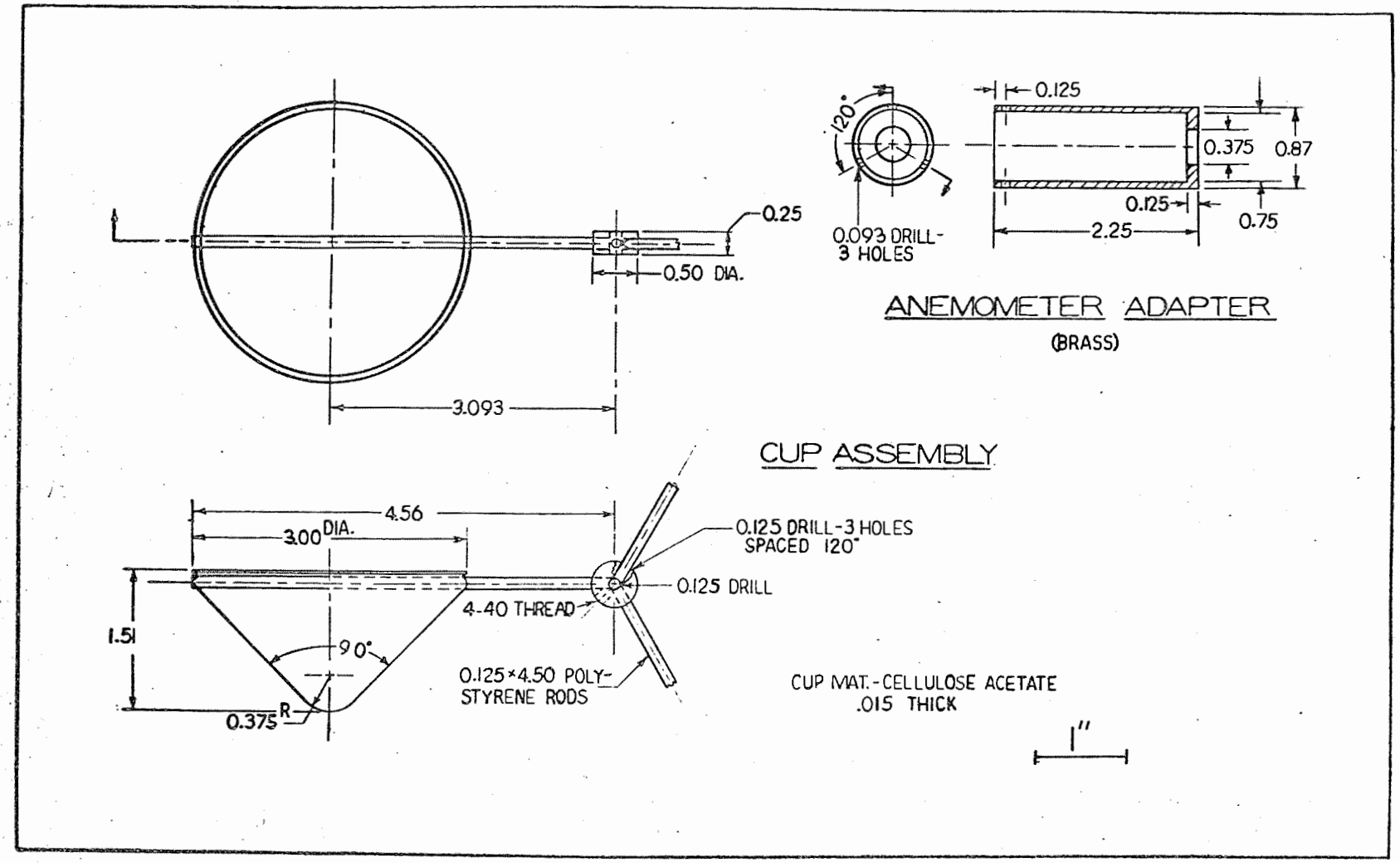

Fig. 1. Construction details for a sensitive cup-type anemometer, Part C.

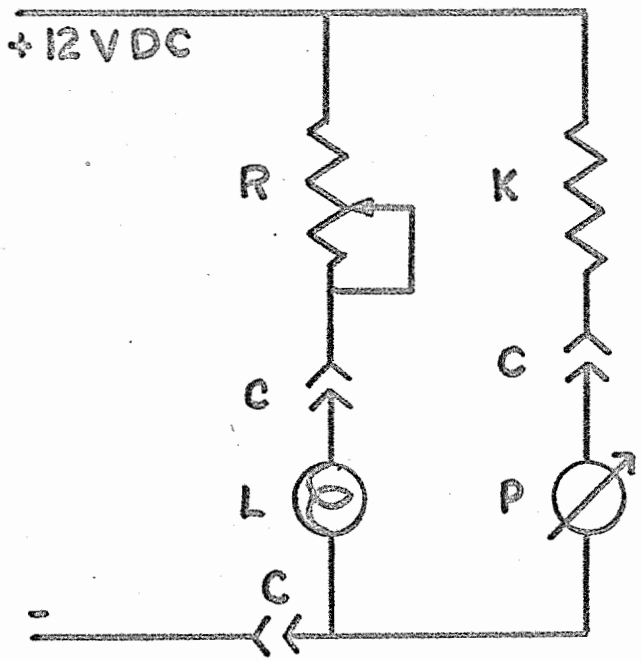

C Connector, Cannon WK-3-31C-3/8
K Relay, Sigma 4R 1000S-SIL
L Lamp, General Electric 685
P Photocell, Sigma 4L18
R Rheostat, Ohmite 0153 type H

Figure 2. Circuit for the sensitive cup-type anemometer.

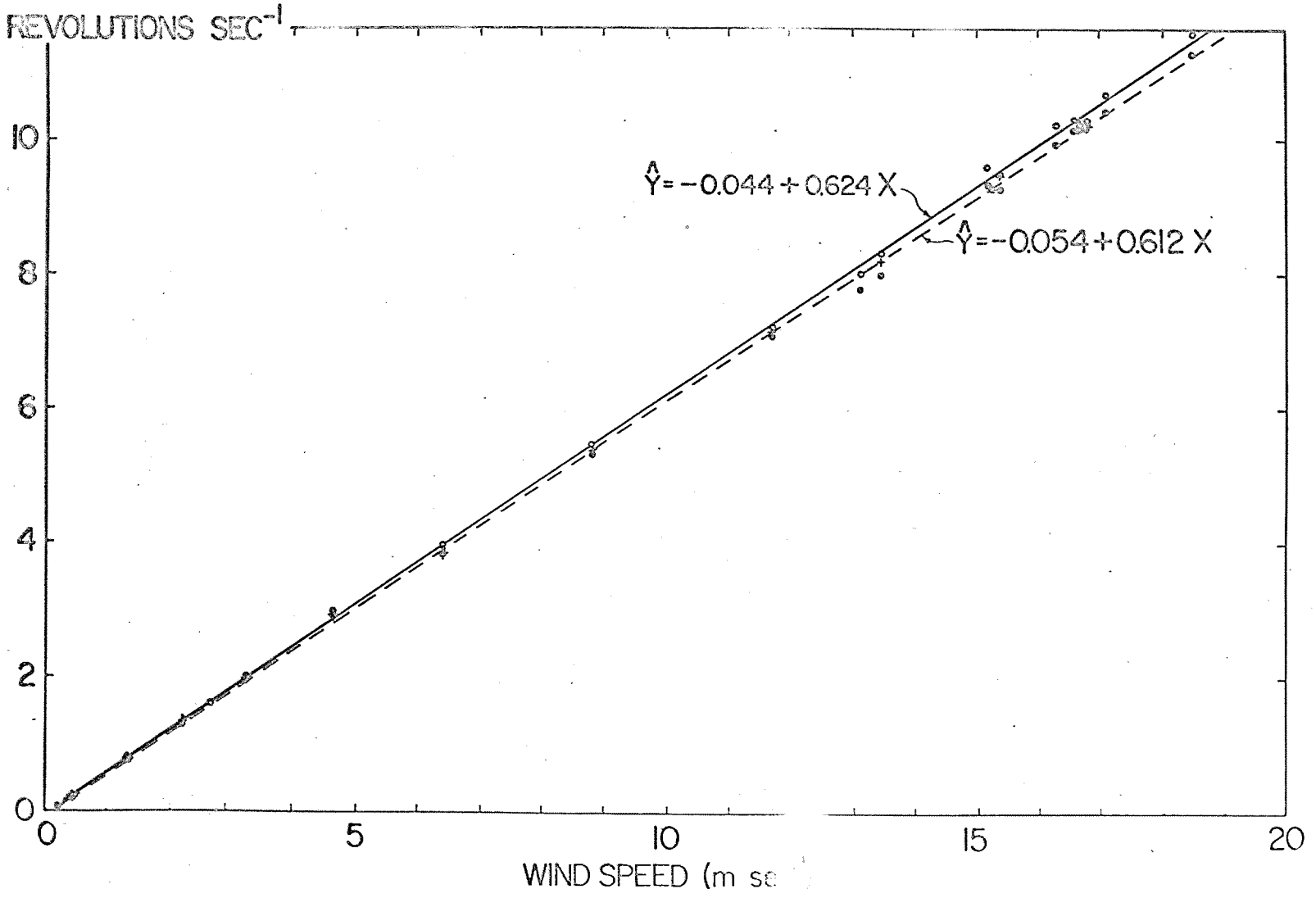

Fig. 3. Calibration results of the sensitive cup-type anemometer with USWCL cup assemblies, with (+) and without (o) edges, and the Beckman and Whitley cup assembly (o).

PART II. A HEATED THERMOCOUPLE ANEMOMETER

1. Introduction

Measurement of wind speeds within a crop canopy requires an anemometer without moving parts because of the low wind speeds encountered and possible interference with the canopy. This suggests the use of thermal-type anemometers. The heated thermocouple anemometer was selected because it is well adapted to our recording system and can be lagged so that mean winds, rather than fluctuations, are obtained by sampling.

The design of the heated thermocouple anemometer extends back to Yaglou (3), who wrapped a fine heating wire around the bulb of the mercury thermometer. When a constant heating current was supplied to a coil, the thermometer would be heated above ambient air temperature. The equation connecting wind speed and temperature was

$$\frac{Q}{(\theta_h - \theta_a)} = K_0 + K_1 V^{1/2} \quad ,$$

where Q is the heat input in milliwatts; θ_h is the temperature of the heated thermocouple θ_a is the temperature of the air; K_0 and K_1 are constants and V is wind speed. This design was also sensitive to ambient temperature.

Hukill (2) described a thermocouple anemometer having one junction heated and the other junction at ambient temperature. This anemometer automatically compensated for changes in the output – wind speed relation due to changes in ambient temperature. This design was further modified for outdoor use by enclosing the thermocouple junctions and the heater wire in small metal spheres, so that both junctions would have the same absorbing surfaces for solar radiation (Fritschen and Shaw, 1).

The major differences between the design presently used and that described by Fritschen and Shaw are that the output is increased by using four junctions, and the time constant is increased so that average winds can be obtained.

2. Construction details

The heated thermocouple anemometers were constructed from the parts shown in Figure 1. The heating element consists of 13.7 cm of 40-gage nichrome resistance wire insulated with 30-gage nylon tubing. Four turns of the insulated resistance wire are wrapped in the groove around part B, with the leads protruding from the bottom holes. Current of 105 milliamperes is supplied to the heating element.

Wind speed is determined by measuring the difference in temperature between the heated and nonheated aluminum discs. This was accomplished by threading through holes in discs A, B, C, and D a 4-junction thermopile constructed from 4-mil manganin and constantan wire. The junctions are located in the middle of discs B and C, with the constantan wire extending from disc B to C and the manganin wire connecting the junctions via discs A, B, C, and D. The thermocouple junctions in discs B and C are insulated from the aluminum ring with a length of 30-gage nylon tubing. The output of the thermopile is recorded on a self-balancing potentiometer.

3. Calibration results

Two heated thermocouple anemometers were calibrated in the wind tunnel for speeds ranging from 0.3 to 4.4 m sec^{-1}. The results obtained are shown in Figure 2. The difference between the curves appears to be due to the location of the thermocouple junctions with respect to the aluminum disc.

A heating current of 105 milliamperes was selected, because sufficient sensitivity was achieved with this heating current over the range of interest while minimizing the temperature of the heated disc. If the temperature of the heated disc were elevated much above ambient, a convective circulation would be induced in still air,

yielding an ambiguous calibration curve. Thus a given millivolt output would represent two wind speeds at low wind movement.

The temperature coefficient of the anemometer was investigated in a temperature-controlled wind tunnel at the U.S. Water Conservation Laboratory. The response of the heated thermocouple anemometer was not altered by ambient temperatures at 15, 25, and 35C.

Time and distance constants were investigated. The time constant, going from high to low wind speeds, was 63 seconds, which was equivalent to 32 m of air. The time constant was 45 seconds (equivalent to 64 m of air) when the sensor was subjected to increased winds. These tests were conducted at various wind speeds ranging from 40 to 180 cm sec^{-1}. It appears that the wind speed obtained from the heated thermocouple anemometer in turbulent air would be greater than the true wind.

4. Summary

A heated thermocouple anemometer was designed to measure wind speed within a plant canopy. The design included lagging the sensor, so that mean wind speeds could be obtained with sufficient sensitivity over the range of interest, less than 3 m sec^{-1}. The construction and calibration results are described.

REFERENCES:

(1) Fritschen, L. J., and Shaw, R. H.
1961. A thermocouple-type anemometer and its use. Bul. Amer. Met. Soc. 42:42–46.

(2) Hukill, W. V.
1941. Characteristics of thermocouple anemometers, in Temperature, Its Measurement and Control in Science and Industry, New York, Reinhold Publishing Corporation, 666–672.

(3) Yaglou, C. P.
1938. The heated thermometer anemometer. Jour. Indus. Hygiene and Toxicology 20:497–510.

PERSONNEL: Leo J. Fritschen

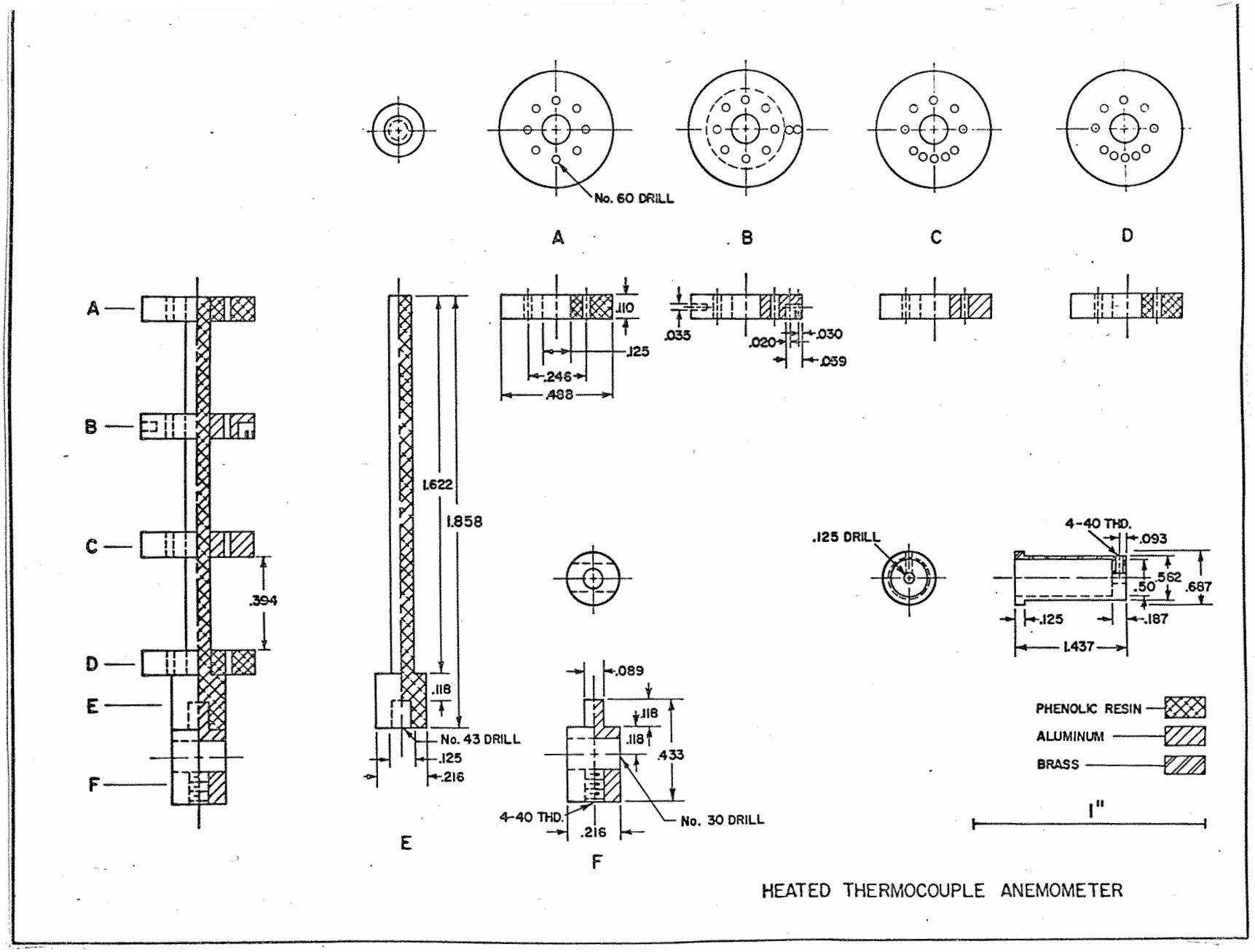

Fig. 1. Construction details for the heated thermocouple anemometer.

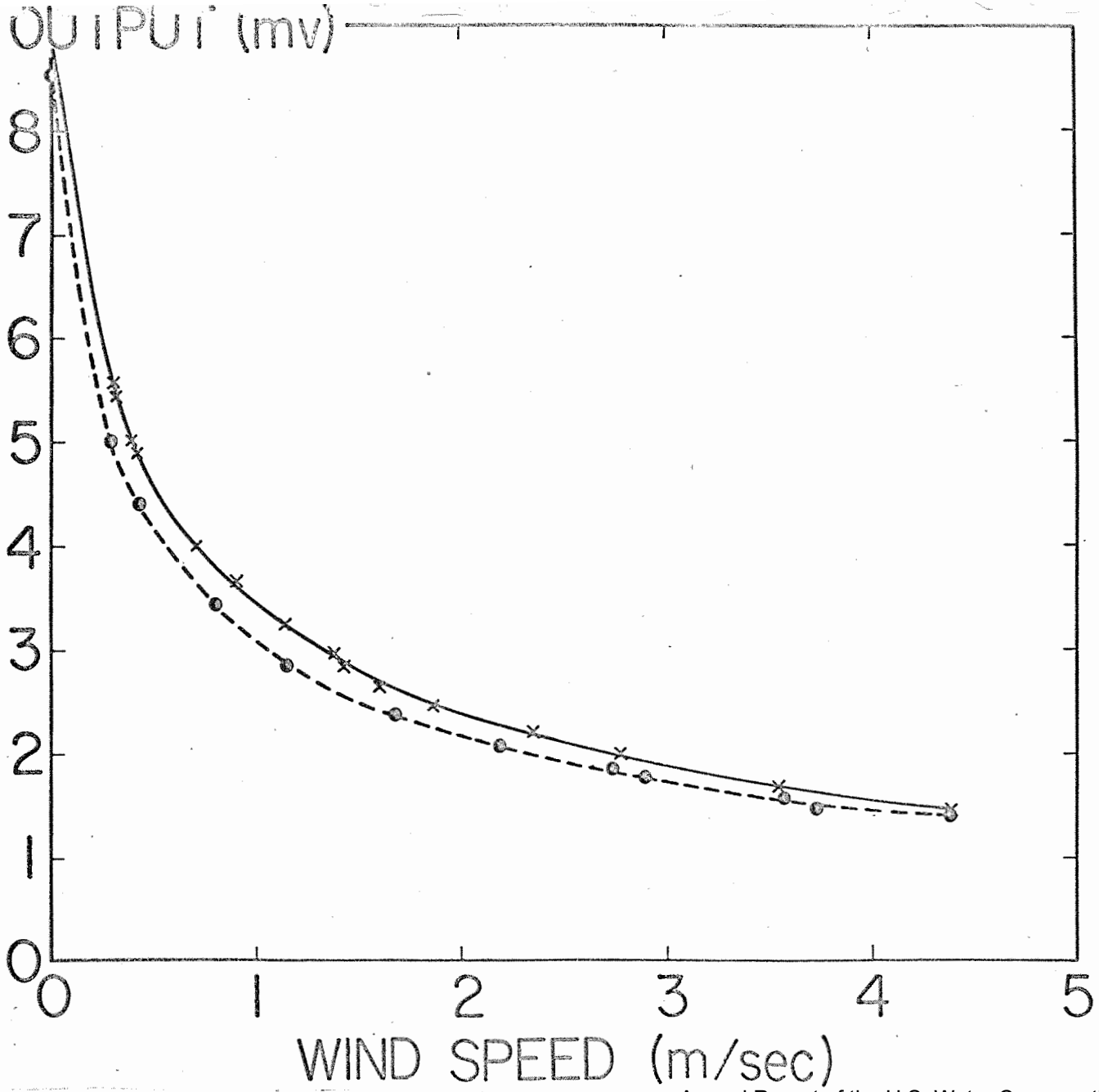

Fig. 2. Calibration curves for two heated thermocouple anemometers.

TITLE: DIRECT MEASUREMENT OF EVAPOTRANSPIRATION AND THE ENERGY BALANCE OF IRRIGATED CROPS

LINE PROJECT: SWC 4-gG2 CODE NO.: Ariz.-WCL-33

INTRODUCTION:

An experiment was carried out to measure the changes in evaporation and energy balance brought about by withholding irrigation water from a cropped surface. As pointed out in the 1964 Annual Report, a numerical value of the canopy's effective resistance to evaporation can be derived from a joint consideration of actual and potential evaporation. This value had never before been compared with a direct and simultaneous measurement of the fundamental parameter involved: the resistance per unit leaf area. The reduction in evaporation that is caused by such an increase in resistance also reverses the general direction of the flow of sensible heat from surface to ambient air and implies a corresponding change in the difference between leaf and air temperature. To verify this aspect, direct measurements were made of the leaf temperature as referred to air temperature over the crop.

PROCEDURE:

The planned schedule for investigating the leaf diffusion resistance of sorghum under field conditions was to establish three long irrigation cycles, each time allowing the soil moisture to be depleted to the point of limiting transpiration. After the soil moisture had been sufficiently depleted, an intensive "dry" measuring period was to be initiated at midnight and continued for 24 hours. Then, as soon after irrigation as possible, an intensive "wet" measuring period of 24 hours was to be conducted.

During these periods, measurements of net radiation, soil heat flux, and leaf temperature from each lysimeter were automatically recorded on punched tape every 15 minutes with a 40-channel data logging system. In addition to these intensive weather data, measurements of the weight of the three lysimeters were automatically recorded on punched tape every 15 minutes with a 10-channel data logging system. Also, measurements of leaf diffusion resistance and leaf thickness were obtained periodically (usually every 30 minutes) during the intensive periods. For the procedure that was followed, see WCL-29).

The average leaf temperature of the canopy in a lysimeter was obtained from four leaf thermocouples wired in parallel. In the square meter of soil there were two rows of sorghum plants, each row with 10 plants. Two representative plants in each row were selected to have copper-constantan thermocouples inserted in the midrib of a mature leaf near the tip of the plant. The third leaf back from the tip was used in June; in July and August the monitoring site was the flag leaf (uppermost, subtending the inflorescence). Good exposure to light and air movement was the main criterion for leaf selection. The three types of plant measurements were carried out either on the same or adjacent leaves (leaf temperature, leaf diffusion resistance, and leaf water content).

The 38-gauge copper-constantan thermocouple was placed in the midrib at a point half way between the leaf tip and the sheath, inserted diagonally so that a section of the lead wires would be buffered by vein tissue. The projecting lead wires were soldered to a 30-gauge insulated wire, which in turn was connected to a 2-conductor 24-gauge stranded, insulated 100-foot cable. This cable led over the ground to a central terminal board, from which an underground cable led to the Datex system which included a zero compensator. From each of the three lysimeters a 100-foot cable led to the central terminal board. The Datex system was set to record leaf temperatures every 15 minutes during intensive runs, or every 5 minutes during the routine measurements of leaf resistance.

In order to compare leaf temperature of plants in the lysimeter with those in the field, two square-meter plots in the field near the lysimeters were instrumented with thermocouples in an arrangement identical to that already described. This was done 7 July; all subsequent measurements of leaf temperature were from both the three lysimeters and the two field sites.

A routine weather station was located in the field at a short distance north of the lysimeters, and solar radiation, net radiation, soil heat flux, air temperature, vapor pressure, and windspeed were automatically recorded on punched tape continuously every 30 minutes with a 6-channel data logging system. Air temperature and vapor

pressure were measured with a hygrothermometer of improved ventilated shield design, shown in Figure 1.

In addition, soil moisture content was measured twice a week in access tubes in each lysimeter and at four field sites. Also, banks of tensiometers were installed near three of the outside access tubes to obtain soil-moisture tension patterns and assess moisture loss by deep percolation. Leaf area index, dry weight, and crop height were obtained at intervals throughout the growing season.

After the conclusion of the three irrigation cycles, computer programs were written for both the 40-channel intensive-weather and 10-channel lysimeter data that had been recorded every 15 minutes on punched tape. Computed values for 15- and 60-minute values of evapotranspiration, net radiation, soil heat flux, and leaf temperature were then obtained for each of the intensive 24-hour periods.

The following intensive periods and irrigation dates resulted during the three long irrigation cycles:

Cycle	Dry	Irrigation	Wet
1 (June)	15	16	18
2 (July)	13	14	20
3 (Aug)	5	6	10

Measurements made during the experiment are tabulated below:

Measurement	Field	Lysimeters	Elevation
Solar radiation (Eppley pyranometer)	1	---	3 m above ground
Net radiation (Fritschen net radiometer)	1	1 at each	1 m above crop
Soil heat flux (Four N.I.L. discs in series)	1	1 at each	1 cm below surface
Air temperature (hygrothermometer)	1	---	2 m above crop
Vapor pressure (hygrothermometer)	1	---	2 m above crop
Windspeed (Casella anemometer)	1	---	2 m above crop
Leaf temperature (four TC in parallel)	2	1 at each	leaves on 4 plants

Measurement	Field	Lysimeters	Elevation
Leaf diffusion resistance (Leaf Resistance Meter)	-	1 at each	top leaf on 2 plants
Leaf thickness (Beta Ray Gauge)	-	1 at each	upper leaf on 1 plant
Soil moisture content (Neutron Meter)	4	1 at each	8 depths from 20-140 cm
Soil moisture tension (Tensiometer)	2	1 in #2	20, 40, 80, 120 and 140 cm

RESULTS:

A. Sorghum Development

Date	Item
May	
03	Planted RS-610 sorghum in lysimeter field in double rows on 40-inch beds.
13	Emergence.
28	Final plant thinning on lysimeters (2 × 10 plants per m^2).
Jun	
01	Plant height, 9 cm.
03	Plant height, 12 cm; beginning of tillering; began harvesting for leaf area index.
10	Height, 21 cm; up to 4 tillers per plant.
15	Height, 49 cm; first intensive measurement period, dry soil.
16	Irrigation.
18	Height, 55 cm; second intensive measurement period.
21	Height, 60 cm; "boot" stage.
24	Height, 73 cm; plant damage from hail.
28	Late "boot" stage
29	Height, 79 cm.
Jul	
02	Emergence of inflorescence from "boot".
05	Height, 80 cm.
07	Instrumented plants at two field sites, at the bottom of access tubes #2 and #3.
08	Height, 82 cm.
13	Height, 82 cm; vigorous plants have grain in the "milk" stage; third intensive measurement period, dry soil.
14	Irrigation.
19	Accelerated lower leaf senescence; grain in "dough" stage; height, 82 cm.
20	Fourth intensive measurement period, wet soil; lower 3-4 leaves dead; upper 4-5 leaves in fairly good condition.
27	Beginning of branching.
Aug	
05	Fifth intensive measurement period, dry soil.
06	Irrigation.
09	Moved plant instrumentation up to the flag leaf.
10	Sixth intensive measurement period, wet soil.
11	All plants harvested from lysimeters #1 and #2 and from both access tube sites (#2 and #3).
13	Grain harvested from lysimeter #3.
20	Remainder of plant material harvested from lysimeter #3; end of experiment.

A graphic summary of the development of the crop is given in Figure 2.

B. Soil Moisture

Soil moisture content in the lysimeters was to be matched with that in the field so that the measurements obtained in the lysimeters during the intensive period would be representative of the entire field. A comparison of the average soil moisture content to a depth of 150 cm between the lysimeters and the field is given for 12 weekly periods in Figure 3. The first four periods include the time during early development of the sorghum stand, which was planted on 3 May and first emerged on 13 May. The last eight periods include the three long irrigation cycles during which soil moisture was allowed to be depleted to the point of limiting transpiration. Matching the soil moisture content measurements more carefully during the early growing season would probably have resulted in a more uniform sorghum stand, but soil compaction differences in the field seemed to also cause stand variation. The most serious failure to match soil moisture contents occurred during the last intensive dry period. During this period the soil moisture content in the first two lysimeters was depleted to the point of permanent wilting before a high leaf diffusion resistance occurred in the third lysimeter in the field. Therefore, replication of measurements was lost for the last intensive wet period. Data from lysimeter #3 were used only.

A comparison of the measured evapotranspiration from the lysimeters with the soil moisture depletion from weekly soil moisture content measurements is shown by the shaded areas in Figure 4. These results indicated that using weekly neutron soil moisture content measurements for estimating evapotranspiration based upon soil moisture depletion can give considerable error. This error is probably caused by failure to assess the soil moisture depletion near the surface with the 20 cm sampling depth. Although the soil moisture depletion for the sixth weekly period underestimated the evapotranspiration as much as 60 percent, total moisture depletion for the last 11 weeks underestimated evapotranspiration by only 12 percent.

Results from the tensiometers were of little value since the older tensiometers developed leaks and the new plastic tensiometers (Lark) were not installed until 15 July. Also, soil moisture tensions that developed during the last intensive dry period exceeded the tensiometer range, and the last two irrigations were not sufficient to cause any appreciable moisture loss by deep percolation.

C. Energy Balance Data

As pointed out before, two types of information were obtained during the course of the experiment: (1) routine measurements of the energy balance over the field as a whole were continuously recorded, and (2) detailed data pertaining to each lysimeter were obtained, together with leaf temperatures and leaf resistances on three pairs of days, each pair straddling an irrigation.

From hourly energy balance data and measured evaporation and wind-speed at 2 m, a first estimate was obtained of the surface roughness on 17, 18, 25, 26, and 27 June. These days followed the irrigation on 16 June. Assuming that potential evaporation existed, a first estimate of z_o was 1.31 cm. It appears low in comparison with literature data; nevertheless, it was used for a set of preliminary calculations.

Next, a rough computation was made of the potential evaporation from daily averages of the necessary weather data, and the ratio to the actually recorded evaporation computed. These values are plotted in Figure 5, as a guide to the normalized evaporation and the effectiveness of the drying treatment. Figure 5 also shows data pertaining to the development of the crop as the weight of the leaf mass per m^2. At the time of the 16 June irrigation the crop was only partially developed; moreover, soil moisture depletion had not advanced very far. The August irrigation took place when seed heads were fully developed; also, only one lysimeter gave representative data. Thus, only the data collected on 13 and 20 July are of the desired quality. Table 1 shows, for the daylight hours, a comparison of energy balance and derived parameters on the day before and after irrigation.

D. Direct and Indirect Evaluation of Canopy Resistance

Elsewhere (WCL-29), a full account is given of the measurement of R_ℓ, the leaf resistance. These measurements were made on sunlit leaves, both top and bottom, and an average hourly value for R_ℓ was obtained and compared with the meteorologically derived parameter R_S (both are measured in seconds per centimeter, but the former is per square centimeter of leaf area, whereas, the latter is per square centimeter of land area). A plot of paired values is given in Figure 6. The R_S values should be viewed as first estimates and are presumed to contribute most of the scatter. Despite the tenuous relationship an estimated regression line is drawn which implies that, as a first estimate, $R_S = 0.5\ R_\ell$.

E. Leaf Temperatures and Sensible Heat Flux Between Air and Surface

Measured leaf temperatures agree qualitatively with the energy balance and stomatal resistance measurements. As we have concluded before from controlled indoor experiments, the leaf temperature referred to ambient appears to be one of the simplest and most reliable indicators of the leaf energy balance.

This is illustrated in Figure 7, which shows by hourly periods, the difference between leaf temperature at five locations (three in the lysimeters and two in between) and the air temperature at 2 m above the surface on, 13 and 20 July, respectively, before and after irrigation.

From the measured temperature difference an estimate of the sensible heat flow in the air can be made. This method is not detailed here, but it is, similarly to the combination method, based upon a logarithmic wind profile, an assumption that clearly does not apply, although it is used in the combination method.

These estimates can be compared with those derived directly from the energy balance

$$A = -(LE + R_n + S) \quad ,$$

and a preliminary set of results is given in Figure 8.

F. Discussion

This experiment represents a first attempt to relate atmospheric and canopy properties, where both determine jointly the evaporation rate and, consequently, the energy balance. The principal result is the comparison of the meteorological estimate of the canopy resistance (R_S) with the direct measurements made on the leaves (R_ℓ). A secondary result is the relation of leaf temperatures to the energy balance, as found by comparing a directly obtained and a calculated value for the sensible heat flux (A).

Many aspects of the observations were tentative and would be done differently if the experiment were to be repeated. In only one case out of three did the moisture depletion result in a meaningful situation, thus restricting the number of useful data. In evaluating the energy balance our knowledge of soil heat flow was deficient, partly because of the difficulty of placing the transducers in a representative location when a furrowed land surface is used. We were reasonably successful in maintaining uniform stand and moisture content between lysimeters and field until the next to the last irrigation when an error was made.

The leaf temperature measurement procedure appeared very satisfactory by pooling four thermocouples and using the multichannel compensated digital recorder, combined with ensuing computer tabulation and calculation. Yet, we do not know how representative the measured temperatures are of the effective canopy temperature.

Leaf resistance measurements, though tedious, appeared consistent and reproducible. The absolute accuracy is still somewhat open (see WCL-29). The most serious deficiency was probably the absence of data to provide a stability correction in the turbulent transfer coefficient estimate, and in the future, temperature profiles should be measured.

Based upon the 13 - 20 July data, we can say that by soil moisture depletion, the evaporation from a well-developed, mostly vegetative stand of sorghum was reduced to less than half the potential value. The energy balance indicated sensible heat losses during the daytime of around 0.4 ly min^{-1}. This agreed with leaf temperatures about 4 to 5 C above air temperature at 200 cm above the crop, but a calculation of the ensuing

sensible heat flux gave much smaller values, around 0.15 ly min^{-1}. This demonstrates the effect of free convection added to forced convection, which is all the calculation accounts for.

Within a few days after irrigation the situation reversed completely. The evaporation was close to its potential value and sensible heat was extracted from the air during the latter part of the day at a rate of about 0.2 ly min^{-1}. Leaf temperatures were now below ambient at 200 cm by anywhere from 0 to 4 C, depending on the time of day. Estimates of sensible heat flux were still less than those measured, although one would expect the opposite.

In all cases, energy balance and temperature gradient agreed perfectly as to the direction of flow (see Figure 8).

The direct measurements of R_ℓ reflected the expected effect of the two conditions on 13 and 20 July, respectively, and the numerical values obtained are of the order or magnitude as those of R_S. As a first result, this is very encouraging since the two measurements are wholly independent. Also, the values for R_ℓ were higher than those for R_S, as one must expect. As a first hypothesis, one would further anticipate a linear relation between the two parameters. This is but dimly shown by the data (see Figure 6), probably in large measure due to the imperfection of the meteorological model. The data suggest that with a leaf area index of about 3.5, $R_S = 0.5R_\ell$. In sorghum, this means that with a 7-fold greater leaf area than land area, the effective surface appears only twice as large, and thus, a considerable mutual interference of the foliage is indicated. Presumably, the lower parts of the canopy to not contribute much to either energy exchange or evaporation. Similar findings have been made with other crops, using different methods.

It is of interest to note that estimates of the ratio R_S/R_ℓ for an orange orchard also gave a value close to 0.5 (see a forthcoming article in Agricultural Meteorology, 1966).

As a preliminary result, the 1965 data indicate that one can, from a simple leaf parameter, estimate the role of the canopy in the evaporation process. Consequently, a means is indicated whereby evaporation below potential rates, when soil water is limiting, can be estimated. However, the quality of some of the required data needs to be improved and further work done before definite conclusions can be drawn.

SUMMARY:

Using a sorghum crop as a test object, a study was made in the summer of 1965 of the relation between directly measured values of leaf resistance to evaporation and calculated values of the canopy resistance.

The required variation of both parameters was induced by allowing the soil water reservoir to become largely depleted and then irrigating the field to restore maximum availability. One set of observations, straddling a mid-July irrigation, yielded significant information.

Using the energy budget approach, the canopy resistance was calculated from measured evaporation rates, the latter found with weighable lysimeters. The leaf resistance was monitored with the cup resistance meter developed here in 1964. Although the precision of measurement is open to improvement, the data show a numerical agreement between the two parameters and suggest that the canopy resistance is about half the leaf resistance for a sorghum stand that is on the verge of pushing out its inflorescences and that has a leaf area index of 3.5.

Leaf temperature measurements made concurrently with the other observations, using fine thermocouples, showed that this parameter agreed always with the energy budget as to the direction of sensible heat flow in the air. Quantitative calculations of the latter quantity did not agree well with the observed values. This is attributed to the inadequacy of the transfer function, which should be corrected for stability in future work.

The study as a whole has clarified the physics of an evaporating crop short of soil water: dehydration of leaf tissue produces partial stomatal closure, and the resultant increase in diffusion resistance changes the partition of radiant energy input. Besides the reduced evaporation rate, the role of the canopy regulation is also evident in that leaf temperature during the day will exceed ambient temperatures, rather than be lower as is the rule with well-watered sorghum.

PERSONNEL: C. H. M. van Bavel, K. J. Brust, W. L. Ehrler, and J. Conaway

Table 1. Energy balance and surface resistance to evaporation of sorghum before and after irrigation. Potential evaporation (E_o) and surface resistance are calculated with the combination method. R_A is an equivalent turbulent "resistance," calculated from windspeed and roughness parameter: z_0 = 1.31 cm

Hourly period	Net radiation minus soil heat flow	Air temperature	Vapor-pressure deficit	Wind-speed	Evaporation	Potential evaporation	E/E_o	R_A	R_S
	cal cm^{-2} min^{-1}	C	mb	m sec^{-1}	mm h^{-1}	mm h^{-1}		sec cm^{-1}	sec cm^{-1}
				13 JULY 1965 (BEFORE IRRIGATION)					
7	0.035	23.3	6.9	0.7	0.05	0.049	1.02	2.27	0.21
8	0.228	26.7	9.9	0.7	0.19	0.206	0.92	2.17	0.78
9	0.487	29.7	12.4	1.8	0.27	0.478	0.56	0.83	2.75
10	0.547	31.4	14.0	1.5	0.30	0.524	0.57	1.00	3.43
11	0.735	32.8	17.4	1.3	0.37	0.690	0.54	1.16	4.82
12	0.816	34.2	19.3	1.2	0.36	0.763	0.47	1.25	6.97
13	0.894	35.5	21.2	2.0	0.37	0.894	0.41	0.75	5.64
14	0.870	36.7	23.3	3.3	0.36	0.976	0.37	0.45	4.35
15	0.777	36.9	23.8	3.4	0.38	0.906	0.42	0.44	3.50
16	0.639	37.4	25.0	3.1	0.35	0.775	0.45	0.48	3.46
17	0.441	37.1	25.1	3.6	0.31	0.643	0.48	0.41	2.65
18	0.175	36.9	25.2	2.9	0.24	0.363	0.66	0.52	1.70
19	0.000	35.0	22.0	2.5	0.13	0.152	0.86	0.60	0.91

Continued

Table 1. Energy balance and surface resistance to evaporation of sorghum before and after irrigation. Potential evaporation (E_o) and surface resistance are calculated with the combination method. R_A is an equivalent turbulent "resistance," calculated from windspeed and roughness parameter: z_0 = 1.31 cm—Continued

Hourly period	Net radiation minus soil heat flow	Air temperature	Vapor-pressure deficit	Wind-speed	Evaporation	Potential evaporation	E/E_o	R_A	R_S
	cal cm^{-2} min^{-1}	C	mb	m sec^{-1}	mm h^{-1}	mm h^{-1}		sec cm^{-1}	sec cm^{-1}
				20 JULY 1965 (AFTER IRRIGATION)					
7	0.048	22.0	7.7	0.7	0.05	0.062	0.81	2.17	1.75
8	0.261	25.8	14.2	1.2	0.26	0.275	0.94	1.25	0.30
9	0.478	28.9	22.7	1.1	0.42	0.478	0.88	1.37	0.84
10	0.652	30.9	29.8	1.0	0.63	0.641	0.98	1.51	0.14
11	0.830	32.3	33.5	1.1	0.81	0.814	1.00	1.37	0.07
12	1.019	34.0	39.5	1.5	0.95	1.052	0.90	1.00	0.59
13	1.108	35.0	44.5	1.6	1.02	1.165	0.88	0.94	0.73
14	1.075	35.7	46.9	2.4	1.16	1.263	0.92	0.62	0.32
15	0.962	36.4	50.8	2.4	1.14	1.189	0.96	0.62	0.15
16	0.691	36.7	51.1	2.2	0.95	0.927	1.02	0.68	0.00
17	0.500	36.7	51.1	2.2	0.71	0.763	0.93	0.68	0.28
18	0.328	36.4	49.3	2.1	0.55	0.588	0.94	0.71	0.29
19	0.050	35.0	41.8	1.3	0.19	0.213	0.89	1.16	0.13

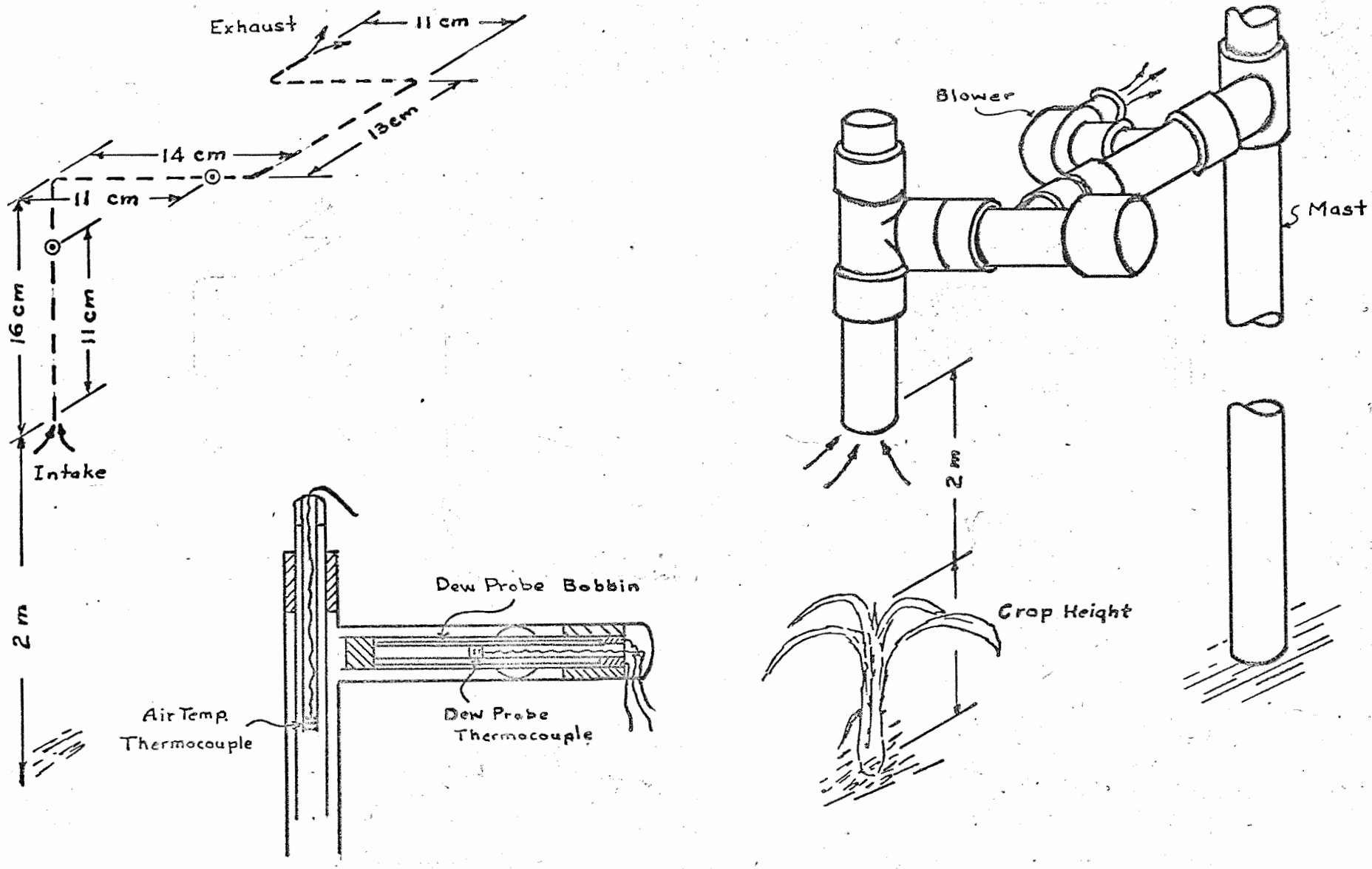

Figure 1. Schematic view (right), section (bottom), and dimensioning (left) of ventilated hygrothermometer. All materials are standard plastic pipe.

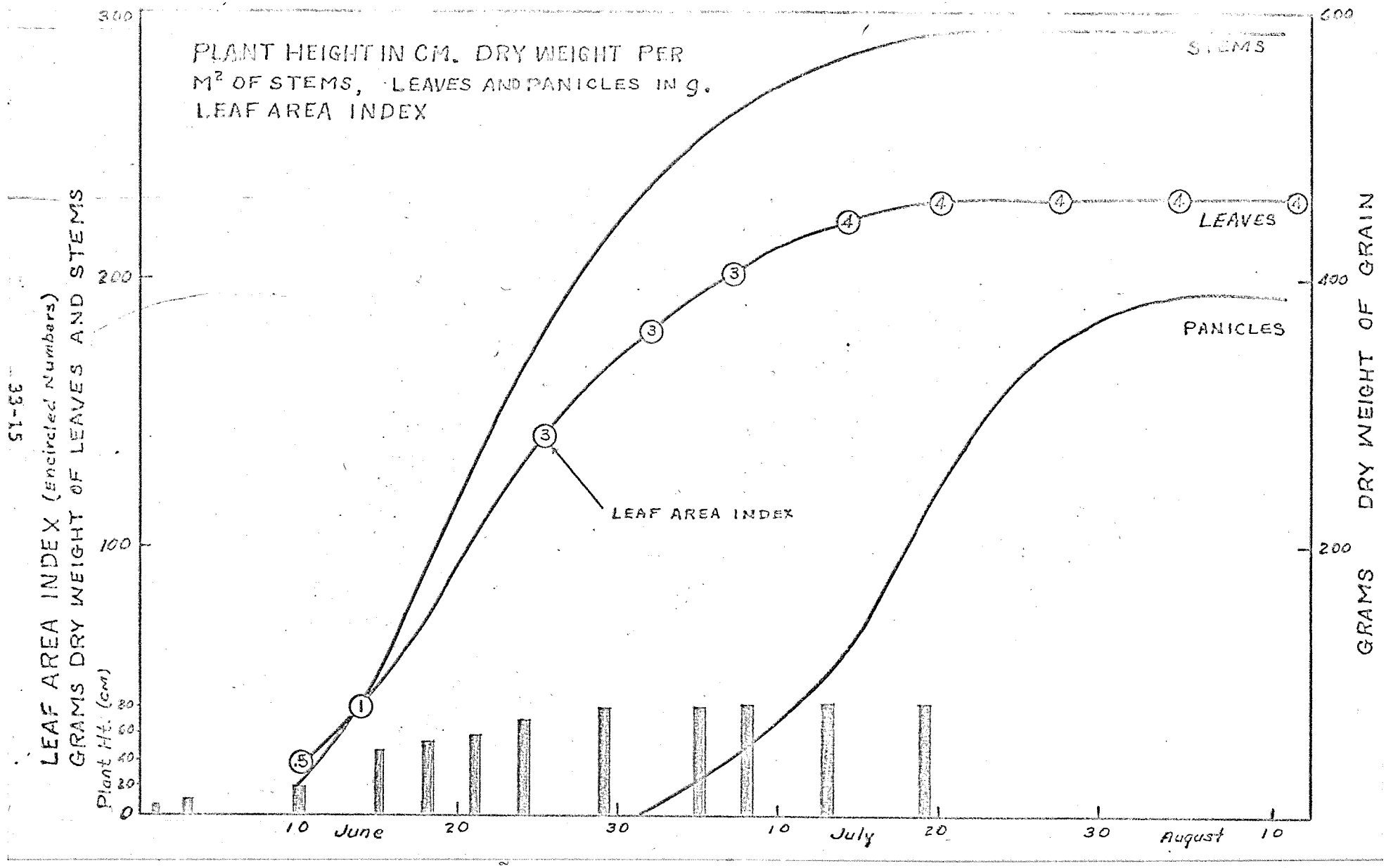

Figure 2. Development of sorghum crop in 1965. Plant height in cm; dry weight per m^2 of stems; leaves, and panicles in grams; also, leaf area index.

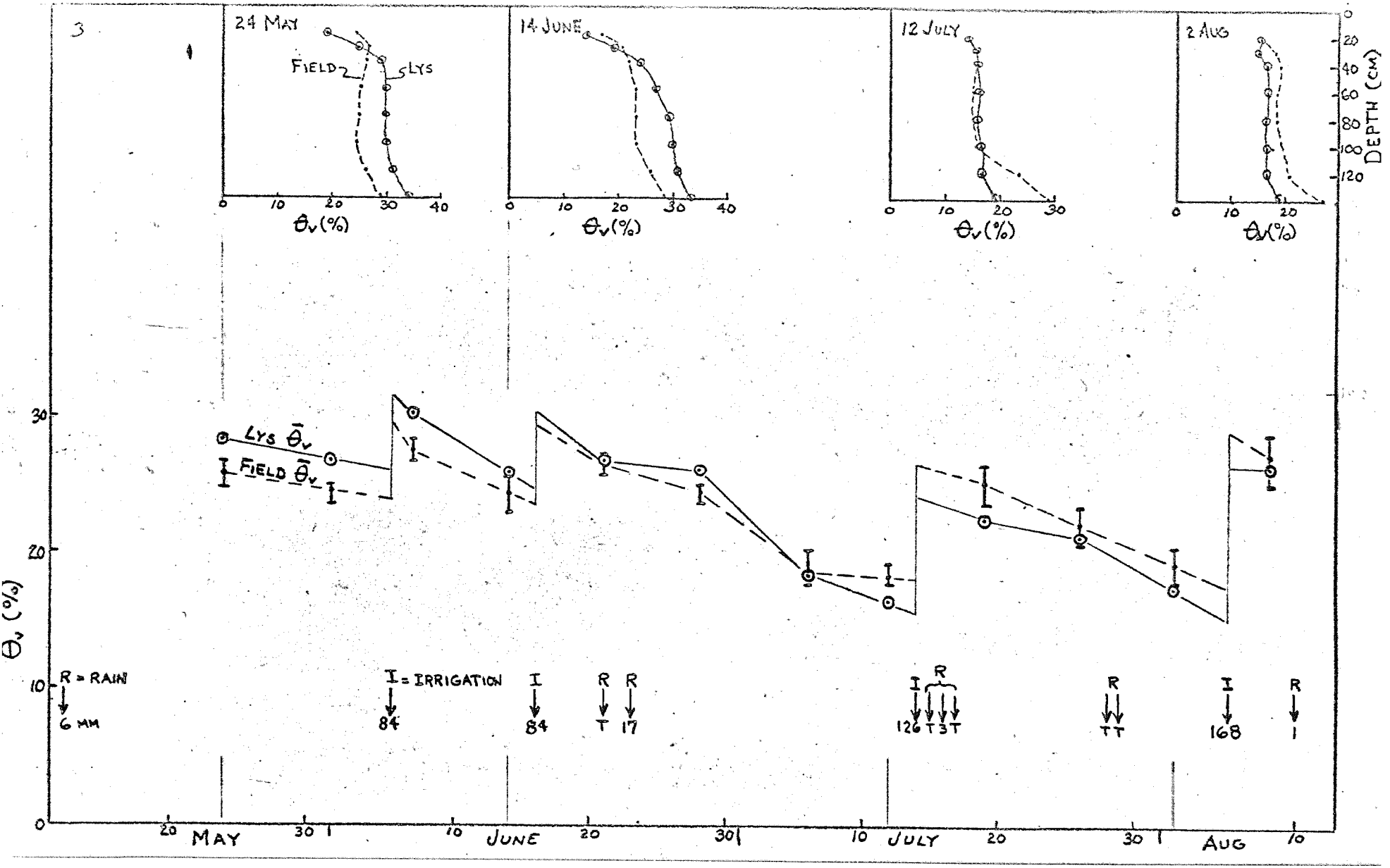

Figure 3. Comparison of weekly total profile water in field and in lysimeters expressed as volume fraction. Also, selected profiles of water content in the two locations.

Annual Report of the U.S. Water Conservation Laboratory

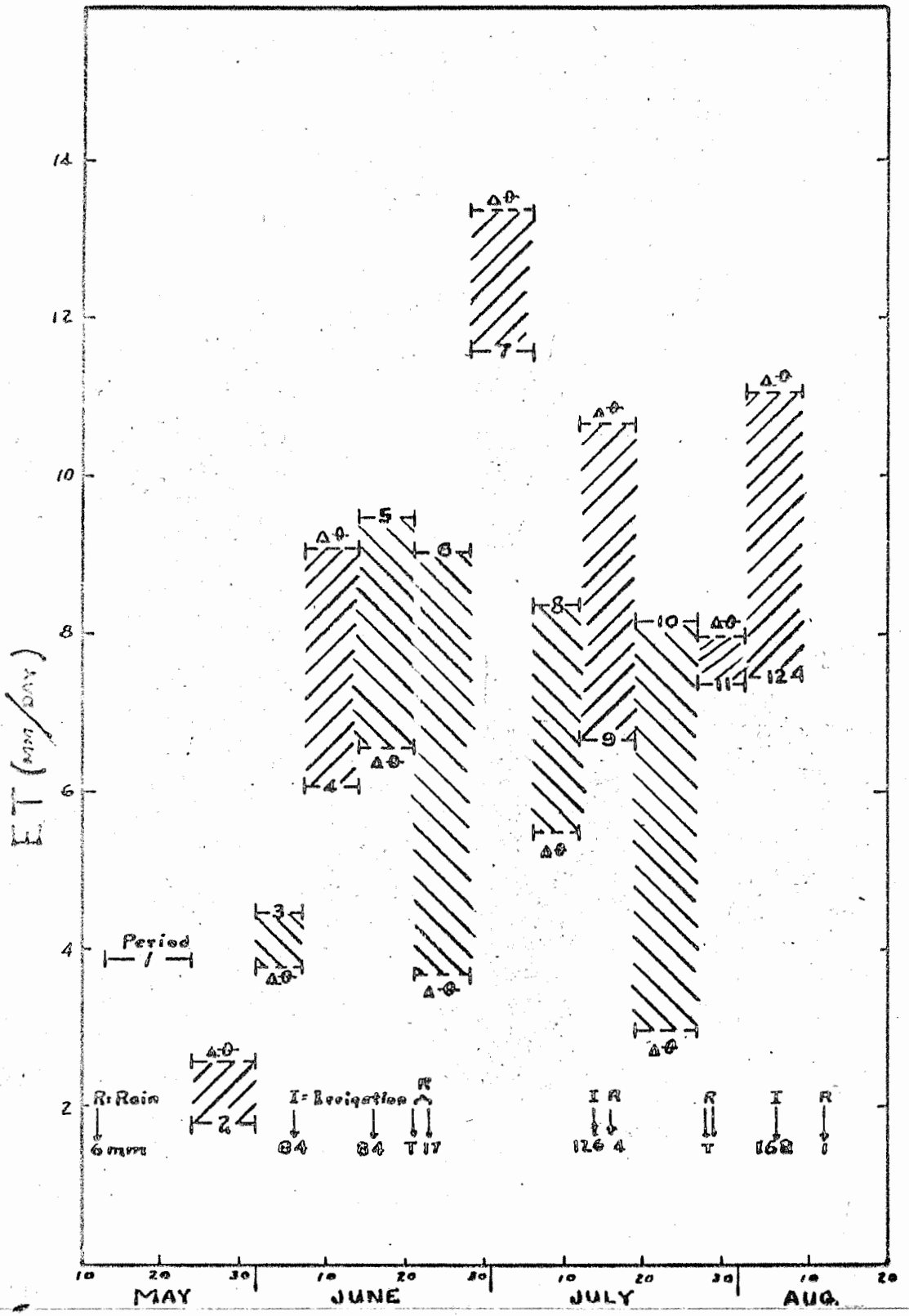

Figure 4. Comparison of evaporation calculated from soil moisture depletion and measured by lysimeters during 12 successive one-week periods.

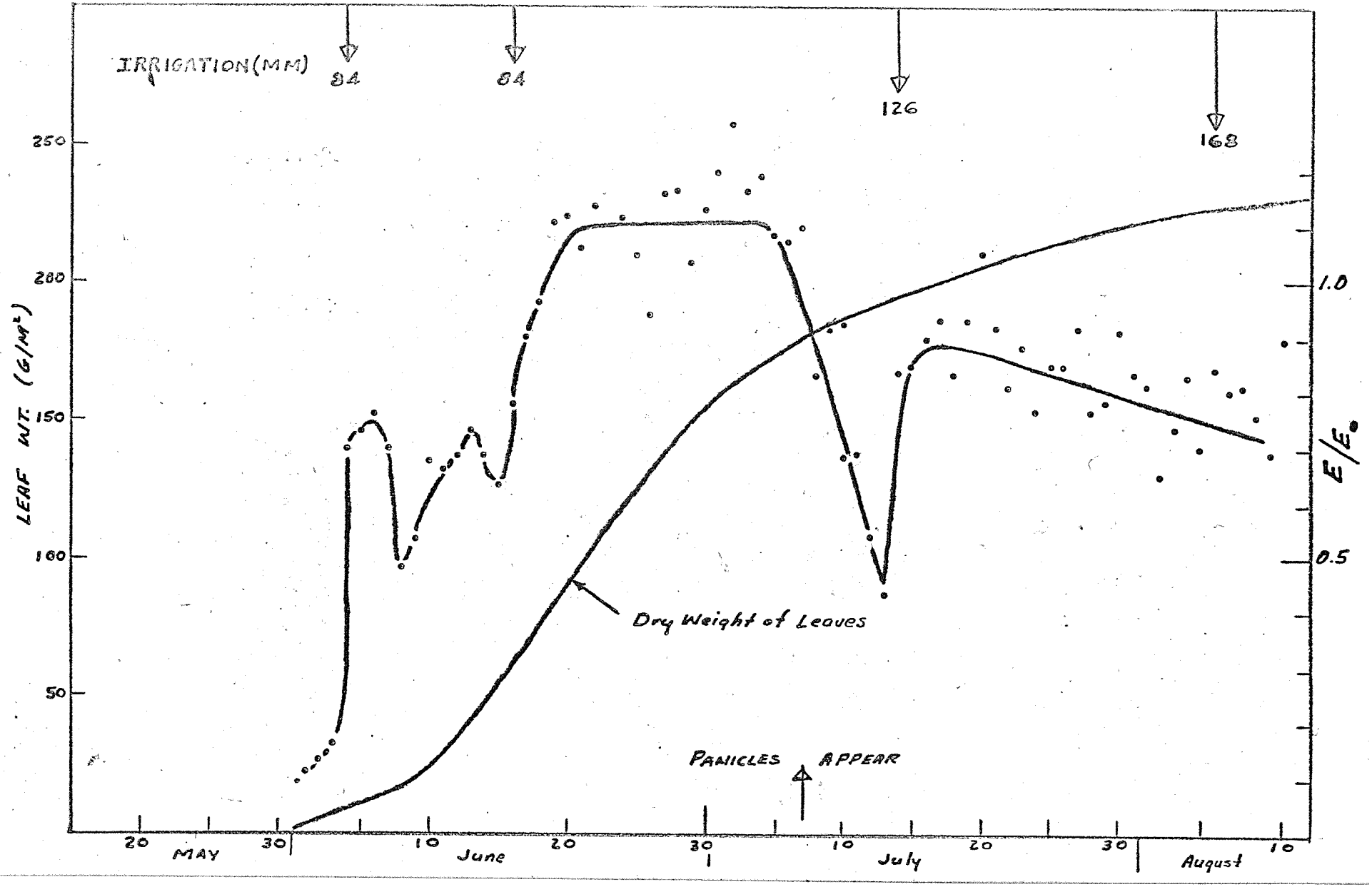

Figure 5. Daily values of the ratio of measured over potential evaporation from sorghum crop in 1965. Also shown are the dry weight of foliage in g m⁻² and irrigation time and quantity.

Annual Report of the U.S. Water Conservation Laboratory

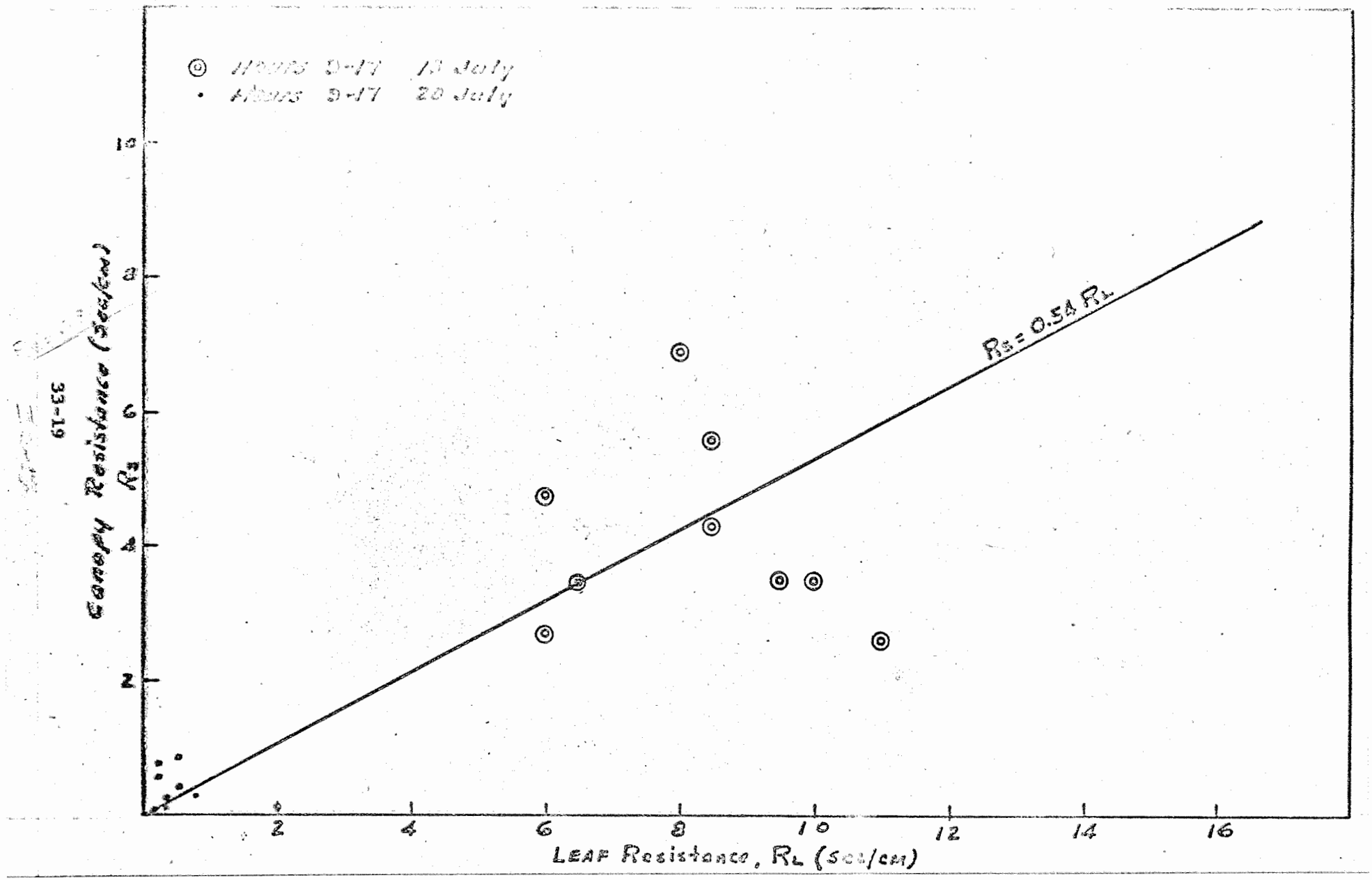

Figure 6. A pair diagram of hourly values of measured leaf resistance (R_L) and calculated canopy resistance (R_S), as obtained during daylight period on 13 and 20 July 1965 on sorghum

Annual Report of the U.S. Water Conservation Laboratory

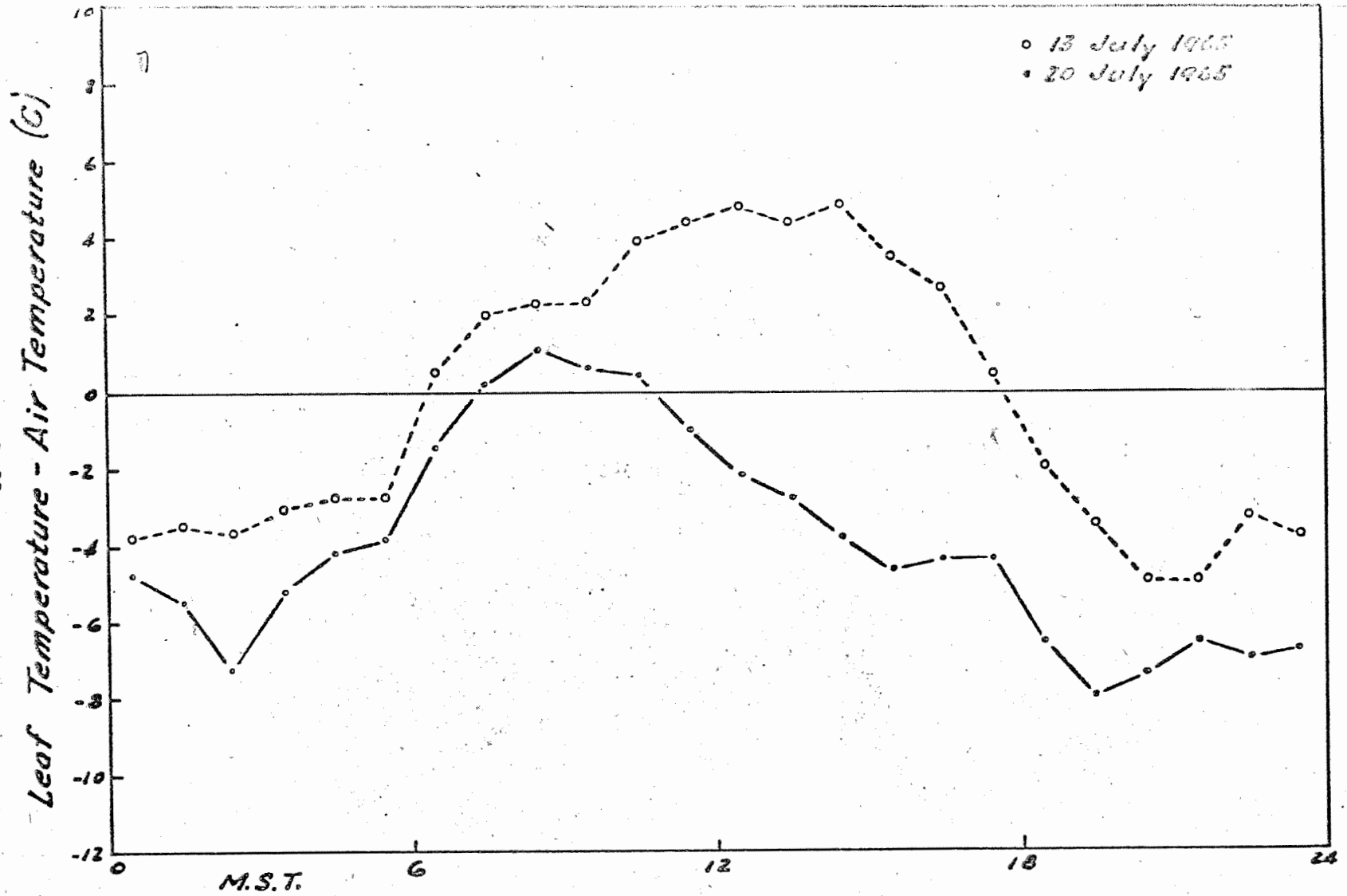

Figure 7. Hourly average of leaf temperature - air temperature at 2 m over the canopy, before irrigation on 13 July 1965, and after irrigation on 20 July 1965.

Annual Report of the U.S. Water Conservation Laboratory

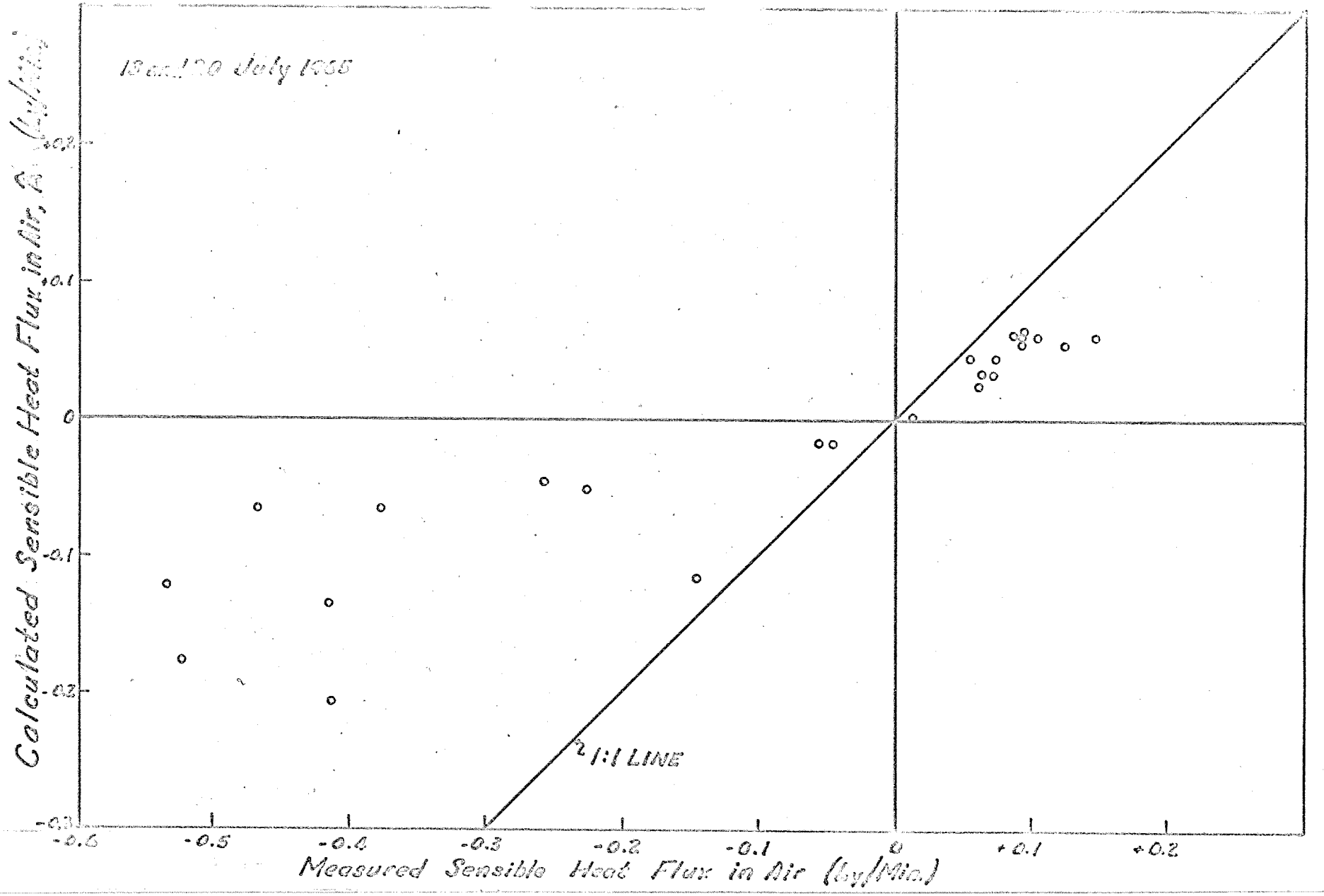

Figure 8. A pair diagram of average hourly values of measured and calculated sensible heat flux in air and of calculated values from leaf and air temperature, both in ly min^{-1}.

TITLE: WATER MANAGEMENT FOR THE EFFICIENT IRRIGATION OF SUGAR BEETS

LINE PROJECT: SWC 5-g2 CODE NO.: Ariz.-WCL-36

INTRODUCTION:

The objective of the experiment is to determine the irrigation requirements of sugar beets for maximum economic yield per unit of water.

Considerable acreages of sugar beets are being grown and more will be grown in the Southwest, mainly in lower California, Arizona, New Mexico, and Texas. Only limited information is available on water management for a long-season-grown sugar beet such as grown in the Southwest. Irrigation water is becoming more scarce in the Southwest, thus information is needed on the most economical use of water in the production of sugar beets.

In 1964, Arizona was given a 20,000-acre sugar beet allotment. Beets will be processed by the Spreckles Sugar Company near Chandler, Arizona, in the fall of 1967. Sugar beets for sugar have not been produced in Arizona since the early 1920's.

Beets for sugar are produced in the Southwest under considerably different conditions than in the Midwest. Beets are planted in the fall, go partially dormant in top growth during December, January, and February, and are exposed to light frosts. Warm weather in March starts rapid growth with increasing water use, attaining a peak use near the last of May.

Existing information on the influence of soil moisture on sugar beets is limited and conflicting. Research in California found no difference in the yield of sugar, even though soil moisture was allowed to reach the permanent wilting point to a depth of four feet between irrigations. Additional information from California showed trends towards increased production on low soil-tension treatments. Studies in Utah showed reductions in yield by both over- and under-irrigation. Analysis of water use in relation to nitrogen levels indicates water use increases with increased nitrogen. Other research indicates that beets need not be wetted below two feet; however, data taken at Mesa, Arizona,

in 1963 and 1964, show that beets use significant amounts of water from the three, four and five foot depths. Studies in California also show substantial water use below two feet.

PROCEDURE:

The experiment is located at the University of Arizona Experiment Farm, Mesa, Arizona.

Design and Procedure

Four borders, each 300 x 33 feet, were split into 60 plots (each 16.5 x 27 feet) containing nine rows of beets, planted October 12, two rows on a 40-inch bed. Ten irrigation treatments were replicated six times in a randomized block design. One hundred units of phosphate and 130 units of nitrogen were applied previous to planting of 301-H monogerm beet seed. An additional 70 units of nitrogen were applied after thinning. The seed was germinated by irrigating up with at least one acre-foot applied at this time. A pre-determined quantity of water was pumped and measured with a Sparling meter into the respective plots at each subsequent irrigation. Hand thinning, normal cultivation and weed control were conducted.

Treatments and Variables

A. Under investigation: (soil moisture)

Treatment 1 - irrigate when less than 40 percent of the available water in the top three feet of soil was depleted.

(1) 1A - irrigate continuously until harvest.

(2) 1A - 3A irrigate until April 20, then like 3A.

(3) 1A - 2A irrigate until April 20, then like 2A.

Treatment 2 - irrigate when 60 percent of the available water in the top three feet was depleted.

(4) 2A - irrigate continuously until harvest.

(5) 2A - 1A irrigate until April 20, then like 1A.

(6) 2A - 3A irrigate until April 20, then like 3A.

Treatment 3 - irrigate when 80 percent of the available water in the top three feet was depleted.

(7) 3A - irrigate continuously until harvest.

(8) 3A - 1A irrigate until April 20, then like 1A.

(9) 3A - 2A irrigate until April 20, then like 2A.

Treatment 4 - irrigate only when a visual moisture stress appeared.

(10) 4A - irrigate continuously until harvest.

The basic treatments, 1A, 2A, and 3A, were designed to cover the regime of very dry to wet. The April change in schedule was designed to determine if such a procedure was desirable from the standpoint of production and water conservation. Measurements of consumptive use made in 1963 and 1964 showed that approximately 50 inches of water were consumptively used. Beets attained a water-use peak the latter part of November and a high peak the last of May. About 65 percent of the water depleted was from the top two feet of soil. About 70 percent of the consumptive use took place after April 1.

Data to be Obtained

1. Quantity of water applied by measurement with a Sparling meter.
2. Soil-moisture depletion by gravimetric sampling.
3. Growth rate measurements and plant physiology.
4. Yield and sucrose measurements on four harvest dates.

Methods of Interpreting Results

1. Analysis of variance

Source	df
Main plots	59
Treatments	9
Replications	5
Error	45

AMENDMENT 1

TITLE: DETERMINATION OF THE RATIO OF ROOT TO TOP GROWTH FOR FALL-PLANTED SUGAR BEETS

LINE PROJECT: SWC 5-g2 CODE NO.: Ariz.-WCL-36

INTRODUCTION:

The objectives of the experiment are: (1) To obtain bi-weekly weights of sugar-beet tops and roots from late February until the last harvest; (2) To obtain a record of the bi-weekly changes in sugar content from the probable first harvest until the last harvest.

At the request of the Spreckles Sugar Company, the nine beet rows acting as a buffer for the original sugar-beet study plot were utilized in a further study to determine the ratio of roots to top growth. It is of economic interest to know when both top and bottom growth attain their peak weights. It is also of interest to know the sugar content throughout the season because of its economic importance as associated with the compulsorily staggered harvest dates and the various yields at these harvest dates.

PROCEDURE:

The experiment is located at the University of Arizona Experiment Farm, Mesa, Arizona.

Treatments and Variables

A. Under investigation: (harvest dates)

1. Eleven harvest dates, starting on February 25, and thereafter at two-week intervals. The February 25 harvest date was indicated as No. 1, and the last harvest as No. 11.

Beets were planted and thinned to about one foot between plants. Plots were irrigated on the same schedule as 2A, a medium treatment scheduled to be irrigated when 60 percent of the available water was depleted from the top three feet of soil. At each of the eleven harvest dates, six lineal feet in each of four rows of beets were harvested. Tops and bottoms were weighed separately. Representative beet samples from each of the four replications were processed, and sugar content

analysis made. The beet area involved was split into 44 plots, each plot nine rows wide and six feet long. Harvest dates were replicated four times in a randomized block design.

Data to be Obtained

1. Weights of tops and bottoms.
2. Sucrose content, starting in June.

Methods of Interpreting Results

1. Analysis of variance

Source	df
Main plots	43
Harvest dates	10
Replications	3
Main plot error	30

AMENDMENT 2

TITLE: EFFECT OF LATE-SEASON SOIL MOISTURE STRESS ON SUCROSE CONTENT OF SUGAR BEETS

LINE PROJECT: SWC 5-g2 CODE NO.: Ariz.-WCL-36

INTRODUCTION:

The objective of the experiment is to investigate the effect on sucrose content of beets if they are allowed to become very dry before each harvest.

Considerable research has been conducted involving the many variables that might affect sucrose content. In some areas, research showed increases in sugar content with increased soil moisture stress. It is also of interest to note the change in yield, if any, when severe stresses are initiated just before harvest.

PROCEDURE:

The experiment is located at the University of Arizona Experiment Farm, Mesa, Arizona.

Treatments and Variables

A. Under investigation: (harvest dates).

1. Two moisture treatments, one wet and the other very dry, were established, starting in June.
2. Harvest was conducted whenever the dry treatments showed visual moisture stress.

Beets were planted and thinned to about one foot between plants. Plots were irrigated on the same schedule as 2A, a medium treatment scheduled for irrigation when 60 percent of the available water was depleted from the top three feet of soil. The buffer area (9 rows wide by 270' long) was divided into eight plots, each 33' long. Yields and sucrose measurements were made whenever dry plots reached a visual soil moisture stress appearance, from four rows, each six feet long. Dry and wet plots were replicated four times.

Data to be Obtained

1. Weight of beets at each harvest date.
2. Sucrose content of beets at each harvest date.

Method of Interpreting Results

1. Analysis of variance

Source	df
Main plots	7
Moisture levels	1
Replications	3
Main plot error	3

FIELD PLAN

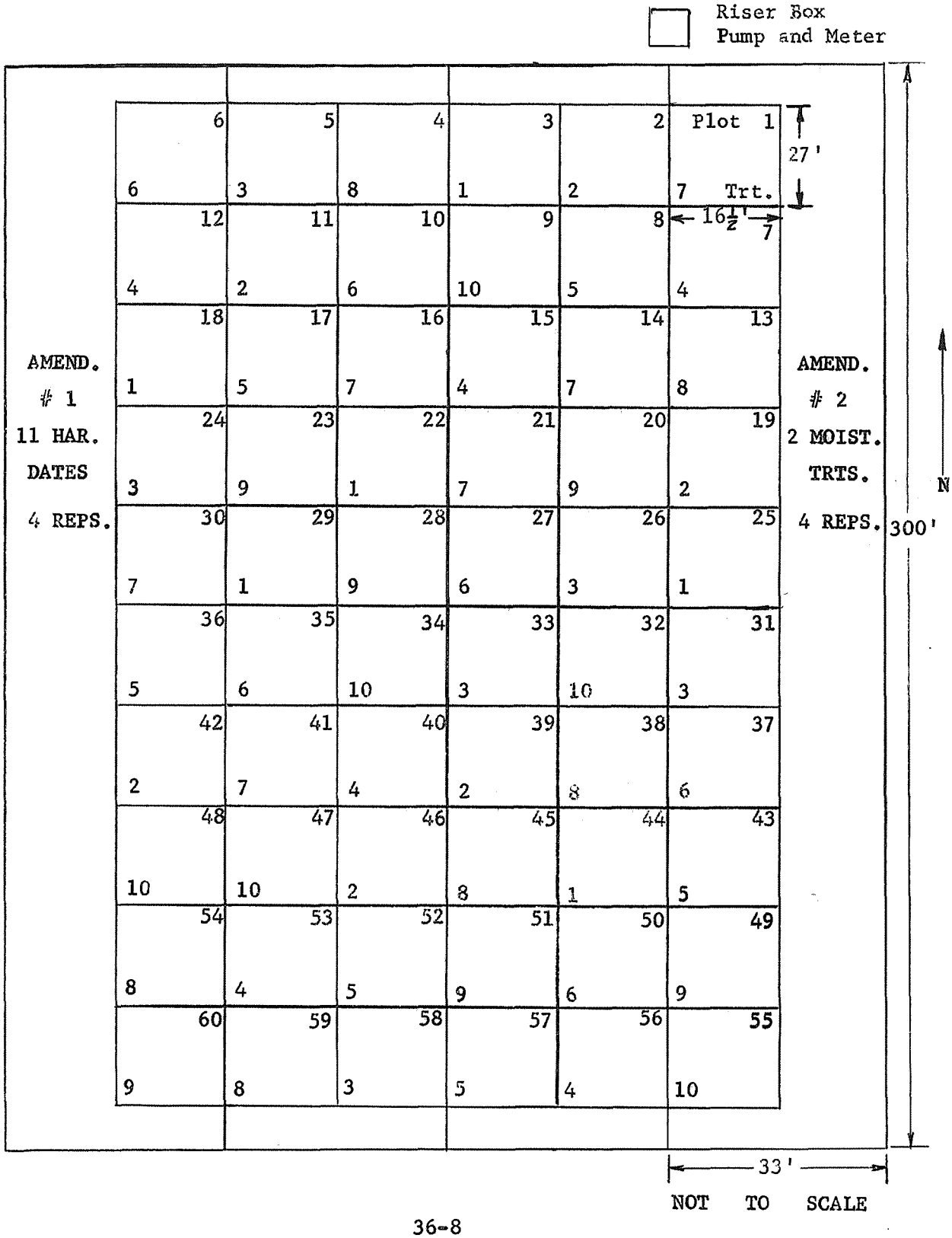
Riser Box
Pump and Meter
Plot 1
Trt.
27'
16½'
AMEND.
1
11 HAR.
DATES
4 REPS.
AMEND.
2
2 MOIST.
TRTS.
4 REPS.
N
300'
33'
NOT TO SCALE

DATES

TRT.	10/12	10/28	11/18	12/15	2/5	3/2	3/5	3/19	3/30	4/2	4/23	5/6	5/10	5/17	5/21	5/27	6/4	6/7	6/16	6/24	6/29	7/8	7/14	TOTAL
1	X	X	X	X	X		X			X	X	X			X		X		X		X		X	14
2	X	X	X	X	X		X			X	X			X				X			X			11
3	X	X	X	X	X		X			X	X		X			X		X		X		X		13
4	X	X	X			X			X		X		X			X		X		X		X		11
5	X	X	X			X			X		X	X			X		X		X		X		X	12
6	X	X	X			X			X		X			X				X			X			9
7	X	X	X					X			X			X				X			X			8
8	X	X	X					X			X	X			X		X		X		X		X	11
9	X	X	X					X			X		X			X		X		X		X		10
10	X	X	X					X			X					X				X			X	8

SCHEDULE OF IRRIGATIONS

RESULTS AND DISCUSSION:

Sugar beets were planted October 12, 1964 and irrigated up. An additional irrigation was given October 28. Plants were thinned to about nine inches between plants, from November 9 to November 12. Plants were side dressed with 70 units of nitrogen on November 12, and all plots were given an irrigation, November 18.

Considerable "yellows" was observed in mid-winter. There was some visual indication that "yellows" was more severe on the wet plots. There was no visual indication that plants on any treatment were damaged because of moisture stress up to April 23, when all plots were given an irrigation.

Visual leaf coloring as indicator of stress could not be observed. The only major visual signs of stress were that lower leaves wilted and fell when extreme stress occurred. Very little bolting developed, but winter temperatures were unusually mild. Spring temperatures were abnormally cool, with frequent light rains in December, January and February.

Beets from the main plot study were harvested June 1 and 21, and July 13 and 27. Yields were taken on six rows, each four feet long. Beets and beet-top measurements were commenced on Amendment No. 1, February 25, and continued at two-week intervals until eleven harvests were made. Each plot harvested consisted of four rows, each four feet long. Beets were harvested on Amendment No. 2 from four rows, each six feet long, June 9 and 22, and July 13 and 27. All beets were counted, weighed, and samples taken for sucrose measurements.

The first three irrigations applied to all plots were not measured other than by soil moisture sampling. All other irrigations were measured with a Sparling Meter. Soil moisture samples were taken on the planting date, at intervals of no more than ten days, before and after each irrigation, and on the final harvest date. Samples were taken on three plots for each treatment and two samples consolidated from each plot. Soil samples were taken at 1-foot increments, through six feet. The average percent soil moisture content before each irrigation was wet 54, medium 58, dry 72, and stress 80.

SUMMARY AND CONCLUSIONS:

Main Study

There is a difference in yields between irrigation treatments ranging from 10 to 18 percent, however only one harvest date, July 13, (Table 1), showed any differences that were statistically significant. In general, the wetter treatments are inferior to treatments in the medium or dry range. Treatments kept dry early in the season (8 and 9) and then changed to a wetter regime in April, seemed to be more desirable from a total beet yield standpoint. Because of the relatively poor beet yield showing of Treatments 1, 2 and 3, one would conclude that a wet regime is inferior. This inference may be partially false since the poor showing could be associated with the incidence of "yellows" or a retarding effect due to keeping the plant succulent during the cold months. Beet roots continued to increase in size as the harvest season was extended. Beet yields for Treatment 4 increased at an average rate of 2,195 lbs per acre per week (Figure 1), from June 1 to July 13, then at a reduced rate of 1,862 lbs per acre per week, until July 27. Because of the general lack of statistical significance between treatments, the inference can be made that the beet plant has the ability to use moisture even when the moisture is under high tension and not show a great reduction in yield of beet roots or in sugar percentage.

Table 2 represents the sugar percentages for all harvest dates. The trend is that beets subject to the dry soil moisture regime during all of the last half of the growing season (Treatments 2, 6, 7), have the highest sugar content. This is more significant for the last two harvest dates.

When the sugar percentages are applied to the beet root yields, (Table 3), the trend is for a dry to medium (9), a medium (4), a dry (7) or a medium to wet (6) to give highest total sugar potential. Sugar percentage is lowest for the first and last harvests. (Figure 1).

Seasonal consumptive use was nearly ten inches less in 1965 than in 1964. Previous years' study showed a small peak use in late November,

which was not evident this year. A cool fall and spring could have been responsible for the lack of a peak and for the lower consumptive use. Even though a range of soil moisture regimes existed, consumptive use measurements were relatively similar. Changes in the way the different irrigation regimes used water were not evident until the middle of April, when the wetter treatments showed greater use of water. The stress treatment showed a definite decrease in use in the middle of June. The effect was indicated by poor yields for the last three harvests. The dry treatment showed a rather constant use throughout the harvest, but data did not indicate that this decrease caused lower yields.

Soil profile depletion shows that if the fifth and sixth foot soil profiles are wetted at planting time, they will have enough water stored to satisfy the seasonal plant needs. Use in the top foot was higher in 1965 than in previous years.

The 1965 data indicates a consumptive use of about 40 inches should be adequate for a late season harvest for maximum yields. Data indicates irrigations could be spaced at three-week intervals during the harvest period to accommodate the required harvest dates. If early irrigations are not needed for purposes of improving germination, maintaining stands, or dissolving fertilizer, it may not be necessary to irrigate until the first part of January. From Figure 4, data shows that only 3.42 inches of water have been used from the root zone by January 1.

AMENDMENT NO. 1

Root tops increase in weight until a peak is reached in the middle of June, then decline very rapidly because leaves begin to mature (Figure 2). The yield of tops reaches a peak of 35 tons per acre. Roots continue to increase in weight with each harvest until the last harvest, July 27. Final beet root yield is 32.3 tons per acre. Sugar percentage increases until July 16, then declines for the remainder of the harvest season. The highest sugar percentage is 13 percent. Beet-top yields could be expected to be much larger if "yellows" does not occur.

AMENDMENT NO. 2

Dry treatments have higher sugar contents for each harvest but lower beet yield per harvest. Plants were irrigated under a medium regime until a dry status was attained on June 9. A 2 1/4 ton difference in root yield was recorded at that time. The same yield difference was measured for the three additional harvests. The rather pronounced decrease in yield occurring when the study was changed from a medium to a dry status should be investigated further and in more detail.

PERSONNEL: Leonard J. Erie and Orrin F. French.

TABLE 1.

MEAN PLOT YIELD IN POUNDS AT HARVEST DATES (6 REPS.)

JUNE 1		JUNE 21		JULY 13			JULY 27	
TRT	$\bar{x}$	TRT	$\bar{x}$	TRT	$\bar{x}$		TRT	$\bar{x}$
4	45.8	9	55.8	8	59.7	a	9	63.3
9	45.8	5	52.7	9	59.0	ab	8	61.7
10	43.8	8	52.4	4	57.9	ab	7	60.3
6	43.1	4	51.6	6	55.6	ab	5	60.2
5	42.6	1	50.6	3	54.7	ab	4	59.5
8	42.6	3	50.3	7	54.4	abc	6	58.3
7	41.7	6	49.8	1	54.1	abc	1	57.9
2	41.4	7	49.2	5	54.0	abc	10	57.8
3	40.5	2	48.1	10	53.7	bc	3	56.9
1	38.5	10	45.8	2	48.6	c	2	56.4
No. Sig.		No Sig.		Sig. 1%			No Sig.	
				LSD 5.9				

To convert plot yields to pounds per acre, multiply ($\bar{x}$)(1089).

TABLE 2.

MEAN SUGAR PERCENTAGE AT HARVEST DATES

JUNE 1		JUNE 21		JULY 13		JULY 27	
TRT	$\bar{x}$ 3 REPS	TRT	$\bar{x}$ 3 REPS	TRT	$\bar{x}$ 6 REPS	TRT	$\bar{x}$ 6 REPS
1	13.5 a	10	14.0	6	14.0 a	6	13.7 a
7	13.2 ab	3	13.6	7	13.8 ab	7	13.6 ab
2	12.9 abc	2	13.5	2	13.8 ab	2	13.1 abc
8	12.8 bc	6	13.4	10	13.8 ab	3	12.9 bcd
6	12.8 bc	4	13.3	1	13.4 abc	8	12.8 bcd
5	12.7 bc	9	13.2	8	13.3 abc	9	12.8 cd
4	12.6 bc	1	13.1	3	13.0 bc	10	12.7 cd
10	12.6 bc	7	13.0	4	13.0 bc	4	12.7 cd
3	12.5 c	5	12.8	5	12.9 bc	5	12.5 cd
9	12.5 c	8	12.7	9	12.6 c	1	12.3 d
Sig. 1%		No Sig.		Sig. 1%		Sig. 1%	
LSD 0.66				LSD 1.01		LSD 0.81	

TABLE 3.

MEAN YIELD OF SUGAR IN POUNDS PER PLOT AT HARVEST DATES (6 REPS)

TRT	$\bar{x}$	TRT	$\bar{x}$	TRT	$\bar{x}$	TRT	x
4	5.78	9	7.34	8	7.92 a	7	8.21
9	5.70	4	6.88	6	7.81 ab	9	8.10
10	5.52	3	6.84	7	7.53 abc	6	7.99
6	5.50	5	6.72	4	7.50 abc	8	7.90
7	5.49	6	6.67	9	7.46 abc	4	7.56
8	5.46	1	6.66	10	7.37 abcd	5	7.50
5	5.43	8	6.63	1	7.24 abcd	2	7.39
2	5.34	2	6.51	3	7.09 bcd	10	7.36
1	5.18	10	6.41	5	6.98 d	3	7.32
3	5.06	7	6.38	2	6.71 d	1	7.11
No Sig.		No Sig.		Sig. 5%		No Sig.	
				LSD 0.72			

To convert plot yields to pounds per acre, multiply ($\bar{x}$)(1089)

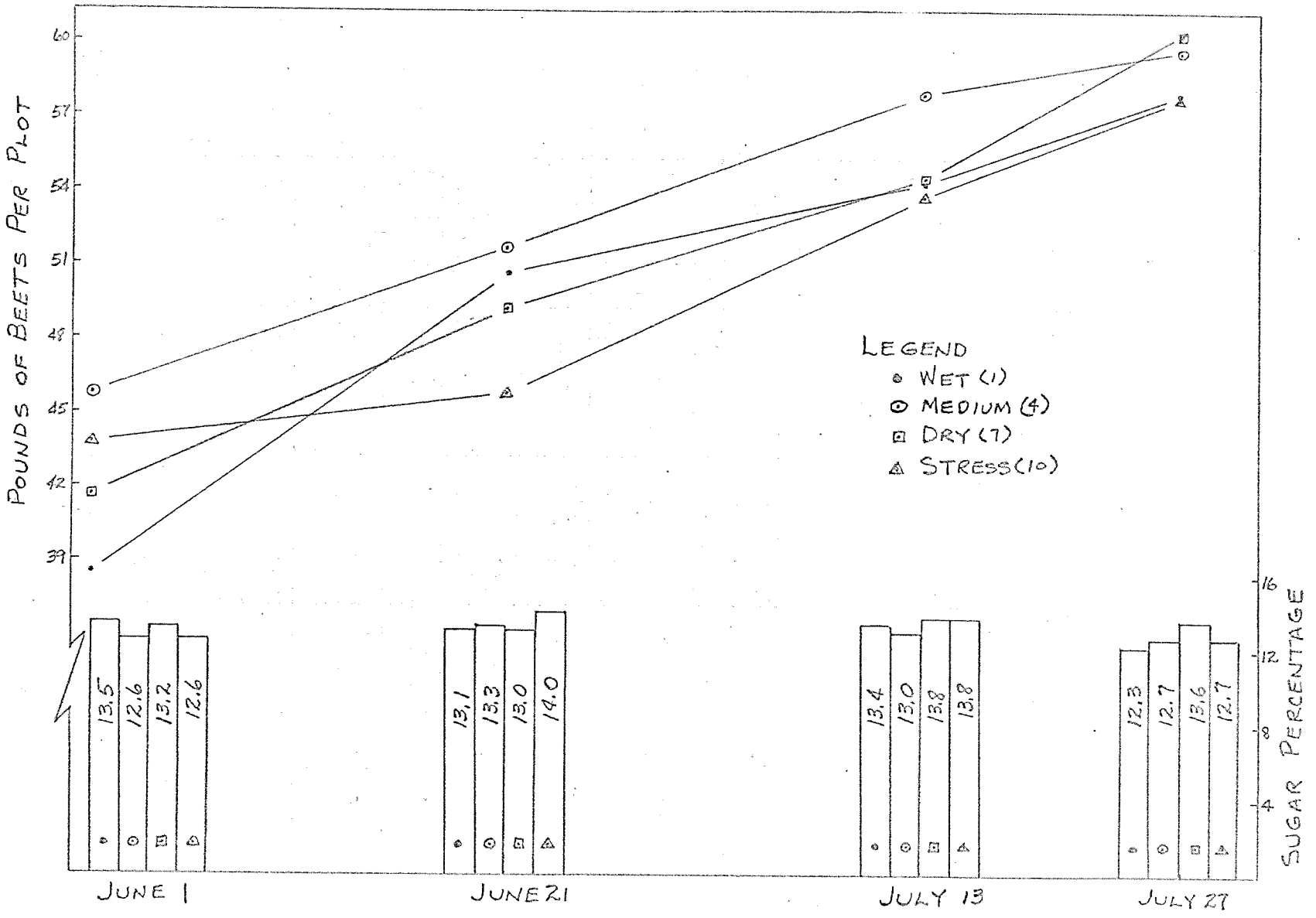

FIG. 1 MEAN PLOT YIELDS AND SUGAR PERCENTAGES FOR SUGA

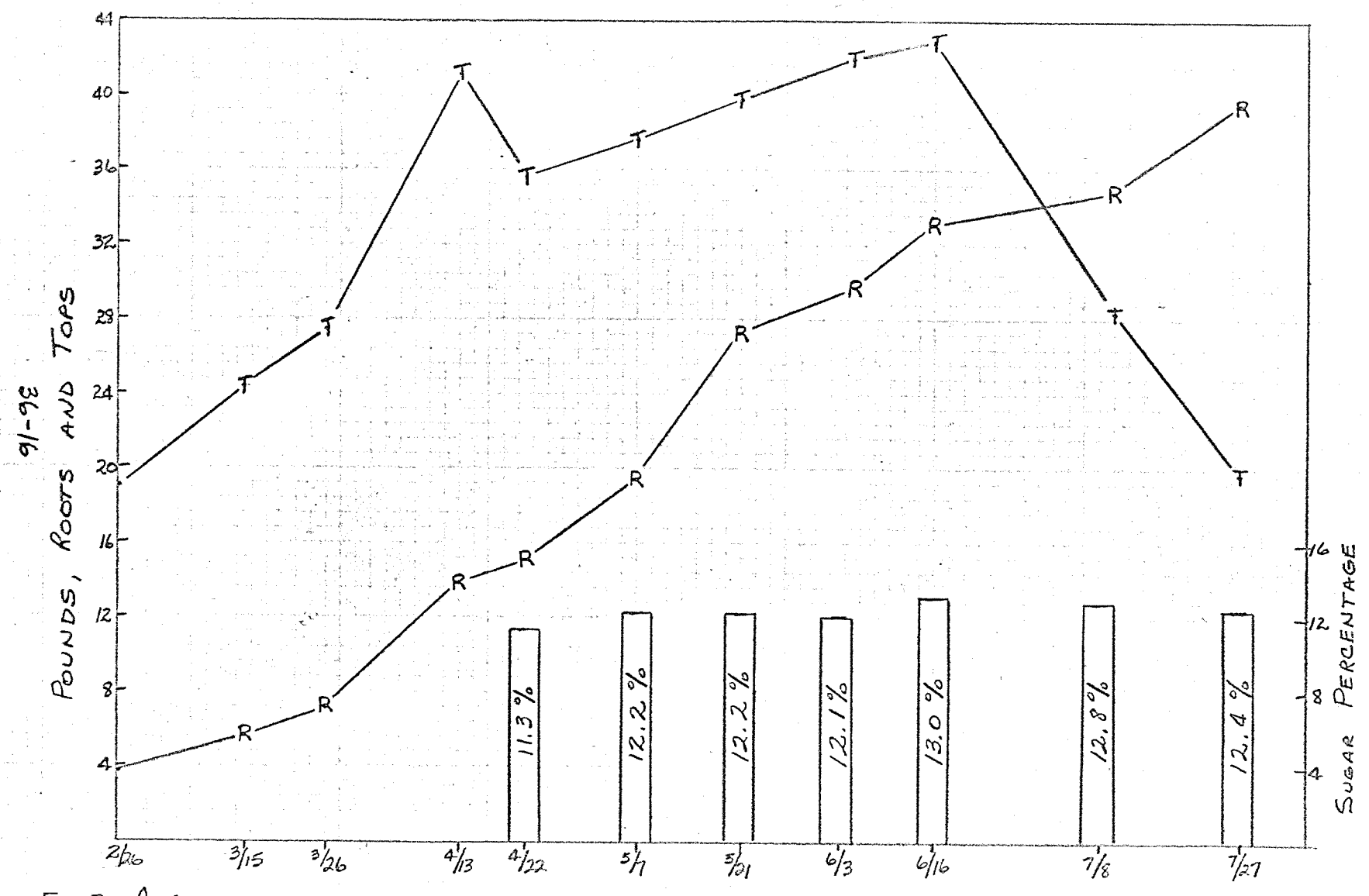

FIG. 2 A COMPARISON OF ROOT AND TOP WEIGHTS OF SUGAR BEETS FOR ELEVEN HARVEST DATES WITH SUGAR PERCENTAGES FOR THE LAST SEVEN DATES. EACH POINT ON THE CURVE IS A MEAN OF 4 REPS.

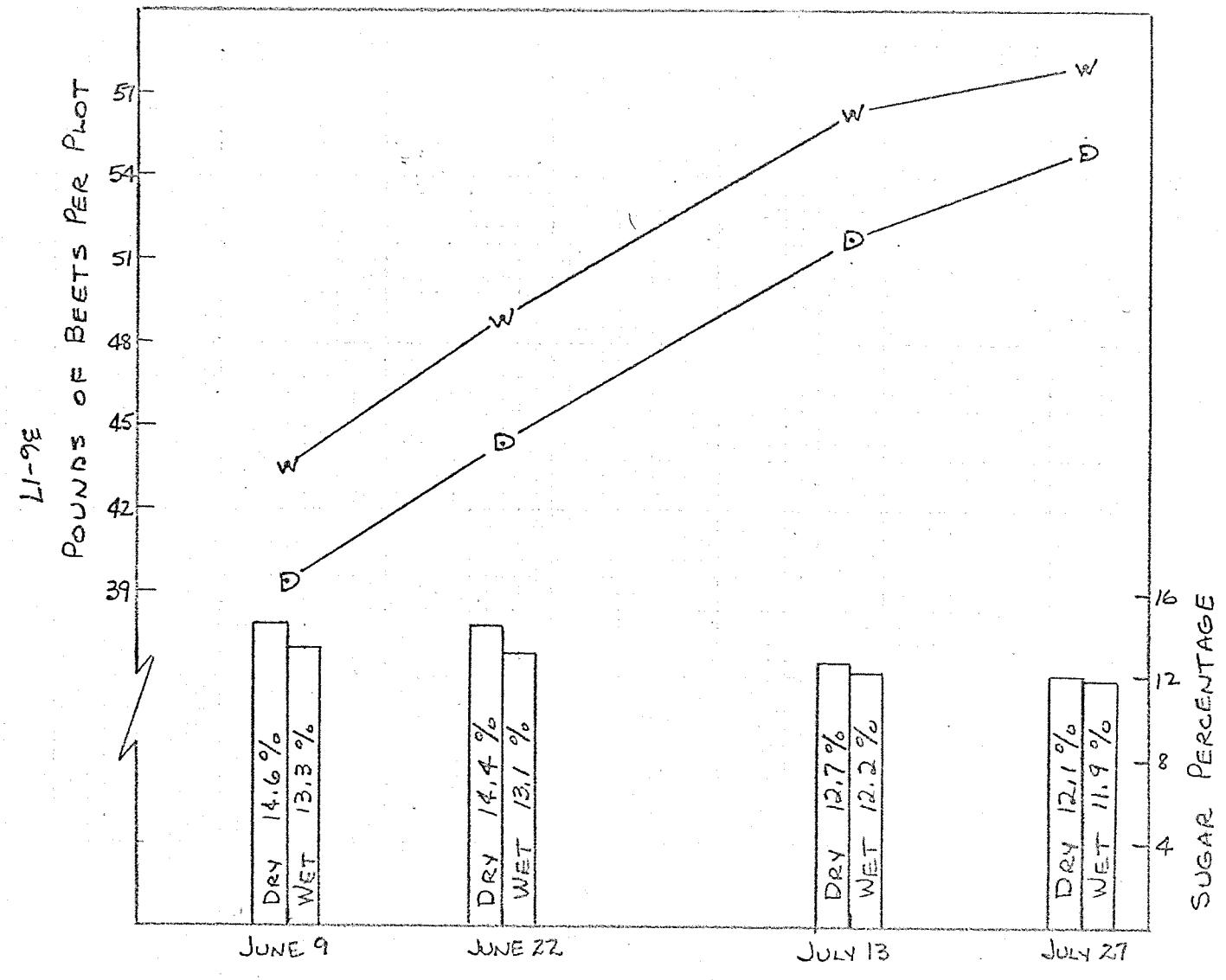

FIG. 3 EFFECT OF LATE-SEASON SOIL MOISTURE STRESS ON YIELDS AND SUGAR PERCENTAGE OF BEETS. EACH POINT ON CURVE IS A MEAN OF 4 REPS.

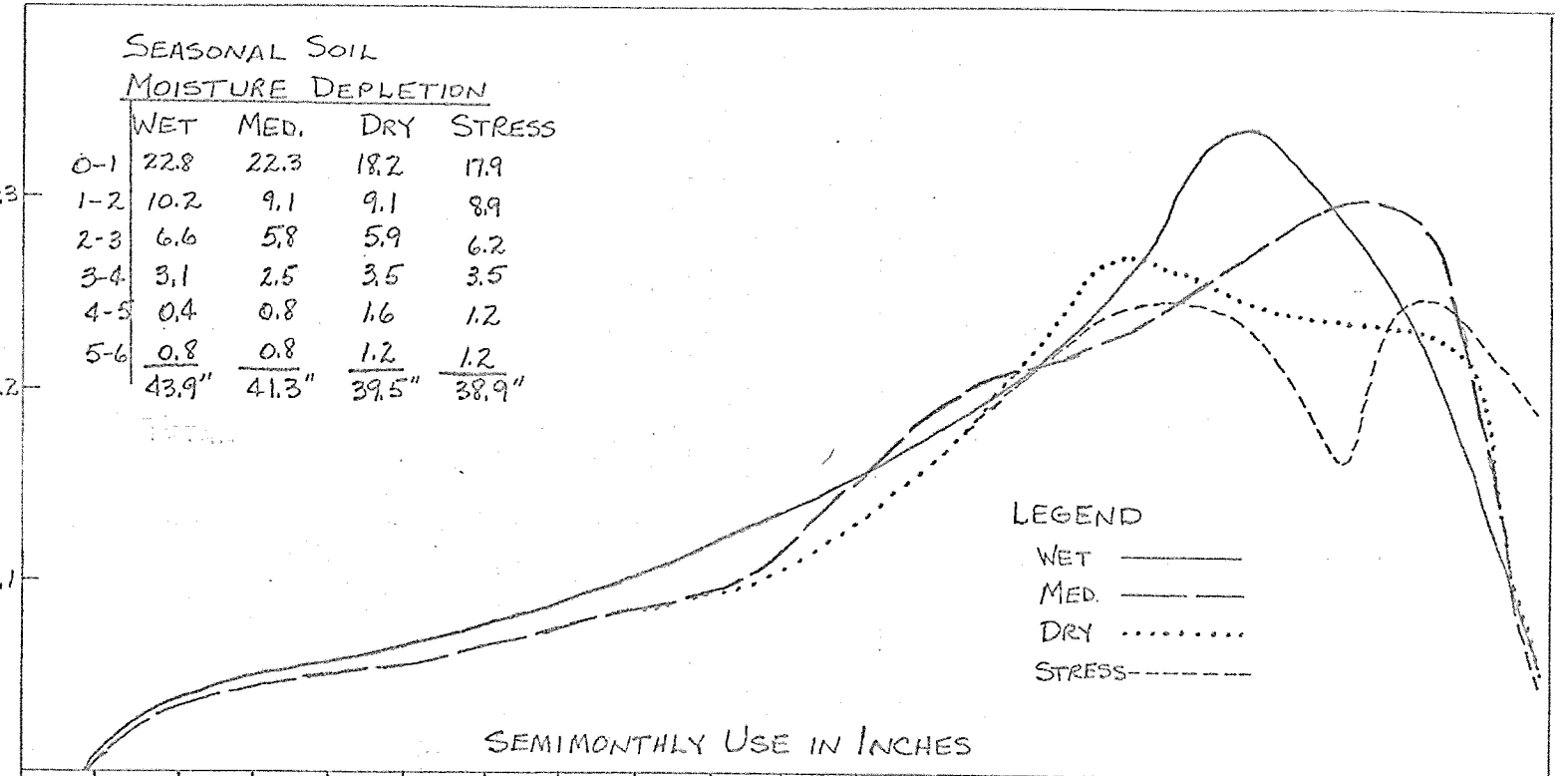

SEASONAL SOIL MOISTURE DEPLETION

	WET	MED.	DRY	STRESS
0-1	22.8	22.3	18.2	17.9
1-2	10.2	9.1	9.1	8.9
2-3	6.6	5.8	5.9	6.2
3-4	3.1	2.5	3.5	3.5
4-5	0.4	0.8	1.6	1.2
5-6	0.8	0.8	1.2	1.2
	43.9"	41.3"	39.5"	38.9"

	OCT.		NOV.		DEC.		JAN.		FEB.		MARCH		APRIL		MAY		JUNE		JULY	
WET	.02	.45	.64	.75	.91	1.14	1.23	1.54	1.54	1.79	2.19	2.64	2.85	3.27	3.87	5.20	4.84	4.20	3.22	1.60
MED.	.02	.38	.58	.72	.78	.94	1.03	1.28	1.23	1.41	2.01	2.77	3.00	3.22	3.36	4.08	4.22	4.50	4.15	1.60
DRY	.02	.38	.58	.72	.78	.94	1.03	1.28	1.23	1.39	1.77	2.35	2.80	3.51	4.05	4.12	3.62	3.54	3.45	1.92
STRESS	.02	.38	.58	.72	.78	.94	1.03	1.28	1.23	1.39	1.77	2.34	2.73	3.30	3.66	3.88	3.15	2.73	3.70	3.28

FIG. 4 MEAN CONSUMPTIVE USE FOR SUGAR BEETS AT MESA, ARIZONA, 1964-65.

TITLE: CLAY DISPERSANTS FOR THE REDUCTION OF SEEPAGE LOSSES FROM RESERVOIRS

LINE PROJECT: SWC 4-gG1 CODE NO.: Ariz.-WCL-37

INTRODUCTION:

Observations and post-treatment soil and water analyses were made during 1965 on two stock ponds treated with sodium salts to reduce seepage. Only water samples could be taken on House Mountain No. 1 pond as it did not go dry during 1965. The Dick Mason pond went dry in June 1965 and soil samples were taken. This latter pond was re-treated with a sodium salt in July to try and reduce its 2 cm day^{-1} seepage loss. The owner raised the spillway level in July 1965 about 30 cm to increase the capacity of the Dick Mason pond.

PROCEDURE:

To observe what happens to the Na^{+}, Ca^{++}, and Mg^{++} status in the two ponds with time, after the ponds are filled with water from the winter rains, ceramic extraction units were installed at depths of 4, 10, 16, and 22 cm in each pond in October 1965. Soil solution extracts will be taken monthly. Assuming that the soil solution is in equilibrium with the exchangeable cations on the soil, it should be possible to determine the SAR (sodium absorption ratio) and ESP (exchangeable sodium percentage) concomitant with low seepage rates.

Dick Mason pond had a seepage rate of 12 cm day^{-1} prior to treating it with TSPP (tetrasodium pyrophosphate) in August 1962. One year after treatment the seepage rate was 0.4 cm day^{-1}. Two years after treatment the seepage rate had increased to 2 cm day^{-1}. Soil samples were taken in June 1965.

To reduce the increased seepage loss, the pond was treated with sodium carbonate (soda ash) in July 1965 at the rate of 7.6 meq/100g in the top 10 cm of soil (5,900 pounds per acre). The salt was broadcast by hand (730 pounds) on the soil surface (5,760 ft^2) and harrowed in to an average depth of 10 cm. This treatment was designed to obtain an ESP of 15 in the treated depth.

RESULTS AND DISCUSSION:

1. House Mountain No. 1 Pond. The seepage rate on this pond measured over a two-week period in late September 1965 was 0.4 cm day^{-1} (evaporation was 0.4 cm day^{-1} for a total loss of 0.8 cm day^{-1}). Water depth at measurement time was about 60 cm. Because of this low seepage loss, which is the same as estimated in the summer of 1964, and the amount of rain during 1965, the pond has held water continuously for the past year--a condition which had not existed previously.

Soil solution extracts will be taken to continually follow the Na^{+}, Ca^{++}, Mg^{++} status in the soil.

2. Dick Mason Pond. An analysis of the soil samples taken in July 1965 showed that the sodium remaining in the upper 10 cm of soil was at a level nearly that of the pretreatment level (0.6 vs 0.4 meq/100g), and that the sodium had moved down into the soil profile (2.9 vs 0.4 meq/100g in the 30-45 cm depth). After treatment with sodium carbonate in July 1965, the pond was filled to overflowing from rains during August and September 1965. For a two-week period during the latter part of September, the seepage rate was measured at 0.4 cm day^{-1} (evaporation was 0.4 cm day^{-1} for a total loss of 0.8 cm day^{-1}). Water depth was about 120 cm.

This post-treatment seepage rate indicates that the sodium carbonate treatment has reduced the seepage loss considerably.

Soil solution extracts will also be taken on this pond.

SUMMARY:

The use of sodium carbonate as a dispersing agent to reduce seepage in two stock ponds was evaluated. House Mountain No. 1, treated with sodium carbonate in August 1963, is holding water well with a seepage rate of only 0.4 cm day^{-1}. The Dick Mason pond was treated with tetrasodium pyrophosphate in August 1962 to reduce the seepage rate from 12 to 0.4 cm day^{-1}. The seepage rate increased from 0.4 to 2.0 cm day^{-1} two years after treatment. In July 1965 the pond was treated with sodium carbonate (at the rate of 5,900 pounds per acre). Measurements in September 1965 showed a seepage rate of 0.4 cm day^{-1}.

Ceramic cups were installed in both ponds in October 1965 so that soil solution extracts can be taken periodically. Measurements of the Na^{+}, Ca^{++}, Mg^{++} status in the soil solution will be made at different depths below the soil surface to determine any changes which may take place with time.

PERSONNEL: R. J. Reginato, L. E. Myers.

TITLE: WATERBORNE SEALANTS TO REDUCE SEEPAGE LOSSES FROM UNLINED CHANNELS AND RESERVOIRS

LINE PROJECT: SWC 4-gG1 CODE NO.: Ariz.-WCL-38

INTRODUCTION:

During 1965, a petroleum emulsion was investigated in the laboratory and in two field tests for suitability as a waterborne seepage-reducing agent.

PROCEDURES:

Laboratory. An evaluation of emulsion B on Beardsley soil was conducted to determine if the poor sealing previously observed (1964 Annual Report) was due to the physical or the chemical properties of the soil. A 1-cm layer of Beardsley soil was packed in cylinders over 14 cm of control soil. Emulsion B at a concentration of one part per thousand was added to water ponded over the layered soils. The supply water was stopped when the emulsion was added to the ponded water. However, a head difference of 3 cm, which corresponded to an initial flow rate of 2.0 cm hr^{-1}, was maintained by periodically lowering the outlet as the ponded water level declined. It was hoped that by this procedure conditions more like those found in the field would be approached.

Field. Emulsion B was added to a section of unlined canal and to one holding pond with a positive displacement gear pump rather than the venturi system used in 1964. This was done to allow the emulsion to be added to the water before coming in contact with air (air causes the asphalt emulsion to "break," rendering it ineffective as a sealant). The canal treated in February 1965 was a 500-ft section of the Beardsley gravity canal near Beardsley, Arizona. It has a 30-sq ft cross-section at a depth of 4.5 ft, and holds approximately 1 acre-ft of water. The holding pond, near Indio, California, is built in a coarse-textured soil and has a capacity of about 1.5 acre-ft at a 5.8-ft depth. It also was treated in February 1965.

RESULTS AND DISCUSSION:

Laboratory. Previous tests of emulsion B on Beardsley soil alone showed poor sealing (39 percent average reduction in seepage rates) with an initial seepage rate of 1.8 cm hr^{-1}. It was

hypothesized that as a surface seal formed on soils with a low impedance (high hydraulic conductivity), a large pressure gradient was established across the seal. The resulting force caused the asphalt to be drawn into the soil pores and a good seal was created (as evidenced on control soil). However, on a soil such as Beardsley, with a high impedance (low hydraulic conductivity), the seal that was formed did not cause such a high pressure gradient. Without this force, the asphalt was not drawn into the soil pores and a porous seal resulted.

Results of the layered-soil cylinder tests showed an average seepage reduction of 91 percent 48 hours after treatment where the initial flow rate was 2.0 cm hr^{-1}. This indicates that the previous problem in sealing Beardsley soil was physical in nature rather than chemical.

Field. Prior to treating the Beardsley canal, Bermuda grass growing within the treatment area was burned off. The average pretreatment seepage rate for the first 60-cm drop in the water level was 1.9 cm hr^{-1}. Immediately after treatment for the same water level drop of 60 cm, the seepage rate was 1.0 cm hr^{-1}, an average seepage reduction of 47 percent. The canal was then allowed to dry. One week after treatment, the canal section was refilled with clear water and the seepage rate was 1.7 cm hr^{-1}, which showed very little residual sealing effect of the material one week after treatment. It was observed that a lush growth of Bermuda grass had essentially destroyed the seal. One month after the first treatment, the same section of canal was retreated with 1000 ppm emulsion B, and the seepage rate immediately after retreatment was 0.8 cm hr^{-1}, a 58-percent reduction.

These results show that a reduction in seepage essentially equal to that found in the laboratory was obtained in the field until the seal was destroyed by Bermuda grass.

The second field trial to determine the effectiveness of emulsion B was conducted in the Indio pond with pretreatment seepage rate of 5 cm hr^{-1}. The soil was poorly graded and highly

porous with a typical textural analysis of 7 percent clay, 7 percent silt and 86 percent sand. Prior to treatment, infiltration cylinders were placed in the pond banks, infiltration measurements were made with clear water, and then emulsion B was added to the water in the cylinders. An infiltration reduction of 70 percent was obtained. Treated with 1000 ppm emulsion B in February 1965, an average seepage reduction of 69 percent was measured over the entire depth of the pond (170 cm) immediately after treatment. In March, the pond was refilled with clear water, and the reduction was still the same, 69 percent. However, in May the pond was refilled with clear water, and a seepage rate of 5 cm hr^{-1} was measured, the same as the pre-treatment rate. Bermuda grass growing through the asphalt emulsion had caused the seal to fail.

The Indio soil has a high hydraulic conductivity and it was hoped that a 90-percent reduction in seepage would be attained with the asphalt emulsion treatment. The reason for the lower reduction apparently relates to the high porosity of the Indio soil which was much coarser than any soil tested in the laboratory. It is probable that the asphalt particles were not able to completely fill the larger soil pores and a partial seal was the result.

SUMMARY AND CONCLUSIONS:

A laboratory experiment and two field trials were conducted to determine the suitability of an asphalt emulsion as a waterborne seepage-reducing agent. In the laboratory, a 1-cm depth of Beardsley soil (fine textured) was packed in cylinders over 14 cm of control soil, (coarse textured) and the emulsion was added to the water ponded over the soil. Tests run previously on 15 cm of Beardsley soil packed in cylinders showed an average reduction of 39 percent in the seepage rate. However, in the layered soil system, seepage was reduced 91 percent.

From these results it was hypothesized that a high pressure gradient would be established across a surface seal formed on a soil with low impedance (high hydraulic conductivity), and the asphalt would be drawn into the soil pores to form a tight seal.

With a soil having high impedance, a large gradient would not be established and the asphalt would deposit on the soil surface to form a porous seal.

In two field tests, a canal section in Beardsley soil and a holding pond in a coarse-textured soil, seepage was reduced about 50 and 70 percent, respectively, as long as the seal remained intact. However, as soon as Bermuda grass grew through the seal, its seepage-reducing effectiveness was destroyed. Weed control is obviously a necessary part of any future application.

Seepage reduction in the Beardsley canal was essentially the same as that obtained with laboratory tests on small cylinders of soil. Similarly, seepage reduction in the Indio pond was essentially the same as that obtained in pre-treatment field tests utilizing infiltration cylinders. It appears that these simple procedures may be used to predict the approximate seepage reduction to be expected in full-scale field applications of pore-plugging petroleum emulsions used as waterborne sealants.

PERSONNEL: R. J. Reginato and L. E. Myers.

TITLE: CRACK SEALANTS FOR CONCRETE LINED CANALS

LINE PROJECT: SWC 4-gG1 CODE NO.: Ariz.-WCL-39

INTRODUCTION:

See Annual Report for 1964 and "Repair of Cracks in Concrete Channel Linings" (1966 manuscript) for general information.

PROCEDURES AND RESULTS:

Sealing Materials. Asphalt emulsion was used as the base material in the formulation of a sprayable crack sealer. Improved extensibility and weathering resistance was obtained by the addition of butyl latex. Asbestos fibers were added to reduce running or slumping of the asphalt on steep slopes. All of these materials are readily available and are classed as nontoxic. Formulation of the crack sealers consisted of combining various amounts of asphalt emulsion, butyl latex, and asbestos fibers. Formulation did not appear critical but there were certain limits. Increasing the amount of butyl latex increased material costs and caused clogging problems with the piston-pump spray equipment first used in this project; too much asbestos also caused a clogging problem. From preliminary laboratory and field observations of the physical properties and spraying characteristics of these mixtures, it was decided that formulations containing approximately 48 percent asphalt, 3 percent actual butyl latex, 14 percent asbestos fibers, and 35 percent water would be reasonably satisfactory. Shortly after the initial testing of laboratory-mixed materials, a commercial sprayable crack sealer became available.

Bonding of pure asphalt to concrete is ordinarily a mechanical process. Adhesion is often poor and the asphalt can be mechanically stripped or peeled from the concrete. The asphalt in the two sprayable sealants, used in these tests had been modified by the addition of cationic antistripping agents. Concrete normally has a negatively charged surface. The addition of cationic antistripping agents to the emulsion causes the asphalt to act as a positively charged material. This creates an electrochemical bond of the treated asphalt to the concrete surface. Such bonding will take place in the presence of water.

Bonding of asphalt to concrete can be improved by the addition of rubber or other materials to increase the tack or stickiness of the asphalt mixture. Two nonsprayable rubberized-asphalt mastics sold commercially for repairing cracks in concrete, were included in the laboratory tests for comparison with the sprayable sealers.

Laboratory Tests. The bonding of four crack sealers to concrete was evaluated in the Laboratory. Tested sealants included a laboratory mixed sprayable material, S_1, a commercially available sprayable material, S_2, and two commercially available rubberized asphalt mastics, M_1 and M_2. Measurements were made in an attempt to determine differences in bonding caused by variations in concrete cleaning, tack coat applications, temperature, and curing time.

Testing procedure consisted of pulling apart two concrete blocks, 2 × 2 × 1-inch in size, which had been bonded together with a 0.05-inch layer of crack sealer between the 1 × 2-inch surfaces. Block surfaces treated included concrete with a 0.05-inch layer of mud on the surface, concrete with mud lightly brushed off, and new, clean concrete. In addition to cleaning, at the time of crack sealer application, the concrete surfaces were either dry, wet with water, or brushed with a tack coat of kerosene which contained a surfactant. After application to the blocks with a putty knife, sealing materials were allowed to cure for periods of 1, 7, and 28 days at a temperature of 77 F and a relative humidity of 40 percent. The blocks were then pulled apart at a rate of 0.25 inch/min in a laboratory testing machine located in a controlled temperature room. Bonds were tested at temperatures of 50, 77, and 104 F. All variations in treatments were run in triplicate. After being pulled apart, the blocks were inspected visually to determine any bonding failures. Results are presented in Table 1. Bond was considered good if both concrete surfaces were completely covered with sealing material after being pulled apart. Bond was considered fair if sealant had pulled free from only one or two small spots, and was considered poor if any appreciable amount of bare concrete was visible.

General conclusions from the laboratory tests are: (1) all four sealants bonded very well to clean concrete, either wet or dry, at all temperatures; (2) no sealant bonded to muddy concrete; (3) bonding to brushed concrete after 28 days curing time was fair to good for S_1, S_2 and M_2 at temperatures above 50 F, but all bonds failed at 50 F; (4) at seven days curing time a kerosene tack coat reduced bonding to clean concrete and did not improve bonding to brushed concrete; at 28 days curing time the bond to clean concrete was not reduced and the bond to brushed concrete was apparently improved.

Durability and ductility of the crack sealers was not studied in the laboratory. A field evaluation of these factors was initiated for the sprayable sealers by applying them to cracks in the concrete linings of operational ditches and canals.

Field Applications. A field test was initiated in May 1964 to determine if the crack sealers would spray easily, how clean the concrete had to be, and if a tack coat was necessary. Three sealers were applied to joints and cracks in the same field ditch where crack movement had been measured. The joints and cracks had either been swept with a bristle broom or thoroughly cleaned with a wire brush. Half had then been sprayed with a tack coat of cut-back asphalt and half were without a tack coat. The sealers applied were S_1 and S_2, plus a clay-type asphalt emulsion modified with butyl latex and asbestos fibers. Sealers were sprayed on the cracks and joints with a high-pressure (2,500 psi) piston pump driven by compressed air. The pump unit functioned properly if spraying was continuous. Intermittent spraying caused all three sealers to break in the pump, forming solid lumps which stopped the equipment.

Silt deposited from irrigation water in the bottom of the ditch was removed with shovels in January 1965 with no damage to the test materials. All materials bonded tightly to the concrete, regardless of whether or not a tack coat was applied, and whether the concrete was wire brushed or merely swept clean.

Inspection of all field sites in October 1965, 17 months after treatment, revealed that S_1 and S_2 crack sealers generally were weathering well, with S_2 remaining slightly more pliable. Both sealers had cracked slightly on about half the south-facing cracks. However, there was little cracking of the sealers placed on the north-facing slope. The crack sealer with the asphalt clay emulsion had hardened and cracked on both sides of the ditch. All three materials, regardless of concrete cleanliness, were bonded tightly and could not be peeled with a knife. It should be pointed out that this field ditch carried water only intermittently and the crack sealers were exposed to air and sunlight for almost all of the 17-month period. Mastic sealer M_1 cracked and peeled from the concrete after one year of exposure in this same farm ditch.

A 500-ft section of the Tempe Canal in the Salt River Valley, Arizona, which is gunite-lined on one side for erosion control, was treated with the commercial sealer S_2 in November 1964. Air temperature at treatment time was 50 F. This material was sprayed with the piston pump on cracks in the paved canal side which has a 1:1 slope and a vertical height of 7 ft. Some cracks had received a tack coat of kerosene and surfactant, and some had not. Some had been swept clean, some wire brushed, and some washed clean with a high-pressure water jet.

Cleaning the cracks with water was done with a 400-500 psi jet from a commercially available pump and sprayer unit usually used for applying insecticides to trees and orchards (Model 10-T, Thuron Sprayer Mfg Co., 765 Coleman Avenue, San Jose, California). The small multiple piston water pump, driven by a 7-1/2 hp gasoline motor, is attached to a 300-gal tank mounted on a trailer. The pump has a capacity of 10 gal/min, and with the proper size orifice in the nozzle, pressures up to 500 psi are attainable. The high pressure water jet blasted the soil out of the cracks and rapidly removed all silt and algae deposited around the edge of the cracks. Fine cracks, covered and hidden by silt and algae, could be quickly uncovered and traced out with the water jet. It also washed the

soil away from the crack area so that the sealer could be sprayed directly on the clean, wet concrete. The high pressure water jet is much faster than hand cleaning with a wire brush or even sand blasting; the latter method requires removal of the sand from the crack area.

About 800 ft of cracks were covered with 40 gal of sealer S_2. Cost of the material given by the manufacturer is about $1.50 per gal depending on volume. The sealer did not slump on the steep side slope even though layers of material up to 1/4 inch thick were sprayed over some cracks. The Tempe Canal was inspected in November 1965 and there was no visual difference between treatments above the water line; all remained pliable and tightly bonded to the concrete. Regardless of the cleanliness of the concrete surface, it was impossible to scrape the sealer from the concrete with a knife. The sealer on most of the cracks covered had started to check slightly above the water line. Below the water line there was no checking visible on any of the treatments. However, on the cracks that had been brushed clean and had not received a tack coat, the sealer had started to peel from the concrete. Material sprayed on cracks brushed clean and primed with a tack coat was bonded tightly to the concrete. Where the sealer was sprayed on the cracks cleaned with the water jet, there were no bonding failures and the sealer could not be separated from the concrete.

Since the Tempe Canal installation, a new type high-pressure (1500 psi) diaphragm pump was obtained for spraying crack sealers (P-series pumps, PCP Corporation, 3537 South Normal, Chicago, Illinois). This pump is driven by a small, integrally mounted 2 1/4-hp gasoline motor and requires no supplemental air compressor. Two men can easily lift the pump. The diaphragm pump creates less shearing action on the sealer than did the previously used piston pump and does not cause the sealer to break within the spraying equipment. A section of farm-sized concrete lined ditch near Tempe, Arizona was treated with crack sealer S_2 in August 1965. No

clogging problems were encountered while spraying the S_2 sealer. About 800 ft of cracks were sprayed with 10 gal of sealer in an hour's time.

Sealing cracks with power spray equipment requires three men: one to clean the cracks with the water jet, one to spray the crack sealing material, and one to drive the equipment truck. Cost of the spray equipment, excluding the truck, is about 2,000 dollars.

Investigations reported by Wallace have shown that after five years of exposure in an operational canal, rubberized-asphalt compounds were keeping joints sealed better and were remaining more resilient than five other general types of crack sealing materials. Experimental material S_1 and developmental material S_2, which were slightly checked after 17 months of exposure to sun and air in the field, are sprayable rubberized-asphalt type sealers. Manufacturers should be able to improve the durability of sprayable crack sealers, at slightly increased cost, to equal that of the mastics.

SUMMARY AND CONCLUSIONS:

A new method for repairing cracks in concrete-lined channels more rapidly and efficiently than previously available methods has been developed. The cracked area is cleaned with a high-pressure water jet (400 psi), and a crack sealer is sprayed (1500 psi) on the wet concrete. Commercially available equipment is used for both of these operations.

From laboratory and field investigations, it was determined that the cleaning and spraying methods mentioned above have several advantages over other repair methods. Cracks in a silt-and-algae-encrusted concrete lining can be rapidly and very effectively located and cleaned with the high pressure water jet, and materials to seal cracks by covering and/or filling can be applied on wet concrete rapidly and effectively with high-pressure spray equipment.

If a high-pressure water jet is not available for cleaning, thorough wire brushing of the cracked area followed by a tack coat of kerosene or cut-back asphalt will provide a good bonding surface for crack sealing materials. However, this procedure is tedious and

costly. Crack sealers sprayed on concrete either washed clean or wire brushed followed by a tack coat have bonded well in one year of exposure in the field.

In recent field trials 800 ft of cracks were covered with 10 gal of sprayable sealer in one hour's time. This work involved three men, one cleaning with the water jet, one spraying the sealer, and one driving the equipment truck. It is our belief that this unique method offers tremendous possibilities for the rapid, economical, and effective repair of concrete channels and other hydraulic structures.

PERSONNEL: R. J. Reginato and L. E. Myers.

TABLE 1.--Bonding of four crack sealers to concrete as affected by curing time, surface pretreatment, temperature, and cleanliness of concrete.

Cure time	Surface	Temp.	Clean				Brushed Mud				Mud			
			S_1	S_2	M_1	M_2	S_1	S_2	M_1	M_2	S_1	S_2	M_1	M_2
days	Tack	F. 77	1/ G	G	G	G	G	G	1/ F	F	1/ P	P	P	P
1	Dry	50	G	G	G	G	F	G	F	G	-	-	-	-
		77	G	G	G	G	G	G	G	G	P	P	P	P
		104	G	G	G	G	G	G	G	G	-	-	-	-
	Wet	77	G	G	G	G	-	-	-	-	-	-	-	-
7	Tack	77	P	F	P	P	P	F	P	P	P	P	P	P
	Dry	50	G	G	G	G	P	P	F	G	-	-	-	-
		77	G	G	G	G	G	G	G	G	P	P	P	P
		104	G	G	G	G	F	G	F	G	-	-	-	-
	Wet	77	G	G	G	G	-	-	-	-	-	-	-	-
28	Tack	77	G	G	G	G	G	G	G	G	-	-	-	-
	Dry	50	G	G	G	G	P	P	P	P	-	-	-	-
		77	G	G	G	G	G	G	F	G	-	-	-	-
		104	G	G	G	G	F	G	P	G	-	-	-	-

1/ Bond: G - good, no exposed concrete
F - Fair, small spot or two of exposed concrete
P - Poor, appreciable exposed concrete

TITLE: DISPERSION AND FLOCCULATION OF SOIL AND CLAY MINERALS AS RELATED TO THE Na AND Ca STATUS OF THE AMBIENT SOLUTION

LINE PROJECT: SWC 4-gG3 CODE NO.: Ariz.-WCL-40

INTRODUCTION:

The objectives of this project have been discussed in the Annual Report of 1964.

PART I. DEFLOCCULATION OF SOIL MATERIALS BY SODIUM SALTS

An additional study included one on the dispersive action of various Na salts on different soil materials and the relation to the composition of the ambient soil solution.

PROCEDURE:

The soil materials used were the Mason and Pine soils located in pond sites, the Big Lake located near a storage reservoir, and the Adelanto and Safford occurring in irrigated areas of the Salt River Valley of Central Arizona. The chemical and physical properties of the soils are listed in Table 1. Note that the Adelanto, Pine, and Safford soils contain free carbonates and also that the Adelanto and Safford contain appreciable soluble salts as indicated by the saturated electrical conductivity measurements. X-ray analysis indicates that montmorillonite is the chief clay mineral constituent.

The sodium salts used were NaCl, Na_2CO_3, Na_2SO_4, and $(NaPO_3)_6$, "hexametaphosphate." The latter hexametaphosphate salt refers to the vitreous sodium phosphate, whose equivalent formula weight was taken as $NaPO_3$.

A specified equivalent of the sodium salt from 0.5 to 32 meq/100g was mixed with 50g of soil and placed in a 1-liter graduate normally used for particle size analysis. Distilled water was added to bring the total volume to 1 liter. The material was suspended with a paddle without the usual pretreatment of mechanical dispersion on a stirrer as is prescribed in the standard mechanical analysis procedure. The clay- and silt-size fractions were determined by the pipette technique. Corrections were made for the soluble salts in solution.

Part of the remaining suspension was centrifuged, filtered, and the filtrate analyzed for the various ionic constitutents by standard

analytical techniques. Ca and Mg were determined by versenate titration, Na by flame spectrophotometer, HCO_3 and CO_3 by acid titration, pH with the glass electrode, and electrical conductivity with conductivity cell-cathode ray Wheatstone bridge.

RESULTS AND DISCUSSION:

The deflocculation behavior of the different soil materials treated with the various sodium salts in respect to the $< 2\mu$ (solid line) and the 2 to 20μ (dashed line) is presented in Figures 1 and 2. For the Big Lake soil, the NaCl treatment caused a decrease in silt- and clay-size fractions with increasing amounts of salt applied. The Na_2SO_4 treatment behaved in a similar manner for the clay-size fraction, whereas the silt-size fraction increased slightly. With the Na_2CO_3 treatment at the 32 meq/100g level, on the other hand, the silt- and clay-size fractions increased to twice that of the check or salt-free treatment. For a similar situation the $(NaPO_3)_6$ treatment tripled the quantity of silt-size fraction and increased the clay-size fraction by a factor of 40. According to Daugherty (3) a soluble complex such as $[Na_{n-4}(CaPO_3)_n]^{-2}$ is formed between Ca ions in solution and $(NaPO_3)_n$. Thus, the Ca is still in solution, but no longer contributes to the flocculation of the particles. In addition, the polyphosphate anion is adsorbed on the soil clay mineral surface with consequent disruption of the charge distribution resulting in the dispersion of the soil particles. Without going into further detail for the other soils, we see from Figures 1 and 2 that the dispersion of the soil particles is greater with the $(NaPO_3)_6$ treatment than the Na_2CO_3, NaCl, and Na_2SO_4 treatments, except in the Adelanto and Pine soils for the $< 2\mu$ fraction where the deflocculation is similar between the Na_2CO_3 and $(NaPO_3)_6$ treatments. An increase in the rate of chemical application resulted in a greater deflocculation for the $(NaPO_3)_6$ and Na_2CO_3 treatments, whereas no change to a decrease in dispersion occurred for the NaCl and Na_2SO_4 treatments, both of which behave similarly, particularly for the $< 2\mu$ fraction; at the higher treatment rates the clay-size fraction flocculated.

An explanation for pond sealing after an NaCl treatment is based, in addition to compaction of the soil as part of the soil treatment,

on the premise that deflocculation is present and the dispersed particles plug the water conducting pores. The laboratory study shows, however, that only a negligible amount of deflocculation occurs for these particular three soils treated with NaCl. Although only a limited number of materials were studied, an alternative explanation for soil sealing in such instances is proposed for such treatment which is based on the interlamellar swelling and also tying-up of part of the soil water by the soil colloid. It has been shown with pure clay minerals that the Na-montmorillonite clay swells to a larger extent than the Ca-saturated clay. Thus, the addition of NaCl to soil results in the formation of Na clay which swells and decreases the effective area of water conducting pores.

The Na, Ca + Mg, and H statuses of the ambient soil solutions are presented for the different materials in Figures 3 and 4. The solution conductivities were also measured, but these only confirm the cationic concentration (Na + Ca + Mg) determinations and consequently, the data are omitted in this report. In case of NaCl addition, the Na increased in direct proportion to the addition, and the Ca + Mg increased in the solution due to exchange reaction. Furthermore, an example showing the comparison of the total Na concentration as added cations to the measured cations is represented in Figure 5 for the Big Lake soil. Any drastic change of the actual from the theoretical as represented by the dotted line would indicate a tying-up of portions of the equivalent replaced cations. As shown for the Big Lake soil, the sum of cation concentrations of Ca, Mg, and Na adds up close to the concentration theoretically possible assuming that all the NaCl went into solution. This is not the case for the other treatments in which Ca ions have been removed by precipitation and also Na ions have been removed from solution by exchange for the replaced Ca in the exchange complex.

Using Figures 3 and 4 we see that, for the Na_2SO_4 treatment, there is less Ca in solution than the NaCl treatment, indicating that there are possibilities of some formation of insoluble $CaSO_4$. On the other hand, with Na_2CO_3, a larger part of the exchangeable Ca cations is tied up as $CaCO_3$. As a consequence, the Na in solution is lower in this

case as a result of the replacement of the Ca by Na in the exchange complex. Consequently, the addition of Na_2CO_3 results in a relatively greater rate of change of the Na to Ca ratio than the NaCl or Na_2SO_4 addition. This is shown in Figure 6 where the sodium adsorption ratio, $SAR = Na/[(Ca + Mg)/2]^{1/2}$, for Big Lake soil as a function of the added Na salts is presented.

The pH of the NaCl, Na_2SO_4, and $(NaPO_3)_6$ treatment remained constant and essentially similar whereas that of Na_2CO_3 increased with treatment rate. Alkaline hydrolysis can occur with the carbonate treatment, whereas none appears possible with the other treatments.

The electrical conductivities of the soil solution for the same equivalent added salt are in the order NaCl > Na_2SO_4 > $(NaPO_3)_6$ > Na_2CO_3. The electrolyte concentration ranges from 1 to 20 meq per liter from the low (0.5 meq/100g) to high (32 meq/100g) treatment levels for the NaCl, whereas the other treatments ranged lower than this [Na_2CO_3, 0.3 to 12 meq/liter; Na_2SO_4, 0.5 to 17 meq/liter; $(NaPO_3)_6$, 0.3 to 12 meq/liter]. At the low rate of salt addition, the nondispersed nature of the materials, particularly with NaCl and Na_2SO_4, may be due to a high enough electrolyte concentration which can cause flocculation of dispersed particles. At least the data for the NaCl and Na_2SO_4 treated materials are consistant with that of Collis-George and Smiles (2) where they attempted to show the relation between total cation concentration, sodium adsorption ratios, and the dispersed or flocculated state of soil material medium. In the case of the Na_2CO_3 treatment, the SAR is sufficiently high for a given electrolyte concentration that deflocculation can occur.

The behavior of the $(NaPO_3)_6$-soil system is different from the other treatments in regard to the Ca status of the ambient solution, which is much higher than even the NaCl treatment. The versenate method is supposed to titrate free Ca ions, which are of interest in this study, and it is possible that some of the complexed Ca-phosphate forms are being converted to the free Ca form during the titration procedure. Ordinarily in the Ca analysis, phosphates interfere to the extent that they cause lower Ca measurement than the actual Ca present in the system.

This is in contrast to the results obtained. Although suitable experimental explanation for this behavior is lacking, this should not detract from the fact that the Na-metaphosphate reacts fundamentally differently from the other Na salts. The Na content in the ambient solution for the phosphate system is lower than the NaCl indicating that some of the exchangeable Ca being removed as the complex phosphate is being replaced by the solution Na.

From the analyses of the ambient solution, the calcium carbonate saturation indices for the different soil materials were calculated for the Na_2CO_3 treatment following the method of Langelier (4) with refinements introduced by Bower, et al. (1). In each calculation, a negative value signifies $CaCO_3$ dissolution while a positive value indicates $CaCO_3$ precipitation from solution of the carbonate material. Each soil showed a distinct relation between the calcium carbonate saturation and the rate of addition of Na_2CO_3. It can be seen from Figure 7 that the higher the original $CaCO_3$ equivalent, the smaller the amount of Na_2CO_3 needed to start the precipitation of Ca. This method appears to be a useful one for characterizing and also determining the formation of $CaCO_3$ precipitation in soil materials with the addition of carbonate materials.

Decker's (4) report on chemical soil sealing indicates that the treatment rates of various salts are in the order of 5 meq/100g. Referring back to Figures 1 and 2, we see that only a small fraction of the total dispersable material is actually being deflocculated at this treatment level. This small quantity of deflocculated material, however, is sufficient to cause a decrease in water flow in the soil medium so that water can be maintained in a pond. Unpublished data of this Laboratory (see project Ariz.-WCL-37 for 1964 and 1965 and Ariz.-WCL-8 for 1963) show that field treatment of the Pine soil with NaCl at a rate of 5 meq/100g was not effective in preventing seepage loss. On the Mason soil, treatment with polyphosphate ($Na_4P_2O_7$ at 5 meq/100g) resulted in seepage reduction of from 12.5 cm per day to 0.75 cm per day, including evaporation, for a period of one and one-half years with consequent reversion to the higher rate of 2.54 cm per day on the second year. On another pond site, Na_2CO_3 treatment (7 meq/100g) decreased

seepage loss to 0.25 cm per day. Preliminary soil analyses on the Mason soil indicate a gradual replacement of the added Na by Ca from the runoff water thus causing an eventual breakdown in the soil seal. By the use of the calcium carbonate saturation index technique, it is proposed to add more Na_2CO_3 to take into account the additional Ca appearing in the pond from the runoff water. From the data of Figures 1 and 2, the treatment rate at which a significant amount of dispersion occurs with the Na salt addition is approximately 5 meq/100g. The limited number of field data available at present indicate that the level of treatment is about optimum to use.

PART II. MAINTAINING AN ADEQUATE CATIONIC ENVIRONMENT IN PONDS FOR SUSTAINING CHEMICAL POND SEALS

The runoff water into ponds carries with it more Ca than Na cations, so that eventually through the process of leaching and exchange the Na-dispersed soil pond seal will revert back to a Ca-flocculated system with an increased seepage rate. The Ca can be "inactivated" by the formation of a precipitate such as $CaCO_3$ by the addition of Na_2CO_3 salt. The question remains, however, as to the amount of salt necessary to maintain the proper Na-Ca balance.

By use of the calcium carbonate saturation index concept originally proposed by Langelier (5) with calculation improvement of Bower, et al. (1), estimations of the calcium "balance" of the pond water can be made.

The calcium saturation index is defined as

$$CaCO_3 \text{ Saturation Index} = pH_a - (pK_2' - pK'_{CaCO_3}) + pCa + pAlk$$

where

pH_a = measure pH of the solution

pK_2' = negative log of the second dissociation constant for H_2CO_3

pK'_{CaCO_3} = negative log of the solubility constant of $CaCO_3$

pCa = negative log of the molal concentration of Ca

pAlk = negative log of the equivalent concentration of the titratable bases, $CO_3 + HCO_3$

A positive value of the $CaCO_3$ saturation index means the precipitation of $CaCO_3$, whereas a negative value indicates the dissolution of the $CaCO_3$ present.

The objective then is to find the amount of Na_2CO_3 necessary to give a $CaCO_3$ saturation index close to zero.

PROCEDURE:

Na_2CO_3 was added to House Mountain and Mason pond water at varying rates of from 0.5 to 8 meq/liter. The pH, Ca, Mg, HCO_3, and CO_3 concentrations in the treated water were determined, and the $CaCO_3$ saturation index was calculated.

RESULTS AND DISCUSSION:

The $CaCO_3$ saturation index and pH of the solution after the addition of Na_2CO_3 to the House Mountain and Mason pond water are presented in Figures 8 and 9, respectively. In both cases, the addition of 0.6 meq/liter (2.6 lbs/1000 gal) of Na_2CO_3 is sufficient to cause the tying-up of Ca ions. Extra addition of Na_2CO_3 is not recommended, since the pH of the water gets to an alkaline level which is not suitable for animal consumption.

Under conditions where elaborate analytical equipment is not available, a check of pH only can be made by litmus paper technique. In this case, the Na_2CO_3 addition should not give a pH higher than 8.5.

SUMMARY:

The dispersive behavior of soils was studied when treated with NaCl, Na_2CO_3, Na_2SO_4, and $(NaPO_3)_6$. Soils differed in the magnitude of deflocculation, but in general were in the order $(NaPO_3)_6 \geqq Na_2CO_3 > Na_2SO_4 = NaCl$. The NaCl and Na_2SO_4 treatments caused flocculation at the higher application rates, whereas greater deflocculation occurred with higher concentration of Na_2CO_3 and $(NaPO_3)_6$. With these two latter chemicals the degree of dispersion can be controlled by the selection of a particular treatment rate. When field treatment rates are compared with the laboratory data on dispersion, the results indicate that only part of the total dispersible soil material is being dispersed, yet with effective pond sealing.

In order to inactivate Ca, which cause flocculation upon entering storage ponds, it is proposed that Na_2CO_3 be added to the runoff water or to the pond water. The proper amount of Na_2CO_3 to be added can be determined by the use of the calcium carbonate saturation index concept. Once the amount to be used is established for a given condition, a pH measurement of the treated water can be used to check the efficiency of the treatment.

REFERENCES:

(1) Bower, C. A., et al.
1965. An index of the tendency of $CaCO_3$ to precipitate from irrigation waters. Soil Sci. Soc. Amer. Proc. 29:91-92.

(2) Collis-George, N., and Smiles, D. E.
1963. An examination of cation balance and moisture characteristic methods of determining the stability of soil aggregates. Jour. Soil Sci. 14:21-32.

(3) Daugherty, T. H.
1948. Sequestration, dispersion, and dilatancy - lecture demonstrations. Jour. Chem. Ed. 25:482-486.

(4) Decker, R.
1965. Sealing small reservoirs with chemical soil dispersants. Proc. Seepage Symposium 1963. USDA ARS 41-90, pp. 112-131.

(5) Langelier, W. F.
1936. The analytical control of anticorrosion water treatment. Jour. Amer. Water Works Assoc. 28:1500-1521.

PERSONNEL: F. S. Nakayama

Table 1. Physical and chemical properties of soil materials.

	Adelanto	Big Lake	Mason	Pine	Safford
(1) Clay (%)	21.4	37.8	48.0	28.6	42.1
(2) Silt (%)	43.1	38.4	36.8	55.8	35.1
(3) Sand (%)	35.5	23.8	15.2	15.6	22.8
(4) pH (Satd. Paste)	7.70	6.53	6.41	7.90	7.68
(5) Exch. Ca (meq/100g)	20.4	12.6	20.2	19.3	37.8
(6) Exch. Mg (meq/100g)	3.4	5.8	16.6	21.2	43.9
(7) Exch. Na (meq/100g)	2.43	0.26	0.11	0.12	16.3
(8) Exch. K (meq/100g)	2.43	0.45	0.41	0.25	1.63
(9) Exch. H (meq/100g)	---	1.8	2.9	---	---
(10) Organic matter (%)	1.13	0.31	2.32	0.49	1.95
(11) $CaCO_3$ equiv. (%)	3.94	0.97	0.94	8.69	2.85
(12) Satd. Cond. (mmho/cm)	9.1	0.19	0.29	0.49	28.4

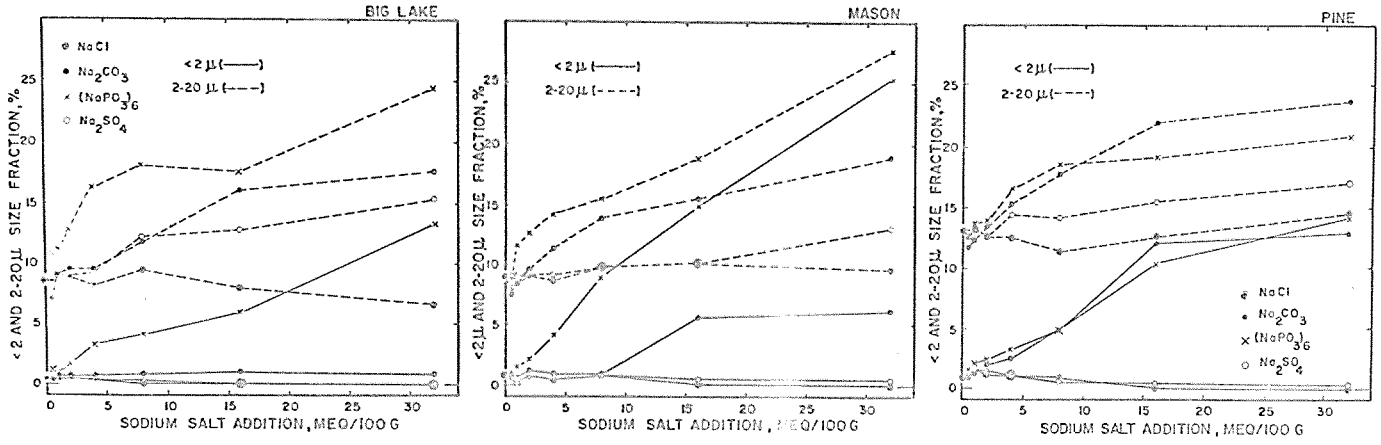

Figure 1. Deflocculation behavior of the Big Lake, Mason, and Pine soils.

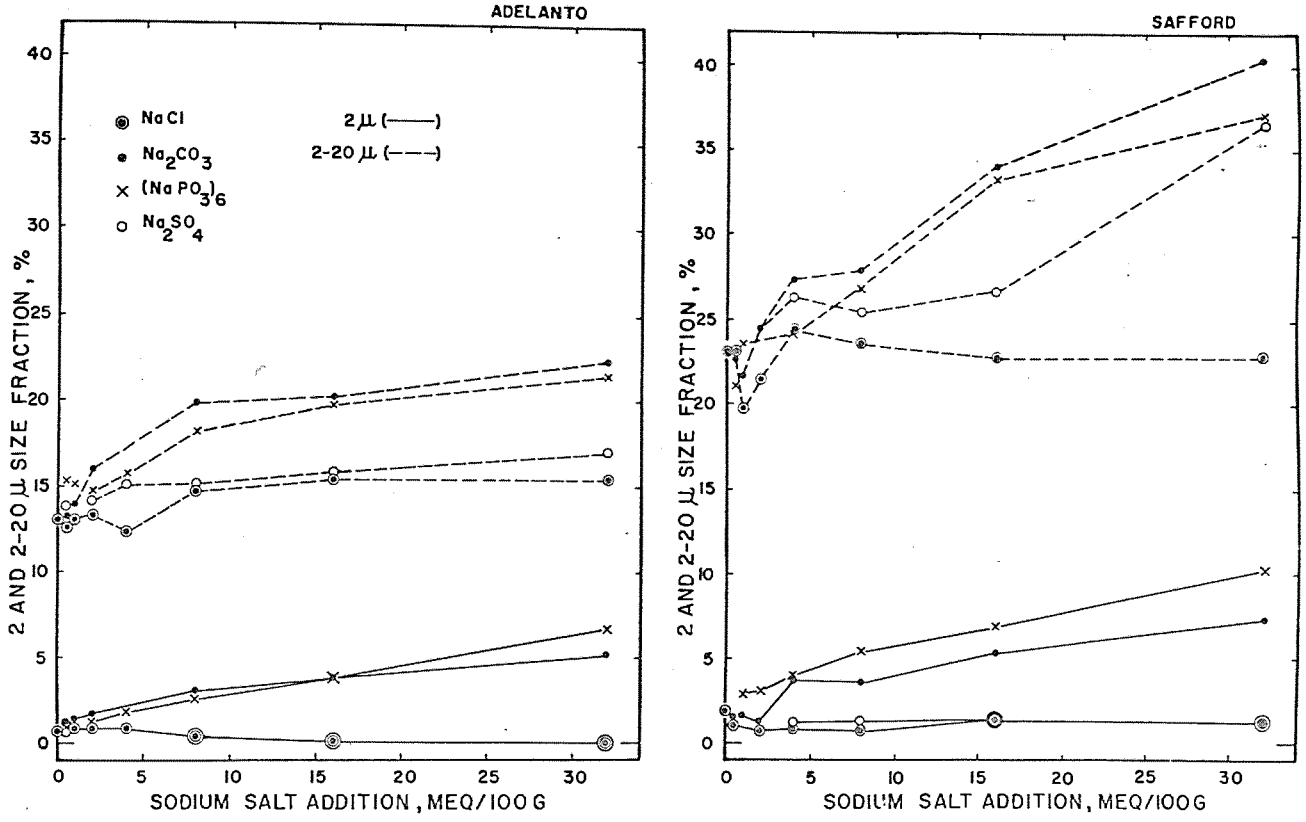

Figure 2. Deflocculation behavior of the Adelanto and Safford soils.

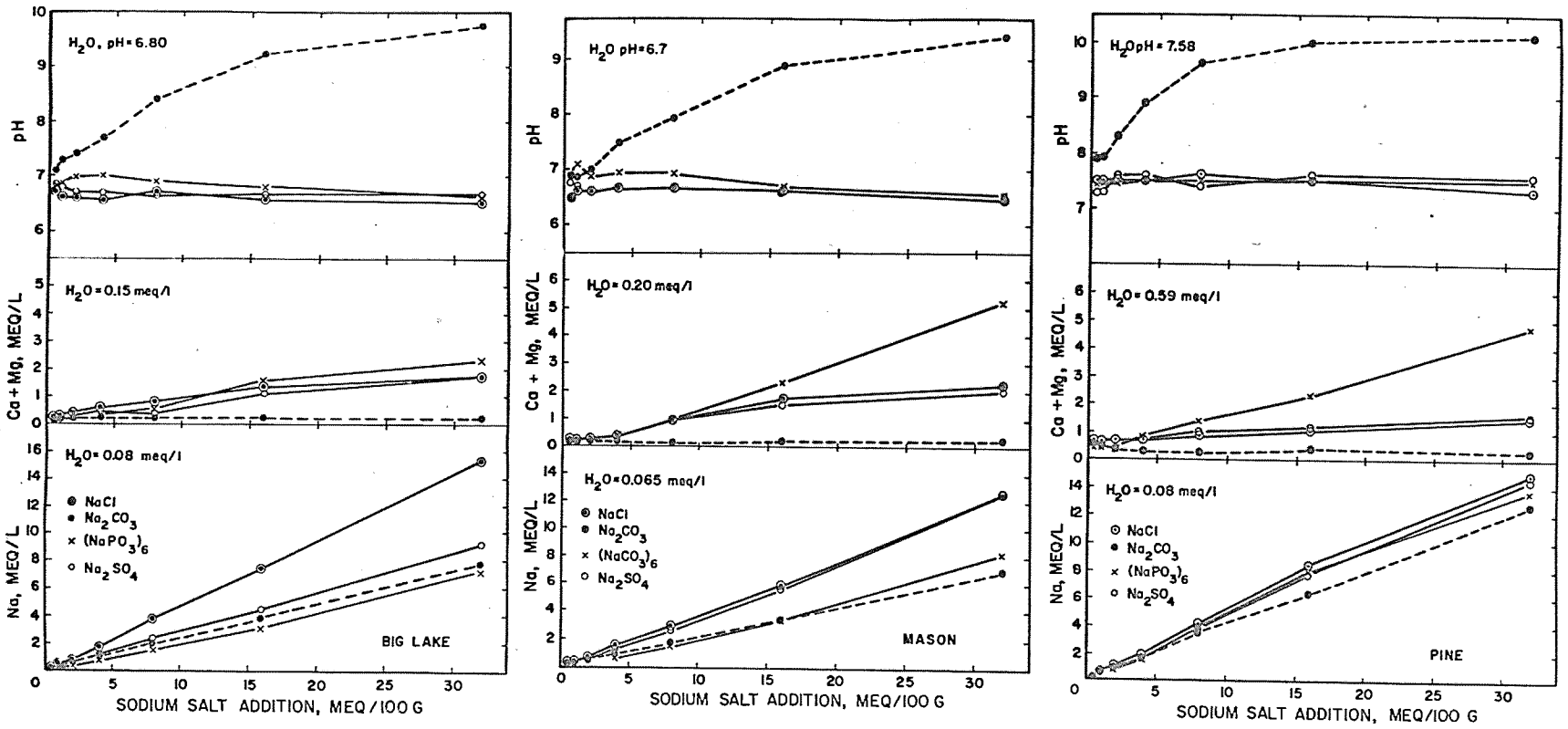

Figure 3. Chemical analysis (pH, Ca + Mg, Na) of ambient soil solution for Big Lake, Mason and Pine soils.

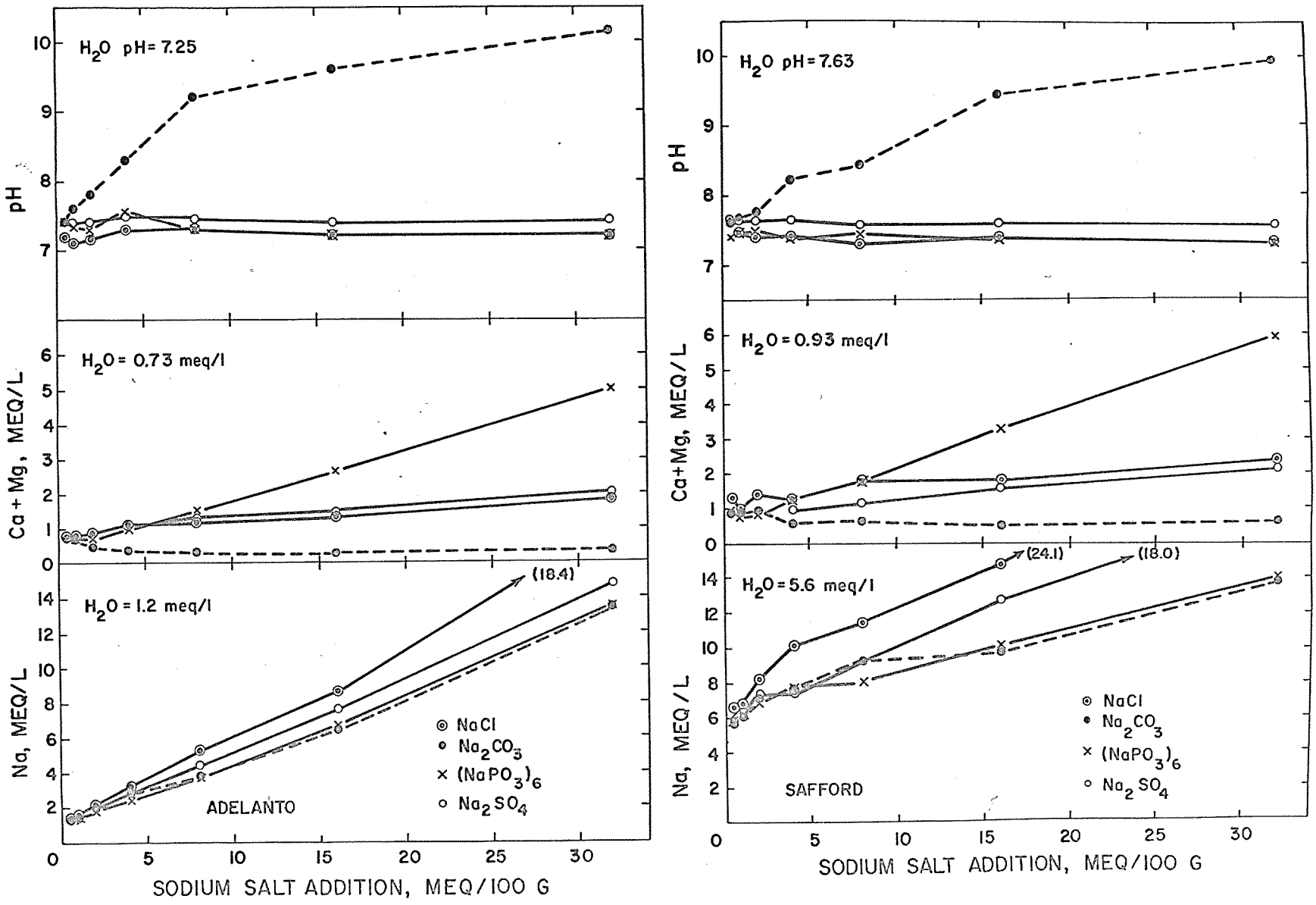

Figure 4. Chemical analysis (pH, Ca + Mg, Na) of ambient soil solution for Adelanto and Safford soils.

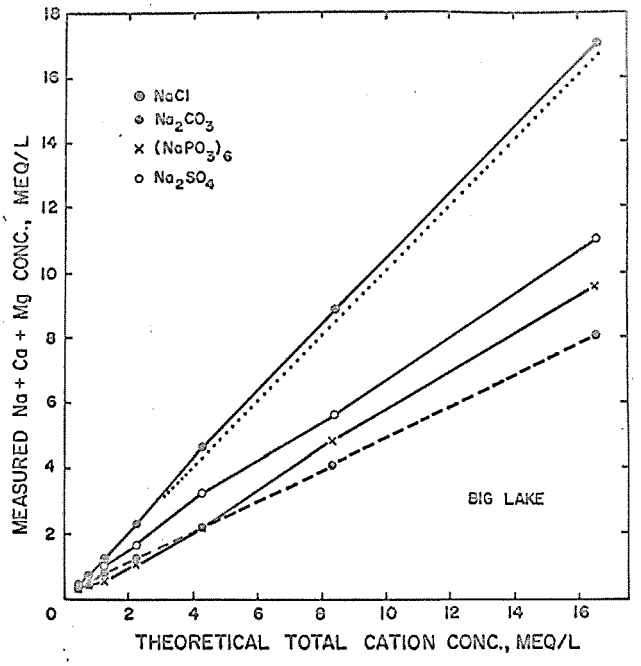

Figure 5. Comparison between the total Na concentration as added cation and the measured cations (Ca + Mg + Na).

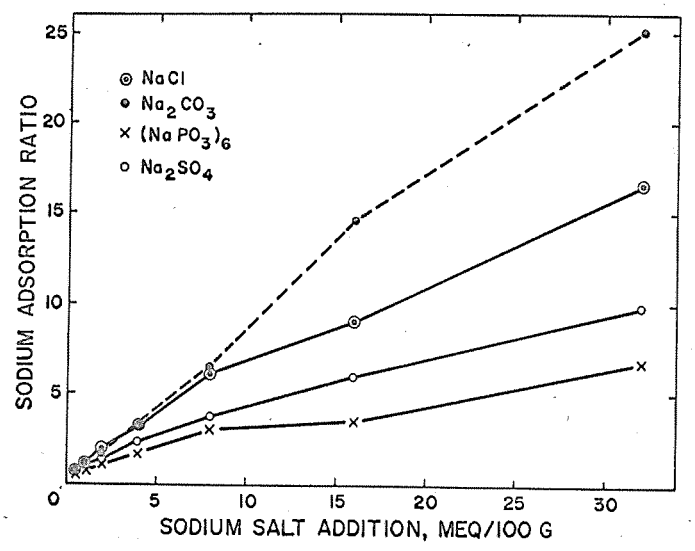

Figure 6. Sodium adsorption ratio for the Big Lake as a function of added Na salts.

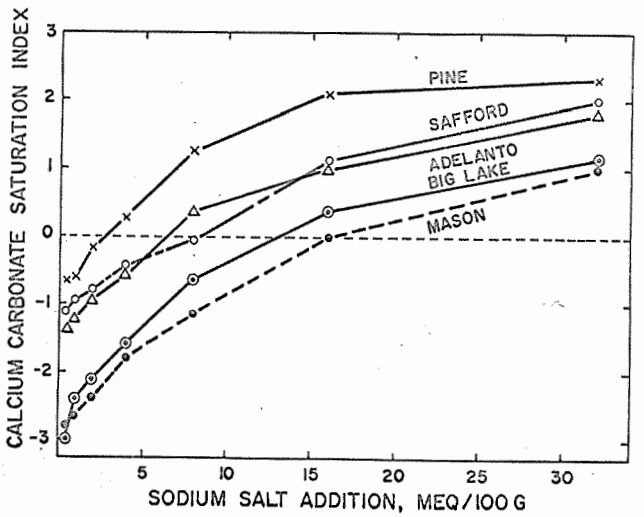

Figure 7. Calcium carbonate saturation index for the ambient solutions for the different soils treated with various levels of Na_2CO_3.

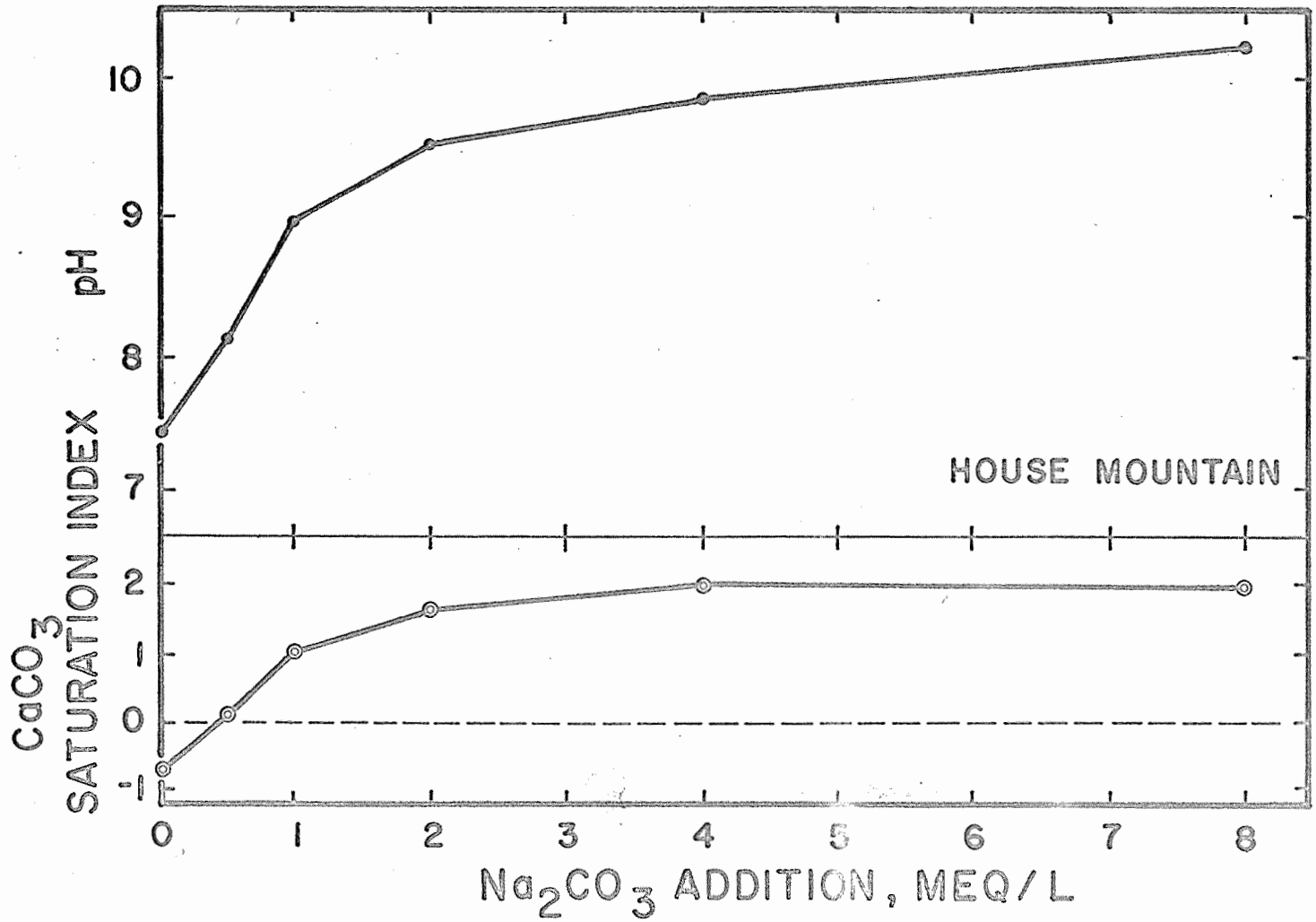

Figure 8. Calcium carbonate saturation index and pH for House Mountain pond water treated with Na_2CO_3.

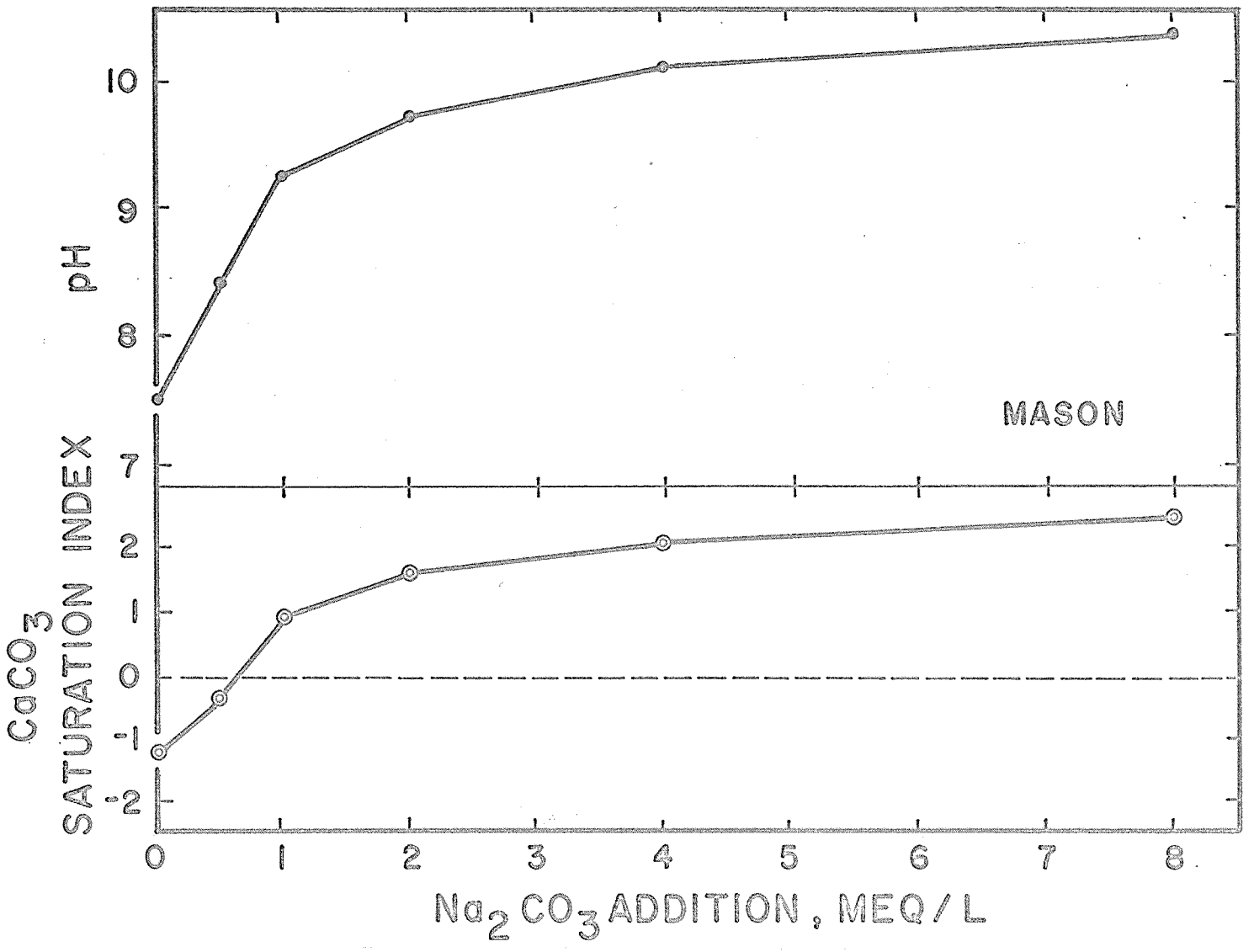

Figure 9. Calcium carbonate saturation index and pH for

TITLE: FIELD MEASUREMENT OF CRITICAL PRESSURE HEAD OF SOILS

LINE PROJECT: SWC 4-gG1 CODE NO.: Ariz.-WCL-41

INTRODUCTION:

The work under this project was continued with the development of a field device for measuring air entry value, P_a, of soil. A technique for estimating the hydraulic conductivity, K, of the wetted zone with the same device was also developed. Studies were performed to investigate the effect of the initial moisture content of the soil on the measured value of P_a. The validity of the data obtained with the field device as estimates of the critical pressure head, P_{cr}, (See Annual Report 1964, Section 24) and the saturated hydraulic conductivity of the soil was determined by comparing P_a and K from the device with P_{cr} and K obtained from systems of porous medium flow in laboratory models. Other comparisons were also made.

In order to avoid confusion with the symbol P_c often used in the literature to describe capillary pressure, the symbol P_c as selected earlier for critical pressure head has been replaced by the symbol P_{cr}.

PROCEDURE:

Field device

The field device, as shown in Figure 1, is operated as follows:

1. The cylinder is driven into the ground to a depth of 8 to 10 cm (a cylindrical driver with sliding weight is used for this purpose).
2. Using a 1-ft section of 1-inch × 2-inch lumber and a hammer, the soil along the inner perimeter of the cylinder is packed down and against the cylinder wall to insure a good bond between the cylinder and the soil. In loose or cracked soil, compacting around the outside of the cylinder may also be necessary.
3. In case of a bare soil surface, the soil is covered with a 1/2- to 1-inch layer of coarse, clean sand. A disk or similar object is placed on the sand in the center of the cylinder to break the water stream from the supply pipe.

4. The surface of the foam rubber gasket is cleaned and a thin coat of grease is applied.
5. The lid-assembly with the air valve open and the gage and supply valves closed is placed on the cylinder. A round bubble-level is placed on the lid to determine the highest point. The lid assembly is then rotated so that the air escape valve is at that highest point.
6. The lid is fastened with four small C-clamps until it rests firmly on the rim of the metal cylinder. Lead weights are placed on the lid to offset the upward hydrostatic force when the supply valve is open.
7. The plastic reservoir at the top of the galvanized pipe is filled with water and the air in the pipe is allowed to escape. The supply valve at the bottom of the galvanized pipe is opened while maintaining the water supply to the plastic reservoir. When the water has driven out the air from inside the cylinder, the air valve is closed.
8. The vacuum gage is removed from the holder and lifted to about the water level in the plastic reservoir. The gage valve at the plastic lid is opened, which causes the needle on the gage to go to zero. Tilting the gage will then reset the memory pointer to zero. The gage valve is closed and the gage is replaced on the gage holder.
9. When the depth of the wet front is expected to be approximately 10 cm, the supply valve is closed. Experience will tell how much water needs to be applied to achieve this depth.
10. The gage valve is opened. When the gage indicates approximately atmospheric pressure inside the cylinder, the weights are removed from the plastic lid.
11. When the memory pointer has lost contact with the gage needle, minimum pressure has occurred. As soon as loss of contact is observed, the memory pointer is read, the gage valve is closed, and the air escape valve is opened. The lid assembly

is removed and the depth of the wet front is measured. This can be done by pushing a quarter-inch rod into the soil and observing the depth where the penetration resistance is considerably increased. Another way is to quickly remove any remaining water in the cylinder, taking the cylinder out of the soil, and digging with a spade to visually determine the position of the wet front. Dyes and electric-conductivity probes may also offer possibilities for wet-front detection. To facilitate accurate assessment of the depth of the wet front, the soil should not be too wet at the time of the test.

12. The value of P_a is calculated by subtracting the gage reading in cm water from the vertical distance between the gage center and the bottom of the wetted zone. The resulting value should be negative.

The measurement of the hydraulic conductivity of the wetted zone is based on the assumption that P_a is a reasonable estimate of the pressure at the "saturation" front. The procedure for K-measurement is as follows:

1. Time and water level readings are taken in the plastic reservoir at the top of the galvanized pipe for approximately the last 5 cm of fall of the water level prior to closing the supply valve. The last time and water level measurement should occur immediately before the supply valve is closed.

The hydraulic conductivity is calculated according to the following equation:

$$K = 2 \frac{\frac{dH}{dt} L}{H_t + L - P_a} \frac{R_r^2}{R_c^2} \qquad (1)$$

where $\frac{dH}{dt}$ = rate of fall of water level in plastic reservoir just before valve at bottom of galvanized pipe is closed. This rate may be obtained by plotting time and water level readings on graph paper and determining the slope of the curve just before the valve closing.

L = depth of wet front below soil surface.

H_t = distance of water level in plastic reservoir above ground level at closure of supply valve.

R_r = radius of plastic reservoir.

R_c = radius of cylinder.

The factor 2 in the equation accounts for the fact that the saturated hydraulic conductivity is about twice the hydraulic conductivity for sorption.[1/]

Box studies

To determine the validity of the results of the field device as estimates of P_{cr} and K, flow models were set up from which P_{cr} and K could be evaluated. The models consisted of soil-filled wooden boxes, 150 cm long, 60 cm wide, and 150 cm high. Three boxes were constructed. Rectangular drains of epoxied sand and gravel were placed along the 60-cm wall at each side of the bottom. The drains were 20 cm high and 10 cm wide. The boxes were filled with air-dry medium river sand (2 replications) and Laveen loam (3 replications) to a depth of approximately 100 cm.

The mechanical analysis of these soils was as follows:

Medium river sand		Laveen loam	
0.5-1 mm	3%	sand	43%
0.3-0.5 mm	39%	silt	44%
0.1-0.3 mm	47%	clay	13%
<0.1 mm	11%		

Each drain was connected to a constant-level reservoir and a system of mainly horizontal flow was established in each box by maintaining a small head difference (2 cm) between the two reservoirs.

The flow per unit width of the box and per unit head-difference was called C (for conductance). The relationship between C per unit

---

1/ R. H. Brooks, ARS-SWC, Fort Collins, Colorado, personal communication.

K and the effective height y of the flow system of saturated hydraulic conductivity was determined by resistance network analog (Figure 2). An example of a flow system obtained by analog is shown in Figure 3. To obtain another measurement of K, the relationship between C/K and the total depth of soil in the box was also determined for the ponded case (Figure 4). For this test, water was standing above the soil surface and identical heads a few centimeters below the water level in the box were maintained in each drain.

To minimize problems associated with air formation and growth of micro-organisms in the soil, water of higher than ambient temperature with liquid chlorine added was used in a recirculatory system. Clogging of the sand and gravel drains was minimized by periodic reversion of the flow direction. The test procedure consisted of the following four steps:

A. Starting with dry soil, water was slowly admitted to both constant-level reservoirs. The reservoirs were set with their level at approximately 25 cm above the bottom of the box. When essentially no more water was absorbed by the soil, a 2-cm head difference between the two reservoirs was established. The resulting flow through the soil in the box was measured until constant.

B. The constant-level reservoirs were raised at small increments until approximately 2 cm below soil surface to saturate the medium without ponding. The reservoirs were then set at a 2-cm head difference and the resulting flow was measured until constant. The upper boundary of the flow system in this case was the surface of the soil.

C. The constant-level reservoirs were raised a small distance above the surface of the soil in the box to create a ponded condition with approximately 5 cm of water standing above the surface of the soil. The constant-level reservoirs were then lowered to 5 cm below the water level in the box. The outflow from each drain was measured.

D. The constant-level reservoirs were slowly lowered to about 25 cm above the bottom of the box and a 2-cm head difference was again established. The flow was measured until constant.

For test B, the height of the saturated flow system, y, was equal to the total height of the soil in the box. Thus, C/K could be evaluated from Figure 2. Knowing C, from flow measurements, K could be calculated. Knowing C for tests A and D, C/K for these tests could then be determined and the corresponding y-values could be evaluated from Figure 2. Subtracting from this y the average height of the water table in the boxes (calculated at the average water level of the constant-head reservoirs above the box bottom), yielded the effective height of the capillary fringe, which is $-P_{cr}$. For the ponded case (test C) the outflow of each pair of drains was averaged to determine C. Using Figure 4, K could then be calculated. In summary, the tests yielded the following data:

Test A	P_{cr} for sorption
Test D	P_{cr} for desorption
Test B	K in mainly horizontal direction
Test C	K in mainly vertical direction

For the same soil materials as used in the boxes, P_a and K were determined with the field device, so that comparisons could be made. These tests were carried out with the soil in a 60 × 60 × 60-cm box. For the Laveen loam, the field device with vacuum gage (Figure 1) was used. For the river sand, the vacuum gage was replaced by a pressure transducer and recorder. This was necessary because of the high infiltration rate, and the fast pressure response after closing the supply valve.

Column studies

In this study, K as calculated with equation (1) was compared with K from permeameter tests, using the vertical columns described in earlier P_{cr}-work (See Annual Report 1964, Section 24). The columns were filled with fine river sand and water was applied and cut off to determine K with equation (1). Water application was then

resumed to saturate the entire column. A flow through the column was maintained and K was calculated from flow rate and head loss for the entire column. Since the latter K referred also to sorption, the factor 2 in equation (1) was omitted for this comparison.

Field studies

A field study was carried out in Adelanto loam south of the laboratory to compare K as calculated with equation (1) with K obtained from previous double-tube tests. The device of Figure 1 was placed in trenches, which were deepened as the test progressed to obtain a profile of K-values. The location of the test was east of the lathhouse on Bermuda grass lawn.

Initial moisture content

The air entry value of the soil should not be affected by the initial moisture content. To verify this, P_a was measured with the columns for 76μ glass beads at 4.1 percent moisture content. The results were compared with previous measurements on air-dry glass beads. In addition, field measurements were carried out with the device of Figure 1 on bare Adelanto loam south of the laboratory during a drying period after severe rain. Of the 24 measurements made, 13 were at soil moisture contents from 8 percent to 14 percent, and 11 at moisture contents of 14 percent to 20 percent.

RESULTS AND DISCUSSION:

Box studies

The results of the studies of the flow systems in the large boxes are shown in Table 1, which also gives the values of P_a and K obtained with the device of Figure 1 for the same soil materials. For the flow models, P_{cr} for sorption is about one-half of P_{cr} for desorption. An exception is box 3 of Laveen loam which yielded a rather unrealistically low value of P_{cr} for sorption. This may have been caused by partial blocking of the flow due to air or microbiological activity in the box. The K-values from the lateral-flow tests and the ponding tests showed good agreement.

For the river sand, P_a and K were not only determined with the field device in the 60 × 60 × 60-cm box, but also with the vertical

columns (See Annual Report 1964). This was done because packing of the sand to sufficient surface density could not be achieved in the small box. The density of the sand in the columns was probably in excess of that in the large boxes. Thus, P_a and K for tests 1, 2 and 3 are probably on the high side, and for tests 4 and 5 on the low side. For test 3, the pressure-trace of the recorder is shown in Figure 5.

For the Laveen loam, the soil packed at 3 percent moisture content probably had a somewhat higher density than the soil that was packed dry, then saturated and allowed to dry in the atmosphere. This is evidenced by P_a and K being somewhat higher for tests 1 and 2 than for tests 3, 4, and 5. Since P_a and K are essentially determined by the larger pores in the soil, they are quite sensitive to soil density. For the finer soils, surface sealing may be difficult to avoid and the values of K for the field device may therefore be on the low side.

Table 1 shows that P_a as determined by the device of Figure 1 gives a good estimate of P_{cr} for desorption. As regards P_{cr} for sorption, Table 1 and reports by other investigators indicate that this value can be estimated at one-half of P_{cr} for desorption. The K-values obtained with the field device according to equation (1) agree reasonably well with the K-values obtained from the flow models.

The flow rates in the model studies of lateral flow (tests A, B, and D) showed a diurnal fluctuation, which was opposite the diurnal fluctuation in barometric pressure. The apparent effect of barometric pressure on flow rate was attributed to expansion or contraction of entrapped air in the soil, which resulted in release or absorption of water with attendant increase or decrease in outflow rate, as the barometric pressure decreased or increased, respectively.

The effect was most noticeable for the slowly permeable Laveen loam, where the outflow rate was low and thus materially affected by release or absorption of the water in the soil. As an example of a typical change in flow rate, an increase from 0.89 to 1.04 cc/min was observed for a pressure drop from 970.5 to 967.6 millibars in a five-hour period. For these data and using Boyle's Law, the air

volume of the soil in the box was approximately calculated as 4.9 percent. Upon completion of the tests, core samples were taken from the soil, which yielded air contents ranging from 5 percent for the lower portion of the box to 7 percent for the upper portion of the box. Since most of the lateral flow was concentrated in the lower part of the box, the calculated and measured air contents of the soil were in excellent agreement. This supports the conclusion that barometric pressure variations were responsible for the variations in outflow rate from the models.

Column studies

The results of the comparison between K determined with equation (1) and associated procedure, and K calculated from flow rate and head loss by considering the entire column as a permeameter, are shown in Table 2. The results are in excellent agreement.

Field studies

The results of the measurements of P_a and K with the field device of Figure 1 in Adelanto loam south of the laboratory are summarized in Table 3. The relatively high (numerically relatively low) values of P_a are due to root holes and worm holes, which were clearly visible in the soil. The K-values assume a relatively constant value at depths greater than 30 cm. This value compares favorably with results from double-tube tests that were carried out several years ago. One such test was performed south of the laboratory at 80-cm depth and it yielded a K-value of 0.036 cm/min. Nine long-duration double-tube tests, carried out east of the laboratory at depths from 80 to 180 cm, yielded $K = 0.066 \pm 0.040$ cm/min.

Initial moisture content

The values of P_a yielded by the column studies on 76μ glass beads at 4.1 percent moisture content ranged from -48 to -61 cm with an average of -55 ± 4.4 cm. This is relatively close to the average P_a-value of dry glass beads, which was -63 ± 4.4 cm (See Annual Report 1964). Part of the difference may be due to the lower air permeability of the moist glass beads. This could have resulted in above-atmospheric pressures of the air below the advancing wet

front, and a recorded value of P_a that is higher (numerically lower) than the actual air entry value of the wetted zone.

The field studies with the device of Figure 1 on bare Adelanto loam southeast of the laboratory yielded the following results:

Moisture content	P_a in cm water	Number of tests
8-14%	-34 ± 11	13
14-20%	-32 ± 7	11

The P_a-values differ less in this case than for the column studies with glass beads. This may be due to the fact that the opportunity for air escape ahead of the wet front is much better for the field device than for the columns.

The results of both studies indicate that the initial moisture content has little or no effect on P_a.

SUMMARY AND CONCLUSIONS:

A field device was developed for measuring the air entry value, P_a, of soil in situ. The device consists basically of a 10-inch infiltration cylinder with lid, a standpipe with reservoir, and a vacuum gage with memory pointer. The principles of operation are identical to that of the vertical columns discussed in Annual Report 1964. The soil is wetted under high head to a depth of 10 to 15 cm, the water supply is turned off to halt the advance of the wet front, and the minimum water pressure in the cylinder prior to the emergence of air bubbles from the soil is measured. Referring this minimum pressure to the depth of the wet front yields P_a. Assuming that P_a is also a reasonable estimate of the pressure head at the advancing wet front, the hydraulic conductivity K of the wetted zone can be calculated from velocity and gradient if the infiltration rate prior to turning off the water supply is measured. The resulting K applies to sorption. Multiplying this value by 2 yields K for saturated conditions.

To determine the validity of P_a and K from the field device as estimates of critical pressure head, P_{cr}, and saturated K, a number of studies was performed. In one study, models of lateral flow in soil were set up in large wooden boxes. The flow systems were

analyzed by resistance network analog to permit determination of P_{cr} and saturated K from discharge measurements at various heights of the water table in the boxes. For the same soil materials in the models, i.e., Laveen loam and medium river sand, P_a and K were determined with the field device in a separate box. The resulting values were in good agreement with P_{cr} and saturated K from the models. A second study consisted of determining K from P_a and the infiltration rate in vertical columns of fine river sand. After the necessary measurements were taken, water application was resumed to wet the entire column, so that K could be determined by permeameter techniques. The agreement between the K-values obtained in both manners was excellent. In a third study, a K-profile was determined with the field device in Adelanto loam south of the laboratory. The resulting values were compared with K-data from double-tube measurements made in previous years. Good agreement existed also in this case. A fourth study concerned the effect of initial moisture content of the soil on the measured value of P_a. Theoretically, there should be no such effect. This was verified in the laboratory for vertical columns of glass beads, and in the field for Adelanto loam in a drying period following severe rainfall.

Based on these studies, the conclusion is made that the values of P_a and K determined by halting the advance of a wet front are acceptable estimates of critical pressure head and saturated hydraulic conductivity. The field device for obtaining P_a and K is simple in construction and operation. Usually, not more than 20 minutes are required per test.

PERSONNEL: Herman Bouwer and Robert C. Rice.

Table 1. Results of evaluation of P_{cr} and K with the flow models, and of P_a and K with the field device.

FLOW MODELS

	Test A P_{cr}-sorption cm water	Test D P_{cr}-desorption cm water	Test B K-lateral cm/min	Test C K-ponded cm/min
River sand				
Box 2	-18	-31	0.79	0.74
Box 3	-15	-25	0.62	0.55
Laveen loam				
Box 1	-22	-47	0.020	0.018
Box 2	-23	-51	0.018	0.015
Box 3	-10	-43	0.011	0.012

FIELD DEVICE

	P_a	K
River sand		
Test 1	-28	0.76
Test 2	-26	0.90
Test 3	-32	0.80
Test 4 1/	-31	0.66
Test 5 1/	-37	0.65
Laveen loam		
Test 1 2/	-47	0.015
Test 2 2/	-48	0.013
Test 3 3/	-51	0.013
Test 4 3/	-57	0.012
Test 5 3/	-50	0.012

1/ Results from vertical columns.
2/ Soil was packed dry, saturated, and air dried in box.
3/ Soil was packed at 3% moisture content.

Table 2. Results of K-determination with equation (1) and with permeameter technique in vertical columns with fine river sand.

Column	P_a cm water	K-eq.(1) cm/min	K-permeameter cm/min
1	-48	0.23	0.21
2	-46	0.18	0.19
3	-46	0.19	0.19
4	-43	0.19	0.20

Table 3. Results of P_a and K evaluation for Adelanto loam south of the laboratory.

Depth	P_a	K	Number of Tests
cm	cm water	cm/min	
0	-14 ± 0.74	0.12 ± 0.015	22
18	-10 ± 1.00	0.060 ± 0.006	22
30	-7.5 ± 0.84	0.042 ± 0.005	21
50	-6.3 ± 0.49	0.044 ± 0.005	21

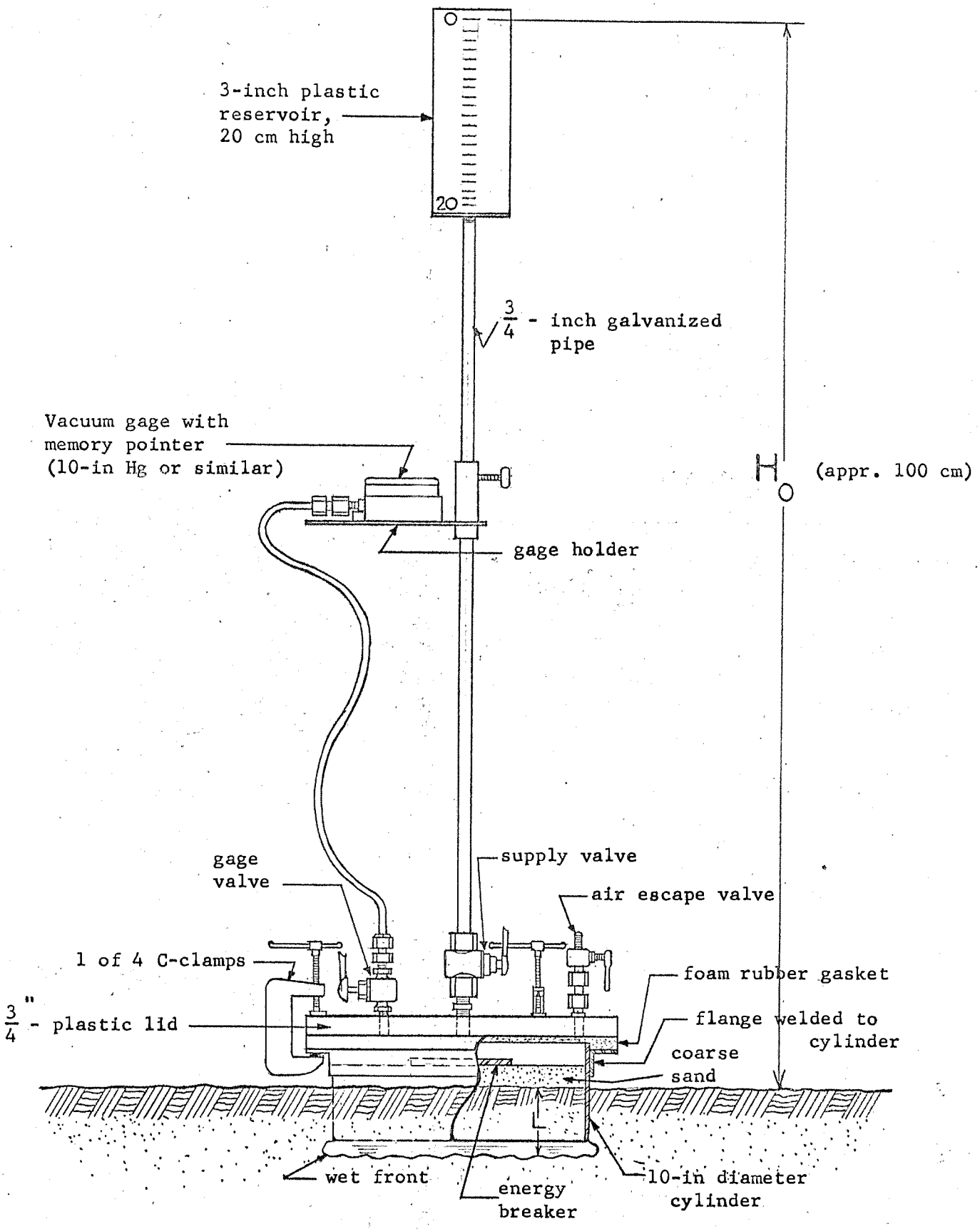

Figure 1. Field device for measuring air entry value and hydraulic conductivity.

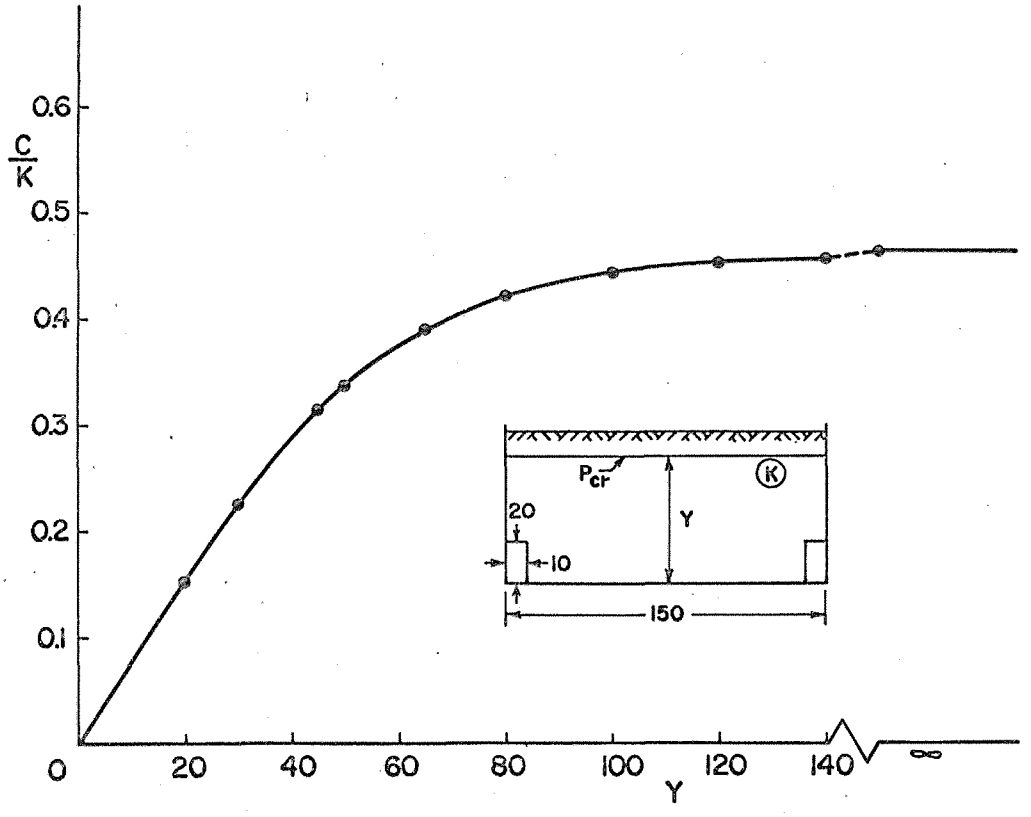

Figure 2. Relationship between C/K and y for lateral flow in models as determined by resistance network analog.

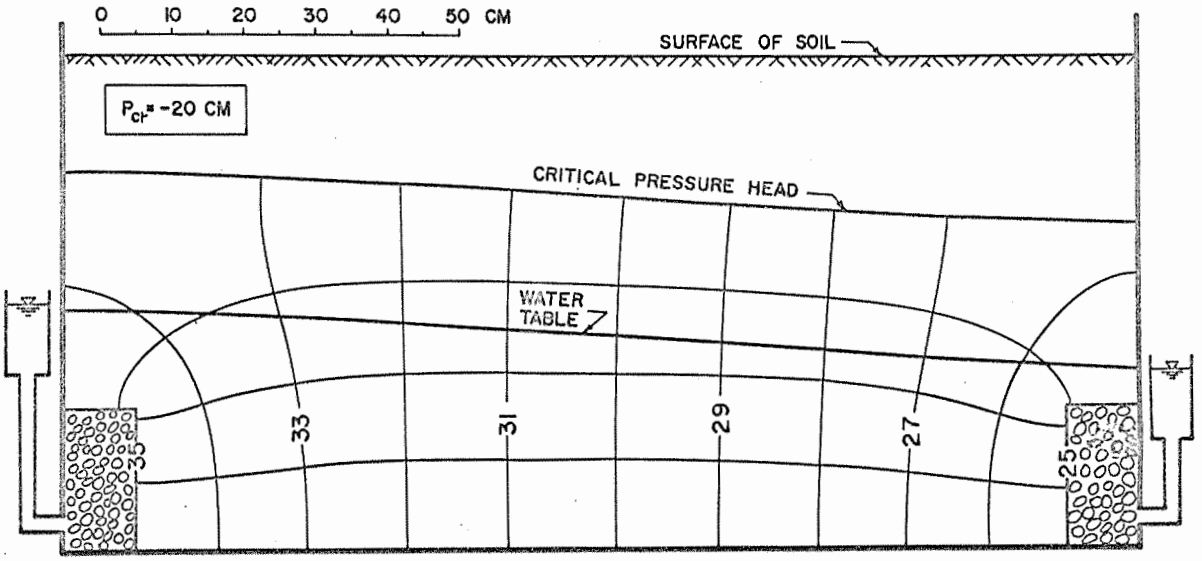

Figure 3. Example of system of lateral flow in the boxes.

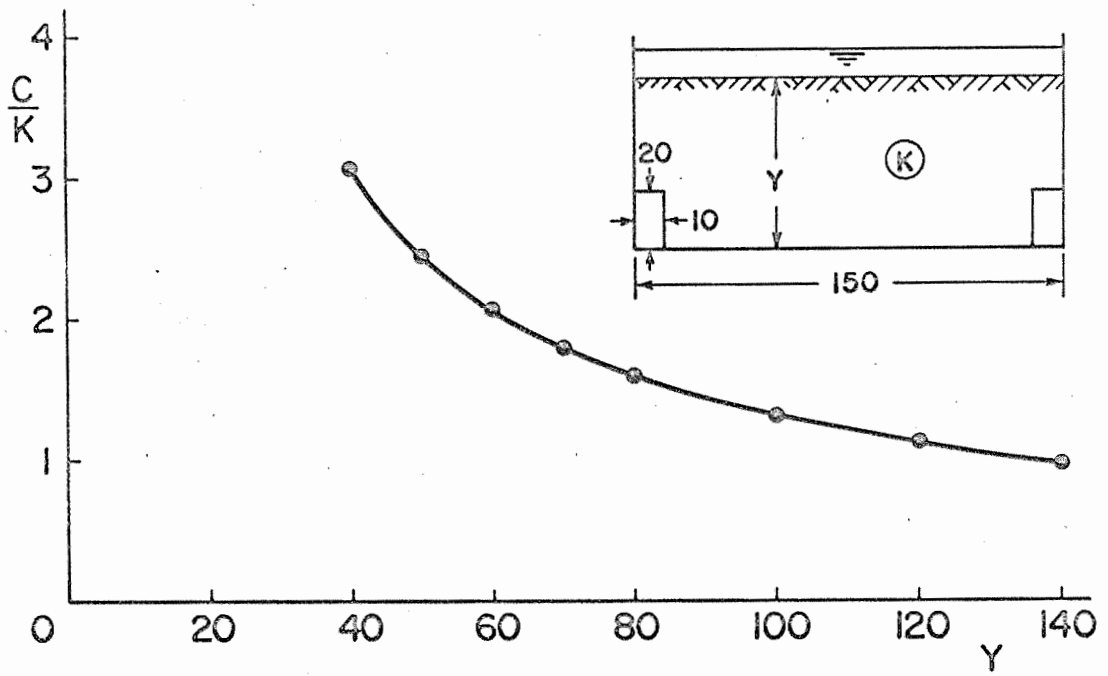

Figure 4. Relationship between C/K and y for ponded case as determined by resistance network analog.

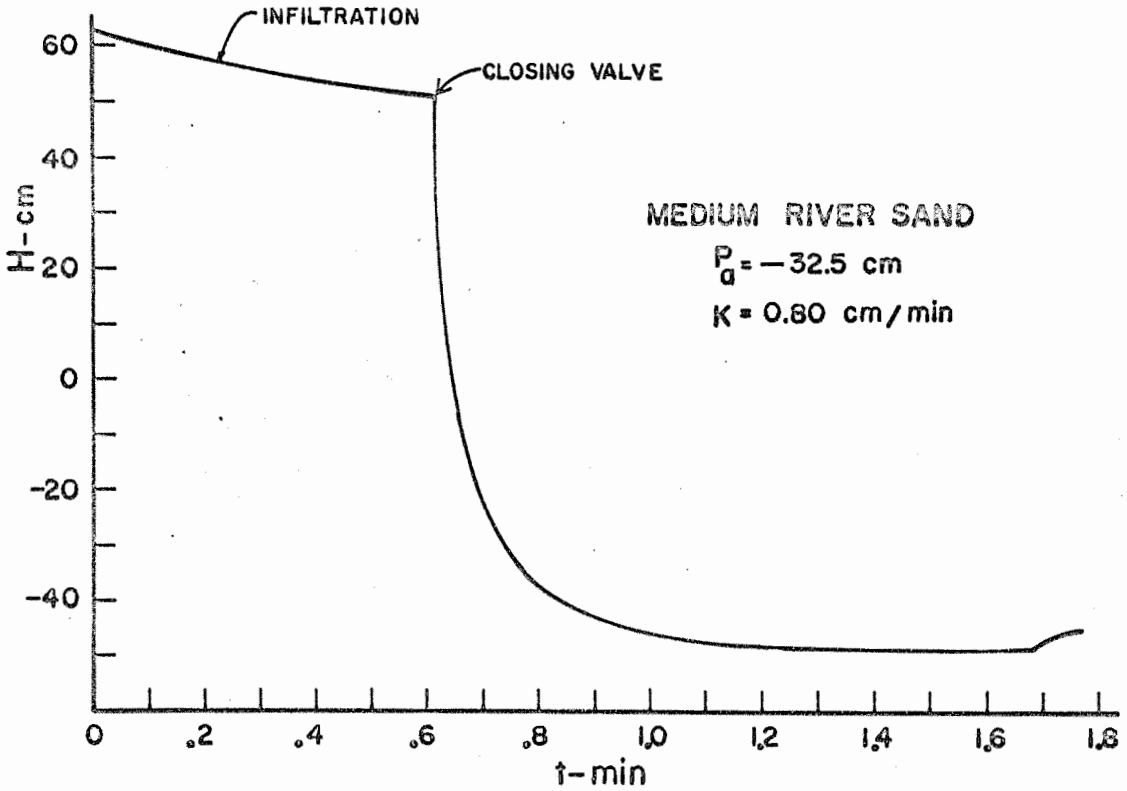

Figure 5. Pressure trace for test 3 of field device in river sand.

TITLE: MATERIALS AND METHODS FOR WATER HARVESTING AND WATER STORAGE IN THE STATE OF HAWAII

LINE PROJECT: SWC 4-gG3 CODE NO: Ariz.-WCL-42

INTRODUCTION:

Water harvesting is feasible and badly needed in the State of Hawaii. Despite high rainfall, which annually exceeds 1,200 gallons per square yard in many locations, porous lava flows and highly permeable soils absorb the water and perennial streams are the exception rather than the rule. Ground water supplies are normally available only at sea level and salt water intrusion often reduces the usefulness of this source. As a result inadequate water supplies plague Hawaiian ranchers, farmers, industries, and householders. Additional water supplies can readily be obtained by water harvesting. Small catchment areas can collect large volumes of water and economic justification of water harvesting structures is readily apparent. The problem restricting the use of water harvesting is the lack of information concerning design criteria and materials specifications suited to Hawaiian conditions.

Site conditions can be conservatively classified as "difficult" at most locations where water harvesting structures are desired. Topography is rough and steep, "soil" often consists of cinders and sharp pieces of broken lava, and earth tremors occur at relatively frequent intervals. If true soil exists, its chemical composition is not ordinarily similar to soil in the mainland states and its physical characteristics are drastically different. Suitable construction materials must be flexible, strong, puncture resistant, watertight, durable, and low in cost. Structural design must consider wind uplift, vegetation encroachment, elimination of downhill creep on steep slopes, control of high-volume super-critical water flow down covered steep slopes, and related problems.

The great interest in water harvesting makes a cooperative research program feasible. During the course of two visits to Hawaii during April and September 1965, arrangements were made for sites, surveys, materials, and installation of experimental water harvesting structures at two sites, one on Hawaii and one on Maui.

PROCEDURE:

The Hawaii site is in a 100-inch rainfall zone on the Kukaiau Ranch. The installation will consist of a 10,000 ft^2 catchment and a 750,000-gal lined reservoir. The catchment will be covered with experimental plastic sheeting provided by the Dow Chemical Company. DuPont will provide a new artificial rubber sheeting for lining the reservoir. A topographic survey of the site has been made by the Soil Conservation Service. Site preparation will be done by the Kukaiau Ranch. Installation will be a joint effort by the Kukaiau Ranch, the Wisdom Rubber Company, and the U.S. Water Conservation Laboratory.

Evaluation of the Kukaiau site will be in terms of problems encountered in construction, followed by periodic inspection to determine performance. Inspection will be performed by SCS and Laboratory personnel to record factors such as weathering, cracking, puncturing, wind damage, creep down slopes, and vegetation damage. Runoff from the catchment will not be measured since experience has shown that this will be essentially 100 percent of rainfall unless the plastic cover is damaged. Rainfall will be measured with a storage type gage. Water surface elevation in the reservoir will be measured at intervals to check inflow and possible seepage loss.

The Maui site is on land made available by the East Maui Irrigation District. Four test plots, 40 × 80 ft, will be installed on 10 to 20 percent slopes with treatments as follows:

(1) Pasture grass,
(2) Two-phase asphalt pavement,
(3) Butyl rubber sheeting, and
(4) Experimental plastic sheeting.

Asphalt will be provided by the Chevron Asphalt Company, butyl sheeting by the Hodgman Rubber Company, and the plastic sheeting by DuPont. A topographic site survey was made by the Soil Conservation Service. Site preparation will be done by the Hawaiian Commercial and Sugar

Company. Installation will be done by Wisdom Rubber Company, Chevron Asphalt Company, HC&S, and our Laboratory.

Evaluation will consist of periodic observations as outlined for the Kukaiau site, plus measurements of rainfall and runoff. Rainfall will be measured by a standard raingage. Runoff from each plot will be measured by venturi flumes equipped with water-stage recorders. Instrumentation will be provided by the Laboratory and maintained by the East Maui Irrigation District.

Installation of the Kukaiau and Maui sites is planned for February 1966.

PERSONNEL: L. E. Myers, G. W. Frasier

TITLE: INTEGRATING VELOCITY PROFILE METERS

LINE PROJECT: SWC 4-gG5 CODE NO.: Ariz.-WCL-43

INTRODUCTION:

Numerous flow velocity devices use impact force or momentum principles for indicating fluid flow velocity. These include pitot tubes, current meters, impact velocity-head-rise rules or sticks, and force-deflection devices. Pitot tubes and current meters provide point velocity measurements, a number of which must be obtained to provide an integrated discharge measurement. Impact rules are of limited accuracy because of the difficulty of reading the velocity head rise, especially at relatively low velocities. The commercial force-deflection meters are usually limited to fixed channel geometries. An adequate analytical treatment of most of these deflection devices is difficult since it involves many variables.

Certain design features are proposed here that simplify mathematical analysis of force-deflection devices as flow velocity meters. Numerous impact or drag elements, such as blades, spheres, cylinders, and discs, may be inserted into the flowing stream to serve as the sensor for such a device. The body force exerted on the element is an indication of the velocity in the channel.

PROCEDURE:

A rectangular plate was selected for initial study because of analytical simplicity and ease of fabrication. Drag force data is available in the literature for many shapes. However, spheres and cylinders exhibit variability in the point of flow separation as the fluid passes around the body, due to changes in the texture or cleanliness of the body surface. With flat plates turned broadside to the flow, the point of separation is the sharp edge. Changes in surface roughness have limited effects, if any.

Analytically, the drag force, F_D, on a rectangular plate in a flowing fluid can be expressed as

$$F_D = \int_0^y C_d \, w \, \frac{v_x^2}{2g} \, b \, dy \qquad [1]$$

where C_d is a drag coefficient, w is the unit weight of the fluid, v_x is the point velocity, g is the gravitational constant, and b is the width of the body having a height of y.

If the rectangular plate is set normal to the flow, then separation always occurs at the edges and C_d varies from approximately 1.90 to 2.00. The total force F_D on a rectangular plate is a function of the velocity distribution in the channel. Since F_D can be measured, the average velocity, $\bar{v}$, can be deduced from a general knowledge of the velocity distribution in channels. For w, g, C_d all constant, equation [1] may be written

$$F_D = \frac{C_d wb}{2g} \int_o^y v_x^2 \, dy \qquad [2]$$

An expression for the integral portion of equation [2], in terms of the average velocity, $\bar{v}$, in the vertical stream section being tested is desirable. Such an expression can be obtained by considering the principles of momentum. The momentum, M, of fluid passing a particular stream cross section in a unit time is commonly expressed as

$$M = \beta \frac{w}{g} A \bar{v}^2 \qquad [3]$$

where A is a stream cross-sectional area, and β is the momentum correction factor. (See King's Handbook of Hydraulics, 4th Ed., p 7.10.)

In terms of point velocities, v_x, equation [3] is

$$M = \frac{w}{g} \int_o^A v_x^2 \, dA \qquad [4]$$

For a single vertical section in a stream cross section, or for an infinitely wide stream the area, A, can be replaced by a unit area of (1 · y) and

$$M = \frac{w}{g} \int_o^y v_x^2 \, dy \qquad [5]$$

where y is the depth of the stream (also the length of a rectangular plate extending to the bottom of the channel). Equating [3] and [5] and solving for the integral portion of equation [5]

$$\int_0^y v_x^2 \, dy = \beta \, y \, \bar{v}^2 \qquad [6]$$

substituting equation [6] into equation [2]

$$F_D = C_d \frac{wb}{2g} \beta \, y \, \bar{v}^2 \qquad [7]$$

or

$$\bar{v} = \sqrt{\frac{2g \, F_D}{\beta \, w \, b \, y \, C_d}} \qquad [8]$$

where β is the momentum correction factor. The usual range of values for β in prismatic channels is between 1.01 and 1.06. The velocity, $\bar{v}$, in a vertical section can thus be determined with equation [8] by measuring the force, F_D, and the length y of a rectangular plate extending from the water surface to the bottom of the stream channel.

The force, F_D, can be determined for a rectangular plate of width b and length y by measuring the force necessary to prevent the plate from pivoting about any edge. This might be done by forcing the bottom of the plate firmly against the bottom of the channel and measuring the force at the upper end. With this method, however, there is no way of determining the center of force, and thus the amount to attribute to the bottom reaction.

If the assumption of small transverse variation in velocity is made, then the force, F_D, can be determined by the torque necessary to prevent rotation about a vertical edge of the plate. The resultant force would act on the vertical centerline of the plate and, since the depth to its point of application is immaterial in the calculation, F_D is defined. The readings from several vertical measurements could be combined to obtain the discharge for the entire channel.

Readout devices that can be used to obtain the force, F_D, may be either electrical, electrical-mechanical, or mechanical. For laboratory

purposes, electrical systems such as strain gauges are convenient, but the associated electrical circuitry and instruments make the cost near prohibitive for wide-scale field application. Therefore, emphasis in this study has been toward mechanical readout systems. The mechanical systems can be simple flexures, such as cantilever beams or torsion bars indicating force exerted on the blade by the degree of flexure; or hydraulic transducers, such as bourdon tubes and hydraulic bellows.

Laboratory Study. Two vane meters have been constructed during the initial phase of this study. Both meters have similar configurations. Meter number 2 is shown diagramatically in Figure 1. Both had blades about 1-inch wide with a usable length of 14 to 16 inches. The major difference between the two meters concerned the method of readout for the force measurement. Meter number 1 used a cantilever flexure indicator made from a 4-inch piece of piano wire. A micrometer screw was used to apply enough lateral force to the free end of the cantilever to maintain the blade perpendicular to the stream flow into which the blade was placed. The deflection, read from the micrometer screw, was converted to force on the blade using a previous force-deflection calibration for the cantilever. With the force, F_D, and the depth of flow, y, the average velocity could be obtained from equation [8].

Meter number 2 used a torsion bar to indicate force. A slot was cut into one edge of the blade and stainless steel hypodermic tubing inset below the surfaces for the entire length of the blade. Piano wire was inserted through the tubing and firmly attached at the bottom end of the blade. The tubing, which was attached rigidly to the blade, acted as a protecting shield for the piano-wire torsion bar and also served as the top bearing for the blade. A dial was attached to the upper end of the torsion bar to measure the torsional deflection necessary to balance the impact force of the flow against the blade. A pointer attached to the blade indicated when balance was achieved.

The accuracy of the meter as a velocity integrator was checked by measuring flow profiles with a pitot tube in a laboratory channel, 1 ft wide and 30 ft long. These profiles were plotted and planimeterd

to determine the average velocity. A measurement at the same location in the channel was also obtained with the integrating velocity meter. This measurement was compared to the average velocity determined with the pitot tube.

RESULTS AND DISCUSSION:

Considerable difficulty was encountered with meter number 1, which used a cantilever and micrometer screw readout system. It was difficult to determine when the blade had been returned to its correct alignment. Since the total deflection was on the order of 0.100 to 0.300 inch, the position of the indicating pointer needed to be only 0.001 to 0.003-inch misaligned, respectively, for 1 percent readout error. With care, adequate lighting, and the use of a magnifying lens, several tests were completed. The results of these tests are summarized in Table 1.

The vane meter indicated discharge velocities 2.4 percent less than those calculated from the pitot tube measurements. This would indicate a need to increase the assumed value of C_d. The value for C_d and β used in equation [8] was $C_d = 1.90$ and $\beta = 1.02$. Graphical determinations of β from the pitot tube data indicated that β in a single vertical strip was very close to unity, varying from 1.000 to 1.003, even though the value for the channel as a whole was as large as 1.026. This requires the value of C_d to increase to approximately 1.98.

A value of $C_d = 2.00$ is sometimes quoted for an infinitely long rectangular blade. It is thought that a value of 2.00 is approached since flow cannot go around the ends of an infinitely long plate. Similarly, in the application here, one end of the blade is very near the channel floor and the other extends beyond the surface such that no flow can pass the ends of the blade. Also, the velocity head rise on the front side of the blade is accompanied by a flow depression behind the blade, thus registering a static force and an impact force, tending to maintain the two-times value for the drag coefficient even near the surface.

Based on the tests in Table 1, the accuracy to be expected with meter number 1 is indicated by the tolerance (two times the standard

deviation) which is equal to 3 percent. This means that ± 3 percent accuracy can be expected 96 percent of the time.

The improvements in meter number 2 should improve the tolerance slightly. Comparison measurements with meter number 2 are yet to be made.

SUMMARY AND CONCLUSIONS:

An impact velocity indicating device, using a rectangular blade in a flowing stream, was analyzed mathematically, constructed, and tested in a laboratory channel. The blade was long enough to extend from the flow surface to the channel floor and was placed broadside to the flow. The total force exerted by the velocity profile was measured as torque about a vertical edge of the blade.

Numerous flow velocity devices such as current meters, pitot tubes, and force deflection devices, use impact force or momentum for indicating fluid velocity. Pitot tubes and current meters provide point velocity measurements, many of which are required to provide an integrated discharge measurement. While some commercial force deflection meters provide a single-measurement discharge reading, they are usually limited to a fixed channel geometry. Also, adequate analytical treatment of the many variables is difficult.

Two meters were constructed, both of similar configuration, with blades 1 inch wide and approximately 18 inches long. Mechanical readout of force-indication was chosen over strain-gauge devices, hopefully to simplify field applications. The first meter used a cantilever flexure indicator fashioned from spring-steel wire. A micrometer screw was used to apply enough lateral force to the free end of the cantilever to maintain the blade perpendicular to the flow. The deflection of the cantilever in relation to a reference pointer attached to the blade was read from the micrometer screw to indicate force on the blades. A magnifying lens and good lighting were necessary to obtain correct alignment of the pointer. The second meter was easier to read since it used a torsion bar running the length of the blade. The torsional deflection was large enough so that correct alignment of the reference pointer was not difficult.

Tests were conducted with the first meter in a laboratory channel by comparing the average profile velocity obtained by using the meter with the average profile velocity obtained by pitot tube techniques. The comparison indicated that the blade had a drag coefficient of 1.98. This approximates the value for infinitely long plates, or situations where flow can pass on only two sides of a plate.

With the first meter, the standard deviation based on 16 tests was $\pm$ 1.5 percent. Thus, the method seems promising and will permit rapid measurements of average velocity in sheet flows and channels. No tests have yet been conducted with the second meter.

PERSONNEL: J. A. Replogle

Table 1. Comparison of average velocities determined with a pitot tube and with the integrating velocity profile meter number 1.

Test No.	Flow depth y ft	Average velocity, $\bar{v}$ Pitot tube ft/sec	Vane meter ft/sec	$\Delta\bar{v}$ %
1	0.522	1.171	1.141	-2.56
2	0.552	1.176	1.208	-1.26
3	0.552	1.235	1.196	-3.16
4	0.552	1.239	1.172	-5.42
5	0.552	1.128	1.116	-1.063
6	0.552	1.161	1.128	-2.84
7	0.552	1.228	1.192	-2.92
8	0.552	1.212	1.162	-4.12
9	0.751	1.522	1.514	-0.53
10	0.775	1.467	1.461	-0.15
11	0.751	1.461	1.461	-0.00
12	0.751	1.491	1.461	-2.01
13	0.751	1.511	1.496	-1.00
14	0.751	1.500	1.508	-0.53
15	0.751	1.508	1.494	-0.93
16	0.770	1.511	1.508	-0.20
Average				-2.39%
			Standard deviation σ =	1.5%

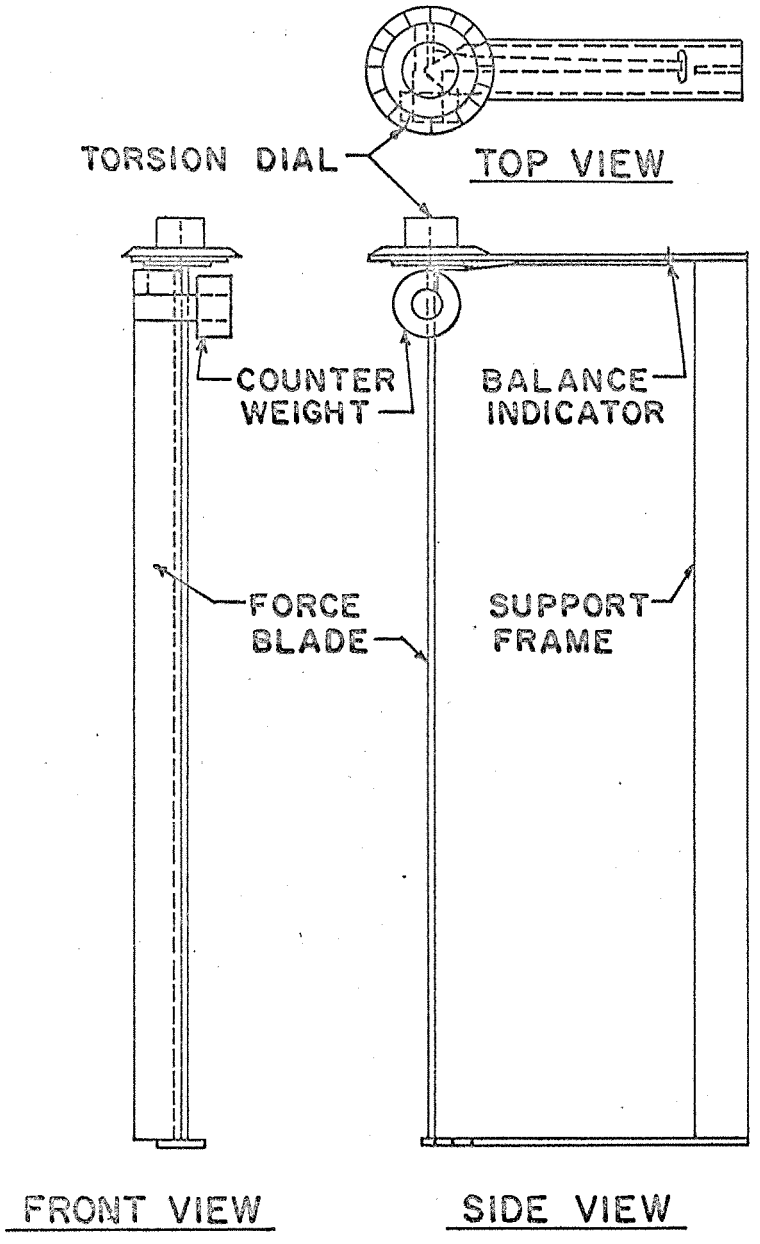

Figure 1. Diagram of integrating velocity profile meter, number 2.

APPENDIX I

MANUSCRIPTS APPROVED AND/OR PUBLISHED IN 1965

	MS Number
Bennett, O. L., Erie, Leonard J., and MacKenzie, A. J. Boll and fiber properties of cotton as affected by management practices. USDA, ARS-41 Series (Submitted).	150
Bouwer, Herman. Applications of seepage meters. Proc., Seepage Symposium, Phoenix, Arizona, Feb. 19-21, 1963. (USDA, ARS 41-90) Pp. 77-81.	93
Bouwer, Herman. Theory of seepage flow systems. Proc., Seepage Symposium, Phoenix, Arizona, Feb. 19-21, 1963. (USDA, ARS 41-90) Pp. 52-56.	94
Bouwer, Herman. Theoretical aspects of seepage from open channels. Jour. Hydraul. Div., Proc. Amer. Soc. Civ. Engin. 91(HY 3):37-59. May, 1965.	131
Bouwer, Herman. Development of design requirements for parallel drains. Proc. Inter-Society Drainage Conf. Chicago, Illinois, Dec. 6-7, 1965. (Submitted).	156
Bouwer, Herman. Closure: Theoretical aspects of seepage from open channels. Jour. Hydraul. Div., Proc. Amer. Soc. Civ. Engin. (Submitted).	158
Ehrler, W. L., Nakayama, F. S., and Van Bavel, C. H. M. Cyclic changes in water balance and transpiration of cotton leaves in a steady environment. Physiologia Plantarum 18(3):766-775, 1965.	126
Erie, Leonard J., French, Orrin F., and Harris, Karl. Consumptive use of water by crops in Arizona. Univ. of Arizona Agric. Experiment Station Technical Bulletin No. 169. September, 1965.	143
Fritschen, Leo J. Miniature net radiometer improvements. Jour. of Appl. Meteorol. 4(4):528-532. Aug. 1965.	137
Fritschen, Leo J. Accuracy of evapotranspiration determinations by the gradient Bowen ratio method. Bul. of Internatl. Assoc. Sci. Hydrol. 10(2):38-48. June, 1965.	142
Fritschen, Leo J. Evapotranspiration rates of field crops determined by the Bowen ratio method. Agron. Jour. (Submitted).	145

	MS Number
Fritschen, Leo J. Net and solar radiation relations over irrigated field crops. Agric. Meteorol. (Submitted).	148
Harris, Karl, Erie, Leonard J., and Fuller, Wallace H. Minimum tillage in the Southwest. Univ. of Arizona Agric. Experiment Sta. and the Cooperative Extension Service Bulletin A-39. February, 1965.	107
Jackson, Ray D., and Taylor, Sterling A. Heat transfer. Chapter 26, Methods of Soil Analysis (Pt. 1), No. 9 in Agronomy Series of Monographs, sponsored by Amer. Soc. Agron. and Amer. Soc. for Testing and Materials. 1965.	33
Jackson, Ray D., Reginato, Robert J., and Van Bavel, C. H M. Comparison of measured and calculated hydraulic conductivities of unsaturated soils. Water Resources Research 1(3):375-380. 1965.	130
Jackson, Ray D. Water vapor diffusion in relatively dry soil: IV. Temperature and pressure effects on sorption diffusion coefficients. Soil Sci. Soc. Amer. Proc. 29(2): 144-148. March-April 1965.	132
Jackson, Ray D., Rose, D. A., and Penman, H. L. The circulation of water in soil under a temperature gradient. Nature 205:314-316. January 16, 1965.	136
Jackson, Ray D., and Van Bavel, C. H. M. Solar distillation of water from soil and plant materials: A simple desert survival technique. Science 149(3690):1377-1378. (September 17, 1965).	146
Jackson, Ray D., and Van Bavel, C. H. M. Pocket-model solar still obtains water for survival. Arid Lands Research Newsletter. (Submitted).	149
Jackson, Ray D., and Van Bavel, C. H. M. Water for survival: An unusual application of plastic film. Proc. 6th Natl. Agric. Plastics Conf., Phoenix, Arizona, November, 1965. (Submitted).	153
Myers, Lloyd E. Evaporation retardants: Application by means of a water soluble matrix. Science 148(3666):70-71. April 2, 1965.	140

	MS Number
Myers, Lloyd E. (Gen. Chairman and Editor) Proceedings, Seepage Symposium, Phoenix, Arizona, Feb. 19-21, 1963. USDA, ARS 41-90. January, 1965.	147
Myers, Lloyd E. Water harvesting with plastic films. Proc. 6th Natl. Agric. Plastics Conf., Phoenix, Arizona, November, 1965. (Submitted).	154
Nakayama, Francis S. Pressure dependence of water vapor pressure in the soil-water system. Soil Sci. Soc. Amer. Proc. 29(3):351. (Letter to the Editor). May-June, 1965.	141
Nakayama, Francis S. Deflocculation of soil materials by sodium salts. Soil Science. (Submitted).	155
Reginato, R. J., and Van Bavel, C. H. M. Soil water measurement with gamma attenuation. Soil Sci. Soc. Amer. Proc. 28(6):721-724. Nov.-Dec. 1964.	112
Replogle, John A., Myers, Lloyd E., and Brust, Kenneth J. Stream flow measurements with fluorescent tracers. Jour. Hydraul. Div., Proc. Amer. Soc. Civ. Engin. (Submitted).	152
Replogle, John A., Myers, Lloyd E., and Brust, Kenneth J. Evaluation of pipe elbows as flow meters. Jour. Irrig. and Drain. Div., Proc. Amer. Soc. Civ. Engin. (To be submitted).	157
Taylor, Sterling A., and Jackson, Ray D. Heat capacity and specific heat. Chapter 25, Methods of Soil Analysis (Pt. 1), No. 9 in Agronomy Series of Monographs, sponsored by Amer. Soc. Agron. and Amer. Soc. for Testing and Materials. 1965.	31
Taylor, Sterling A., and Jackson, Ray D. Temperature. Chapter 24, Methods of Soil Analysis (Pt. 1), No. 9 in Agronomy Series of Monographs, sponsored by Amer. Soc. Agron. and Amer. Soc. for Testing and Materials. 1965.	32
Van Bavel, C. H. M. Composition of the Soil Atmosphere. Chapter 22, Methods of Soil Analysis (Pt. 1), No. 9 in Agronomy Series of Monographs, sponsored by Amer. Soc. Agron. and Amer. Soc. for Testing and Materials. 1965.	40

	MS Number
Van Bavel, C. H. M., and Reginato, R. J. Precision lysimetry for direct measurement of evaporative flux. Proc., Symposium on Methodology of Plant Eco-Physiology, Montpellier, France, April 1962. (Published by UNESCO, Sept. 1965). Pp. 129-135.	65
Van Bavel, C. H. M., and Fritschen, L. J. Energy balance of bare surfaces in an arid climate. Proc., Symposium on Methodology of Plant Eco-Physiology, Montpellier, France, April 1962. (Published by UNESCO, Sept. 1965). Pp. 99-107.	66
Van Bavel, C. H. M. Neutron scattering measurement of soil moisture: Development and current status. Proc., Internatl. Symposium on Humidity and Moisture, Washington, D. C. May, 1963. Pp. 171-184.	106
Van Bavel, C. H. M., Nakayama, F. S., and Ehrler, W. L. Measuring transpiration resistance of leaves. Plant Physiol. 40(3):535-540. May, 1965.	135
Van Bavel, C. H. M. Potential evaporation: The combination concept and its experimental verification. Water Resources Research. (Submitted).	151

Reports -- The following reports of the U. S. Water Conservation Laboratory were released during the year. Such reports are not considered as formal publications, are not distributed to libraries, and should not be cited:

Fritschen, L., and Mullins, K. Miniature net radiometer instruction manual. WCL Report No. 5. October, 1965.

Jackson, Ray D., and Van Bavel, C. H. M. Water for survival. WCL Report No. 4. June, 1965. (Revised: Sept. 1965).

Van Bavel, C. H. M. Report of a trip to the United Kingdom, Netherlands, Austria, Germany, Sweden and Denmark. (15 Sept. - 18 Oct. 1964). WCL Report No. 3. January, 1965.